

**Production of Renewable Diesel from Lignocellulosic biomass through Fast pyrolysis and  
Hydroprocessing Technology**

by

Madhumita Patel

A thesis submitted in partial fulfillment of the requirements for the degree of

Doctor of Philosophy

in

Engineering Management

Department of Mechanical Engineering

University of Alberta

© Madhumita Patel, 2019

# Abstract

Increasing environmental concerns, global warming, and greenhouse gas emissions due to fossil fuel use point to an urgent need for clean renewable energy sources that can replace petroleum-derived fuels. Lignocellulosic biomass, a renewable resource, can be converted to bio-oil by fast pyrolysis and further upgraded to renewable diesel through hydroprocessing. Because biomass behaves as if it is carbon neutral, its use does not increase atmospheric greenhouse gases. To conduct fast pyrolysis experiments to produce bio-oil, a stainless steel fluidized bed was fabricated with an internal diameter and height of 10 and 120 cm, respectively. Bio-oil produced through fast pyrolysis cannot replace conventional petro-diesel, however, because it is highly unstable, polar, has a high oxygen content, and is immiscible with hydrocarbon. Therefore, upgrading is necessary as it removes oxygen-containing compounds from bio-oil through the hydrodeoxygenation reaction using hydroprocessing technology. The ultimate product from this process is hydrogenation-derived renewable diesel (HDRD), also known as renewable diesel or green diesel. Renewable diesel is closer in composition to petroleum diesel, has better chemical stability, and can have better cold flow properties than biodiesel (which is another renewable fuel). The main focus of this research is to (1) explore different lignocellulosic biomasses available in Canada, (2) study the thermochemical properties of the above-mentioned biomass, (3) conduct fast pyrolysis experiments to produce bio-oil with different process conditions, (4) develop a process model for a centralized fast pyrolysis and hydroprocessing facility (5) develop a cost model to estimate the renewable diesel cost, and (6) compare how a centralized pyrolysis plant and a decentralized pyrolysis plant produce bio-oil. For every feedstock, a process and techno-economic model is

developed using an Aspen Plus® simulation. The production cost is reported in \$ L<sup>-1</sup>. Of all the lignocellulosic biomass, woody biomass performed better than agricultural residues in terms of renewable diesel production cost and net energy ratio. The outcomes from this research will be helpful in commercializing and optimizing centralized or decentralized pyrolysis and hydroprocessing facilities to produce renewable diesel from Canadian biomass feedstock. In addition, it will help to reduce the emissions and carbon footprint from the oil and gas industry.

## Preface

This thesis is an original intellectual product of the author, Madhumita Patel. Some parts of this work are published as:

Chapter 2 of this thesis was published as Patel M, Kumar A. Production of renewable diesel through the hydroprocessing of lignocellulosic biomass derived bio oil: a review, *Renewable and Sustainable Energy Reviews*, 2016, 58:1293-1307 and Patel M, Zhang X, Kumar A. Techno-economic and life cycle assessment of lignocellulosic biomass-based thermochemical conversion technologies: a review, *Renewable and Sustainable Energy Reviews*, 2015, 53: 1486-1499

Chapter 3 of this thesis was published as Patel M, Oyedun AO, Kumar A, Gupta R. Predicting the biomass conversion performance in a fluidized bed reactor using an isoconversional model-free method, *The Canadian Journal of Chemical Engineering*. 2018 (in Press). Dr Rajender Gupta supervised the project, assisted with data interpretation and proofread the manuscript prior to submission.

Chapter 4 of this thesis was published as Patel M, Oyedun A, Kumar A, Gupta R. A techno-economic assessment of renewable diesel and gasoline production from aspen hardwood, *Waste and Biomass Valorization*, 2018, 9: 1-16. The fluidized bed experiment were carried out by Madhumita Patel in collaboration with Dr. Adetoyese O. Oyedun. The process and cost model were developed by Madhumita Patel. Dr Rajender Gupta and Dr Amit Kumar supervised this work.

A version of chapter 5 is submitted to Fuel Processing Technology as “What Is The Production Cost of Renewable Diesel from Woody Biomass and Agricultural Residue Based on Experimentation? A Comparative Assessment” coauthored by Madhumita Patel, Dr. Adetoyese O. Oyedun, Dr. Amit Kumar and Dr Rajender Gupta. The fluidized bed experiments were carried out by Madhumita Patel in collaboration with Dr. Adetoyese O. Oyedun. The process and cost model were developed by Madhumita Patel. Dr Rajender Gupta and Dr Amit Kumar supervised this work.

A version of chapter 6 is submitted to Biomass and Bioenergy as “The Development of a Cost Model for Two Supply Chain Network Scenarios for Decentralized Pyrolysis System Scenarios to Produce Bio-oil” coauthored by Madhumita Patel, Dr. Adetoyese O. Oyedun, Dr. Amit Kumar and Dr John Doucette. Madhumita Patel was responsible for defining the problem, developing equations for decentralized pyrolysis system, cost model, data interpretation and manuscript preparation.

Dr. Amit Kumar was the supervisory author on this work and was involved throughout the research in concept formation and manuscript edits. Dr Rajender Gupta and Dr John Doucette was also supervisory author for the part of the thesis.

*This thesis is dedicated to my daughter and my husband,  
Aasmi and Shantanu,  
For their unconditional love, believe, support and  
encouragement*

# Acknowledgements

I would like to thank my supervisor, Dr. Amit Kumar for providing me the opportunity to conduct this research. His immense knowledge, invaluable advice and active participation in every step of this research have helped to complete this thesis. His guidance helped me in all the time of research and writing of this thesis. I thoroughly enjoyed working with Dr. Kumar and I deeply appreciate the knowledge and experiences that I have learned over the course of my graduate studies at the University of Alberta. This work would not have been possible without the funding provided by the Natural Sciences and Engineering Research Council of Canada (NSERC), Alberta Agriculture and Rural Development (AARD), and North West Upgrading Inc. (NWU). I am very grateful for their financial support.

I would like to thank the rest of my supervisory committee: Dr. Rajender Gupta and Dr. John Doucette for their insightful comments and questions, which helped me to broaden my research from various perspectives. Dr Rajender Gupta, one of the humblest people I have ever known. His continuous advice, encouragement and patience helped me to carry out the experimental work in his laboratory.

I highly appreciate the assistance extended by Dr. Adetoyese O. Oyedun (Toye), and Dr. Xiaolei Zhang throughout the research work. I am also thankful to Dr. Deepak Pudasaine Rahman for his help during my experiments. I would like to thank Dr. Mahdi Vaezi for continuous encouragement and friendship throughout this period. I would also like to thank Dr. Abayomi (Femi) Olufemi Oni and Dr. Mahdi Vaezi for peer reviewing of my manuscripts.

This work could not have been completed without the support of the staff at the Department of Mechanical Engineering. Special thanks to Teresa Gray, Gail Dowler and Richard Groulx for their administrative

support. I would also like to thank technicians specially Clark from Machine shop of Chemical Engineering Department for helping in modifying and fabricating the reactor.

I wish to acknowledge Ms. Astrid Blodgett for editing/proofreading countless pages from my papers and thesis. Her suggestions throughout the editing periods helped me to polish my writing styles. From my bottom of my heart, I want to thank Rachel Schofield, project administrator for Dr. Kumar's group, for helping in administrative stuffs.

I want to acknowledge and thank my friends in the Sustainable Energy Research Group (SERG) for sharing the burden and joy of graduate school with me. I would also take this opportunity to thank my friends Satarupa, Garima, Balwinder, Anum, Krishna, Sidhant, Sahil and Rishik for their constant friendship, support and encouragement.

Finally, I would like to thank my parents Ms. Kamalini and Mr. Alekh Patel and my in laws Ms. Nirati and Karunakar Patel for their belief in me even in the dullest phase of life. Without their support the thesis would not have happened. Here I want to take this opportunity to thank my uncle Dr. Arun Patel and aunty Ms. Ranju Patel for their advice, blessing and constant confidence that has made me strong and passionate about achieving dreams.

# Contents

<b>Abstract.....</b>	<b>ii</b>
<b>Preface.....</b>	<b>v</b>
<b>Acknowledgment.....</b>	<b>vi</b>
<b>Chapter 1: Introduction .....</b>	<b>1</b>
1.1 Background .....	1
1.2 Objectives of this research .....	5
1.3 Scope and limitation.....	6
1.4 Organization of the thesis.....	7
<b>Chapter 2: Production of Renewable Diesel through the Hydroprocessing of Lignocellulosic Biomass-derived Bio-oil: A Review .....</b>	<b>10</b>
2.1 Introduction .....	10
2.2 Biomass feedstock.....	14
2.3 Bio-oil.....	17
2.4 Hydroprocessing to convert bio-oil into renewable diesel.....	20
2.4.1 Hydroprocessing .....	20
2.5 Operating parameters .....	26
2.5.1 Catalyst .....	26
2.5.2 Catalyst deactivation.....	39
2.5.3 Temperature .....	41
2.6 Techno-economic analysis of the fast pyrolysis process .....	43
2.7 Techno-economic analysis of hydroprocessing technology.....	46
2.8 Status of HDRD production.....	48
2.9 Issues with hydroprocessing.....	49
2.9.1 Economic analysis .....	49
2.9.2 Gaps in knowledge.....	50
2.10 Conclusions .....	51

### **Chapter 3: Predicting the Biomass Conversion Performance in a Fluidized Bed Reactor**

#### **using Isoconversional Model Free Method..... 66**

3.1	Introduction .....	66
3.2	Basic Pyrolysis Kinetics.....	70
3.3	Experimental Methodology.....	73
3.3.1	Material Preparation and Characterization .....	73
3.3.2	Thermogravimetric Analysis .....	75
3.3.3	Pyrolysis in A Fluidized Bed Reactor and Operating Conditions .....	76
3.4	Results and Discussion.....	79
3.4.1	Thermogravimetric Analysis .....	79
3.4.2	Fast Pyrolysis in Fluidized Bed .....	87
3.5	Comparison of Predicted Biomass Conversion in Fluidized Experiments Using Kinetics from the TGA .....	91
3.6	Comparison with Other Kinetic Studies in the Literature.....	92
3.7	Conclusions .....	93

### **Chapter 4: A Techno-Economic Assessment of Renewable Diesel and Gasoline**

#### **Production from Aspen Hardwood..... 100**

4.1	Introduction .....	100
4.2	Material and methods.....	105
4.2.1	Feedstock .....	105
4.2.2	Experimental set-up .....	106
4.2.3	Characterization of products.....	106
4.2.4	Bio-oil upgrading (hydroprocessing).....	108
4.3	Modelling.....	109
4.3.1	Process modeling .....	109
4.3.2	Techno-economic model.....	113
4.4	Results and Discussion.....	120
4.4.1	Process Model Results for 2000 dry t d <sup>-1</sup> Plant Capacity.....	120
4.4.2	Economic study on the base case of a 2000 t d <sup>-1</sup> aspen woodchip plant .....	121
4.4.3	Influence of plant size on production cost .....	123

4.4.4	Comparison production cost of transportation fuels with published results and actual petro-fuel production .....	126
4.4.5	Sensitivity study .....	127
4.4.6	Uncertainty analysis .....	129
4.5	Conclusion .....	131
<b>Chapter 5: What Is the Production Cost of Renewable Diesel from Woody Biomass and Agricultural Residue Based on Experimentation? A Comparative Assessment ..... 137</b>		
5.1	Introduction .....	137
5.2	Materials and method .....	141
5.2.1	Feedstock preparation .....	141
5.2.2	Experimental set-up .....	143
5.2.3	Product characterization .....	143
5.3	Modelling .....	145
5.3.1	Process modelling .....	145
5.3.2	Economic parameters .....	148
5.4	Result and discussion .....	153
5.4.1	Results of Experimental work on fast pyrolysis in fluidized bed reactor .....	153
5.4.2	Techno-economic model .....	157
5.5	Conclusion .....	167
<b>Chapter 6: Development of Cost Model of Supply Chain Network for Two Scenarios of Decentralized pyrolysis system to Produce Bio-oil ..... 175</b>		
6.1	Introduction .....	175
6.2	Method .....	179
6.2.1	Centralized pyrolysis plant .....	179
6.2.2	Mobile pyrolysis system .....	180
6.3	Generic model development for an MPS .....	181
6.3.1	Scenario 1- Truncated .....	183
6.3.2	Scenario 2 – Radial .....	188
6.4	Description of economic parameters .....	191
6.4.1	Field cost .....	192
6.4.2	Biomass and bio-oil transportation cost .....	194

6.4.3	Capital cost.....	194
6.4.4	Operational cost .....	196
6.4.5	Biomass and bio-oil storage costs.....	196
6.4.6	Biochar transportation cost .....	197
6.4.7	Product cost.....	197
6.4.8	Uncertainty analysis.....	197
6.5	Results and discussion.....	197
6.5.1	Estimate of the number of MPS units required for different capacities .....	198
6.5.2	MPS capital costs.....	199
6.5.3	Biomass transportation distance in scenarios 1 and 2.....	199
6.5.4	Bio-oil transportation distance in scenarios 1 and 2 .....	202
6.5.5	Relocation distance .....	203
6.5.6	Bio-oil production cost .....	205
6.5.7	Bio-oil cost variations with changing centralized plant capacity .....	208
6.5.8	Uncertainty analysis.....	209
6.6	Conclusion.....	212
<b>Chapter 7: Conclusions and Recommendations .....</b>		<b>218</b>
7.1	Conclusions .....	218
7.1.1	Status of fast pyrolysis and hydroprocessing technology.....	219
7.1.2	Identification of Canadian biomass and its pyrolysis kinetics using TGA and fluidized bed reactor .....	220
7.1.3	Process modelling and techno-economic assessment of the centralized fast pyrolysis and hydroprocessing technology .....	223
7.1.4	Development of the supply chain networks for the decentralized pyrolysis system .....	228
7.2	Recommendation for future work .....	230
<b>Appendix A.....</b>		<b>259</b>
<b>Appendix B .....</b>		<b>268</b>

## List of Figures

Figure 2.1. General flow diagram for hydroprocessing technology .....	13
Figure 2.2. Classification of biomass.....	16
Figure 2.3. Reaction mechanism for the hydroprocessing of bio-oil (Venderbosch et al., 2010) 23	23
Figure 2.4. Reaction mechanism for guaiacol .....	24
Figure 2.5. Reaction mechanism for phenol .....	25
Figure 2.6. Performance of noble metal catalysts and benchmark catalysts for liquid (oil) yield and oxygen content in oil yield.....	34
Figure 2.7. The effect of temperature on the performance of noble metal carbon-supported catalysts .....	42
Figure 2.8. The effect of temperature on oil, char, and gas yield for the HDO of bio-oil from sawdust.....	43
Figure 3.1. Non-isothermal solid kinetic methods.....	67
Figure 3.2, Schematic diagram of a fluidized bed reactor .....	77
Figure 3.3. TGA curves of four different biomass samples as a function of temperature at a heating rate of 10°C min <sup>-1</sup> in nitrogen atmosphere .....	80
Figure 3.4. Detailed DTG curves of spruce and aspen as a function of temperature at a heating rate of 10 °C min <sup>-1</sup> in nitrogen atmosphere .....	80
Figure 3.5. The TGA curve of spruce with detailed thermal decomposition zones as a function of temperature at a heating rate of 10 °C min <sup>-1</sup> in nitrogen atmosphere.....	81
Figure 3.6. TGA curves of spruce at four different heating rates .....	84
Figure 3.7. DTG curves of spruce at four different heating rates .....	84
Figure 3.8. FWO plot of spruce hardwood for a range of conversions .....	85
Figure 3.9. Variation of E <sub>a</sub> with conversion using FWO method.....	86
Figure 3.10. Effects of temperature on biomass conversion in the fluidized bed reactor at a fixed particle size (0.425 – 1mm): (a) aspen and spruce and (b) corn stover and wheat straw .....	88

Figure 3.11. Effects of particle size distribution on biomass conversion at 490 °C in the fluidized bed reactor.....	89
Figure 3.12. Prediction of $E_a$ from the fluidized bed reactor for (a) aspen, (b) spruce, (c) corn stover, and (d) straw .....	90
Figure 3.13. Predicted, experimental, and corrected predicted biomass conversion for (a) aspen, (b) spruce, (c) straw, and (d) corn stover.....	92
Figure 4.1. Schematic diagram of process flow sheet for fast pyrolysis and hydroprocessing pathway.....	104
Figure 4.2. Mass flow diagram of fast pyrolysis and hydroprocessing technology for a 2000 t d <sup>-1</sup> aspen feedstock plant.....	110
Figure 4.3. Breakdown of installed cost of 2000 t d <sup>-1</sup> capacity aspen plant.....	122
Figure 4.4. Cost distribution for 2000 t d <sup>-1</sup> capacity plant.....	123
Figure 4.5. Variation of total project investment cost with capacity.....	124
Figure 4.6. Renewable diesel and gasoline production cost with different capacities .....	125
Figure 4.7. Cost distribution for 500 t d <sup>-1</sup> and 5000 t d <sup>-1</sup> capacity plant.....	126
Figure 4.8. Sensitivity of renewable diesel and gasoline production cost.....	128
Figure 4.9. Uncertainty analysis of diesel and gasoline production cost.....	130
Figure 5.1. Experimental methodology for fast pyrolysis process .....	144
Figure 5.2. Schematic process diagram of fast pyrolysis and hydroprocessing technology.....	145
Figure 5.3. Effects of temperature on product distribution for fast pyrolysis of biomass with (a) spruce, (b) corn stover, and (c) wheat straw .....	154
Figure 5.4. Effects of particle size distribution on bio-oil and biochar yield at 460°C for corn stover and wheat straw and at 490°C for spruce in an inert nitrogen atmosphere.....	155
Figure 5.5. Distribution of purchased equipment cost for hydrogen production scenario for spruce wood.....	158
Figure 5.6. Distribution of operating cost on present worth of renewable diesel for a plant capacity of 2000 t d <sup>-1</sup> based on techno-economic model .....	160
Figure 5.7. Sensitivity analysis for renewable diesel from (e) Effects of biochar selling price on renewable diesel cost, (b) Spruce: H <sub>2</sub> purchase, (c) Spruce: H <sub>2</sub> production (d) Corn stover: H <sub>2</sub> production, and (e) Wheat straw: H <sub>2</sub> production .....	165

Figure 6.1. Two MPS allocation configurations: (a) truncated and (b) radial and (c) centralized unit .....	179
Figure 6.2. Schematic of an MPS unit .....	180
Figure 6.3. MPS allocation in area As for scenario 1: Truncated.....	184
Figure 6.4 Bio-oil transportation distance (a), biomass transportation distance (b) and MPS relocation distance (c) for the truncated scenario .....	185
Figure 6.5. Distribution areas into subsectors, radial scenario .....	189
Figure 6.6. Bio-oil transportation distance (a), biomass transportation distance (b) and MPS relocation distance (c) for the radial scenario .....	190
Figure 6.7. Change in the number of MPS units with plant capacity .....	198
Figure 6.8. The development of the scale factor for an MPS plant and Changes in capital cost with MPS capacity .....	199
Figure 6.9. Biomass transportation distance with variations in MPS capacity: (a) truncated and (b) radial configurations .....	201
Figure 6.10. Bio-oil transportation distance with variations in MPS capacity: (a) truncated and (b) radial configurations .....	203
Figure 6.11. MPS relocation distance with variations in MPS capacity: (a) truncated and (b) radial configurations .....	204
Figure 6.12. Bio-oil production costs for a 100 dry t d <sup>-1</sup> MPS plant in the truncated and radial configurations .....	207
Figure 6.13. Bio-oil production costs for centralized and decentralized pyrolysis plants .....	209
Figure 6.14. Uncertainty analysis for bio-oil production cost for 100 dry t d <sup>-1</sup> capacity .....	211
Figure 7.1. Reaction mechanism for the hydroprocessing of bio-oil.....	220
Figure 7.2. Detailed DTG curves of spruce and aspen as a function of temperature at a heating rate of 10 °C min <sup>-1</sup> in nitrogen atmosphere .....	221
Figure 7.3. Predicted, experimental, and corrected predicted biomass conversion for (a) aspen, (b) spruce, (c) straw, and (d) corn stover.....	222
Figure 7.4. Effects of temperature on product distribution for fast pyrolysis of biomass with (a) spruce, (b) corn stover, and (c) wheat straw .....	224
Figure 7.5. Distribution of purchased equipment cost for hydrogen production scenario for spruce wood.....	226

Figure 7.6. Renewable diesel and gasoline production cost with different capacities .....	227
Figure 7.7. Effects of biochar cost on renewable diesel cost.....	227
Figure 7.8. Bio-oil production costs for centralized and decentralized pyrolysis plant .....	230

## List of Tables

Table 2-1. Comparison between biodiesel, renewable diesel, and petro-diesel .....	12
Table 2-2. Composition of woody biomass .....	17
Table 2-3. Elemental composition and physical properties of bio-oil .....	18
Table 2-4. Reactions involved in hydroprocessing.....	21
Table 2-5. Summary of operating conditions for hydroprocessing bio-oil.....	29
Table 2-6. Summary of operating conditions for hydroprocessing model compounds in bio-oil .....	31
Table 2-7. Earlier techno-economic analyses of the fast pyrolysis process .....	45
Table 2-8. Earlier techno-economic analyses of the hydroprocessing technology.....	47
Table 2-9. Commercial renewable diesel plants .....	48
Table 3-1. Ultimate and proximate analyses of biomass samples .....	74
Table 3-2. Typical chemical analysis of biomass samples .....	74
Table 3-3. Peak temperature, range of active pyrolysis, and rate of decomposition of biomass samples from DTG plot .....	82
Table 3-4. Comparison of $E_a$ from the TGA and fluidized bed reactor .....	91
Table 3-5. Comparison of $E_a$ results from the literature .....	93
Table 4-1. Proximate and ultimate analyses of aspen woodchip .....	105
Table 4-2. Composition of bio-oil and uncondensed gases from fast pyrolysis of aspen woodchip .....	107
Table 4-3. Detailed equipment cost for the 2000 t d <sup>-1</sup> biomass plant .....	115
Table 4-4. Methodology for estimating plant capital cost .....	117
Table 4-5. Key assumptions for the development of the techno-economic model.....	117
Table 4-6. Components of feedstock cost.....	118
Table 4-7. Unit price of components used in the model .....	119
Table 4-8. Summary of key results from the techno-economic study .....	121
Table 5-1. Typical chemical analysis of biomass samples .....	142

Table 5-2. Process conditions and model details for the equipment used in the process simulation .....	146
Table 5-3. Method for the estimation of plant capital cost.....	149
Table 5-4. Key assumptions for techno-economic model development.....	150
Table 5-5. Input data on biomass yield and delivery cost for the techno-economic model .....	152
Table 5-6. Experimental results on the composition of bio-oil by feedstock .....	157
Table 5-7. Summary of main cost estimates for a size of 2000 dry t d <sup>-1</sup> plant .....	159
Table 5-8. Variation of renewable production cost as a function of biochar selling price .....	161
Table 6-1. Whole tree biomass properties .....	192
Table 6-2. Field cost, transportation cost, and storage cost for an MPS unit .....	193
Table 6-3. MPS plant characteristics and cost input.....	195
Table 6-4. Bio-oil production costs in two frameworks, centralized and MPS .....	205
Table 6-5. Cost distribution of bio-oil production costs for an MPS.....	206
Table 6-6. Cost distribution of 100 dry t d-1 for four different relocation scenarios .....	208
Table 7-1. Cost distribution of bio-oil production costs for an MPS.....	229

## List of Symbols

GHG	Greenhouse gas emission
HDO	Hydrodeoxygenation
TGA	Thermogravimetric analysis
DTG	Derivative thermogravimetric
$\alpha$	Extent of reaction (conversion)
$k(T)$	Rate constant of the reaction ( $s^{-1}$ )
$f(\alpha)$	Reaction model
$m_i$	Initial mass of the sample (kg)
$m_a$	Actual mass of the sample at time $t$ (kg)
$m_f$	Final mass of the sample after the end of the reaction (kg)
$T$	Absolute temperature (K)
$R$	Gas constant ( $8.314 \text{ J K}^{-1} \text{ mol}^{-1}$ )
$A$	Pre-exponential factor ( $\text{min}^{-1}$ )
$E_a$	Activation energy ( $\text{kJ mol}^{-1}$ )
$B$	Linear heating rate
$M_t$	Biochar remaining after time $t$ (kg)
$M_0$	The biomass fed to the reactor (kg)
$t$	Time (min)
FWO	Flynn-Wall-Ozawa
MPS	Mobile pyrolysis system
$N$	No of MPS units
$A$	Capacity of centralized plant, dry $t \text{ d}^{-1}$
$A_l$	Bio-oil produced in a centralized plant, dry $t \text{ d}^{-1}$
$B_l$	Capacity of an MPS unit, dry $t \text{ d}^{-1}$
$Z$	Bio-oil used by an MPS to produce electricity, dry $t \text{ d}^{-1}$
$M$	Number of relocations by an MPS in a year

$A_s$	Area required for an MPS in relocation time, M ha/relocation time
$T$	Lifetime of an MPS in years
$R$	Radius of the entire area required for the harvesting for T years
$A'$	Area required for entire lifetime of all MPS units for T years
HDO	Hydrodeoxygenation
TEA	Techno-economic Analysis

# **Chapter 1: Introduction**

## **1.1 Background**

The world continuously faces new challenges from greenhouse gas (GHG) emissions due to the use of fossil fuels (mainly, coal, natural gas, and petroleum products) to fulfil our daily energy requirement. The modern economic sector, that is, industry uses large amounts of energy produced from conventional energy sources. In 2016, globally the contributions for energy production were 33.3%, 28.1%, 24.1%, 10% and 4.5%, respectively, from petroleum, coal, natural gas, renewable, and nuclear sources (BP plc, 2017). Generally, coal and natural gas are used to produce electricity and heating, and petroleum fuels are used in the transportation sector. Fossil fuel use continues to increase because they are cheap, convenient, reliable, available, stable, and abundant and have an economic benefit and high calorific value. However, there are adverse effects of fossil fuel use on the ecosystem. Therefore, there is a pressing need to explore alternatives such as renewable fuels.

From 1970 to 2011, GHG emissions from burning fossil fuels and industrial processes made up around 78% of global emissions (Environmental Protection Agency, 2014). According to the Government of Canada, GHG emissions in Canada increased by about 18.5% between 1990 and 2013. GHG emissions from the oil and gas industry, the transportation sector, and the heat and electricity generation increased by 39%, 49%, and 8%, respectively, from 1990 to 2013 (Environment and Climate Change Canada, 2017). The large increase in the transportation sector resulted from changes in vehicle type in both passenger and freight transport. In the last few decades, light duty gasoline trucks (SUVs, vans, pickup trucks) have been used more than cars for passenger transportation, and semi-trailer truck use for freight transportation has increased significantly compared to rail, marine transport, because of increased trade between provinces and

countries (Climate Change Connection, 2013). The adverse effects on the environment of increased GHG emissions are dangerous and risky and need to be addressed urgently.

There are currently three options available to address the environmental problem resulting from GHG emissions: first is carbon capture and sequestration (CCS); second is the switching` to renewable alternatives and third is to increase efficiency of energy use. The first option, to sequester GHG emissions from fossil fuel use, is an emerging, and risky option and requires large investment for full it to be deployed at commercial scale. Recently, many CCS projects on small-scale has faced challenges because of the high cost of capturing, liquefying, transporting, and sequestration of carbon dioxide (Greenpeace International, 2016). To commercialize this technology and make it sustainable, more research and development are required.

The second option is to use renewable resources to reduce dependence on fossil fuel use and subsequently reduce GHG emissions. Broadly, renewable resources are solar, wind, hydro, nuclear, and biomass. All these resources are good candidates to produce heat and electricity. Biomass is the only renewable alternative among all that can be converted to biofuels (renewable diesel, biodiesel, bio gasoline, jet fuel, etc.) whose can be used for substitution of the conventional petroleum products.

The third option includes improvement of energy efficiency of the current energy use. These categories of options are low hanging fruits and are being implemented in various sectors and at different scales. Several jurisdictions around the world have programs to encourage consumers both residential and industrial to improve their energy efficiencies. According to Energy Efficiency Alberta (2018), existing inefficient equipment can be upgraded through more efficient energy saving options or adaption of renewable alternative in both industrial and residential scales. Till date, they are using solar as the renewable resources. But in 2019, other renewable resources such wind, biomass, geothermal energy can be adopted for the upgrading of inefficient equipment to same energy and money (Energy Efficiency Alberta, 2018).

In general, conventional petroleum products are chosen in the transportation sector because of their high energy density and low cost. Diesel is widely accepted for long distance transportation and gasoline is preferred in passenger vehicles. However, high petro-fuel consumption in the transportation sector made up 25% of global GHG emissions in 2015 (United Nations, 2018) . To replace petro-fuels, three alternatives are available: electric vehicles, fuel cells, and biofuels. The popularity of electric vehicles and fuel cells (batteries) is low compared to biofuels because of the high energy density of biofuels and the existing infrastructure of the distribution and consumption system to fulfil supply and demand globally. Neither electric vehicles nor fuel cells are reliable or economically feasible currently as infrastructure for refilling, and storage stations have not been developed. The only viable and sustainable alternative to replace petroleum fuels currently is biomass-derived biofuel.

In several jurisdictions blending renewable fuels with conventional petro-fuels is done to achieve GHG emissions and this is increasing to further achieve the reduction targets by 2030 set in a number of these jurisdictions. In Canada, the percentage of blending varies by province, but a minimum 2% by weight in the conventional gasoline and diesel is required. According to Alberta's Renewable Fuels Standard (RFS), commercial fuel producers must blend 5% renewable alcohol in gasoline and 2% of renewable diesel in diesel before selling to consumers. To meet the RFS requirement to reduce GHG emissions by at least 25%, it is necessary to replace an equivalent amount of renewable fuel with conventional petroleum fuels (Alberta Environment and Parks, 2018).

Biodiesel and renewable diesel are two renewable fuels that satisfy the ASTM standard for petroleum-based diesel fuel (ASTM D975) (Fenwick, 2018), but the production method and composition of the fuels are different. Biodiesel is produced through transesterification, a process in which vegetable oil reacts with alcohol such as methanol or ethanol in the presence of a catalyst to produce biodiesel; glycerol is the by-product. Biodiesel is composed primarily of monoalkyl esters of long-chain fatty acids. Renewable diesel, also known as “green diesel” and “second

generation biodiesel,” is produced from the fast pyrolysis and catalytic hydroprocessing of lignocellulosic biomass. Renewable diesel is composed of hydrocarbons (paraffin, alkanes, aromatics, etc.), similar to petro-diesel (Neste, 2016). In fast pyrolysis, lignocellulosic biomass is converted to bio-oil, biochar, and non-condensable gases in a pyrolyzer. The operating conditions in the pyrolyzer are a temperature of 400-600°C, atmospheric pressure, a very high heating rate at around 2s, and the absence of oxygen. Following pyrolysis, the bio-oil, the intermediate for renewable diesel, is processed in a two-stage hydrotreater, then in a butanizer and a hydrocracker to produce renewable diesel with some gasoline. The hydrotreater and hydrocracker are maintained at high temperature and pressure conditions in the presence of hydrogen and heterogeneous catalysts. Further details on the renewable diesel production is discussed in subsequent chapters.

Because of the significant differences in composition and production technology, the fuel properties of renewable diesel and biodiesel are vastly different. Biodiesel is produced from vegetable oils from biomass such as canola, can be used in existing diesel engines, is nearly carbon neutral over the life cycle and good fuel efficiency, is produced and distributed locally, and is biodegradable and nontoxic (Hassan & Kalam, 2013). But it has a big drawback related to cold flow properties that cannot be ignored in countries like Canada. Because of its higher cloud and pour points, biodiesel forms a gel at low temperatures. Biodiesel has other disadvantages: it is produced from food-based feedstocks, which leads to increase in food prices and food shortages; filters clog due to the high viscosity of vegetable oil; it emits more NO<sub>x</sub> than petro-diesel, etc. Because renewable diesel is composed of hydrocarbons, it is superior to biodiesel in cold countries. Although renewable diesel has many good fuel properties, there is no published study on the use of Canadian lignocellulosic biomass (e.g. forest biomass or agricultural biomass such as straw or corn stover) to produce renewable diesel or a techno-economic assessment of such production through fast pyrolysis and hydroprocessing technology.

In Canada, there are 347 million hectares of forest, an estimated 9% of the world’s forests (Natural Resources Canada, 2017). With proper harvesting practices and land use planning, these forests can be used as a resource for biofuels. In Western Canada, moreover, more than 27 million tonnes

of agricultural residue are available, after the removal of the straw used for soil conservation and livestock feeding and bedding (Sokhansanj et al., 2006). These lignocellulosic feedstocks are good candidates for the production of renewable diesel.

In this study, four lignocellulosic feedstocks (aspen, spruce, corn stover, and wheat straw) were considered to produce renewable diesel through fast pyrolysis and hydroprocessing technology. Miller and Kumar (2014) conducted a techno-economic assessment of renewable diesel production from Canadian seed-based feedstocks (canola and camelina) Several techno-economic assessment studies have been done on the production of renewable fuels and electricity (Brown et al., 2013; Jones et al., 2013; Shemfe et al., 2015; Wright et al., 2010; Zhang et al., 2013). However, in the literature, there is no evidence of the technical and economic feasibility of renewable diesel production from the four Canadian lignocellulosic feedstocks and in Canadian conditions are listed above through fast pyrolysis and hydroprocessing technology. In general, bio-oil, as an intermediate for renewable diesel, can be produced through a centralized fast pyrolysis system or distributed pyrolysis system.. This work sets out to understand the thermal and pyrolysis kinetics of different lignocellulosic Canadian biomass feedstocks and simulates the production of renewable diesel through fast pyrolysis and hydroprocessing technology. The research explores both the technical and the economic aspects of this process. Finally, this work compares, for the first time, centralized and decentralized systems in the production of bio-oil. Further details on the different systems are provided in subsequent chapters. This work aims to understand the technical and economic aspects of pyrolysis and hydroprocessing technology and to reduce greenhouse gas emissions for the transportation sector.

## **1.2 Objectives of this research**

The novel contribution of this research is in the area of the renewable transportation fuels from lignocellulosic biomass feedstocks. The aim of this research is to study the production technology, scale, and economics in order to help to establish standalone, environmentally friendly, and cost-competitive biofuels from lignocellulosic biomass. The specific objectives of this research are to:

1. Carry out experimental research for a thermogravimetric study to understand the pyrolysis kinetics and thermochemical properties of four Canadian lignocellulosic biomass (aspen woodchips, spruce woodchips, wheat straw, and corn stover) for the production of renewable diesel.
2. Design and fabricate a lab-scale fluidized bed reactor to produce bio-oil, an intermediate to renewable diesel, through fast pyrolysis process from woody and agricultural biomass and characterize the properties of the bio-oil.
3. Develop a process model to establish the energy and material balance required to produce renewable diesel through fast pyrolysis and hydroprocessing..
4. Develop and compare detailed data-intensive techno-economic models to estimate the production cost of renewable fuel from the various lignocellulosic biomass types and determine both the optimum feedstock and production plant capacity.
5. Develop supply chain networks for the decentralized mobile pyrolysis plant used to produce bio-oil for a base case plant capacity of 2000 dry tonnes/day and compare the results with a centralized plant of the same capacity.
6. Develop a model to understand the trade-off between bio-oil production cost vs. plant capacity for the two systems to define the favorable zones for the respective systems.

### **1.3 Scope and limitation**

1. The fast pyrolysis experiments are conducted on a lab-scale fluidized bed reactor consisting of a vertical tube 10 cm in diameter and 120 cm high.
2. The four selected Canadian lignocellulosic feedstocks considered are spruce, aspen, corn stover, and wheat straw.
3. Two configurations for the allocation of the mobile pyrolysis units are considered.
4. The cost of renewable diesel from the biomass is estimated for Western Canada. The results could be used in other jurisdictions by modifying local costs.

## 1.4 Organization of the thesis

This thesis consists of seven chapters and each chapter, except the introduction and conclusion, is an independent paper. Most of these have been published and some have been submitted for publication in peer-reviewed literature. In other words, this thesis is a consolidation of papers and each chapter is intended to be read independently. As a result, some concepts and data are repeated.

1. The first chapter briefly introduces the renewable fuels, technologies, and overall objectives of this research.
2. The second chapter reviews in detail the available literature on the technical and economic feasibility of hydroprocessing technology for upgrading fast pyrolysis oil. The chapter discusses the catalysts, reaction mechanism, and process conditions of hydroprocessing technology.
3. The third chapter investigates the pyrolysis kinetics and thermochemical properties of the feedstocks using a thermogravimetric analyzer and also predicts biomass conversion in a fluidized bed using TGA kinetics.
4. The fourth chapter examines the detailed process and techno-economic model results of the use of aspen woody biomass to produce renewable diesel. The process model includes biomass harvesting, biomass transportation, biomass pretreatment, fast pyrolysis, and hydroprocessing technology.
5. The fifth chapter examines and compares the experimental and economic feasibility of renewable diesel production using three biomass feedstocks, spruce woodchips, corn stover, and wheat straw. For process modeling, two hydrogen production scenarios are considered, hydrogen production and hydrogen purchase. Finally, the net energy ratio (NER) is estimated for all the biomass feedstocks.
6. The sixth chapter investigates the optimization framework for the mobile pyrolysis system for the production of bio-oil and compares the results with the centralized pyrolysis system.
7. Finally, chapter seven summarizes the study and makes recommendations for future work

## References

- Alberta Environment and Parks. 2018. Renewable Fuels Standard, available at <http://aep.alberta.ca/climate-change/programs-and-services/renewable-fuels-standard/default.aspx>. Accessed on 7 May 2018
- BP Statistical Review of World Energy. 2017, available at <https://www.bp.com/content/dam/bp/en/corporate/pdf/energy-economics/statistical-review-2017/bp-statistical-review-of-world-energy-2017-full-report.pdf>. Accessed on 7 May 2018.
- Brown, T.R., Thilakarathne, R., Brown, R.C., Hu, G. 2013. Techno-economic analysis of biomass to transportation fuels and electricity via fast pyrolysis and hydroprocessing. *Fuel*, **106**, 463-469.
- Climate Change Connection. 2013. GHG Emissions - Canada, available at <http://climatechangeconnection.org/emissions/ghg-emissions-canada/canada-emissions-by-sector/>. Accessed on 7 May 2018.
- Energy Efficiency Alberta. 2018. The future is bright, available at <https://www.encyalberta.ca/>. Accessed on 15 October 2018.
- Environment and Climate Change Canada. 2017. Canadian environmental sustainability indicators greenhouse gas emissions, available at [http://www.ec.gc.ca/indicateurs-indicators/18F3BB9C-43A1-491E-9835-76C8DB9DDFA3/GHGEmissions\\_EN.pdf](http://www.ec.gc.ca/indicateurs-indicators/18F3BB9C-43A1-491E-9835-76C8DB9DDFA3/GHGEmissions_EN.pdf). Accessed on 15 August 2018.
- Environmental Protection Agency. 2014. Global Greenhouse Gas Emissions Data, available at <https://www.epa.gov/ghgemissions/global-greenhouse-gas-emissions-data>. Accessed on 7 May 2018.
- Fenwick, S. 2018. Renewable fuels for diesel applications, available at [https://cleancities.energy.gov/files/u/news\\_events/document/document\\_url/183/Fenwick\\_-\\_NBB\\_-\\_Clean\\_Cities\\_Renewable\\_Diesel.pdf](https://cleancities.energy.gov/files/u/news_events/document/document_url/183/Fenwick_-_NBB_-_Clean_Cities_Renewable_Diesel.pdf). Accessed on 7 May 2018
- Greenpeace International. 2016. Carbon capture and storage a costly, risky distraction, available at <https://www.greenpeace.org/archive-international/en/campaigns/climate-change/Solutions/Reject-false-solutions/Reject-carbon-capture--storage/>. Accessed on 7 May 2018.

- Hassan, M.H., Kalam, M.A. 2013. An overview of biofuel as a renewable energy source: development and challenges. *Procedia Engineering*, **56**, 39-53.
- Jones, S.B., Meyer, P.A., Snowden-Swan, L.J., Padmaperuma, A.B., Tan, E., Dutta, A., Jacobson, J., Cafferty, K. 2013. Process design and economics for the conversion of lignocellulosic biomass to hydrocarbon fuels: fast pyrolysis and hydrotreating bio-oil pathway. Pacific Northwest National Laboratory (PNNL), Richland, WA (US), available at <https://www.nrel.gov/docs/fy14osti/61178.pdf>. Accessed on 8 May 2107
- Miller, P., Kumar, A. 2014. Techno-economic assessment of hydrogenation-derived renewable diesel production from canola and camelina. *Sustainable Energy Technologies and Assessments*, **6**, 105-115.
- Natural Resources Canada. 2017. How much forest does Canada have?, available at <http://www.nrcan.gc.ca/forests/report/area/17601>. Accessed on 7 May 2018.
- Neste. 2016. Neste renewable diesel handbook, available at [https://www.neste.com/sites/default/files/attachments/neste\\_renewable\\_diesel\\_handbook.pdf](https://www.neste.com/sites/default/files/attachments/neste_renewable_diesel_handbook.pdf). Accessed on 7 May 2018.
- Shemfe, M.B., Gu, S., Ranganathan, P. 2015. Techno-economic performance analysis of biofuel production and miniature electric power generation from biomass fast pyrolysis and bio-oil upgrading. *Fuel*, **143**, 361-372.
- Sokhansanj, S., Mani, S., Stumborg, M., Samson, R., Fenton, J. 2006. Production and distribution of cereal straw on the Canadian prairies. *Canadian Biosystems Engineering*, **48**, 3.
- United Nations. 2018. National greenhouse gas inventory data for the period 1990–2015, available at <https://unfccc.int/sites/default/files/resource/docs/2017/sbi/eng/18.pdf>. Accessed on 15 October 2018.
- Wright, M.M., Daugaard, D.E., Satrio, J.A., Brown, R.C. 2010. Techno-economic analysis of biomass fast pyrolysis to transportation fuels. *Fuel*, **89**, S2-S10.
- Zhang, Y., Brown, T.R., Hu, G., Brown, R.C. 2013. Techno-economic analysis of two bio-oil upgrading pathways. *Chemical Engineering Journal*, **225**, 895-904.

# **Chapter 2: Production of Renewable Diesel through the Hydroprocessing of Lignocellulosic Biomass-derived Bio-oil: A Review<sup>1</sup>**

## **2.1 Introduction**

Increasing environmental concerns and the depletion of fossil fuels are the main factors behind the urgent need for renewable fuels. Canada's Federal Renewable Fuels Regulations requires that at least 5% renewable fuel (based on the volume of petroleum based fuel) (Environment Canada). Biomass is a renewable product that, when processed and upgraded to a transportation fuel, can be used in place of petroleum-based liquid fuels.

Ethanol, biodiesel, and renewable diesel are the three renewable fuels that satisfy current regulations and policies of many jurisdictions (Canadian Renewable Fuels Association; United States Environmental Protection Agency). Ethanol is produced from grains and thus is considered a first-generation biofuel. Ethanol, produced by the fermentation, is also considered as a clean biofuel and a gasoline alternate. Extensive research has been done on ethanol production from

---

<sup>1</sup>This chapter is a combination of two published review papers in *Renewable & Sustainable Energy Reviews*. The first paper is Patel M, Kumar A. Production of renewable diesel through the hydroprocessing of lignocellulosic biomass-derived bio-oil: A review, *Renewable and Sustainable Energy Reviews*, 2016, 97: 151-160. The second is Patel M, Zhang X, Kumar A. Techno-economic and life cycle assessment of lignocellulosic biomass-based thermochemical conversion technologies: a review, *Renewable and Sustainable Energy Reviews*, 2015, 53: 1486-1499.

biomass over the last two decades (Bothast & Schlicher, 2005; Dias et al., 2011; Goldemberg et al., 2008; Quintero et al., 2008; Sánchez & Cardona, 2008). A major challenge in the use of first generation liquid biofuels is that they are also used as food (Environmental Issues).

Biodiesel is produced from the transesterification of vegetable oils produced from grains and has been proven to be a promising renewable fuel with the potential to reduce GHGs significantly of (Canadian Renewable Fuels Association). Biodiesel produces less pollution than petro-diesel and biodegradable; it has no sulfur, which increases the life of the catalytic converter; it is miscible with hydrocarbons and nontoxic; and it has lubricating properties, which can increase the life of diesel engines (Department of Energy). But there are some drawbacks to biodiesel that need specific attention. Biodiesel performs poorly in cold temperatures (Berkeley Biodiesel; Department of Energy). In addition, biodiesel alone is not sufficient to fill consumer demand for clean energy.

The third option, a renewable diesel derived through hydrodeoxygenation (HDO), also known as “green diesel” and “second generation biodiesel,” is produced from the catalytic hydroprocessing of vegetable oil from grains and has been used interchangeably with petro-diesel (Knothe, 2010).. Several governments have mandated that diesel from renewable sources should be blended with conventional diesel (e.g., the Canadian government has mandated that all diesel fuel should have an average of 2% renewable diesel (Environment News Service)). Renewable diesel is composed primarily of long-chain alkanes and short- and branched-chain alkane and negligible aromatics. The cetane number is high for long-chain alkanes and low for short- and branched-chain alkanes. For cold countries like Canada, shorter alkanes and isomerized compounds are preferred over long-chain alkanes due to their high cloud point, which allows the fuel to flow more easily (Knothe, 2010). Table 2.1 shows a comparison of biodiesel, renewable diesel, and petro-diesel (Bezergianni & Dimitriadis, 2013; Knothe, 2010; Krishna et al., 2014; Lehto et al., 2013; Mittelbach, 1996; Saravanan & Nagarajan, 2014). Some properties of renewable diesel are similar to and some are superior to petro-diesel. The low aromatic content of renewable diesel leads to cleaner combustion and better cold-flow properties than biodiesel.

**Table 2-1. Comparison between biodiesel, renewable diesel, and petro-diesel**

<b>Property</b>	<b>Biodiesel</b>	<b>Renewable diesel</b>	<b>Petro-diesel</b>
Density (g ml <sup>-1</sup> )	0.885-0.9	0.77-0.83	0.85
Sulfur (ppmwt)	0 - 0.012	<10	12
Cetane number	45 -72.7	80 – 99	54.57
Flash point (°C)	96-188	68-120	52-136
Net heating value (MJ kg <sup>-1</sup> )	37.1-40.4	42-44	42-45
CFPP (°C)	(-13)-15	>20	-6
Cloud point (°C)	(-3) – 17	(-25) – 30	-5
Pour point (°C)	(-15) -16	(-3) – 29	-21
Kinematic viscosity (mm <sup>2</sup> s <sup>-1</sup> )	1.9 - 6.0 (@ 40°C)	1.9 - 4.1(@ 40 °C)	1.9 - 4.1(@ 40 °C)

Renewable sources of energy could be an alternative that can replace fossil fuels. Among all the renewable sources, biomass is the only resource that can be directly converted to high value end products (bioenergy and biofuel) in any form (solid, liquid, or gas) using thermochemical conversion technology (Hamelinck & Faaij, 2006). These technologies rely on lignocellulosic biomass feedstock (e.g., agricultural residue, forest residue,) to form various fuels and chemicals (Demirbaş, 2001). Lignocellulosic biomass feedstocks do not compete with food sources are getting a lot of attention.

The thermochemical conversion of biomass to useful end products can occur through one over several: pyrolysis, gasification, liquefaction, combustion, carbonization, and co-firing. Pyrolysis is considered to be the starting point of all thermochemical conversion technologies because it involves all chemical reactions to form solid, liquid, and gas as the main products with zero concentration of oxygen. Fast pyrolysis is widely used to enhance the liquid yield with moderate temperature and very low residence time. During the fast pyrolysis process, biomass is heated in a pyrolyzer in the absence of oxygen to 400– 550 °C at atmospheric pressure for a residence time of <2s (Azargohar et al., 2013; Bridgwater, 1999; Bridgwater, 2012; Bridgwater et al., 1999; Kim et al., 2013a; Peters et al., 2014). This bio-oil is a complex mixture of different organic compounds derived from the thermal decomposition of cellulose, hemi-cellulose, and lignin.. All organic compounds are present in the organic oil phase, whose density is higher

than water's and gives bio-oil high viscosity. The acidity of bio-oil promotes a condensation reaction that accelerates aging and a declination of bio-oil properties and makes the bio-oil immiscible with petro-fuels. Therefore, bio-oil should be upgraded so that it can be directly used as a fuel or mixed with crude oil. Moreover, bio-oil is highly unstable because of the presence of unsaturated carbon, which is active during polymerization and condensation (Elliott & Neuenschwander, 1998; Ferrari et al., 2002a; Gandarias et al., 2008; Ward, 1993; Wildschut et al., 2010a).

Upgrading bio-oil to a transportation fuel can be done through hydroprocessing, a well-established technology in the refinery industry (Ward, 1993). Figure 2.1 shows the general flow diagram for hydroprocessing. Hydroprocessing is a combination of two technologies, hydrotreating and hydrocracking. Through these processes, bio-oil can be upgraded to a product whose properties are similar to or better than those of petroleum fuels. There have been few studies done on the production of renewable diesel from hydroprocessing technology using lignocellulosic biomass-based intermediates.

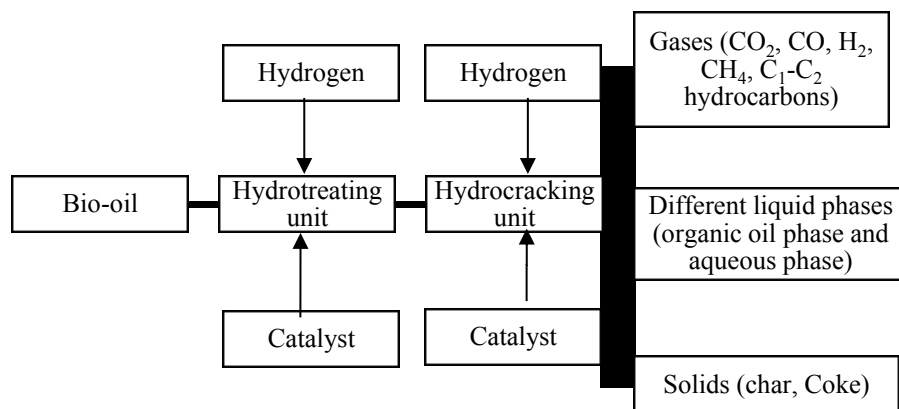


**Figure 2.1. General flow diagram for hydroprocessing technology**

An investigation of the technical and economic aspects of a technology is mandatory to commercialize it. The principal means of evaluating a new technology is a techno-economic assessment. While fast pyrolysis is a well-established and understood technology at both the pilot

and commercial scale, most techno-economic studies of are from the mid to late 1980s. Hydroprocessing for bio-oil is still in the demonstration stage and not yet commercialized. Moreover, little has been published on this topic. The detailed understanding of different pathways for the conversion of model compounds/fast pyrolysis oil to renewable diesel and the effect of different process parameters on hydroprocessing need to be addressed. Simultaneously, this paper also focuses on the economic features of these thermochemical conversion routes can be reflected through a TEA, where the production cost of each product is summarized and compared for different conversion routes. The overall objective of this chapter to conduct a review of renewable diesel production from lignocellulosic biomass-based intermediates, i.e. bio-oil including techno-economic assessments through fast pyrolysis and hydroprocessing technology.

## **2.2 Biomass feedstock**

Biomass is a generic term for organic hydrocarbon materials, primarily carbon, hydrogen, oxygen, nitrogen, and sulfur, though sulfur and nitrogen are present only in insignificant amounts. Biomass contains some inorganic impurities such as ash, whose concentration varies from species to species. Ash concentration is around 5-10% by weight in agricultural residues and much less in softwood, approximately 1% by wt (ECN Phyllis2; Yaman, 2004).

Figure 2.2 shows biomass feedstock classifications (Antizar-Ladislao & Turrion-Gomez, 2008; McKendry, 2002; Naik et al., 2010; Yaman, 2004). These feedstocks are divided into two categories depending on their end use: food and non-food/lignocellulosic biomass feedstock.

Biomass food feedstocks are classified into two categories, starch sugar crops and oil seed vegetable plants. The major starch sugar crops are rice, wheat, maize, root vegetables (potatoes and cassava), sugarcane, and barley. This feedstock contains primarily starch and is made up of a large number of glucose units. Bioethanol and biodiesel are formed from starch sugar crops through fermentation and transesterification, respectively, using different catalysts. Oil seed vegetable plants, the other food category, include coconut, corn, cottonseed, olive, palm, rapeseed, sunflower, sesame seed, soybean, mustard, canola, camellia, jatropha, and pine. The vegetable oil

is extracted through solvent extraction process.. Feedstocks differ from one country to the next depending on climate and soil conditions (Richardson et al., 2013).

Biofuels from first-generation biomass (food feedstock) are limited in their ability to achieve government targets for the replacement of fossil fuels. Increasing concern about these issues has led to an increase in the interest in developing biofuels from non-food biomass.

Non-food biomass, also known as lignocellulosic or second-generation biomass, is emerging as a source for biofuel production that can replace refinery crude oil as feedstocks for the production of transportation fuels. In this review paper, the focus is on lignocellulosic biomass feedstock due to its advantages over other feedstocks. Non-food biomass feedstock can be divided into three broad categories, shown in Figure 2.2. They are mainly agricultural, forest, and municipal waste feedstock. Lignocellulosic biomass is the non-edible portion of major food crops that is currently underused and could be used for biofuel production. Agricultural feedstock has four categories, shown in Figure 2.2. Straw and vegetation waste include bagasse, vegetable wastes, and residues from the production of cereals. Energy crops such as willow, poplar, and switchgrass are grown specifically for energy production. They have a high yield per unit area compared to conventional crops and trees (McKendry, 2002) and are commonly used for the production of biofuels. The moisture content of agricultural residues is between 10 and 20 wt%, which is an advantage for the fast pyrolysis process (Serrano et al., 2011). Forest biomass includes whole tree, forest residue, and wood waste. Forest residues consist of tree branches and tops, and wood waste includes saw mill wastes and rotten and dead trees. These types of feedstock are always available and accessible for bio-oil production.

As mentioned, municipal wastes can be used to produce biofuels (CBCnews). Waste from the paper industry accounts for up to 40% of all the waste in the United States that has biodegradable components (Environmental Protection Agency U.S.). Municipal waste also includes everyday items such as product packaging, grass clippings, furniture, clothing, bottles, food scraps, newspapers, etc. Around 80% of these wastes are biodegradable and could be considered an

alternate sustainable source of biofuels (Environmental Protection Agency U.S.; Environmental Protection Agency U.S.). The main advantage of using municipal waste as feedstock for biofuel production is because in most jurisdictions, municipal waste is landfilled; its use will save land because the amount of material sent to landfills will decrease.

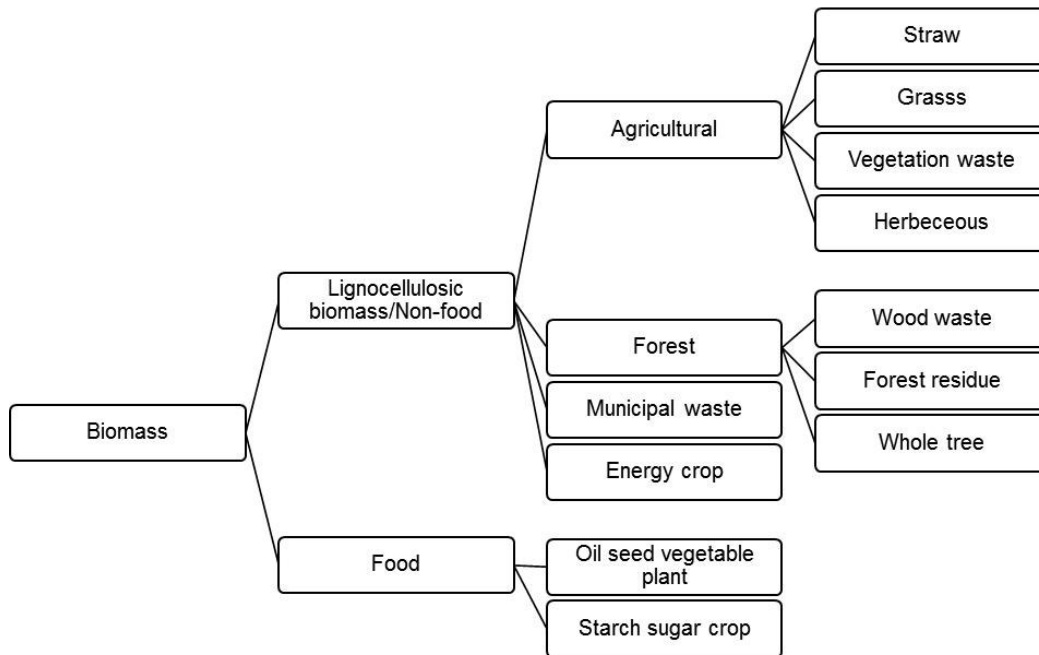


**Figure 2.2. Classification of biomass**

Cellulose, hemicelluloses, and lignin are the three important organic compounds in biomass. Their weight percentages are in the ranges of approximately 30-50, 20-40, and 10-20, respectively (Dakar; EuroBioRef; Galletti & Antonetti; McKendry, 2002; McMillan, 1994; Sun & Cheng, 2002).. Feedstock is categorized based on the proportion of cellulose and lignin. For example, hardwood consists of tightly bound cellulose with low concentrations of lignin; softwood is the opposite. Table 2.2 summarizes the composition of woody biomass (Diffen; Zhang et al., 2005).

**Table 2-2. Composition of woody biomass**

<b>Biomass</b>	<b>Cellulose</b>	<b>Hemicellulose</b>	<b>Lignin</b>	<b>Extractives</b>
Softwood	42% +/- 2%	27% +/- 2%	28% +/- 3%	3% +/- 2%
Hardwood	45% +/- 2%	30% +/- 2%	20% +/- 4%	5% +/- 3%
Sawdust	45.2%	20%	24.3%	9%

### **2.3 Bio-oil**

Several thermal, mechanical, and biological methods are used to convert lignocellulosic biomass to more valuable products. Renewable diesel production from lignocellulosic biomass requires converting lignocellulosic biomass to an intermediate known as bio-oil. Bio-oil can be produced through fast pyrolysis. Its production depends significantly on the feed type, moisture content, temperature, residence time, and ash content. In this process, biomass is heated in a pyrolyzer in absence of oxygen to 450-550 °C at an atmospheric pressure for a residence time of < 2s (Azargohar et al., 2013; Bridgwater, 1999; Bridgwater, 2012; Bridgwater et al., 1999; Kim et al., 2013b; Peters et al., 2014). As residence time is very short, liquid yield is high and there is low ash content in the product. A product analysis found that liquid yield is around 75-80 wt% and the rest are gaseous components and char, which is a solid (Bridgwater, 2012). The bio-oil obtained from this process has a higher heating value than raw biomass and can be directly used as an intermediate to convert lignocellulosic biomass into a transportation fuel (Czernik & Bridgwater, 2004; Lu et al., 2009).

In general, bio-oil is a viscous, polar, dark-brown, free-flowing liquid. It is a complex mixture of different organic compounds derived from the thermal decomposition of cellulose, hemicellulose, and lignin. Bio-oil mainly consists of acids, alcohols, aldehydes, esters, ketones, sugars, phenols, phenol derivatives, nitrogen compounds, and a large proportion (20-30wt%) of lignin-derived oligomers (Environmental Protection Agency U.S.; Tsai et al., 2007; VTT Technical Research Centre of Finland; Zhang et al., 2007). As biomass contains a significant amount of moisture, the bio-oil derived from this process carries significant amounts of water (around 15-30 wt%), which

leads to phase separation, either aqueous or organic oil, in bio-oil. All organic compounds are present in the organic oil phase, whose density is more than that of water and gives bio-oil high viscosity. The acidity of bio-oil promotes a condensation reaction that accelerates aging and a declination of bio-oil properties and makes the bio-oil immiscible with petro-fuels. Therefore bio-oil should be upgraded so that it can directly be used as a fuel or mixed with crude oil. Moreover, bio-oil is highly unstable because of the presence of unsaturated carbon, which is active during polymerization and condensation (Elliott, 1998; Ferrari et al., 2002a; Gandarias et al., 2008; Ward, 1993; Wildschut et al., 2010a).

The heating value of bio-oil is 16-20 MJ kg<sup>-1</sup> (Bridgwater, 2003; Wildschut et al., 2009b; Zhang et al., 2005), which is significantly higher than that of raw biomass but lower than that of crude oil, whose value is around 35-40 MJ kg<sup>-1</sup> (Bezergianni & Dimitriadis, 2013; Lehto et al., 2013). The low heating value of bio-oil compared to crude oil is due to the presence of high molecular-weight oxygenated compounds. The highly unstable nature of bio-oil can be attributed to its deteriorating heating values. This deterioration occurs over time due to polymerization and condensation between the oxygen compounds themselves.

The catalyst has a significant effect on the fast pyrolysis process. According to Wang et al. (Wang et al., 2012), bio-oil from a fast catalytic pyrolysis process in the presence of a mesoporous ZSM-5 zeolite catalyst was more stable than bio-oil from a non-catalytic pyrolysis process. Generally the oxygen content in non-catalytic bio-oil is around 40-50 wt%, but in the catalytic pyrolysis process, the oxygen content could be reduced significantly depending on the catalyst type and feed condition (Wang et al., 2012). Wang et al. (2012) found that oxygen can be removed partially or fully by the catalytic pyrolysis. However, the catalytic pyrolysis is uneconomical due to the high cost of catalysts. Table 2.3 shows the elemental composition and physical properties of bio-oil derived from different lignocellulosic biomass.

**Table 2-3. Elemental composition and physical properties of bio-oil**

<b>Feedstock for bio-oil</b>	<b>C</b>	<b>H</b>	<b>O</b>	<b>N</b>	<b>S</b>	<b>HHV (MJ kg<sup>-1</sup>)</b>	<b>pH</b>	<b>Moisture content</b>	<b>Reference</b>
Beech wood	51.1	7.3	41.6			20.3	3		(Wildschut et al., 2009b)
Typical wood	55-58	5.5-7	35-40	0-0.2		16-19	3	15-30	(Bridgwater, 2003)
Pine wood	40.1	7.6	52.1	0.1					(Ardiyanti et al., 2012a)
Rice husk	39.92	8.15	51.29	0.61	0.03	16.5	3	28	(Lu et al., 2008)
Beech wood	58.6	6.2	35.2					27.8	(Wildschut et al., 2010a)
Pine sawdust	38.8	7.7	53.4	0.09	0.02			26	(Elliott et al., 2012)
Eucalyptus	44.8	7.2	48.1	0.2					(Elliott, 1998)
Hybrid poplar	46.7	7.6	45.7	0.2	0.03			18.9	(Elliott, 1998)
Whole tree poplar	49.06	6.3	43.6	1			2	18.7	
White spruce	49.6	6.4	43.1	0.2			2	22.4	(Piskorz & Scott, 1987)
Red maple	48.5	6.1					2	18	
Poplar	49.5	6.05	44.4	0.07			2	18.6	
Sawdust	60.4	6.9	31.8	0.9		21.3			(Zhang et al., 2005)

Bio-oil can be stored at a refinery before transportation. There are two ways to store oil. For short periods, it can be stored in a stainless steel or olefin polymer vessel that does not get corroded by the bio-oil (Bridgwater, 1999). For long periods, the oil is blended with methanol (10% by weight), which prevents polymerization and condensation (Sarkar & Kumar, 2010).

## 2.4 Hydroprocessing to convert bio-oil into renewable diesel

### 2.4.1 *Hydroprocessing*

Hydroprocessing is a generic term for a combination of two technologies, hydrocracking and hydrotreating (Ward, 1993). Through hydrocracking and hydrotreating (See Figure 2.1), bio-oil is processed into a product with properties similar to those of petroleum fuel. In hydroprocessing technology, feed is initially processed in a hydrotreating unit and then it is put into a hydrocracker unit (Ward, 1993). The hydrotreating unit is a primary pretreatment unit that hydrogenates unsaturated hydrocarbons and removes heteroatoms from the feedstocks. The basic reactions in the hydrotreater are hydrodesulfurization (HDS), hydrodenitrogenation (HDN), hydrodeoxygenation (HDO), and hydrodearomatization (HDA). In biomass-derived oil, oxygenates are the main components (sulfur and nitrogen compounds are found in insignificant quantities). Therefore, HDO is critical in the removal of the oxygen heteroatom from the feedstock. Hydrodealkylation, hydrocracking, isomerization of alkanes, and hydrodecyclization are key reactions that occur simultaneously in the hydrocracking unit. A few more reactions occur in the hydrotreater and hydrocracker without hydrogen: decarboxylation, decarbonylation, the water-gas shift reaction, methanation, and coke formation (Haldor Topsoe). The general reactions involved in hydroprocessing are summarized in Table 2.4.

Oxygen, nitrogen, and sulfur are removed in the hydrotreater in the form of water, ammonia, and hydrogen sulfide, respectively. These reactions take place in the presence of hydrogen and a catalyst. The main component of the hydrotreating unit is the reactor, which consists of a high-pressure reactor vessel, the proprietary catalyst, and internal technology. The pressure range is considerable, between 50-200 bars, and the temperature varies from 300-400 °C (Elliott, 1998; Gandarias et al., 2008). Different researchers have used different kinds of reactors. Tang et al. (2009) reported that hydrotreating is an efficient way to convert aldehydes and unsaturated compounds into more stable compounds by removing oxygen atoms from the compounds. Through this process, an unstable form of bio-oil is converted to a stable one through the removal of unsaturated oxygen compounds (Wildschut et al., 2010a). Depending on the temperature, the hydrotreating process is considered to be high severity or low severity (Elliott & G., 1996). High-

severity hydrotreating is complete hydrodeoxygenation and low-severity hydrotreating is partial hydrodeoxygenation.

**Table 2-4. Reactions involved in hydroprocessing**

<b>Hydrotreating unit (removal of heteroatom)</b>
Hydrodeoxygenation (HDO) : $R - OH + H_2 \rightarrow R - H + H_2O$
Hydrodesulphurization (HDS) : $R - SH + H_2 \rightarrow R - H + H_2S$
Hydrodenitrogenation (HDN) : $Pyridine + H_2 \rightarrow Pentane + NH_3$
<b>Hydrocracking unit</b>
Hydrodealkylation : $R - C_6H_5 + H_2 \rightarrow C_6H_6 + R - H$
Hydrocracking : $R1 - CH_2 - CH_2 - R2 + H_2 \rightarrow R1 - CH_3 + R2 - CH_3$
Isomerization of alkanes : $Pentane \rightarrow Isopentane$
<b>Other simultaneous reactions</b>
Decarboxylation : $R - COOH \rightarrow RH + CO_2$
Water gas shift reactor : $CO_2 + H_2 \rightarrow CO + H_2O$
Decarbonylation : $R - CHO \rightarrow R - H + CO$
Coke formation : $Polyaromatics \rightarrow Coke$

As the moisture content of bio-oil is high, the liquid product derived from hydrotreating unit has two phases: the aqueous phase and the oil phase (Ardiyanti et al., 2011). Depending on the severity of hydrotreatment, the treated oil from the hydrotreating unit is free of heteroatoms, but it has non-polar, high-molecular weight organic compounds in the oil phase. Therefore the oil is further processed in a hydrocracking unit in the presence of a catalyst and hydrogen at high temperature and pressure conditions. As the name suggests, higher molecular compounds break into smaller molecular weight compounds through hydrodealkylation, hydrocracking, and isomerization (see Table 2.4). During hydroalkylation, the branched alkane is removed from the main alkane chain by the addition of hydrogen, thus forming two individual alkane molecules whose molecular weights are significantly lower than the original alkane molecules. During a hydrocracking reaction, one long-chain alkane is broken down into two small molecular weight alkanes in the

presence of hydrogen. During isomerization, the branched alkanes, which are formed during the isomerization reaction, have the same carbon atoms as the reactant.

Among other reactions, decarboxylation, decarbonylation, and the water-gas shift reaction are desired, whereas methanation and coke formation are undesired (Haldor Topsoe). Reaction mechanisms for the hydroprocessing of bio-oil and model compounds involve different reactions depending on the catalyst and operating conditions and are discussed in the next section of this paper.

#### *2.4.1.1 Typical reaction pathways during hydrodeoxygenation of Bio-oil*

Venderbosch et al. (2010) developed a reaction network for the hydroprocessing of bio-oil using a Ru/C catalyst; the network is shown in Figure 2.3. Ardiyanti et al. (2012a) studied bio-oil on non-sulfide bimetallic Ni-Cu catalysts with an alumina support and deduced that the reaction network of this bio-oil was the same as that described by Venderbosch et al.(2010). The authors consider two modes for bio-oil: catalytic hydrogenation (hydroprocessing) and thermal, non-catalytic repolymerization. Because hydroprocessing takes place at high temperature and pressure conditions, repolymerization leads to the formation of soluble, higher molecular weight fragments in the absence of a catalyst, which, following further condensation reactions, gives char. This is undesired and should be reduced as much as possible. The hydrogenation of bio-oil takes place in the presence of a catalyst and hydrogen, which should be dominating in the mechanism. In the initial phase of hydrotreating, the unstable, polar, and highly viscous bio-oil is converted to stabilized oil by hydrogenation at a temperature greater than 80 °C. Then hydrodeoxygenation is the dominating reaction in the hydrotreater, when the temperature is increased to more than 250 °C and the pressure is maintained at 200 bars. The liquid product from the hydrotreater contains non-polar, high molecular weight fragments in the oil phase associated with an aqueous phase. After that, in the hydrocracker, non-polar, high molecular weight compounds along with the aqueous phase are converted into lower molecular weight fragments at high temperature and pressure conditions. The resulting blend from the hydrocracker has properties similar to petrodiesel. This is the generic reaction mechanism for the hydroprocessing of bio-oil (Venderbosch et al., 2010).

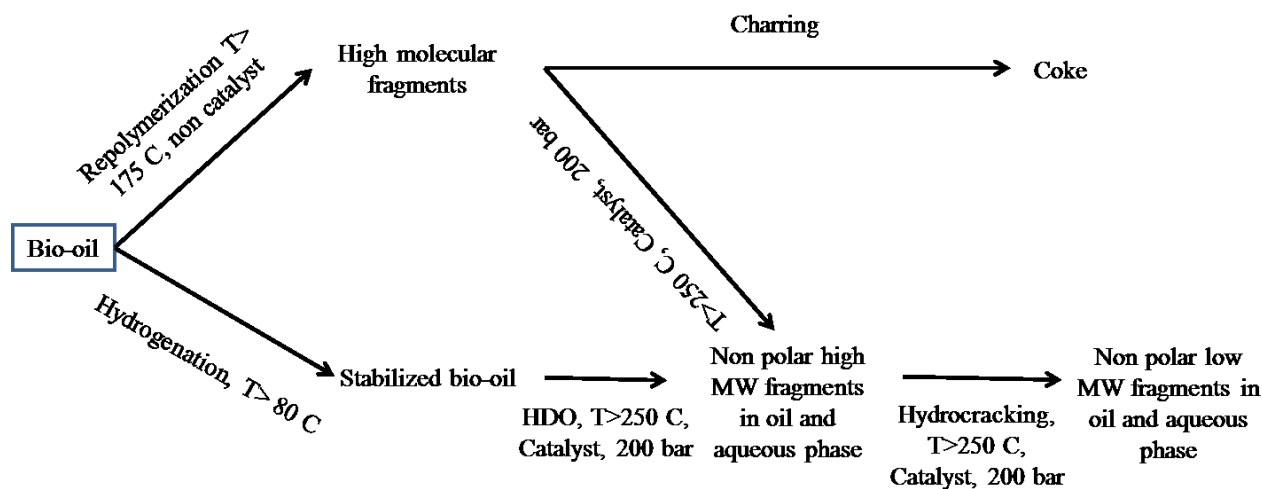


**Figure 2.3. Reaction mechanism for the hydroprocessing of bio-oil (Venderbosch et al., 2010)**

#### 2.4.1.2 Guaiacol

Guaiacol is considered another important model compound of bio-oil obtained from lignin fractions of lignocellulosic biomass fast pyrolysis. Guaiacol contains two oxygen molecules, hydroxyl (C-OH) and methoxy (C-OCH<sub>3</sub>) groups. There are three positions of the methoxy group in guaiacol molecules: para, meta, and ortho.

The reaction mechanism for the conversion of guaiacol to hydrocarbons on different catalysts has been studied by several researchers (Bui et al., 2011a; Centeno et al., 1995; de la Puente et al., 1999; Ferrari et al., 2002a; Gutierrez et al., 2009; Sepúlveda et al., 2011). The general reaction scheme of guaiacol conversion to hydrocarbons is summarized in Figure 2.4. The conversion of guaiacol to phenol takes place in two different paths. The first is the direct conversion of guaiacol to phenol by demethoxylation (elimination of -OCH<sub>3</sub>) without any intermediary. The second path consists of two consecutive steps: the conversion of guaiacol to catechol by demethylation and the conversion of catechol to phenol by hydrogenolysis. Phenol then directly forms benzene by hydrodeoxygenation or follows subsequent hydrogenation of the aromatic ring to give cyclohexane and methyl pentane as the final products. Guaiacol and catechol have a tendency to form coke due

to polymerization depending on the acidity of the catalysts, but the detrimental effect of these molecules can be avoided by proper selection of a catalyst system. The reaction mechanism varies for different catalyst systems mainly depending on the metals and support used.

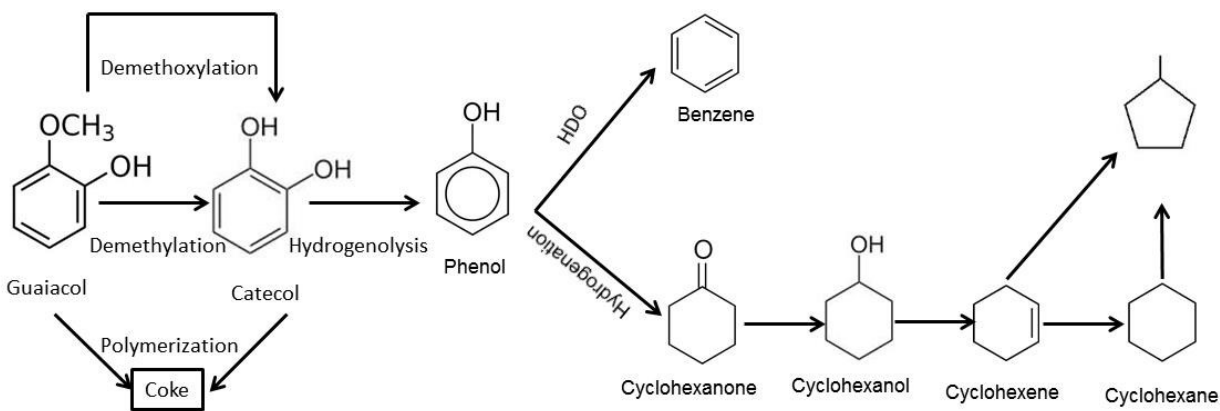


**Figure 2.4. Reaction mechanism for guaiacol**

#### 2.4.1.3 Phenol

Bio-oil derived from the fast pyrolysis process contains around 10-20 wt% phenol and phenol-derived compounds. Therefore phenols were considered a model compound with low reactivity in HDO. The conversion pathways of phenol into high-valued hydrocarbons by hydroprocessing have been studied by different researchers (Bu et al., 2012; Echeandia et al., 2010; Gevert et al., 1987; Laurent & Delmon, 1993; Yang et al., 2009; Zhao et al., 2011). The reaction mechanism for phenol is shown in Figure 2.5.

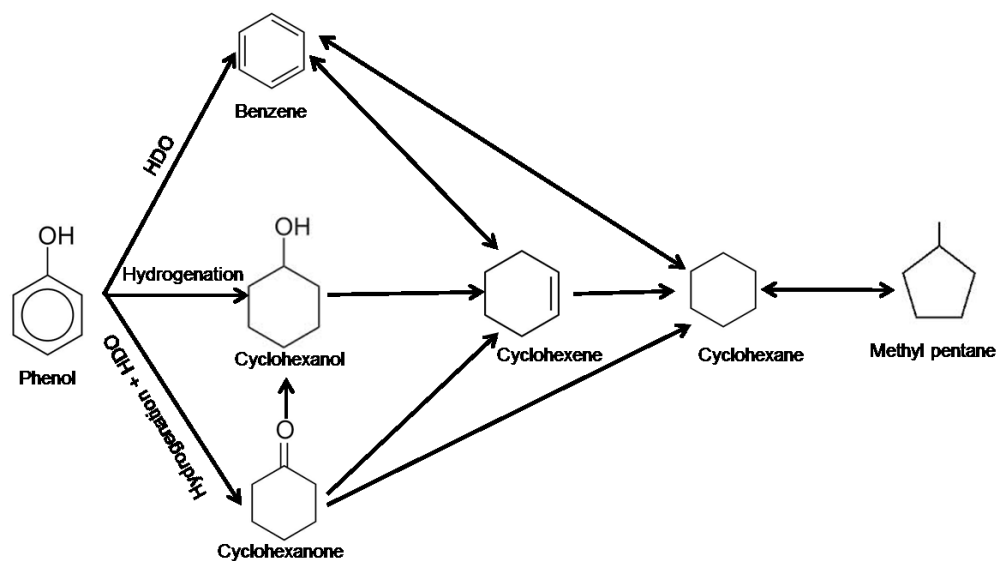


**Figure 2.5. Reaction mechanism for phenol**

There are three independent paths for the HDO of phenol: the first is direct elimination of oxygen from the aromatic chain by C-O bond cleavage (direct hydrodeoxygenation) in the presence of hydrogen to form benzene followed by cyclohexene and cyclohexane; the second path is hydrogenation of the aromatic ring (phenol) to form an intermediate, i.e., cyclohexanol, which is immediately followed by oxygen removal to form cyclohexene and cyclohexane; and the third pathway is a combination of hydrogenation and hydrodeoxygenation of phenol to cyclohexanone followed by subsequent hydrogenation to form cyclohexanol, cyclohexene, and cyclohexane. All three pathways ultimately lead to the formation of cyclohexane, which can also isomerize to form methyl cyclopentane. These paths are completely dependent on the operating parameters of the hydroprocessing reactions. Depending on the surface morphology, compositions of metal, support, and temperature, different intermediate and products are formed (Bu et al., 2012; Echeandia et al., 2010; Gevert et al., 1987; Laurent & Delmon, 1993; Yang et al., 2009; Zhao et al., 2011).

## 2.5 Operating parameters

### 2.5.1 Catalyst

A catalyst plays an important role in the final composition of renewable diesel. Researchers have used a variety of catalysts to hydroprocess bio-oil. Mainly the catalysts fall into one of two categories: transition metal catalysts and sulfide catalysts. Either sulfide Ni-Mo or sulfided Co-Mo supported on gamma alumina is used as a catalyst for removing sulfur compounds from crude oil (Ward, 1993). Since both hydrodeoxygenation and hydrodesulfurization use hydrogen as a reactant to remove the heteroatom from the respective feedstock, sulfide Ni-Mo/sulfide Co-Mo supported on gamma alumina is considered to be the reference catalyst for hydroprocessing bio-oil. In these catalysts, Mo acts as the active site for these heteroatoms and Co/Ni as the promoter for hydrodeoxygenation. Table 2.5 and 2.6 show the operating conditions used for hydroprocessing bio-oil and model compounds.

#### 2.5.1.1 Sulfided NiMo/CoMo metals

Sulfided forms of NiMo/CoMo metals have been studied on different supports for hydroprocessing bio-oil and model compounds (Bui et al., 2011a; Bunch et al., 2007; Zhang et al., 2003). Ni and Co are used as promoters to increase the activity of molybdenum sulfide, and it is believed that promoters donate electrons to Mo, which weakens the metal-sulfide bond. The reactions for different oxygenate compounds have been studied on this sulfide NiMo/CoMo catalyst, and it can be deduced that reaction paths depend on the catalyst surface. The activity of the sulfided catalysts rapidly decreases with time due to the loss of MoS<sub>2</sub> active sites and the presence of H<sub>2</sub>O due to HDO; thus, a continuous supply of a sulfiding agent such as H<sub>2</sub>S is required to preserve the sulfided catalysts from oxidation by oxygenated compounds or a reduction of the sulfided phase by hydrogen (Yoshimura et al., 1991).

The effect of H<sub>2</sub>S and H<sub>2</sub>O on sulfide NiMo/CoMo catalysts has been studied for different model compounds (Laurent & Delmon, 1993; Senol et al., 2005). Senol et al. (2005) have studied the effect of water on the HDO of aliphatic esters on sulfide NiMo/CoMo catalysts supported on gamma alumina. They concluded that water decreases the conversion of esters and suppresses the

deoxygenation reaction. Between dehydration and the decarboxylation reaction, water mainly affects the decarboxylation reaction and suppresses the formation of C<sub>6</sub> hydrogen.

Laurent et al. (1994b) studied the effect of H<sub>2</sub>S and water on the HDO of carbonyl, carboxylic, and guaiacyl groups with sulfide NiMo/CoMo catalysts supported on gamma alumina and deduced that H<sub>2</sub>S increases the Bronsted acidity on the sulfide phase during the reaction. The Bronsted acidity is also responsible for the decarboxylation reaction. Isomerization and hydrocracking are also promoted by the presence of H<sub>2</sub>S. Hydrogen sulfide enables the fine control of the activity and selectivity of sulfided hydrotreating catalysts. Among CoMo and NiMo, it was concluded that H<sub>2</sub>S depresses the activity of Ni compared to Co for the ketonic and carboxylic model compounds. The superior promoting effect of Co has also been agreed upon by Bui et al. (2011a) for the HDO of guaiacol.

The impregnation order of metals in a bimetallic catalyst is an important parameter for catalyst activity and selectivity of hydrodeoxygenation. Ferrari et al. (2002b) have investigated the impregnation order for metals (Co and Ni) loading on carbon support at the time of catalyst preparation. According to these authors, Co was dominantly impregnated on the external surface of the support and Mo was deposited inside the micropores of the support. Therefore, it seemed better to add Co after Mo so that Co became responsible for the remobilization of Mo that had migrated to the external part of the grain. Changing the impregnation order caused Mo-Co interactions to form a thick layer of metal oxide crystal. This layer covered the external surface, leading to a reduction in catalyst activity and product selectivity.

The addition of phosphorus as a promoter to a Mo-based traditional refinery catalyst was studied for a hydrotreating activity of bio-oil and model compounds (Gishti et al., 1984; Yang et al., 2009; Zhang et al., 2005). Phosphorus enhances Mo dispersion on the support, reduces coke formation, increases packing of MoS<sub>2</sub> crystallites, and creates new Lewis and Bronsted acid sites on the support surface (Decanio et al., 1991; Yang et al., 2009; Zhang et al., 2005). At the time of catalyst preparation, phosphorus forms phosphor molybdate complexes that augment HDN reactions in the

hydroprocessing unit. Zhang et al. (2005) found that in the presence of P, the oxygen content in raw bio-oil obtained from sawdust was reduced from 41.8% to 3% by weight and the heating value increased from 21.3 to 41.4 MJ kg<sup>-1</sup>.

#### *2.5.1.2 Noble metals*

Studies have also been conducted on noble metals used as catalysts for hydroprocessing bio-oil and model compounds (see Table 2.5 and 2.6). It was seen that noble metals perform better than traditional refinery catalysts in terms of oil yield and degree of hydrodeoxygenation. While Ru is widely used, Rh, Pt, and Pd are commonly used noble metal catalysts for the hydroprocessing of bio-oil and model compounds.

**Table 2-5. Summary of operating conditions for hydroprocessing bio-oil**

Feedstock	Reactor Type	Reactor Dimension	Catalyst Used	Temperature °C	Pressure bar	SV(h <sup>-1</sup> )	Reference	HHV MJ kg <sup>-1</sup>	HDO (wt%)	Oil Yield (wt%)	pH
Beech wood	Autoclave	100ml volume	Ru/C, Ru/TiO <sub>2</sub> , Ru/Al <sub>2</sub> O <sub>3</sub> , Pt/C, and Pd/C	250 & 350	100 & 200		(Wildschut et al., 2009b)	40	90	60% wt%	
Pine wood	Parr	100ml volume	Ni-Cu/Al <sub>2</sub> O <sub>3</sub>	350	100		(Ardiyanti et al., 2012a)	98	75	35-43	
Vacuum pyrolysis oil	Autoclave		Ru/γAl <sub>2</sub> O <sub>3</sub> & NiO-WO <sub>3</sub> /γAl <sub>2</sub> O <sub>3</sub>	325	172		(Gagnon & Kaliaguine, 1988)				
Pine sawdust and bark	Trickle bed	¾" OD, 0.065" thickness & 32" long	Pt/Al <sub>2</sub> O <sub>3</sub> /SiO <sub>2</sub> , sulfided CoMo/γ-Al <sub>2</sub> O <sub>3</sub> , Ni-W/γ-Al <sub>2</sub> O <sub>3</sub> , Ni-Mo/γ-Al <sub>2</sub> O <sub>3</sub> .	350-400	52.72-104.33	WHSV 0.5-3	(Sheu et al., 1988)				
Rice husk	Autoclave	100ml	Pd/SO <sub>4</sub> <sup>2-</sup> /ZrO <sub>2</sub> /SBA-15	280	85-105		(Tang et al., 2009)	20.1			5
Fast pyrolysis oil	Stainless steel parr	50ml	Pt/Al <sub>2</sub> O <sub>3</sub> . & Pt/MZ-5 (MZ-mesoporous zeolite)	200	40	LHSV 2,4,6	(Wang et al., 2012)		55		
Fast pyrolysis oil	Batch autoclave	100 ml	Ru/C	350	200		(Wildschut et al., 2010b)			55	
Beech wood	Batch autoclave	100ml	Ru/C	350	200		(Wildschut et al., 2010a)			65	
Pine sawdust	Fixed-bed catalytic reactor	1" ID & 32" long	Sulfide Ru/C, NiMoS, CoMoS, NiMoS/C, CoMoS/C, CoMoS/Al <sub>2</sub> O <sub>3</sub>	150-450	138	LHSV=0.19	(Elliott et al., 2012)			35-45	
Pinewood	Batch autoclave	100ml	Rh/ZrO <sub>2</sub> Pd/ZrO <sub>2</sub> Pt/ZrO <sub>2</sub> RhPt/ZrO <sub>2</sub> RhPd/ZrO <sub>2</sub> PdPt/ZrO <sub>2</sub> CoMo/Al <sub>2</sub> O <sub>3</sub>	350	35		(Ardiyanti et al., 2011)			37-47	

Feedstock	Reactor Type	Reactor Dimension	Catalyst Used	Temperature °C	Pressure bar	SV(h <sup>-1</sup> )	Reference	HHV MJ kg <sup>-1</sup>	HDO (wt%)	Oil Yield (wt%)	pH
Sawdust from Pinus insignis	Fixed-bed	9mm ID	HZSM-5	400,450 &500	1.01	WHSV = 0.237 & 0.474	(Gayubo et al., 2004)				
Eucalyptus & hybrid poplar	Continuous feed fixed bed		NiMo/Al <sub>2</sub> O <sub>3</sub> &CoMo/Spinel	355-365		WHSV = 0.54-0.7	(Elliott & G., 1996)		90-96	40-53	
Rice husk	Autoclave	100ml	Aluminum silicate	260	78		(Peng et al., 2008)	21			6
Sawdust	Autoclave	500 ml	Sulfided CoMoP/γAl <sub>2</sub> O <sub>3</sub>	340-400	1.6-2.8		(Zhang et al., 2005)	41.4		60-75	

**Table 2-6. Summary of operating conditions for hydroprocessing model compounds in bio-oil**

Model Compound	Reactor Type	Reactor Dimension	Catalyst Used	Temperature °C	Pressure bar	SV(h <sup>-1</sup> )	Reference	HDO (wt%)	Oil Yield (wt%)
Benzofuran	Fixed-bed	4 mm i.d.	Sulfided Ni-Mo/ $\gamma$ Al <sub>2</sub> O <sub>3</sub>	200-320	35		( <a href="#">Bunch et al., 2007</a> )		
Guaiacol	Fixed-bed tabular		MoS <sub>2</sub> , CoMoS, MoS <sub>2</sub> / $\gamma$ Al <sub>2</sub> O <sub>3</sub> , CoMoS/ $\gamma$ Al <sub>2</sub> O <sub>3</sub>	300	40		( <a href="#">Bui et al., 2011a</a> )		
Phenol and substituted phenol	Conversion		CoMo/ $\gamma$ Al <sub>2</sub> O <sub>3</sub>	250-400	3.0 - 8.2		( <a href="#">Ahmad et al., 2010</a> )		
Guaiacol, Cresol, Dibenzofuran	Continuous flow fixed-bed	10mm ID & 420mm long	Pt/ $\gamma$ Al <sub>2</sub> O <sub>3</sub> & Pt/MZ-5 (MZ-mesoporous zeolite)	200	40	LHSV = 2,4,6	( <a href="#">Wang et al., 2012</a> )		
Phenol	Parr autoclave	100ml	Ru/C	250	100		( <a href="#">Wildschut et al., 2010a</a> )		55
Guaiacol	Batch reactor		Mo <sub>2</sub> N/C	300	50		( <a href="#">Sepúlveda et al., 2011</a> )		
D-Glucose, D-Cellobiose, D-Sorbitol	Batch autoclave	100ml	Ru/C	250	100		( <a href="#">Wildschut et al., 2009a</a> )		61%
Anisole	Continuous fixed bed	3mm ID	Ni-Cu/ $\gamma$ Al <sub>2</sub> O <sub>3</sub>	300	10	WHSV = 3-6	( <a href="#">Ardiyanti et al., 2012a</a> )	70-98	
2-ethylphenol	Fixed-bed	1,25cm ID & 40cm long	Mo/ $\gamma$ Al <sub>2</sub> O <sub>3</sub> , CoMo/ $\gamma$ Al <sub>2</sub> O <sub>3</sub> , NiMo/ $\gamma$ Al <sub>2</sub> O <sub>3</sub>	340	70		( <a href="#">Romero et al., 2010</a> )		
Phenol	Micro reactor system	14ml	CoMo/MgO, CoMoP/MgO	300-450	50		( <a href="#">Yang et al., 2009</a> )		

Model Compound	Reactor Type	Reactor Dimension	Catalyst Used	Temperature °C	Pressure bar	SV(h <sup>-1</sup> )	Reference	HDO (wt%)	Oil Yield (wt%)
Phenol	Bench-scale fixed-bed catalytic	9mm ID & 300mm long	Ni-W/C	150-300	15	WHSV – 0.5	( <u>Echeandia et al., 2010</u> )	85-98	
Methyl substituted phenol	Batch autoclave	300cm <sup>3</sup>	CoMo/ $\gamma$ Al <sub>2</sub> O <sub>3</sub>	300	50		( <u>Gevert et al., 1987</u> )		
Guaiacol	Stainless steel batch	40 ml	Rh/ZrO <sub>2</sub> , Pd/ ZrO <sub>2</sub> , Pt/ ZrO <sub>2</sub> , RhPt/ ZrO <sub>2</sub> , RhPd/ ZrO <sub>2</sub> , PtPd/ ZrO <sub>2</sub>	100 & 300	80		( <u>Gutierrez et al., 2009</u> )		

Ardiyanti et al. (2011) investigated mono- and bimetallic noble catalysts (Pt, Pd, and Rh) on zirconia support for the catalytic hydrotreatment of bio-oil. The results were compared with the traditional sulfided CoMo catalyst. Among noble metals, Pd showed the highest activity, followed by Rh, with Pt having the lowest due to incomplete reduction at the time of reaction. Ardiyanti et al. (2011) reported the activity based on hydrogen uptake as follows:

Pd/ZrO<sub>2</sub> > Rh/ZrO<sub>2</sub> > RhPd//ZrO<sub>2</sub> ≈ PdPt/ZrO<sub>2</sub> > RhPt/ZrO<sub>2</sub> > Pt/ZrO<sub>2</sub> > CoMo/Al<sub>2</sub>O<sub>3</sub>

There is not much difference in oil yield for a bimetallic catalyst as compared to a monometallic one. The extent of leaching determined for metal and support were done by inductively coupled plasma-optical emission spectroscopy ICP-OES. Ardiyanti et al. (2011) observed that with a sulfided CoMo on an alumina catalyst, Co and Al leached to the aqueous phase after reaction, whereas leaching was negligible for noble metal catalysts.

Venderbosch et al. (2010) studied Ru supported on C to stabilize the bio-oil for mild hydrotreating, which is the first step in hydroprocessing. The coke-formation tendency of this stabilized oil is comparatively low compared to the non-stabilized oil. The same Ru on a C catalyst has also been tested by Wildschut et al. (2010a) for the hydrotreatment of fast bio-oil from beech wood in a batch reactor. The effect of reaction time on oil yield and elemental composition of product phases was studied. It was inferred that an increase in reduction time leads to a significant decrease in oil yield due to transformation during the liquid phase to the gaseous phase (Wildschut et al., 2010a).

Figure 2.6 presents the results from another study of noble metal catalysts. These outcomes were compared with the benchmark catalyst study by Wildschut et al. (2009b). Ru/C, Ru/TiO<sub>2</sub>, Ru/Al<sub>2</sub>O<sub>3</sub>, Pd/C, and Pt/C were tested during beech wood oil hydroprocessing in an autoclave following a reaction time of 4h for noble metal catalysts. Three different phases of liquid were reported: a slightly yellow aqueous phase, an oil phase with a density higher than that of water (top oil), and an oil phase with density lower than water (bottom oil). The top oil had a better H/C and O/C ratio than the bottom oil phase. Pd/C appeared better in terms of oil yield and oxygen

content, followed by Ru/C. Both Pd/C and Ru/C performed comparatively far better than the benchmark catalysts (Wildschut et al., 2009b).

The outcome of Pd metal supported on C was investigated by Elliott et al. (2012) for a range of bio-oils. The bio-oil was obtained from various mixed wood feedstocks in a bench-scale continuous-flow fixed-bed reactor for reaction times varying from 8-102 h. The oxygen content in the upgraded oils from different feedstock was reduced to 0-1 wt% from 40-60 wt%.

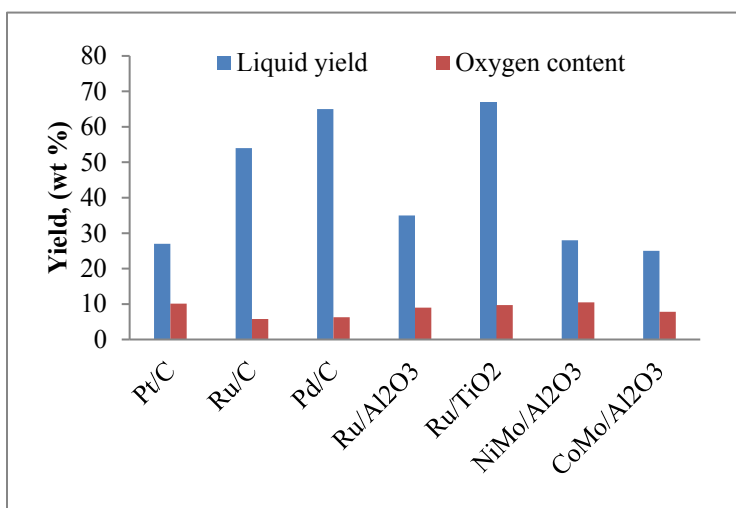


**Figure 2.6. Performance of noble metal catalysts and benchmark catalysts for liquid (oil) yield and oxygen content in oil yield.**

In summary, noble metals (Rh, Ru, Pd, and Pt) are most promising catalysts for the hydroprocessing of bio-oil obtained from lignocellulosic biomass than the traditional sulfide NiMo/CoMo catalyst supported on gamma alumina. For the benchmark catalyst, metal loading is considerably higher (more than 10 times) than the metal loading for a noble metal catalyst. But the activity on a per gram catalyst basis is higher for noble metals than for benchmark ones by a factor of two (Ardiyanti et al., 2011). Noble metals have a high selectivity for hydrogenation reactions and require more hydrogen, which in turn raises the operating cost. Noble metals can be easily

poisoned by small amounts of sulfur compounds present in bio-oil, and these are expensive. These reasons make them unattractive for the hydroprocessing technique.

### 2.5.1.3 Inexpensive transition metals

Although it is difficult to replace a noble metal catalyst in terms of performance, different researchers have tried various alternatives. A series of inexpensive transition metals was tested in hydroprocessing experiments in different reactor systems. Echeandia et al. (2010) studied a Ni-W catalyst supported on active C for the HDO of phenol in a bench-scale fixed-bed catalytic reactor with a hydrogen flow of  $2.5 \text{ l h}^{-1}$  and a reaction time of 4 h. They (Echeandia et al., 2010) also studied the effect of W precursors (silicotungstic [SI], phosphotungstic [P], and tungstic acid [W]). Total elimination of oxygen compounds was reported at 573 K over Ni-W(P)/C and Ni-W(SI)/C catalysts. The synergistic effect between Ni and W supported on C reduced the catalyst deactivation during the reaction. Another study of a Ni-based catalyst, for bio-oil obtained from pine wood, was carried out by Ardiyanti et al. (2012b) in a batch reactor. The study's results in terms of catalyst activity are as follows:

$\text{NiCu/TiO}_2 > \text{NiCu}/\delta\text{-Al}_2\text{O}_3 > \text{NiCu/CeO}_2\text{-ZrO}_2 > \text{NiCu/ZrO}_2$

NiCu/TiO<sub>2</sub> catalysts showed the best performance in terms of hydrogen uptake, stability, and catalyst activity, but leaching and coke formation were significant for these catalysts compared to noble metal catalysts.

Ardiyanti et al. (2012a) studied the variation in ratio of Ni to Cu metal loading on delta alumina support in a batch autoclave for the hydroprocessing of bio-oil obtained from pine wood for a reaction time of 4 h. They reported the activity of catalysts as follows:

$\text{Ru/C} > 16\text{Ni}2\text{Cu} > 13.8\text{Ni}6.83\text{Cu} > 13.3\text{Ni}11.8\text{Cu} > 9.92\text{Ni}18.2\text{Cu}$

The activity of these catalysts decreased with an increase in Cu content as Ni is excellent for HDO. But leaching and coking tendencies were improved considerably during reaction. It should be noted here that the viscosity of the upgraded oil was higher than the original bio-oil (Baldauf et al., 1994; Bartholomew, 2001; Forzatti & Lietti, 1999; Wildschut et al., 2009a).

In summary, for the upgrading of bio-oil from lignocellulosic biomass, both benchmark sulfided NiMo/CoMo supported on alumina and transition metal catalysts are available. The ideal selection of proper catalysts for different feedstocks is still in debate. Research is required to learn the properties and morphology of catalysts to determine the most suitable catalyst.

#### *2.5.1.4 Catalyst support*

Support is an important part of a catalyst system in the hydroprocessing of bio-oil. Alumina, carbon, TiO<sub>2</sub>, ZrO<sub>2</sub>, and CeO<sub>2</sub> are generally used as carriers (Ardiyanti et al., 2011; Ardiyanti et al., 2012b; Bui et al., 2011b; de la Puente et al., 1999; Ferrari et al., 2002a; Gutierrez et al., 2009). Alumina has been widely used in the oil upgrading industry to remove S from crude oil. Therefore, many authors have tried to use gamma alumina for hydrodeoxygenation in bio-oil upgrading. They found that alumina is susceptible to attack by acidic water at elevated conditions and later its reaction with water leads to a reduction of surface area (Laurent & Delmon, 1994a). At the time of reaction, promoters such as Ni/Co can react with Al<sub>2</sub>O<sub>3</sub> as it is not inert and can occupy the octahedral or tetrahedral sites in the external layers depending on the catalyst preparation conditions (Laurent & Delmon, 1993). This strong interaction between promoter and support reduces the dispersion of the Mo sulfide phase, which lowers the activity of the HDO. Further, the crystalline phase of gamma alumina converts to the boehmite phase, which is useless for this reaction (Wildschut et al., 2009b). Another problem for gamma alumina is the viscosity of the upgraded oil, which is higher than the original bio-oil. The higher viscosity affects the product quality and quantity because of the oil's tendency to stick to the walls, plates, impeller, and piping of the reactor, thereby reducing the reactor's efficiency. Weak Lewis-type acidic sites on the support surface lead to large coke formation during HDO (de la Puente et al., 1999). Centeno et al. (1995) reported that alumina-supported CoMo catalysts had the highest rate of decarboxylation

and deesterification selectivity for guaiacol hydrodeoxygenation. But at the same time, surface area and pore volume of alumina support decreased with the HDO reaction.

As an alternative, activated carbon has been identified as a promising support for HDO (Echeandia et al., 2010; Ferrari et al., 2001; Ferrari et al., 2002a; Ferrari et al., 2002b; Sepúlveda et al., 2011; Venderbosch et al., 2010; Wildschut et al., 2010a; Wildschut et al., 2009b). Compared to gamma alumina, carbon is superior in terms of textural properties (surface area, meso- and microporosity, pore volume), thermal stability, and hydrophobic nature. Ferrari et al. (2002b) investigated four different kinds of carbon support with different origins for CoMo catalysts: Merck carbon from coconut shells, Norit carbon from chemical activation of wood, and Chemviron and BKK from the thermal treatment of bituminous coal. Even though variation in properties was negligible, the surface area of carbon support varied significantly. Merck and Norit had high surface areas and microporous volumes, followed by Chemviron. The last was BKK, with the most developed non-microporous volume. On the basis of activity of HDO for guaiacol, the order was as follows:

Norit> BKK>Chemviron>Merck

Sepulveda et al. (2011) investigated three different types of commercial carbon support (Norit, Pica, and udu) varying in pore size distribution and micropore/mesopore volume ratios for a Mo<sub>2</sub>N catalyst for the hydrodeoxygenation of 2-methoxyphenol. They also observed that Mo<sub>2</sub>N/Norit had the highest mesopore diameter resulting in the most open porous structure. High mesoporosity in carbon support facilitated reactant diffusion to the internal surface where the active sites were located. Echeandia et al. (2010) reported that adsorption of water on active sites produced from an HDO reaction can be prevented by the hydrophobic nature of carbon support that ultimately reduces the rate of deactivation of catalysts. Carbon remains inert at the time of an HDO reaction, which is a great advantage for transition metals because all transition metals present in precursors will be converted into active sulfide forms. According to Wildschut et al. (), oil yield and degree of hydrodeoxygenation were highest for carbon support. Carbon support also had a low catalyst deactivation due to the neutral nature of carbon. The presence of some impurities like titanium and

strontium in carbon support can change the electronic structure of active sites that might be undesirable for an HDO reaction. The high microporosity is another disadvantage for carbon material because for high molecular weight compounds which remains unused (Sepúlveda et al., 2011).

Silica has been often used for HDO reactions due to its inert character (like carbon) and smaller interaction with the sulfided phase. Popov et al. (2010) studied silica support for the HDO of phenolic molecule and reported that the phenolic compound interacted through H bonding. Phenate formation on a silica surface was very low compared to alumina support, as two-thirds of the surface was covered by phenate compounds.

MgO and ZrO<sub>2</sub> support are also recognized as good basic supports for hydroprocessing reactions (Ardiyanti et al., 2011; Yang et al., 2009). Yang et al. (2009) investigated CoMo catalysts supported on MgO for the hydroprocessing of phenol. They noticed excellent coke resistance for coking reactions for two reasons: first, MoO<sub>3</sub>/MoS<sub>2</sub> was acidic in nature and highly dispersed on the MgO surface due to the basic nature of the support and second, MoO<sub>3</sub>/MoS<sub>2</sub> increased the edge plane area for promoters due to the formation of short edge-bonded MoS<sub>2</sub> slabs. ZrO<sub>2</sub> is identified as an inert material for hydroprocessing reactions. ZrO<sub>2</sub> has high stability towards the coke formation because it is less acidic and has less affinity towards water, which increases the activity of the HDO.

In summary, the selection of the appropriate support for the HDO reaction is required to get the desired product. Coke formation is another point of concern to reduce catalyst deactivation for the reaction. Overall, carbon can be thought of as a promising carrier for this process, with appropriate mesoporosity.

### 2.5.2 *Catalyst deactivation*

Catalyst deactivation is loss of catalyst activity and product selectivity with reaction time, which is considered a great loss for an HDO reaction. The cost to replace and regenerate a catalyst is too expensive for industry. Catalyst deactivation takes place due to six reasons: (1) poisoning due to strong chemisorption of impurities like sulfur and nitrogen to active sites, (2) fouling/coking due to physical deposition of coke onto the surface of the catalyst, (3) thermal degradation/sintering due to collapse of the catalyst and support surface area because of crystallite growth, (4) vapor compound formation accompanied by transport, (5) vapor-solid (catalyst) and/or solid-solid reactions that are reactions of fluid, support, or promoters in the catalytic phase that lead to an inactive phase, and (6) loss of internal pores at the time of attrition/crushing (Bartholomew, 2001; Forzatti & Lietti, 1999). Although these are the reasons for catalyst deactivation, in the literature the most frequent reason cited is coking/fouling (Baldauf et al., 1994; Gevert et al., 1994; Laurent & Delmon, 1994b; Laurent & Delmon, 1994c; Wildschut et al., 2009a).

Carbon and coke are the two main sources of coking. Carbon forms from a Boudouard reaction ( $2\text{CO} \rightleftharpoons 2\text{CO}_2 + \text{C}$ ), where CO dissociates to form carbon on the catalyst surface, and coke is produced from decomposition or condensation of high molecular weight hydrocarbon compounds on the active sites of the metal and support surface. Coke deposits may deactivate the catalyst either by covering the active sites or by pore blocking (Echeandia et al., 2010). The composition of coke (high molecular weight to graphite form) varies depending on the feed composition and reaction conditions. Reactants with two oxygen-containing functional groups in the benzene ring form coke with greater ease than those with one oxygen-containing substituent. Centeno et al. (1995) investigated a sulfided CoMo catalyst-supported gamma alumina for a HDO guaiacol model compound present in bio-oil and observed that coke was produced from the interaction of guaiacol with the gamma- $\text{Al}_2\text{O}_3$  support rather than with the active metals. This is due to acidity, which plays an important role in coking, as Lewis sites are responsible for binding species to the catalyst surface and Bronsted sites donate protons to the deposited species to form carbonaceous materials. But other supports, like activated carbon and  $\text{ZrO}_2$ , remain inert at the time of HDO; therefore, coking is comparatively low relative to gamma support (Ardiyanti et al., 2011; Ardiyanti et al., 2012b; Bui et al., 2011b; Echeandia et al., 2010).

In a traditional catalyst, Ni is used as a promoter to accelerate the activity of Mo. But Ni tends to form coke at high temperatures, and coking tendency increases with reaction time. Ardiyanti et al. (2012b) reported that the viscosity of the upgraded oil was more than that of the original bio-oil due to the formation of high molecular weight compounds that further converted to coke on the catalyst surface.

Coking is not a big problem in noble metal catalysts as they are mostly affected by sintering. As bio-oil produced from biomass is not completely free from sulfur and nitrogen, sulfur and nitrogen compounds act as impurities for these metals. As chemisorption of sulfur compounds on the catalyst surface is rapid and irreversible, sulfur compounds make the catalyst inactive for HDO. Ardiyanti et al. (2011) studied catalyst deactivation for Rh-based catalysts for a reaction time of 4 h. Deposition of carbonaceous materials after 1 h (2.6 wt%) was similar to after 4 h (2.7 wt%). The reason was high polymerization and char formation at the initial stage of reaction time, but with increased reaction time, the gasification rate of feed was enough to balance the formation of carbonaceous deposits while maintaining a constant temperature (Ardiyanti et al., 2011).

The composition of lignocellulosic biomass plays an important role in the deactivation of a catalyst. As bio-oil contains around 40-50 wt% O-containing compounds, some compounds are highly unstable and may readily polymerize to form coke on the catalyst surface (Furimsky, 2000). Coke formation can be reduced by proper selection of the catalyst, support, temperature, and hydrogen pressure during a HDO reaction. The addition of extra hydrogen during the reaction can reduce coke formation by converting unsaturated compounds to a stable saturated molecule.

### 2.5.3 *Temperature*

Temperature is an important controlling factor for the hydroprocessing of bio-oil from lignocellulosic biomass. In terms of temperature, the hydrotreating process is divided into two categories: high-severity hydrotreating or deep HDO, and low-severity hydrotreating or mild HDO. High-severity hydrotreating involves complete hydrodeoxygenation with minimal hydrogenation at temperatures ranging from 350-400 °C and pressures greater than 200 bar (Wildschut et al., 2009b). For low-severity hydrotreating, the temperature is maintained between 175 and 250 °C, and the pressure is greater than 100 bar, with partial hydrodeoxygenation and reasonable hydrogenation to stabilize the unstable bio-oil. A combination of these steps significantly reduces the oxygen content of bio-oil.

In mild HDO, crude bio-oil becomes more stable through the removal or transfer of unstable compounds to stable ones (Elliott, 1998). Acetic acid makes bio-oil unstable. But there is no significant change in oxygen content and viscosity in the upgraded oil. The dominating reaction in mild HDO is the hydrogenation of carbon-carbon double bond with the partial HDO of aldehydes and ketones. Due to complete hydrodeoxygenation at a deep HDO condition, upgraded bio-oil contains low concentrations of oxygen. But hydrogen consumption increases significantly with the complete removal of oxygen molecules (Wildschut et al., 2009b).

Wildschut et al. (2009b) studied the hydroprocessing of bio-oil from beech wood using noble metal carbon-supported catalysts at both low-severity (250 °C) and high-severity hydrotreating (350 °C) temperature conditions. They reported that the yield of both oil and gaseous components increased significantly with a decrease in char yield when the temperature increased from 250 to 350 °C. The reason for the increase in liquid yield at high temperatures is due to a complete HDO reaction, which requires excess hydrogen. The excess hydrogen and the carbon dioxide that forms during decarboxylation increases the gas phase concentration at high temperatures (Wildschut et al., 2009b). Figure 2.7 shows the oxygen content of upgraded bio-oil for beech wood after low- and high-severity hydrotreating. It was found that after high-severity hydrotreating, the oxygen content decreased significantly from the initial value of 42 wt% in the original bio-oil.

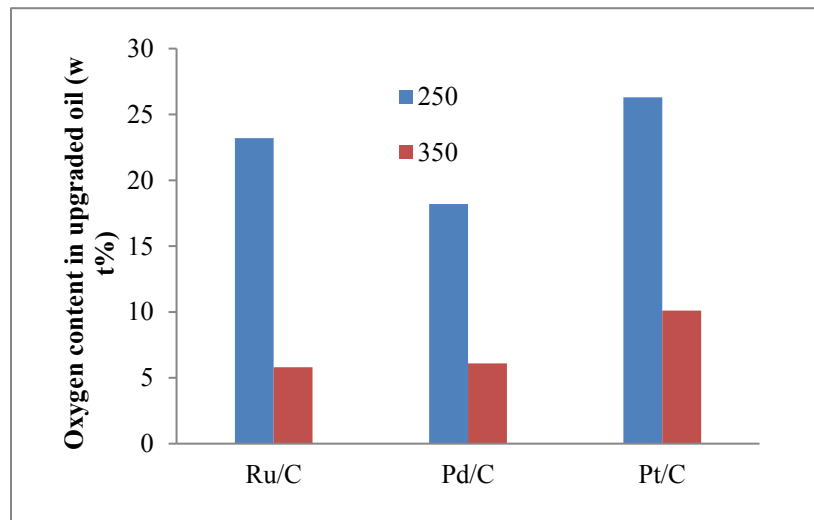


**Figure 2.7. The effect of temperature on the performance of noble metal carbon-supported catalysts.**

In another study, Wildschut and co-workers reported that at high-severity hydrotreating conditions, CO<sub>2</sub> was the dominating gaseous component in the gaseous phase due to unfavorable decarboxylation reactions at high temperatures (Wildschut et al., 2010b). A methanation reaction also started at high temperatures, a reaction not observed at low temperatures.

Zhang et al. (2005) investigated the effect of temperature on the HDO of bio-oil from sawdust in a 500 ml autoclave using a sulfided Co–Mo–P catalyst. Figure 2.8 shows the effect of temperature on liquid, char, and gas yield. Oil yield was low at low temperatures and increased with temperature, but after a certain temperature there was no change in yield. The yield of char and gaseous components was dependent on the temperature. Char yield decreased with a rise in temperature because at low temperatures unstable components were deposited as char due to low volatility, and gaseous components increased with temperature.

In summary, the HDO of bio-oil is affected to a large extent by temperature. As temperature increases with time, the degree of deoxygenation changes and significantly reduces the oxygen

concentration in bio-oil. At high temperatures, coke formation on the catalyst surface could be a main concern and needs more attention.

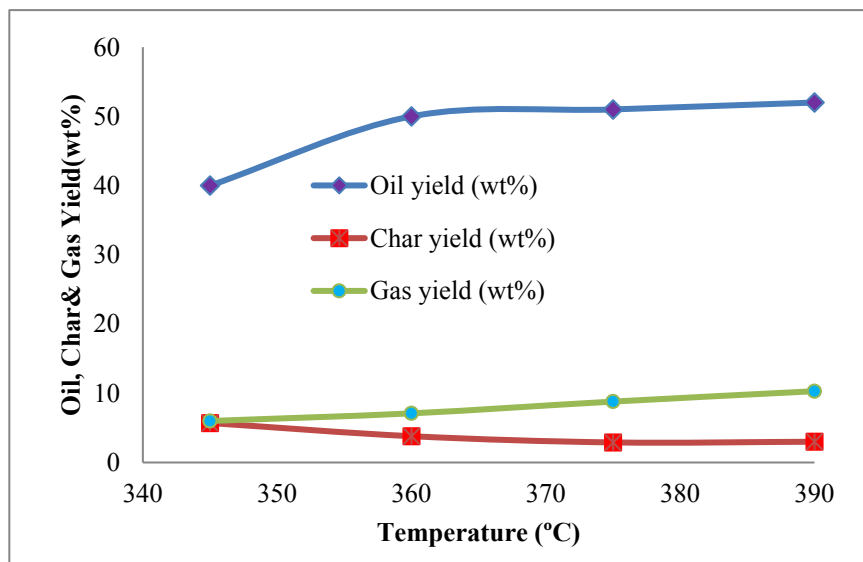


Figure 2.8. The effect of temperature on oil, char, and gas yield for the HDO of bio-oil from sawdust.

## 2.6 Techno-economic analysis of the fast pyrolysis process

An investigation of the technical and economic aspects of a technology is mandatory to commercialize it. The principal means of evaluating a new technology is a techno-economic assessment. While fast pyrolysis is a well-established and understood technology at both the pilot and commercial scale, most techno-economic studies of are from the mid to late 1980s. In 1992, Solantausta et al. (1992) summarized the experimental developments in biomass liquefaction and pyrolysis systems and carried out techno-economic studies for different feedstocks (wood, peat, and straw) for a 1000 t d<sup>-1</sup> plant. The data used for these techno-economic analyses were taken from experimental work done by the International Energy Agency (IEA) Biomass Agreement liquefaction activities from 1983 to 1991. The IEA estimated bio-oil production costs of 117 \$ t<sup>-1</sup>-488 \$ t<sup>-1</sup> for different feedstocks and IEA concluded that pyrolysis processes offered better

potential than the high-pressure liquefaction technology. Gregoire and Bain (Gregoire & Bain, 1994a) did a techno-economic assessment of the production of biocrude from wood chips for a 1000 t d<sup>-1</sup> plant. The selling price of bio-oil was 0.11 \$ kg<sup>-1</sup> for a 15% after tax internal rate of return. They also performed a sensitivity analysis on the process and economic parameters to understand the effects on plant profitability and concluded that financing method, feedstock cost, plant location, plant capacity, and depreciation method were the most important parameters. Ringer et al. (2006a) carried out a detailed technical and economic assessment of bio-oil production from commercial pine wood chips. They developed an Aspen Plus<sup>®</sup> model that included feedstock preparation, fast pyrolysis, and steam and power generation processes and reported the cost of bio-oil to be 7.62 \$ GJ<sup>-1</sup> on a lower heating value basis for a 550 t d<sup>-1</sup> plant (Ringer et al., 2006a). In the UK, Brown et al. (2012a) investigated the production costs of bio-oil from two different energy crops. Their model includes the sale of biochar as a by-product of pyrolysis and concludes that bio-oil production costs from energy crops can be equivalent to distillate fuel oil costs (Rogers & Brammer, 2012a). Staff at the University of New Hampshire researched the technical, environmental, and economic feasibility of bio-oil facility using low-grade wood chips for three different plant capacities: 100, 200, and 400 t d<sup>-1</sup> wet wood. The bio-oil cost was 1.21 \$ gal<sup>-1</sup>, 0.99\$ gal<sup>-1</sup>, and 0.89\$ gal<sup>-1</sup> for the three capacities (LaClaire et al., 2004). Table 2.7 summarizes the techno-economic assessment of fast pyrolysis from different feedstocks. The cost of bio-oil is reported in terms of \$ L<sup>-1</sup>. All the cost numbers are adjusted to the 2016 US dollar.

**Table 2-7. Earlier techno-economic analyses of the fast pyrolysis process**

Year	Feedstock	Capacity	Location	Bio-oil cost (\$ L <sup>-1</sup> ) <sup>2</sup>	Bio-oil yield (wt%)	Reference
2015	Wood residue	2316 ton d <sup>-1</sup>	South-western Nigeria	0.26	60	(Popoola et al., 2015)
2013	Willow tree	55 dry t d <sup>-1</sup>	Belgium	0.17	65	(Kuppens et al., 2015)
1998	Rice husk	0.3, 100 and 1000 kg h <sup>-1</sup>	Malaysia	22.47, 0.45 and 0.22		(Islam & Ani, 2000)
2006	Wood chips	550 dry t d <sup>-1</sup>	USA	0.13	60	(Ringer et al., 2006b)
2010	SRC Willow and miscanthus	50-800 dry t d <sup>-1</sup>	UK	0.25-0.5	60-65	(Rogers & Brammer, 2012b)
2002	Low grade wood	100, 200 and 400 t d <sup>-1</sup>	USA	0.32-0.26 and 0.24	72	(Farak et al., 2004)
1992	Wood, peat and straw	1000 dry t d <sup>-1</sup>	USA	0.17-0.40		(Solantausta et al., 1992)
1994	Wood chips	900 dry t d <sup>-1</sup>	NREL, USA	0.17		(Gregoire & Bain, 1994a)

<sup>2</sup> Cost is in 2016 USD.

## 2.7 Techno-economic analysis of hydroprocessing technology

Upgrading bio-oil to a transportation fuel can be done through hydroprocessing, a well-established technology in the refinery industry (Ward, 1993). Hydroprocessing involves two steps: hydrotreating and hydrocracking. Hydroprocessing for bio-oil is still in the demonstration stage and not yet commercialized. Moreover, little has been published on this topic which are summarized in Table 2.8. Wright et al. (2010) did a techno-economic analysis on upgrading bio-oil through the fast pyrolysis of corn stover to naphtha and diesel. They investigated two different scenarios, one in which the hydrogen is purchased and the other in which it was produced, and concluded that it is cheaper to produce of transportation fuel in the first scenario (Wright et al., 2010). Brown et al. (2013) expanded that study by updating the techno-economic analysis of fast pyrolysis and hydroprocessing from the same corn stover feedstock by incorporating recent literature data . They assessed the conversion of corn stover to gasoline and diesel in a 2000 t d<sup>-1</sup> plant and concluded that the fuel produced could be competitive with the petro-fuels (Brown et al., 2013). Zhang et al. (2013) investigated the economic feasibility of two bio-oil upgrading pathways: two-stage hydrotreating followed by fluid catalytic cracking, and single-stage hydrotreating followed by hydrocracking, each for a 2000 t d<sup>-1</sup> facility . They found that the facility employing the first pathway with hydrogen production via natural gas reforming generated a higher internal rate of return (IRR) . In these studies, the authors investigated the production costs of various transportation fuels from corn stover and mixed wood using different upgrading conditions for a 2000 t d<sup>-1</sup> plant capacity. However, the effects of variations in plant capacity on the production costs of transportation fuel are not available in literature

**Table 2-8. Earlier techno-economic analyses of the hydroprocessing technology**

Bio-product	Feedstock	Location	Technology	Capacity (dry tonnes/day)	Base year	Production cost (2014 USD)	Reference
Diesel	Lignocellulosic biomass	Karlsruhe, Germany	Gasification syngas-FT synthesis-diesel		2010	1.72-1.77 \$ L <sup>-1</sup>	(Trippe et al., 2013)
	Coal	Karlsruhe, Germany	Gasification syngas-FT synthesis-diesel		2010	1.09 \$ L <sup>-1</sup>	(Trippe et al., 2013)
gasoline & diesel	Woody biomass	Ames, USA	Mild catalyst pyrolysis	2000	2011	1.03\$ L <sup>-1</sup>	(Thilakaratne et al., 2014)
	Woody biomass	Ames, USA	Mild catalyst pyrolysis with cogeneration of electricity and hydrogen	2000	2011	0.85\$ L <sup>-1</sup>	(Thilakaratne et al., 2014)
	Stover	Ames, USA	Fast pyrolysis + hydroprocessing	2000	2011	0.72\$ L <sup>-1</sup>	(Brown et al., 2013)
naphtha & diesel	Corn stover	Ames, USA	Gasification + Fischer-Tropsch synthesis and hydroprocessing	2000	2007	1.22-1.52\$ L <sup>-1</sup>	(Swanson et al., 2010)
	Corn stover	Ames, USA	Fast pyrolysis + upgrading, with hydrogen generation on-site	2000	2007	0.94\$ L <sup>-1</sup>	(Wright et al., 2010)
	Corn stover	Ames, USA	Fast pyrolysis + upgrading, with merchant hydrogen	2000	2007	0.64\$ L <sup>-1</sup>	(Wright et al., 2010)

## 2.8 Status of HDRD production

Today some companies are paying attention to renewable diesel production – for example, ConocoPhillips (ConocoPhillips; Green Car Congress), Neste Oil (Neste Oil; Neste Oil; Neste Oil), Petrobras in Brazil (BiofuelsDigest) – and others plan to produce renewable diesel, e.g., Nippon Oil in Japan (The University of California Davis & The University of California Berkeley), BP in Australia (BP), and Syntroleum (Syntroleum), Tyson (Tyson), and UOP-Eni in the United States (Honeywell). All the existing companies are using vegetable oil and animal fat as the feedstock for renewable diesel production. ConocoPhillips uses vegetable oil and crude oil, Neste’s plant processes vegetable and animal fats, and Brazilian Petrobras uses co-processed vegetable oils. Table 2.9 summarizes the commercial producers of renewable diesel. However, substantial research is still needed in order for renewable diesel to replace diesel and gasoline on a large scale.

**Table 2-9. Commercial renewable diesel plants**

Company	Plant Location	Capacity	On-Stream	Reference
ConocoPhillips	Cork, Ireland	1000 bbl d <sup>-1</sup>	2006	(Green Car Congress)
Neste Oil	Rotterdam, Netherlands	800,000 t y <sup>-1</sup>	2010	(Neste Oil)
Neste Oil	Singapore	800,00 t y <sup>-1</sup>	2010	(Neste Oil)
Neste Oil	Porvoo, Finland	190000 t y <sup>-1</sup>	2007	(Neste Oil)
Neste Oil	Porvoo, Finland	190000 t y <sup>-1</sup>	2009	(Neste Oil)

## 2.9 Issues with hydroprocessing

### 2.9.1 *Economic analysis*

Economic viability is an important factor for any process when it is compared with a developed process. According to Elliott and Neuenschwander, there are four major cost considerations in bio-oil hydroprocessing: raw bio-oil cost, capital cost, hydrogen cost, and relative product value (Elliott, 1998). A number of techno-economic studies are available on the production of bio-oil from biomass (Cottam & Bridgwater, 1994; Gregoire & Bain, 1994b; Islam & Ani, 2000; Ringer et al., 2006b), but very limited study has been done on the techno-economic assessment of the upgrading of bio-oil using hydroprocessing technologies (Wright et al., 2010). The National Renewable Energy Laboratory (NREL) has completed a techno-economic assessment of bio-oil from corn stover to transportation fuel that includes both naphtha-range and diesel-range distillation fractions (Wright et al., 2010). The NREL did the analysis for two scenarios for bio-oil upgrading through hydroprocessing: on-site hydrogen production and a hydrogen purchase scenario. According to their results, costs were lower in the second scenario due to the difference in capital costs of a hydrogen reforming plant. Production costs of transportation fuels from pyrolysis-derived biofuels are competitive with production costs of other renewable fuels (biodiesel); however, the technology is relatively immature, and so there is a high level of uncertainty. Another techno-economic assessment was done by a team from the Pacific Northwest National Laboratory for the production of diesel and gasoline from hybrid poplar via fast pyrolysis, hydrotreating, and hydrocracking (Jones et al., 2009). The team observed that this method could be financially attractive if the pyrolysis plant was located within an existing refinery in order to reduce the capital costs of the hydrotreating unit and the steam reforming unit.

A stand-alone renewable diesel unit requires a large capital investment as the material required for handling bio-oil is expensive. But the overall cost can be optimized by building the new unit near the existing refineries in order to make use of an existing hydrogen facility, as well as electricity, steam, and a recycle gases management unit (Eco Resources Consultants).

Capital costs for a pyrolysis unit, a hydrotreating unit, and a hydrogen reforming unit contribute approximately 85% of the total costs, and each unit has an equal weight.. There could be a large reduction in capital costs if the hydrotreating unit of an existing refinery is used. As the hydrotreating unit is operated at high pressure and temperature conditions, more care should be taken to determine the space velocity (volumetric flow rate of the feed/volume of the reactor) to reduce the capital cost (Wright et al., 2010).

The cost of the bio-oil is the largest component in the hydrotreating product costs; therefore, the product yield is a primary consideration for process optimization. The composition of renewable diesel varies depending on the composition of the bio-oil. For improved cold-flow properties, we need more short and isomerized alkenes than long-chain alkenes, and these properties depend completely on the elemental composition of the bio-oil.

Hydrogen also makes up a significant portion of the total cost. The optimization of hydrogen could be done following careful study of reaction mechanisms of different oxygenate compounds, where hydrogen is consumed in excess amounts. Unstable compounds such as acetic acid, olefins, etc., could be removed before hydrotreating (Wright et al., 2010).

### 2.9.2 *Gaps in knowledge*

More experimental work is required to determine optimal operating conditions, e.g., catalyst, catalyst deactivation, temperature and pressure in the hydroprocessing unit, to control product yield. The reactor configuration plays an important role in reaction rates and mass transfer of feed. Channeling, clogging, and entrainment are major problems in reactors due to uneven distribution of materials. Selection of proper metal and support is important to reduce catalyst deactivation, which is reported as the main concern in this upgrading process.

Carbon deposition on a noble metal catalyst is comparatively lower than on the benchmark catalyst (gamma alumina-supported sulfide NiMo/CoMo catalyst), but a noble metal catalyst is affected

by small concentrations of sulfur present in feedstock and highly expensive compared to transition metal catalysts. Due to the acidic nature of gamma alumina, gamma alumina is not so effective for this process compared to activated carbon and MgO, which remain inert throughout the reaction. Therefore, the optimization of metal and the support system is required to get catalysts that are technically and economically feasible.

Temperature is another key operating parameter for the hydroprocessing process in the elimination of oxygen compounds in order to increase the heating value of renewable diesel. At high temperatures and pressures, the concentration of oxygen is reduced significantly, from 40-50 wt% to 3-8 wt%, but high temperature hydroprocessing is associated with high hydrogen consumption and low oil yield. Therefore more research is required to optimize the relationship between hydrogen consumption, oil yield, and temperature, given that oil yield and hydrogen consumption significantly affect the costs of crude bio-oil and hydrogen production. In other words, optimization of operating conditions is necessary for better product yield.

More research is required in production of renewable diesel from lignocellulosic biomass to make this economically feasible.

## **2.10 Conclusions**

Biomass-derived biofuels have the potential to replace fossil fuels and are the only renewable carbon resource that has a short production cycle and is carbon neutral. Among all biofuels, renewable diesel is the only fuel that can directly replace petro-diesel with one of a more superior quality than the minimum diesel standard requirement decided by fuel regulators. Commercialization of renewable diesel is yet to be attained due to the following technological gaps and economic disparities.

- Technological gaps include the consideration of bio-oil composition from different feedstocks, catalyst selection, and the temperature of the hydroprocessing process. The

oxygen content of bio-oil makes hydroprocessing more challenging, so effort should be put toward reducing the oxygen content in bio-oil before it is put into the hydrotreater.

- Catalytic pyrolysis should be implemented in place of non-catalytic pyrolysis to reduce the oxygen content and stabilize the bio-oil before further processing.
- More research should be done in the area of catalyst regeneration and recycling to increase the lifetime of catalysts.
- A process can be practically feasible if it is economically sound; however, studies on costs are lacking. Work on different feedstocks ought to be carried out to support the development of large-scale processes.
- Although several challenges are associated with hydroprocessing, several factors, such as environmental concerns, population rise, and depletion of fossil fuels, need attention so that energy can be directed toward renewable diesel serving as a transportation fuel to fulfill our future needs. Hence this topic will continue to be one of the most energetic topics of research until bio-oil is commercialized.

## References

- Ahmad, M.M., Nordin, M.F., Azizan, M.T. 2010. Upgrading of bio-oil into high-value hydrocarbons via hydrodeoxygenation. *American Journal of Applied Sciences*, **7**(6), 746-755.
- Antizar-Ladislao, B., Turrion-Gomez, J.L. 2008. Second-generation biofuels and local bioenergy systems. *Biofuels Bioproducts & Biorefining-Biofpr*, **2**(5), 455-469.
- Ardiyanti, A.R., Gutierrez, A., Honkela, M.L., Krause, A.O.I., Heeres, H.J. 2011. Hydrotreatment of wood-based pyrolysis oil using zirconia-supported mono- and bimetallic (Pt, Pd, Rh) catalysts. *Applied Catalysis A: General*, **407**(1–2), 56-66.
- Ardiyanti, A.R., Khromova, S.A., Venderbosch, R.H., Yakovlev, V.A., Heeres, H.J. 2012a. Catalytic hydrotreatment of fast-pyrolysis oil using non-sulfided bimetallic Ni-Cu catalysts on a  $\delta$ -Al<sub>2</sub>O<sub>3</sub> support. *Applied Catalysis B: Environmental*, **117–118**(0), 105-117.
- Ardiyanti, A.R., Khromova, S.A., Venderbosch, R.H., Yakovlev, V.A., Melián-Cabrera, I.V., Heeres, H.J. 2012b. Catalytic hydrotreatment of fast pyrolysis oil using bimetallic Ni–Cu catalysts on various supports. *Applied Catalysis A: General*, **449**(0), 121-130.
- Azargohar, R., Jacobson, K.L., Powell, E.E., Dalai, A.K. 2013. Evaluation of properties of fast pyrolysis products obtained, from Canadian waste biomass. *Journal of Analytical and Applied Pyrolysis*, **104**(0), 330-340.
- Baldauf, W., Balfanz, U., Rupp, M. 1994. Upgrading of flash pyrolysis oil and utilization in refineries. *Biomass and Bioenergy*, **7**(1-6), 237-244.
- Bartholomew, C.H. 2001. Mechanisms of catalyst deactivation. *Applied Catalysis A: General*, **212**(1–2), 17-60.
- Berkeley Biodiesel. Advantages and Disadvantages of Biodiesel Fuel, <http://www.berkeleybiodiesel.org/advantages-and-disadvantages-of-biodiesel.html>, Accessed: September 2013.
- Bezergianni, S., Dimitriadis, A. 2013. Comparison between different types of renewable diesel. *Renewable and Sustainable Energy Reviews*, **21**(0), 110-116.
- BiofuelsDigest. The lowdown on making jet fuel and diesel from biomass, <http://www.biofuelsdigest.com/bdigest/2012/08/31/the-lowdown-on-making-jet-fuel-and-diesel-from-biomass/>. Accessed: October 2013.

- Bothast, R.J., Schlicher, M.A. 2005. Biotechnological processes for conversion of corn into ethanol. *Applied Microbiology and Biotechnology*, **67**(1), 19-25.
- BP. Biofuels, <http://www.bp.com/sectiongenericarticle.do?categoryId=9026466&contentId=7048815>. Accessed: October 2013.
- Bridgwater, A.V. 1999. Principles and practice of biomass fast pyrolysis processes for liquids. *Journal of Analytical and Applied Pyrolysis*, **51**(1–2), 3-22.
- Bridgwater, A.V. 2003. Renewable fuels and chemicals by thermal processing of biomass. *Chemical Engineering Journal*, **91**(2–3), 87-102.
- Bridgwater, A.V. 2012. Review of fast pyrolysis of biomass and product upgrading. *Biomass and Bioenergy*, **38**(0), 68-94.
- Bridgwater, A.V., Meier, D., Radlein, D. 1999. An overview of fast pyrolysis of biomass. *Organic Geochemistry*, **30**(12), 1479-1493.
- Brown, T.R., Thilakaratne, R., Brown, R.C., Hu, G. 2013. Techno-economic analysis of biomass to transportation fuels and electricity via fast pyrolysis and hydroprocessing. *Fuel*, **106**, 463-469.
- Bu, Q., Lei, H., Zacher, A.H., Wang, L., Ren, S., Liang, J., Wei, Y., Liu, Y., Tang, J., Zhang, Q., Ruan, R. 2012. A review of catalytic hydrodeoxygenation of lignin-derived phenols from biomass pyrolysis. *Bioresource Technology*, **124**(0), 470-477.
- Bui, V.N., Laurenti, D., Afanasiev, P., Geantet, C. 2011a. Hydrodeoxygenation of guaiacol with CoMo catalysts. Part I: Promoting effect of cobalt on HDO selectivity and activity. *Applied Catalysis B-Environmental*, **101**(3-4), 239-245.
- Bui, V.N., Laurenti, D., Delichere, P., Geantet, C. 2011b. Hydrodeoxygenation of guaiacol Part II: Support effect for CoMoS catalysts on HDO activity and selectivity. *Applied Catalysis B-Environmental*, **101**(3-4), 246-255.
- Bunch, A.Y., Wang, X., Ozkan, U.S. 2007. Hydrodeoxygenation of benzofuran over sulfided and reduced Ni–Mo/ $\gamma$ -Al<sub>2</sub>O<sub>3</sub> catalysts: Effect of H<sub>2</sub>S. *Journal of Molecular Catalysis A: Chemical*, **270**(1–2), 264-272.
- Canadian Renewable Fuels Association. Federal Programs, <http://www.greenfuels.org/en/public-policy/federal-programs.aspx>, Accessed: September 2013.

- CBCnews. Researcher aims to create biofuel from pulp waste, <http://www.cbc.ca/news/canada/thunder-bay/researcher-aims-to-create-biofuel-from-pulp-waste-1.1197581>. Accessed: October 2013.
- Centeno, A., Laurent, E., Delmon, B. 1995. Influence of the Support of CoMo Sulfide Catalysts and of the Addition of Potassium and Platinum on the Catalytic Performances for the Hydrodeoxygenation of Carbonyl, Carboxyl, and Guaiacol-Type Molecules. *Journal of Catalysis*, **154**(2), 288-298.
- ConocoPhillips. Who We Are, <http://www.conocophillips.com/who-we-are/our-legacy/history/Pages/1990-Present.aspx>. Accessed: September 2013.
- Cottam, M.L., Bridgwater, A.V. 1994. Techno-economic modelling of biomass flash pyrolysis and upgrading systems. *Biomass and Bioenergy*, **7**(1-6), 267-273.
- Czernik, S., Bridgwater, A.V. 2004. Overview of Applications of Biomass Fast Pyrolysis Oil. *Energy & Fuels*, **18**(2), 590-598.
- Dakar, M. Challenges of Ethanol Lignocellulosic Production from Biomass, <http://www.katzen.com/ethanol101/Lignocellulosic%20Biomass.pdf>. Accessed: October 2013.
- de la Puente, G., Gil, A., Pis, J.J., Grange, P. 1999. Effects of support surface chemistry in hydrodeoxygenation reactions over CoMo/activated carbon sulfided catalysts. *Langmuir*, **15**(18), 5800-5806.
- Decanio, E.C., Edwards, J.C., Scalzo, T.R., Storm, D.A., Bruno, J.W. 1991. FT-IR and solid-state NMR investigation of phosphorus promoted hydrotreating catalyst precursors. *Journal of Catalysis*, **132**(2), 498-511.
- Demirbaş, A. 2001. Biomass resource facilities and biomass conversion processing for fuels and chemicals. *Energy Conversion and Management*, **42**(11), 1357-1378.
- Department of Energy, U.S. Biodiesel, <http://www.fueleconomy.gov/feg/biodiesel.shtml>. Accessed: September 2013.
- Dias, M.O.S., Modesto, M., Ensinas, A.V., Nebra, S.A., Filho, R.M., Rossell, C.E.V. 2011. Improving bioethanol production from sugarcane: evaluation of distillation, thermal integration and cogeneration systems. *Energy*, **36**(6), 3691-3703.
- Diffen. Hardwood vs Softwood, [http://www.diffen.com/difference/Hardwood\\_vs\\_Softwood](http://www.diffen.com/difference/Hardwood_vs_Softwood). Accessed: September 2013.

- Echeandia, S., Arias, P.L., Barrio, V.L., Pawelec, B., Fierro, J.L.G. 2010. Synergy effect in the HDO of phenol over Ni–W catalysts supported on active carbon: Effect of tungsten precursors. *Applied Catalysis B: Environmental*, **101**(1–2), 1-12.
- ECN Phyllis2. ECN Phyllis classification, <https://www.ecn.nl/phyllis2/Browse/Standard/ECN-Phyllis>. Accessed: October 2013.
- Eco Resources Consultants. Study of Hydrogenation Derived Renewable Diesel as a Renewable Fuel Option in North America, [http://oee.nrcan.gc.ca/sites/oee.nrcan.gc.ca/files/files/pdf/transportation/alternative-fuels/resources/pdf/HDRD\\_Final\\_Report\\_eng.pdf](http://oee.nrcan.gc.ca/sites/oee.nrcan.gc.ca/files/files/pdf/transportation/alternative-fuels/resources/pdf/HDRD_Final_Report_eng.pdf). Accessed: October 2013.
- Elliott, D.C., G., N.G. 1996. *Developments in thermochemical biomass conversion. First Edition ed.* Kluwer Academic Publishers, London, UK.
- Elliott, D.C., Hart, T.R., Neuenschwander, G.G., Rotness, L.J., Olarte, M.V., Zacher, A.H., Solantausta, Y. 2012. Catalytic Hydroprocessing of Fast Pyrolysis Bio-oil from Pine Sawdust. *Energy & Fuels*, **26**(6), 3891-3896.
- Elliott, D.C., Neuenschwander, G.G. 1998. Liquid fuels by low-severity hydrotreating of biocrude. *Fuel and Energy Abstracts*, **39**(4), 259.
- Elliott, D.C.a.N., G. G. 1998. Liquid fuels by low-severity hydrotreating of biocrude. *Fuel and Energy Abstracts*, **39**(4), 259.
- Environment Canada. Federal Renewable Fuels Regulations: Overview, <http://www.ec.gc.ca/energie-energy/default.asp?lang=En&n=828C9342-1>, Accessed: September 2013
- Environment News Service. Canada Requires Two Percent Renewable Diesel Fuels 2011, <http://www.ens-newswire.com/ens/feb2011/2011-02-14-01.html>. Accessed September 2013.
- Environmental Issues. What are the Drawbacks of Using Ethanol?, [http://environment.about.com/od/ethanolfaq/f/ethanol\\_problem.htm](http://environment.about.com/od/ethanolfaq/f/ethanol_problem.htm), Accessed: September 2013.
- Environmental Protection Agency U.S. General Overview of What's In America's Trash, <http://www.epa.gov/osw/wycd/catbook/what.htm>. Assessed September 2013.

- Environmental Protection Agency U.S. Municipal Solid Waste in the United States, <http://www.epa.gov/wastes/nonhaz/municipal/pubs/msw2009rpt.pdf>, Accessed: September 2013.
- EuroBioRef. Conversion of cellulose, hemicellulose and lignin into platform molecules: biotechnological approach, [http://www.eurobioref.org/Summer\\_School/Lectures\\_Slides/day3/Lectures/L06\\_A.Frolander.pdf](http://www.eurobioref.org/Summer_School/Lectures_Slides/day3/Lectures/L06_A.Frolander.pdf). Accessed: October 2013.
- Farag, I.H., LaClaire, C.E., Barrett, C.J. 2004. Technical, environmental and economic feasibility of bio-oil in new hampshire's north country. University of New Hampshire.
- Ferrari, M., Bosmans, S., Maggi, R., Delmon, B., Grange, P. 2001. CoMo/carbon hydrodeoxygenation catalysts: influence of the hydrogen sulfide partial pressure and of the sulfidation temperature. *Catalysis Today*, **65**(2-4), 257-264.
- Ferrari, M., Delmon, B., Grange, P. 2002a. Influence of the active phase loading in carbon supported molybdenum-cobalt catalysts for hydrodeoxygenation reactions. *Microporous and Mesoporous Materials*, **56**(3), 279-290.
- Ferrari, M., Delmon, B., Grange, P. 2002b. Influence of the impregnation order of molybdenum and cobalt in carbon-supported catalysts for hydrodeoxygenation reactions. *Carbon*, **40**(4), 497-511.
- Forzatti, P., Lietti, L. 1999. Catalyst deactivation. *Catalysis Today*, **52**(2-3), 165-181.
- Furimsky, E. 2000. Catalytic hydrodeoxygenation. *Applied Catalysis A: General*, **199**(2), 147-190.
- Gagnon, J., Kaliaguine, S. 1988. Catalytic Hydrotreatment of Vacuum Pyrolysis Oils from Wood. *Industrial & Engineering Chemistry Research*, **27**(10), 1783-1788.
- Galletti, A.M.R., Antonetti, C. Biomass pre-treatment: separation of cellulose, hemicellulose and lignin. Existing technologies and perspectives, [http://www.eurobioref.org/Summer\\_School/Lectures\\_Slides/day2/Lectures/L04\\_AG%20Raspolli.pdf](http://www.eurobioref.org/Summer_School/Lectures_Slides/day2/Lectures/L04_AG%20Raspolli.pdf). Access: October 2013.
- Gandarias, I., Barrio, V.L., Requies, J., Arias, P.L., Cambra, J.F., Güemez, M.B. 2008. From biomass to fuels: Hydrotreating of oxygenated compounds. *International Journal of Hydrogen Energy*, **33**(13), 3485-3488.

- Gayubo, A.G., Aguayo, A.T., Atutxa, A., Prieto, R., Bilbao, J. 2004. Deactivation of a HZSM-5 zeolite catalyst in the transformation of the aqueous fraction of biomass pyrolysis oil into hydrocarbons. *Energy & Fuels*, **18**(6), 1640-1647.
- Gevert, B.S., Otterstedt, J.E., Massoth, F.E. 1987. Kinetics of the HDO of methyl-substituted phenols. *Applied Catalysis*, **31**(1), 119-131.
- Gevert, S.B., Eriksson, M., Eriksson, P., Massoth, F.E. 1994. Direct hydrodeoxygenation and hydrogenation of 2,6- and 3,5-dimethylphenol over sulphided CoMo catalyst. *Applied Catalysis A, General*, **117**(2), 151-162.
- Gishti, K., Iannibello, A., Marengo, S., Morelli, G., Tittarelli, P. 1984. On the role of phosphate anion in the MoO<sub>3</sub>-Al<sub>2</sub>O<sub>3</sub> based catalysts. *Applied Catalysis*, **12**(4), 381-393.
- Goldemberg, J., Coelho, S.T., Guardabassi, P. 2008. The sustainability of ethanol production from sugarcane. *Energy Policy*, **36**(6), 2086-2097.
- Green Car Congress. ConocoPhillips Begins Production of Renewable Diesel Fuel at Whitegate Refinery at Whitegate Refinery, [http://www.greencarcongress.com/2006/12/conocophillips\\_.html](http://www.greencarcongress.com/2006/12/conocophillips_.html). Accessed: September 2013.
- Gregoire, C.E., Bain, R.L. 1994a. Technoeconomic analysis of the production of biocrude from wood. *Biomass and Bioenergy*, **7**(1), 275-283.
- Gregoire, C.E., Bain, R.L. 1994b. Technoeconomic analysis of the production of biocrude from wood. *Biomass and Bioenergy*, **7**(1-6), 275-283.
- Gutierrez, A., Kaila, R.K., Honkela, M.L., Slioor, R., Krause, A.O.I. 2009. Hydrodeoxygenation of guaiacol on noble metal catalysts. *Catalysis Today*, **147**(3-4), 239-246.
- Haldor Topsoe. Novel hydrotreating technology for production of green diesel. [http://www.topsoe.com/business\\_areas/refining/~media/PDF%20files/Refining/novel\\_hydrotreating\\_technology\\_for\\_production\\_of\\_green\\_diesel.ashx](http://www.topsoe.com/business_areas/refining/~media/PDF%20files/Refining/novel_hydrotreating_technology_for_production_of_green_diesel.ashx). Accessed: October 2013.
- Hamelinck, C.N., Faaij, A.P.C. 2006. Outlook for advanced biofuels. *Energy Policy*, **34**(17), 3268-3283.
- Honeywell. Honeywell Green Diesel™ To Be Produced From Bio Feedstocks In U.S. Facility, <http://honeywell.com/News/Pages/Honeywell-Green-Diesel-To-Be-Produced-From-Bio-Feedstocks-In-US-Facility.aspx>. Accessed: October 2013

- Islam, M.N., Ani, F.N. 2000. Techno-economics of rice husk pyrolysis, conversion with catalytic treatment to produce liquid fuel. *Bioresource Technology*, **73**(1), 67-75.
- Jones, S.B., Valkenburg, C., Walton, C.W., Elliott, D.C., Holladay, J.E., Stevens, D.J., Kinchin, C., Czernik, S. 2009. Production of Gasoline and Diesel from Biomass via fast pyrolysis, hydrotreating and hydrocracking: A design case. Pacific Northwest National Laboratory. PNNL-18284.
- Kim, K.H., Kim, T.-S., Lee, S.-M., Choi, D., Yeo, H., Choi, I.-G., Choi, J.W. 2013a. Comparison of physicochemical features of biooils and biochars produced from various woody biomasses by fast pyrolysis. *Renewable Energy*, **50**, 188-195.
- Kim, K.H., Kim, T.-S., Lee, S.-M., Choi, D., Yeo, H., Choi, I.-G., Choi, J.W. 2013b. Comparison of physicochemical features of biooils and biochars produced from various woody biomasses by fast pyrolysis. *Renewable Energy*, **50**(0), 188-195.
- Knothe, G. 2010. Biodiesel and renewable diesel: A comparison. *Progress in Energy and Combustion Science*, **36**(3), 364-373.
- Krishna, M.V.S.M., Rao, V.V.R.S., Reddy, T.K.K., Murthy, P.V.K. 2014. Comparative studies on performance evaluation of DI diesel engine with high grade low heat rejection combustion chamber with carbureted alcohols and crude jatropha oil. *Renewable and Sustainable Energy Reviews*, **36**, 1-19.
- Kuppens, T., Van Dael, M., Vanreppelen, K., Thewys, T., Yperman, J., Carleer, R., Schreurs, S., Van Passel, S. 2015. Techno-economic assessment of fast pyrolysis for the valorization of short rotation coppice cultivated for phytoextraction. *Journal of Cleaner Production*, **88**, 336-344.
- LaClaire, C.E., Barrett, C.J., Hall, K. 2004. Technical, environmental and economic feasibility of bio-oil in new hampshire's north country. *Durham, NH: University of New Hampshire*.
- Laurent, E., Delmon, B. 1993. Influence of Oxygen-Containing, Nitrogen-Containing, and Sulfur-Containing-Compounds on the Hydrodeoxygenation of Phenols over Sulfided Como/Gamma-Al<sub>2</sub>O<sub>3</sub> and Nimo/Gamma-Al<sub>2</sub>O<sub>3</sub> Catalysts. *Industrial & Engineering Chemistry Research*, **32**(11), 2516-2524.
- Laurent, E., Delmon, B. 1994a. Influence of water in the deactivation of a sulfided NiMo Gamma-Al<sub>2</sub>O<sub>3</sub> catalyst during hydrodeoxygenation. *Journal of Catalysis*, **146**(1), 281-291.

- Laurent, E., Delmon, B. 1994b. Study of the hydrodeoxygenation of carbonyl, carboxylic and guaiacyl groups over sulfided CoMo/ $\gamma$ -Al<sub>2</sub>O<sub>3</sub> and NiMo/ $\gamma$ -Al<sub>2</sub>O<sub>3</sub> catalyst .2. Influence of water, ammonia and hydrogen-sulfide. *Applied Catalysis a-General*, **109**(1), 97-115.
- Laurent, E., Delmon, B. 1994c. Study of the hydrodeoxygenation of carbonyl, carboxylic and guaiacyl groups over sulfided CoMo/ $\gamma$ -Al<sub>2</sub>O<sub>3</sub> and NiMo/ $\gamma$ -Al<sub>2</sub>O<sub>3</sub> catalysts. I. Catalytic reaction schemes. *Applied Catalysis A, General*, **109**(1), 77-96.
- Lehto, J., Oasmaa, A., Solantausta, Y., Kyto, M., Chiaramonti, D. 2013. Fuel oil quality and combustion of fast pyrolysis bio-oils VTT Technical Research Centre of Finland.
- Lu, Q., Li, W.-Z., Zhu, X.-F. 2009. Overview of fuel properties of biomass fast pyrolysis oils. *Energy Conversion and Management*, **50**(5), 1376-1383.
- Lu, Q., Yang, X.-l., Zhu, X.-f. 2008. Analysis on chemical and physical properties of bio-oil pyrolyzed from rice husk. *Journal of Analytical and Applied Pyrolysis*, **82**(2), 191-198.
- McKendry, P. 2002. Energy production from biomass (part 1): overview of biomass. *Bioresource Technology*, **83**(1), 37-46.
- McMillan, J.D. 1994. Pretreatment of lignocellulosic biomass. *ACS symposium series*. ACS Publications. pp. 292-324.
- Mittelbach, M. 1996. Diesel fuel derived from vegetable oils, VI: Specifications and quality control of biodiesel. *Bioresource Technology*, **56**(1), 7-11.
- Naik, S.N., Goud, V.V., Rout, P.K., Dalai, A.K. 2010. Production of first and second generation biofuels: A comprehensive review. *Renewable and Sustainable Energy Reviews*, **14**(2), 578-597.
- Neste Oil. Neste Oil's renewable diesel plant in Rotterdam – the largest and most advanced in Europe,  
<https://www.google.ca/url?sa=t&rct=j&q=&esrc=s&source=web&cd=3&ved=0CD0QFjAC&url=http%3A%2F%2Fwww.nesteoil.com%2Fbinary.asp%3Fpath%3D1%3B41%3B540%3B2384%3B18010%3B18129%26field%3DFileAttachment&ei=Wh7CUrDDDdjm oASWjoKACQ&usg=AFQjCNEBIcF65ghlNNqdmHoFAk02aLRrQw&bvm=bv.58187178,d.cGU&cad=rja>. Accessed: September 2013.
- Neste Oil. Neste Oil's Singapore refinery – the world's largest and most advanced,  
<https://www.google.ca/url?sa=t&rct=j&q=&esrc=s&source=web&cd=4&ved=0CEMQFj>

AD&url=http%3A%2F%2Fwww.nesteoil.com%2Fbinary.asp%3Fpath%3D1%3B41%3B540%3B2384%3B18010%3B21058%26field%3DFileAttachment&ei=Wh7CUrDDDDjm oASWjoKACQ&usg=AFQjCNHCqV9a\_uQc68FRDapb-1Ds89Yn3Q&bvm=bv.58187178,d.cGU&cad=rja. Accessed: September 2013.

Neste Oil Production Capacity, <http://www.nesteoil.com/default.asp?path=1,41,11991,22708,22720>. accessed: October 2013.

Peng, J., Chen, P., Lou, H., Zheng, X.M. 2008. Upgrading of bio-oil over aluminum silicate in supercritical ethanol. *Energy & Fuels*, **22**(5), 3489-3492.

Peters, J.F., Petrakopoulou, F., Dufour, J. 2014. Exergetic analysis of a fast pyrolysis process for bio-oil production. *Fuel Processing Technology*, **119**(0), 245-255.

Piskorz, J., Scott, D.S. 1987. The Composition of Oils Obtained by the Fast Pyrolysis of Different Woods. *Abstracts of Papers of the American Chemical Society*, **193**, 58-Cell.

Popoola, L.T., Adeoye, B.K., Grema, A.S., Yusuff, A.S., Adeyi, A.A. 2015. Process economic analysis of bio-oil production from wood residue using pyrolysis in South-Western Nigeria. *Journal of Applied Chemical Science International* **2**(1), 12-23.

Popov, A., Kondratieva, E., Goupil, J.M., Mariey, L., Bazin, P., Gilson, J.P., Travert, A., Mauge, F. 2010. Bio-oils hydrodeoxygenation: adsorption of phenolic molecules on oxidic catalyst supports. *Journal of Physical Chemistry C*, **114**(37), 15661-15670.

Quintero, J.A., Montoya, M.I., Sánchez, O.J., Giraldo, O.H., Cardona, C.A. 2008. Fuel ethanol production from sugarcane and corn: Comparative analysis for a Colombian case. *Energy*, **33**(3), 385-399.

Richardson, A.D., Keenan, T.F., Migliavacca, M., Ryu, Y., Sonnentag, O., Toomey, M. 2013. Climate change, phenology, and phenological control of vegetation feedbacks to the climate system. *Agricultural and Forest Meteorology*, **169**(0), 156-173.

Ringer, M., Putsche, V., Scahill, J. 2006a. Large-Scale Pyrolysis Oil. *Assessment*.

Ringer, M., Putsche, V., Scahill, J. 2006b. Large-scale pyrolysis oil production: A technology assessment and economic analysis. National renewable energy laboratory. NREL/TP-510-37779

Rogers, J., Brammer, J. 2012a. Estimation of the production cost of fast pyrolysis bio-oil. *Biomass and bioenergy*, **36**, 208-217.

- Rogers, J.G., Brammer, J.G. 2012b. Estimation of the production cost of fast pyrolysis bio-oil. *Biomass and Bioenergy*, **36**(0), 208-217.
- Romero, Y., Richard, F., Brunet, S. 2010. Hydrodeoxygenation of 2-ethylphenol as a model compound of bio-crude over sulfided Mo-based catalysts: Promoting effect and reaction mechanism. *Applied Catalysis B: Environmental*, **98**(3-4), 213-223.
- Sánchez, Ó.J., Cardona, C.A. 2008. Trends in biotechnological production of fuel ethanol from different feedstocks. *Bioresource Technology*, **99**(13), 5270-5295.
- Saravanan, S., Nagarajan, G. 2014. Comparison of influencing factors of diesel with crude rice bran oil methyl ester in multi response optimization of NOx emission. *Ain Shams Engineering Journal*, **5**(4), 1241-1248.
- Sarkar, S., Kumar, A. 2010. Large-scale biohydrogen production from bio-oil. *Bioresource Technology*, **101**(19), 7350-7361.
- Senol, O.I., Viljava, T.R., Krause, A.O.I. 2005. Hydrodeoxygenation of aliphatic esters on sulphided NiMo/gamma-Al<sub>2</sub>O<sub>3</sub> and CoMo/gamma-Al<sub>2</sub>O<sub>3</sub> catalyst: The effect of water. *Catalysis Today*, **106**(1-4), 186-189.
- Sepúlveda, C., Leiva, K., García, R., Radovic, L.R., Ghampson, I.T., DeSisto, W.J., Fierro, J.L.G., Escalona, N. 2011. Hydrodeoxygenation of 2-methoxyphenol over Mo<sub>2</sub>N catalysts supported on activated carbons. *Catalysis Today*, **172**(1), 232-239.
- Serrano, C., Monedero, E., Lapuerta, M., Portero, H. 2011. Effect of moisture content, particle size and pine addition on quality parameters of barley straw pellets. *Fuel Processing Technology*, **92**(3), 699-706.
- Sheu, Y.-H.E., Anthony, R.G., Soltes, E.J. 1988. Kinetic studies of upgrading pine pyrolytic oil by hydrotreatment. *Fuel Processing Technology*, **19**(1), 31-50.
- Solantausta, Y., Beckman, D., Bridgwater, A.V., Diebold, J.P., Elliott, D.C. 1992. International Energy Agency Bioenergy Agreement Progress and Achievements 1989-1991 Assessment of liquefaction and pyrolysis systems. *Biomass and Bioenergy*, **2**(1), 279-297.
- Sun, Y., Cheng, J. 2002. Hydrolysis of lignocellulosic materials for ethanol production: a review. *Bioresource Technology*, **83**(1), 1-11.
- Swanson, R.M., Platon, A., Satrio, J.A., Brown, R.C. 2010. Techno-economic analysis of biomass-to-liquids production based on gasification. *Fuel*, **89**, Supplement 1(0), S11-S19.

- Syntroleum. Synthetic fuels technology for a clean future, <http://www.syntroleum.com/profiles/investor/fullpage.asp?BzID=2029&to=cp&Nav=0&LangID=1&s=0&ID=11912>. Accessed: October 2013.
- Tang, Z., Lu, Q., Zhang, Y., Zhu, X.F., Guo, Q.X. 2009. One Step Bio-Oil Upgrading through Hydrotreatment, Esterification, and Cracking. *Industrial & Engineering Chemistry Research*, **48**(15), 6923-6929.
- The University of California Davis, The University of California Berkeley. California Renewable Diesel Multimedia Evaluation, [http://www.arb.ca.gov/fuels/multimedia/RenewableDieselTierI\\_DftFinal.pdf](http://www.arb.ca.gov/fuels/multimedia/RenewableDieselTierI_DftFinal.pdf). Accessed: October 2013.
- Thilakaratne, R., Brown, T., Li, Y., Hu, G., Brown, R. 2014. Mild catalytic pyrolysis of biomass for production of transportation fuels: a techno-economic analysis. *Green Chemistry*, **16**(2), 627-636.
- Trippe, F., Fröhling, M., Schultmann, F., Stahl, R., Henrich, E., Dalai, A. 2013. Comprehensive techno-economic assessment of dimethyl ether (DME) synthesis and Fischer–Tropsch synthesis as alternative process steps within biomass-to-liquid production. *Fuel Processing Technology*, **106**(0), 577-586.
- Tsai, W.T., Lee, M.K., Chang, Y.M. 2007. Fast pyrolysis of rice husk: Product yields and compositions. *Bioresource Technology*, **98**(1), 22-28.
- Tyson. Welcome to Tyson Renewable Energy, <http://renewableenergy.tyson.com/>. Accessed: October 2013.
- United States Environmental Protection Agency. Renewable fuels: regulations & standards, <http://www.epa.gov/otaq/fuels/renewablefuels/regulations.htm>. Accessed: October 2013.
- Venderbosch, R.H., Ardiyanti, A.R., Wildschut, J., Oasmaa, A., Heeresb, H.J. 2010. Stabilization of biomass-derived pyrolysis oils. *Journal of Chemical Technology and Biotechnology*, **85**(5), 674-686.
- VTT Technical Research Centre of Finland. Stability of fast pyrolysis bio-oils and upgraded products, <http://www.gastechnology.org/tcbiomass2013/tcb2013/04-Oasmaa-tcbiomass2013-presentation-Thur.pdf>, Accessed: October 2013.

- Wang, Y., He, T., Liu, K., Wu, J., Fang, Y. 2012. From biomass to advanced bio-fuel by catalytic pyrolysis/hydro-processing: Hydrodeoxygenation of bio-oil derived from biomass catalytic pyrolysis. *Bioresource Technology*, **108**(0), 280-284.
- Ward, J.W. 1993. Hydrocracking processes and catalysts. *Fuel Processing Technology*, **35**(1-2), 55-85.
- Wildschut, J., Arentz, J., Rasrendra, C.B., Venderbosch, R.H., Heeres, H.J. 2009a. Catalytic hydrotreatment of fast pyrolysis oil: Model studies on reaction pathways for the carbohydrate fraction. *Environmental Progress and Sustainable Energy*, **28**(3), 450-460.
- Wildschut, J., Iqbal, M., Mahfud, F.H., Melian-Cabrera, I., Venderbosch, R.H., Heeres, H.J. 2010a. Insights in the hydrotreatment of fast pyrolysis oil using a ruthenium on carbon catalyst. *Energy & Environmental Science*, **3**(7), 962-970.
- Wildschut, J., Mahfud, F.H., Venderbosch, R.H., Heeres, H.J. 2009b. Hydrotreatment of Fast Pyrolysis Oil Using Heterogeneous Noble-Metal Catalysts. *Industrial & Engineering Chemistry Research*, **48**(23), 10324-10334.
- Wildschut, J., Melian-Cabrera, I., Heeres, H.J. 2010b. Catalyst studies on the hydrotreatment of fast pyrolysis oil. *Applied Catalysis B-Environmental*, **99**(1-2), 298-306.
- Wright, M.M., Daugaard, D.E., Satrio, J.A., Brown, R.C. 2010. Techno-economic analysis of biomass fast pyrolysis to transportation fuels. *Fuel*, **89**, S2-S10.
- Yaman, S. 2004. Pyrolysis of biomass to produce fuels and chemical feedstocks. *Energy Conversion and Management*, **45**(5), 651-671.
- Yang, Y., Gilbert, A., Xu, C. 2009. Hydrodeoxygenation of bio-crude in supercritical hexane with sulfided CoMo and CoMoP catalysts supported on MgO: A model compound study using phenol. *Applied Catalysis A: General*, **360**(2), 242-249.
- Yoshimura, Y., Sato, T., Shimada, H., Matsubayashi, N., Nishijima, A. 1991. Influences of oxygen-containing substances on deactivation of sulfided molybdate catalysts. *Applied Catalysis*, **73**(1), 55-63.
- Zhang, Q., Chang, J., Wang, T., Xu, Y. 2007. Review of biomass pyrolysis oil properties and upgrading research. *Energy Conversion and Management*, **48**(1), 87-92.
- Zhang, S., Yan, Y., Li, T., Ren, Z. 2005. Upgrading of liquid fuel from the pyrolysis of biomass. *Bioresource Technology*, **96**(5), 545-550.

- Zhang, S.P., Yan, Y.J., Ren, J.W., Li, T.C. 2003. Study of hydrodeoxygenation of bio-oil from the fast pyrolysis of biomass. *Energy Sources*, **25**(1), 57-65.
- Zhang, Y., Brown, T.R., Hu, G., Brown, R.C. 2013. Techno-economic analysis of two bio-oil upgrading pathways. *Chemical Engineering Journal*, **225**, 895-904.
- Zhao, C., He, J., Lemonidou, A.A., Li, X., Lercher, J.A. 2011. Aqueous-phase hydrodeoxygenation of bio-derived phenols to cycloalkanes. *Journal of Catalysis*, **280**(1), 8-16.

## **Chapter 3: Predicting the Biomass Conversion Performance in a Fluidized Bed Reactor using Isoconversional Model Free Method<sup>3</sup>**

### **3.1 Introduction**

Globalization and industrialization have direct and indirect effects on the environment due to increased consumption of fossil fuels, which results in global warming and greenhouse effects. The continuous use of fossil fuels ultimately threatens the ecosystem, as the global environment was already degrading. Therefore, for the last few decades researchers have been focusing on renewable resources such as solar, wind, biomass, hydro, etc. Of all the renewable resources, biomass is gaining significant attention as it can be directly converted to transportation fuels and replace fossil fuels (Parikka, 2004; Patel & Kumar, 2016).

There are both thermochemical and biological technologies available to convert lignocellulosic biomass to different end products such as biofuels and chemicals. But thermochemical conversion is considered the most promising (Patel et al., 2016). Pyrolysis is considered the fundamental process for all thermochemical conversions because it can convert biomass to a solid, liquid, or gas in the absence of oxygen (Goyal et al., 2008). To produce biofuels equivalent to fossil fuel,

---

<sup>3</sup>A version of this chapter has been published in The Canadian Journal of Chemical Engineering: Patel M, Oyedun A, Kumar A, Gupta R. Predicting the biomass conversion performance in a fluidized bed reactor using isoconversional model free method" in **The Canadian Journal of Chemical Engineering** (in press)

fast pyrolysis is widely used as it enhances the liquid yield with moderate temperature and pressure condition at low residence times in a fixed bed or fluidized bed reactor (Patel et al., 2016). Fluidized bed reactor is widely used for fast pyrolysis technology to produce liquid fuel (Burton & Wu, 2017; Choi et al., 2017; Morin et al., 2016; Patel et al., 2018; Soria-Verdugo et al., 2017; Zhang et al., 2017). The advantages of this type of reactor are; uniform temperature, low investment, good gas solid contact, ability to handle varieties of feedstock with wide particle size distribution, low maintenance and high heating rate etc. (Warnecke, 2000).

For complete utilization of biomass through pyrolysis, it is required to investigate the kinetics of pyrolysis and thermal degradation/decomposition of the solid to biochar. Thermogravimetric analysis is the right platform for estimating the pyrolysis kinetic of biomass by two methods: isothermal and non-isothermal analysis. Basically these two methods are used to estimate kinetic parameters in term of activation energy ( $E_a$ ) and pre-exponential factor ( $A$ ). Compared to the isothermal method, non-isothermal method is more convenient and accurate in terms of the  $E_a$  and  $A$  (Vyazovkin & Wight, 1999). Non-isothermal solid kinetic methods are divided into two groups, which are listed in Figure 3.1.

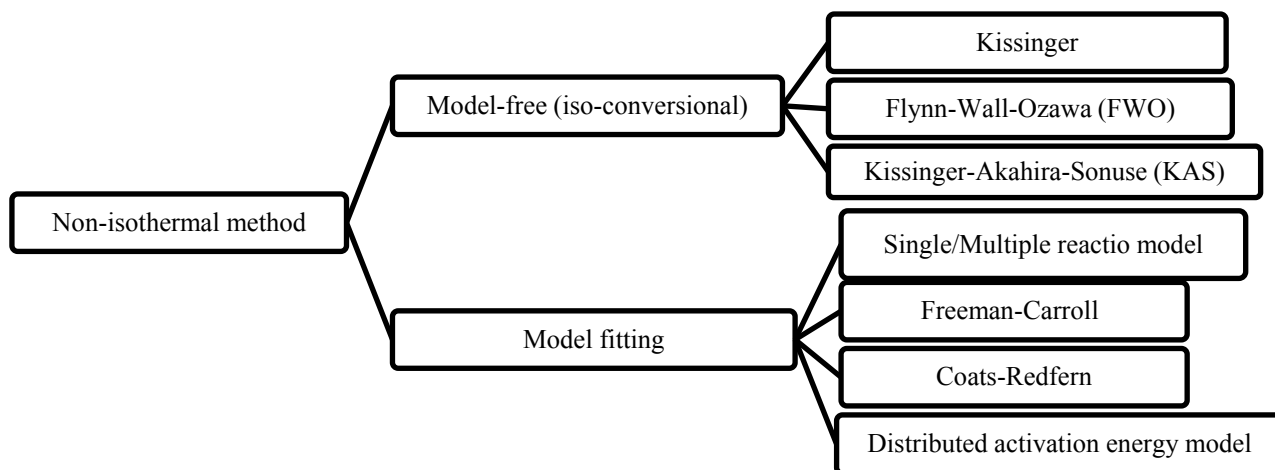


**Figure 3.1. Non-isothermal solid kinetic methods**

In the past, model fitting methods (single or multiple reaction model, Coats Redfern method etc.) were used more than model-free methods because kinetic parameters could easily be determined from a single set of experiments (Ceylan & Topçu, 2014; Hu et al., 2007; Li & Suzuki, 2009; Rosselló et al., 2016; Várhegyi et al., 1997; Vyazovkin & Wight, 1999). But overall model fitting methods predict highly uncertain values for the Arrhenius parameters as they use very limited non-isothermal experimental data and all the experiments are performed at single heating rate. On the other hand, the isoconversional model-free method predicts more accurate values of kinetic parameters since it uses the extent of the conversion of the biomass with time or temperature. A study by ICTAC Kinetics Committee also investigated the reliability of different thermal analysis method including model free and model fitting method and recommended to avoid the method which use single heating rate program to enhance the accuracy of the model (Vyazovkin & Wight, 1999). Therefore, the model-free method is highly trustworthy compared to the model fitting method for estimating reliable and consistent kinetic information for non-isothermal data. The  $E_a$  can be determined without assuming or estimating any form of reaction model. The estimated  $E_a$  at corresponding conversion are almost similar for Flynn-Wall-Ozawa (FWO) and Kissinger-Akahira-Sonuse (KAS) (Huang et al., 2016; Słopiecka et al., 2012).

Previous literatures have been published on estimation of kinetic parameters of biomass degradation to biochar using model free method (Chandrasekaran et al., 2017; Damartzis et al., 2011; Hu et al., 2016; Huang et al., 2016; Lopez-Velazquez et al., 2013; Mishra et al., 2015; Muktham et al., 2016; Quan et al., 2016; Słopiecka et al., 2012; Varma & Mondal, 2016). Huang et al., (2016) investigated the pyrolysis kinetics of soybean straw using KAS and FWO method in an inert Argon atmosphere and reported that initially  $E_a$  increased smoothly as conversion increased to 0.1 to 0.3, then it maintained a constant trend till 0.6 and decreased drastically from  $176 \text{ kJ mol}^{-1}$  to around  $50 \text{ kJ mol}^{-1}$  as conversion increased from 0.6 to 0.7. The reason stated for increase and flat trend off  $E_a$  due to the cellulose and hemicellulose content and drastically decreased in  $E_a$  due to lignin decomposition which required low energy. Chandrasekaran et al.,(2017) studied the pyrolysis kinetics of *Prosopis juliflora* using KAS, FWO and Friedman model and presented different trend of  $E_a$  with the conversion from the previous study. First,  $E_a$  increased, then decreased and further increased with increase in extent of conversion and the

reason was the involvement of multistep reactions instead of single step reaction mechanism for the decomposition of biomass. Muktham et al. (2016) studied the thermal behavior of de-oiled karanja seed cake biomass using model free thermogravimetric analysis. They found that  $E_a$  decreased with increase in conversion, as high conversion observed at high temperature and the energy required at elevated temperature was lower than the lower temperature. Quan et al. (2016) investigated the kinetic and thermochemical behavior of three components of biomass: cellulose, hemicellulose and lignin using FWO method and presented completely different behavior of  $E_a$  for these individual feedstock. They estimated the average  $E_a$  for cellulose, hemicellulose and lignin to be  $141 \text{ kJ mol}^{-1}$ ,  $126 \text{ kJ mol}^{-1}$  and  $167 \text{ kJ mol}^{-1}$ , respectively. According to them,  $E_a$  required was highest for lignin in contradiction to the Huang et al.,(2016). There are other studies available in the literature regarding the estimation of  $E_a$  for the different kind of biomass using model free method (Abdelouahed et al., 2017; Hu et al., 2016; Kantarelis et al., 2011; Maia & de Morais, 2016; Mishra et al., 2015; Polat et al., 2016; Varma & Mondal, 2016).

From the above studies, it can be concluded that the trend of  $E_a$  varies due to the composition and properties of biomass, operating condition of TGA and the method used for the analysis. Therefore, it is essential to estimate the kinetic parameters for the specific Canadian feedstock which will further help in designing the reactor, downstream process and the cost estimation of the entire pyrolysis and upgrading process to produce biofuels from the biomass. In literature, there are only two papers reported on the pyrolysis kinetics of Canadian forest residue and wheat straw with limited analysis (Harun & Afzal, 2010; Mani et al., 2010).

The specific objectives of this study are to:

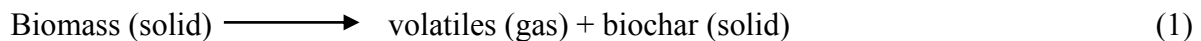
- To estimate the kinetic parameters from thermogravimetric analysis for different feedstocks using isoconversional model free method
- To investigate the effect of temperatures and particle size on the char yield in fluidized bed reactor
- To apply kinetic parameters obtained from TGA to predict the biochar yield in the fluidized bed experiments

- To study the effect of particle size on the biomass conversion to char in the fluidized bed reactor

This study focused on the investigation of thermal degradation and pyrolysis kinetics using a model free thermogravimetric analysis of four Canadian feedstocks: two Canadian woody biomass (spruce and aspen) and two Canadian agricultural residues (corn stover and wheat straw). The kinetic parameters were estimated using isoconversional FWO method for decomposition of biomass to bio-char. To perform thermogravimetric analysis, four sets of heating rate ( $2\text{ }^{\circ}\text{C min}^{-1}$ ,  $5\text{ }^{\circ}\text{C min}^{-1}$ ,  $10\text{ }^{\circ}\text{C min}^{-1}$  and  $15\text{ }^{\circ}\text{C min}^{-1}$ ) were considered for a temperature range of  $30 - 900^{\circ}\text{C}$  in a nitrogen atmosphere. Simultaneously, the thermal degradation of these feedstocks to biochar through fast pyrolysis were investigated in a fluidized bed reactor at different temperatures and for different particle size distributions. We estimated the  $E_a$  from the fluidized bed using simple Arrhenius model and compared with the TGA kinetic parameters from FWO method. The global kinetic parameters (the average for all the conversions) obtained from the TGA were used to simulate biomass conversion at different temperatures and for particle size of  $0.425\text{-}1\text{mm}$  were compared with experimental biochar data obtained at different temperatures in the fluidized bed reactor, which gave very interesting results.

### 3.2 Basic Pyrolysis Kinetics

In general, when biomass is heated in a nitrogen-controlled atmosphere with zero concentration of oxygen at a constant heating rate, the biomass will decompose into volatiles and biochar. This can be illustrated by Equation (1):



The kinetics of the thermal decomposition of lignocellulosic biomass is complicated as it involves a set of both parallel and series reactions. But a TGA is the right platform from which information

on overall reactions can be obtained rather than on the individual reactions for the calculation of kinetic parameters.

The estimation of the kinetic parameters of the decomposition of the lignocellulosic biomass from the TGA data is based on the rate expressed in Equation (2):

$$\frac{d\alpha}{dt} = k(T)f(\alpha) \quad (2)$$

where:

$\alpha$  extent of reaction (conversion)

t time (min)

k (T) rate constant of the reaction ( $s^{-1}$ )

f( $\alpha$ ) reaction model

The extent of reaction,  $\alpha$ , is defined in terms of the weight loss of the biomass sample or formation of volatiles and can be expressed as:

$$\alpha = \frac{m_i - m_a}{m_i - m_f} \quad (3)$$

where:

$m_i$  initial mass of the sample (kg)

$m_a$  actual mass of the sample at time t (kg)

$m_f$  final mass of the sample after the end of the reaction (kg)

The rate constant,  $k(T)$ , is defined according to the Arrhenius equation, as follows:

$$k(T) = A \exp\left(-\frac{E_a}{RT}\right) \quad (4)$$

where:

$E_a$  activation energy ( $\text{kJ mol}^{-1}$ )

$T$  absolute temperature (K)

$R$  gas constant ( $8.314 \text{ J K}^{-1} \text{ mol}^{-1}$ )

$A$  pre-exponential factor ( $\text{min}^{-1}$ )

The mathematical expression for the reaction model,  $f(\alpha)$  is represented by Equation (5):

$$f(\alpha) = (1 - \alpha)^n \quad (5)$$

where  $n$  is the order of the reaction. For this study  $n$  was considered to be 1.

The substitution of Equations (4) and (5) in Equation (2) results in Equation (6), which is the fundamental expression used to calculate the kinetic parameters for solid state decomposition reactions.

$$\frac{d\alpha}{dt} = A e^{-\frac{E_a}{RT}} (1 - \alpha) \quad (6)$$

For non-isothermal thermogravimetric experiments at the linear heating rate  $\beta = dT/dt$ , Equation (6) can be revised as follows:

$$\frac{d\alpha}{dt} = \beta \frac{d\alpha}{dT} = A e^{\frac{-E_a}{RT}} (1 - \alpha) \quad (7)$$

And can be further simplified to:

$$\frac{d\alpha}{dt} = \frac{A}{\beta} e^{\frac{-E_a}{RT}} (1 - \alpha) \quad (8)$$

### 3.3 Experimental Methodology

#### 3.3.1 *Material Preparation and Characterization*

For this study, four different lignocellulosic biomass feedstocks were selected: aspen hardwood, spruce softwood, corn stover, and wheat straw. Corn stover (*Zea mays* ssp. *mays* L.) and wheat straw (*Triticum aestivum* L.) were collected from farms in southern Alberta and in northern Alberta, Canada, respectively. Aspen (*Populus tremuloides* –) and spruce (*Picea abies*) wood chips were gathered from Weyerhaeuser in Edson and in Drayton Valley, Alberta, respectively. These feedstocks were selected based on the availability in Western Canada. The particle sizes of the supplied feedstocks were 6 – 10 mm. This particle size was too large for the TGA experiments and fluidized bed fast pyrolysis. Therefore, the feedstocks were ground to less than 1 mm using a grinder and sieved through mechanical screens ranging from a mesh size of 2 mm to less than 0.125 mm. For fast pyrolysis in the fluidized bed reactor, three ranges of particle size distribution were considered: 0.125-0.425 mm, 0.425-1 mm and 1-2 mm (average particle diameter of 0.275, 0.7125 and 1.5 mm). For the TGA experiments, samples were taken from the mesh size of 0.425-1 mm. The prepared samples were stored in properly sealed glass bottles to prevent contact with atmospheric moisture. The proximate and ultimate analysis and chemical composition of these biomass feedstocks were summarized in Table 3.1. A proximate analysis was conducted through thermogravimetric analysis (701, LECO, St. Joseph, MI, USA) and an ultimate analysis was carried out using an Elemental Analyzer (EA1108, Carlo Erba, Val de Reuil, France) for CHNS (carbon, hydrogen, nitrogen, and sulfur) and oxygen was estimated by difference. Table 3.2 shows

the typical chemical composition of all biomass feedstock (Bilba et al., 2013; Burhenne et al., 2013; Demirbaş, 1997; Öhgren et al., 2007; Pettersen, 1984; Yildiz et al., 2006; Zhu et al., 2009). According to chemical analysis, woody biomass is rich in cellulose and lignin whereas agricultural residues content more ash and low lignin.

**Table 3-1. Ultimate and proximate analyses of biomass samples**

	<b>Wheat straw</b>	<b>Corn stover</b>	<b>Aspen hardwood</b>	<b>Spruce softwood</b>
Proximate analysis (dry basis)				
Ash	6.3	6.1	0.32	0.5
Volatile	75.4	76.3	83.3	82.3
Fixed carbon	18.3	17.6	16.3	17.2
Moisture	4.1	6.2	3.2	3.9
Ultimate analysis (dry basis)				
Nitrogen	0.8	1.2	0.2	0.2
Carbon	42.2	41.5	46.5	47.5
Hydrogen	5.7	5.6	5.6	6.4
Sulfur	0.03	0.05	0	0
Oxygen	51.1	50.3	47.3	45.9

**Table 3-2. Typical chemical analysis of biomass samples**

	<b>Cellulose</b>	<b>Hemicellulose</b>	<b>Lignin</b>	<b>Ash</b>	<b>Reference</b>
Aspen hardwood	45-55	30-35	22-30	0.1-1	(Bilba et al., 2013; Demirbaş, 1997; Pettersen, 1984)
Spruce softwood	40-50	20-30	25-35	0.5-1	(Bilba et al., 2013; Burhenne et al., 2013; Demirbaş, 1997; Yildiz et al., 2006)
Wheat straw	25-35	40-45	15-22	5-12	(Burhenne et al., 2013; Demirbaş, 1997)
Corn stover	40-50	28-32	12-20	4-8	(Demirbaş, 1997; Öhgren et al., 2007; Zhu et al., 2009)

### 3.3.2 Thermogravimetric Analysis

The TGA of lignocellulosic biomass is performed using a Thermogravimetric Analyzer SDT Q600 (New Castle, DE, USA). To maintain pyrolysis conditions, high-purity nitrogen was used as carrier gas at a constant flow rate of 50 mL/min throughout the run. About 10-11 mg of prepared biomass samples were placed in the alumina crucible and for accuracy all the experiments were repeated three times. For all feedstocks, thermogravimetric analyses were performed at four different heating rates: 2, 5, 10, and 15 °C min<sup>-1</sup>. The temperature used for the decomposition study ranges from room temperature to 900 °C. At the end of all the experiments, the isothermal condition was maintained for 15 minutes. During the experiments, weight loss was monitored with temperature and time in a nitrogen-controlled atmosphere. A Type R thermocouple was used to monitor the temperature in the thermogravimetric analyzer. The data for the TGA and derivative thermogravimetric (DTG) curves for different feedstocks obtained from the TGA equipment were analyzed using TA instruments Universal Analysis 2000 software. The data extracted from this software were used to calculate E<sub>a</sub> and A. To estimate the kinetic parameters, Flynn-Wall-Ozawa method was used.

#### *The Flynn-Wall-Ozawa method*

The FWO method is an integral iso-conversional model-free method. In this method, it is assumed that the E<sub>a</sub> is not constant with changes in conversion. So the corresponding temperatures for conversion at different heating rates are different. This method is derived by three scientists, Joseph Flynn, Leo Wall, and Takeo Ozawa (Flynn & Wall, 1966; Ozawa, 1965; Venkatesh et al., 2013), and the final form is represented by Equation (9) as follows:

$$\ln\beta_i = \ln \frac{A_\alpha E_\alpha}{Rg(\alpha)} - 5.331 - 1.052 \frac{E_\alpha}{RT_{\alpha i}} \quad (9)$$

where  $g(\alpha)$  is constant at a constant conversion and  $i$  represents the given value of the heating rate. The apparent E<sub>a</sub> of the biomass can be estimated from the slope of the plot of  $\ln(\beta)$  vs.  $1/T$ .

### 3.3.3 *Pyrolysis in A Fluidized Bed Reactor and Operating Conditions*

The fast pyrolysis of four Canadian biomass feedstocks ranging from woody biomass to agricultural residues was carried out in a laboratory-scale batch fluidized bed reactor. All the experiments were conducted in an inert nitrogen atmosphere. A schematic diagram of the fluidized bed reactor is shown in Figure 3.2. The main components of the set-up were a two-valve feeder, fluidized bed reactor, cyclone separator, and condensers. The reactor was made of stainless steel and its internal diameter and height were 10 and 100 cm, respectively. A 35 cm high detachable reactor bed was situated at one end of the reactor (as shown in Figure 3.2) and a perforated plate was embedded at the bottom of the bed for the uniform distribution of the nitrogen gas to the fluidized sand bed. The reactor consisted of a vertical split furnace with three heated zones, and the temperature of the experiments was monitored with a K-type thermocouple. The temperature calibration was conducted to estimate errors in reaction temperature, which were  $\pm 5\%$ .

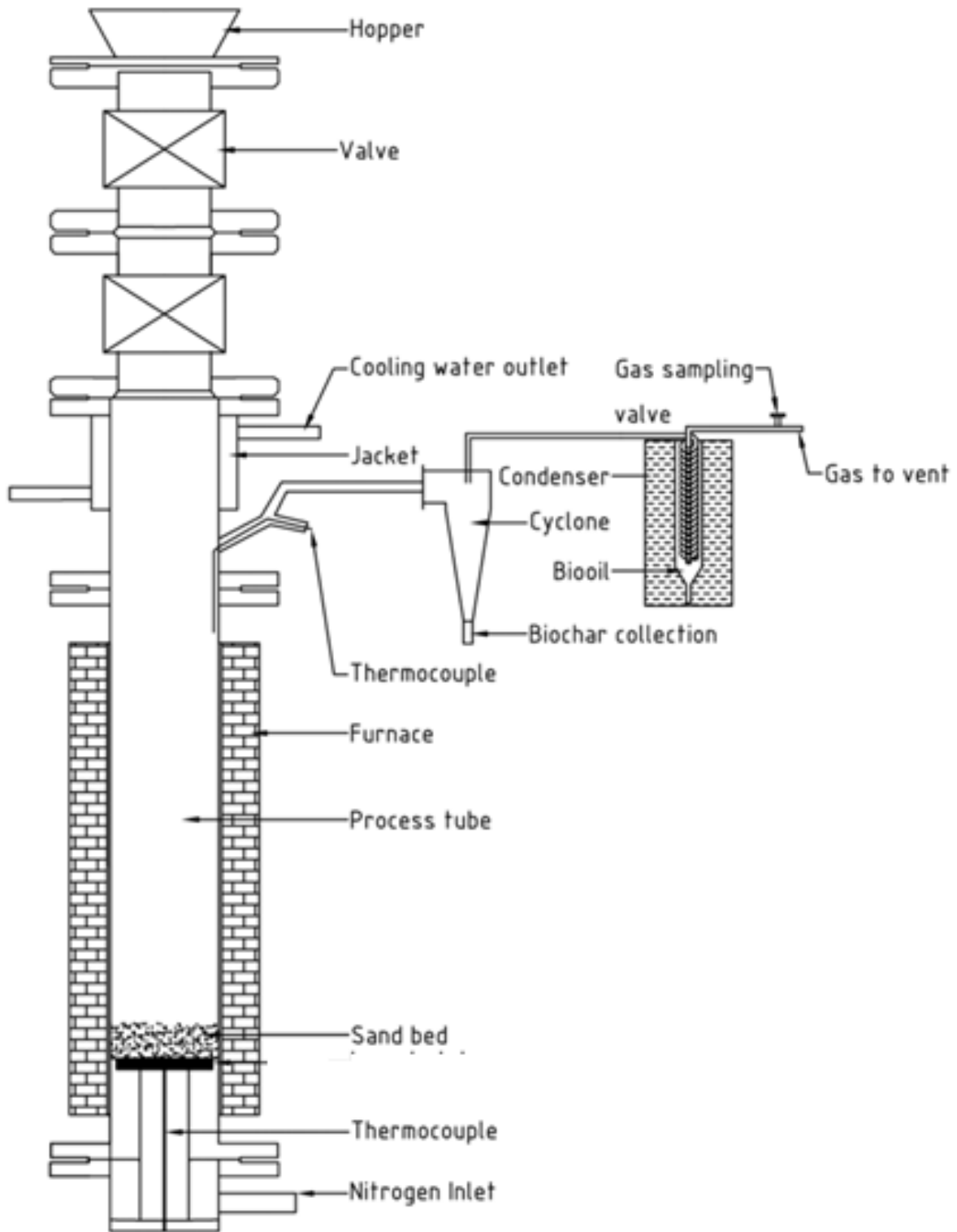


Figure 3.2, Schematic diagram of a fluidized bed reactor

The end products from these fast pyrolysis experiments were bio-oil, non-condensable gases, and biochar. All the experiments were carried out for a range of temperatures (400 – 520 °C) and three particle size distributions for all four biomass feedstocks. Biochar was collected from the reactor bed and the biochar collector of the cyclone separator. After biochar separation, pyrolysis vapor was passed through a series of condensers that were placed in a bucket of ice and water for proper condensation. Finally, non-condensable gases were passed to the vent.

In the fluidized bed reactor, 250 g of sand with a mean particle size of 230  $\mu\text{m}$  was used as the bed material, and nitrogen, the fluidizing medium, was introduced from the bottom of the reactor. The minimum fluidization velocity of the sand was calculated using Wen and Yu's correlation (Wen & Yu, 1966), 5 L  $\text{min}^{-1}$  at room temperature. 50 g of biomass was introduced into the reactor after the targeted temperature was reached in the reactor. It is important to note that this study focused on comparing kinetics from both the fluidized bed and the TGA study; therefore, only the biochar amount was estimated and other products were not reported.

#### *Arrhenius model*

To compare the kinetic parameters obtained in the TGA with fluidized bed, global  $E_a$  was calculated from the fluidized bed pyrolysis data. To calculate  $E_a$ , first order reaction kinetics was considered, as shown below:

$$-\frac{dm}{dt} = km \tag{10}$$

$$\int_{M_0}^{M_t} \frac{dm}{m} = \int_0^t -kdt \tag{11}$$

$$M_t = M_0 e^{-kt} \quad (12)$$

where  $M_t$  is biochar remaining after time  $t$  (kg)

$M_0$  is the biomass fed to the reactor (kg)

$t$  is time (min)

$k$  is the rate constant for the first order reaction, which can be estimated from Equation (4).

## 3.4 Results and Discussion

### 3.4.1 *Thermogravimetric Analysis*

#### 3.4.1.1 *Thermal degradation of biomass feedstocks in TGA*

This study conducted a thermogravimetric analysis of four different lignocellulosic biomass feedstocks: aspen, spruce, wheat straw, and corn stover. Figure 3.3 shows the TGA thermograms of the four feedstocks, while Figure 3.4 shows the derivative thermogravimetric (DTG) curves for a heating rate of  $10 \text{ }^\circ\text{C min}^{-1}$  in a nitrogen-controlled atmosphere for woody biomass (spruce and aspen) and agricultural residues (wheat straw and corn stover). DTG plot is the quantitative representation of TGA thermograms in terms of decomposition rate, pyrolysis zones with peak, peak temperature and the temperature ranges for the corresponding pyrolysis zone.

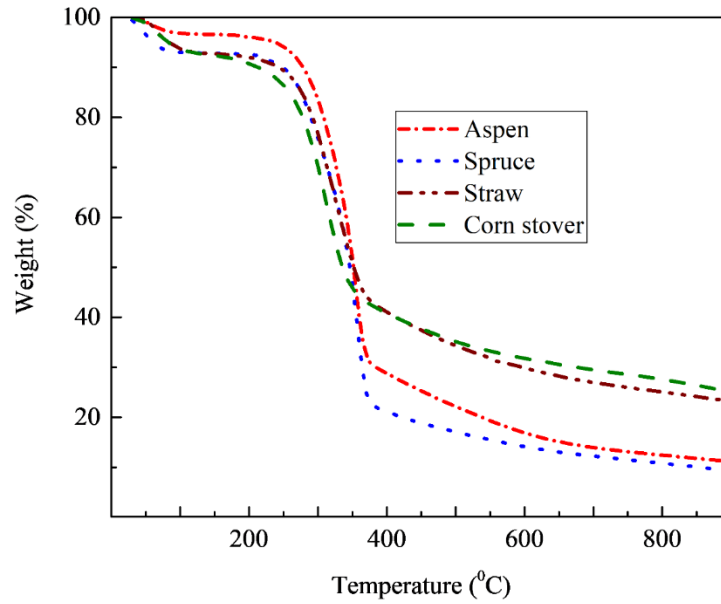


**Figure 3.3. TGA curves of four different biomass samples as a function of temperature at a heating rate of  $10^{\circ}\text{C min}^{-1}$  in nitrogen atmosphere**

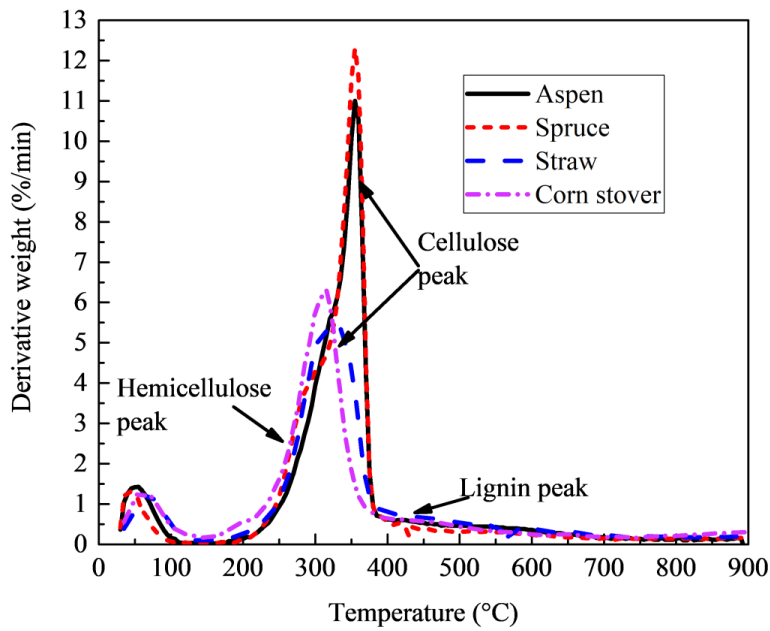


**Figure 3.4. Detailed DTG curves of spruce and aspen as a function of temperature at a heating rate of  $10^{\circ}\text{C min}^{-1}$  in nitrogen atmosphere**

Figure 3.5 shows the detailed distribution of the three stages in the pyrolysis process in a nitrogen atmosphere. Table 3.3 summarizes the results of the thermal degradation for the four feedstocks at a heating rate of  $10\text{ }^{\circ}\text{C min}^{-1}$ . For all four feedstocks, these three zones were repeated, as can be observed in TGA thermograms and DTG plot (Figure 3.3 and 3.4). Stage 1 represents the moisture removal and the percentage weight losses at this stage for spruce, aspen, wheat straw, and corn stover were 7%, 4%, 6.3%, and 6.4%, respectively. Biomass dehydration took place between room temperature and  $110\text{ }^{\circ}\text{C}$  which corresponds to the first peak in the DTG plot (see Figure 3.4).

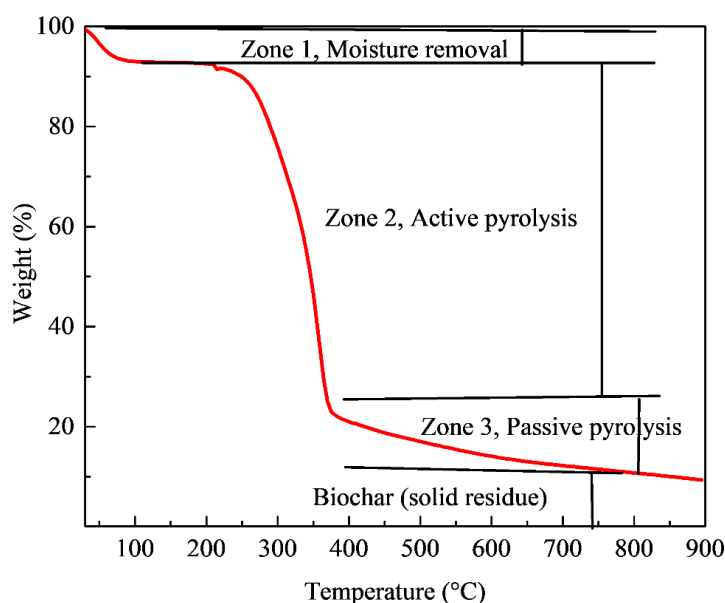


**Figure 3.5. The TGA curve of spruce with detailed thermal decomposition zones as a function of temperature at a heating rate of  $10\text{ }^{\circ}\text{C min}^{-1}$  in nitrogen atmosphere**

After moisture removal, active pyrolysis started, and the majority of the weight loss occurred at this stage. The active pyrolysis temperature varied with the feedstock and is given in Table 3.3. The onset temperature of stage 2 was between  $180\text{ }^{\circ}\text{C}$  and  $200\text{ }^{\circ}\text{C}$  for all feedstocks. The peak temperatures, where the rate of devolatilization was higher, were  $358\text{ }^{\circ}\text{C}$ ,  $371\text{ }^{\circ}\text{C}$ ,  $317\text{ }^{\circ}\text{C}$ , and  $305\text{ }^{\circ}\text{C}$ , respectively, for aspen, spruce, wheat straw, and corn stover. The decomposition rates for these feedstocks were  $12.3\text{ wt}\% \text{ min}^{-1}$ ,  $11\text{ wt}\% \text{ min}^{-1}$ ,  $5.5\text{ wt}\% \text{ min}^{-1}$ , and  $6.3\text{ wt}\% \text{ min}^{-1}$ , respectively

which is shown in the DTG plot. The rate of devolatilization (decomposition rate) for woody biomass (aspen and spruce) was much higher than that of agricultural residue (wheat straw and corn stover) because of high volatiles content and low ash content. The difference in peak temperature for different feedstocks can also be related to the elemental composition of the biomass. From the composition and chemical analysis, it can be seen that carbon content and volatiles were lower for agricultural residues, so the onset temperature active pyrolysis zone for agricultural residue was started a little ahead of temperature woody feedstock. In the active pyrolysis zone, one big peak with a small shoulder at the starting point of can be observed clearly in the Figure 3.4 for all the feedstocks, although the peaks were more distinct for woody biomass. The small shoulder represented the decomposition of the hemicellulose present in the feedstocks, which usually occurred at low temperature between 200 – 250 °C (Damartzis et al., 2011; Garcia-Maraver et al., 2013). The cellulose decomposition of the biomass was shown by the big peak of a stage-two devolatilization zone. The decomposition of hemicellulose and cellulose was distinctly visible in the DTG plot of aspen and spruce. The area under shoulder was lower than under peak 2 because cellulose was the dominating composition compared to hemicellulose and lignin (Burhenne et al., 2013). Hemicellulose decomposition started around 200 - 250 °C followed by cellulose decomposition, which initiated just after that and continued till 400 – 450 °C depending on the feedstock.

**Table 3-3. Peak temperature, range of active pyrolysis, and rate of decomposition of biomass samples from DTG plot**

Biomass feedstock	Moisture loss (wt%)	Onset of devolatilization (°C)	Temperature range of active pyrolysis (°C)	Peak temperature, $T_m$ (°C)	Maximum rate of decomposition (wt% min <sup>-1</sup> )	Volatiles evaporated (%wt)	Solid left (wt%)
Aspen	7.0	195	195-420	358	12.3	70.0	9.4
Spruce	4.0	200	200-415	371	11.1	66.5	11.2
Wheat straw	6.3	170	170-390	317	5.5	51.3	23.3
Corn stover	6.4	180	180-385	305	6.3	48.7	25.3

The third zone on the TGA thermograms was passive pyrolysis. After the end of the second stage, the third stage started and was basically the lignin decomposition region (Damartzis et al., 2011; Garcia-Maraver et al., 2013). In this zone, the total degradation and rate of thermal decomposition were low and continued to 900 °C. The decomposition rate was significant at 400-600 °C for all the feedstocks in this zone and above that decomposition was very low. The solids left at the end of the reaction were biochar. The amount of biochar at the end of the reaction was 9.4, 11.2, 23.3, and 25.3 wt%, respectively, for spruce, aspen, wheat straw, and corn stover. The biochar for the woody biomass was considerably lower than for wheat straw and corn stover due to the higher ash content of agricultural residues.

#### *3.4.1.2 Effect of heating rate*

The effect of heating rate on the TGA and the DTG for spruce softwood is illustrated in Figure 3.6 and 3.7, respectively. The response of all the feedstocks to the different heating rates was similar to that of spruce. From these figures, it can be observed that heating rate affected the TGA and the DTG curves, position of peak temperature, biochar yield, and decomposition rate at peak temperature. All the data points in both curves shifted towards the right with an increase in heating rate and the amount of biochar remaining was 9.1 wt%, 8.0 wt%, 4.5 wt%, and 1.2 wt%, respectively, for heating rates of 15 °C min<sup>-1</sup>, 10 °C min<sup>-1</sup>, 5 °C min<sup>-1</sup>, and 2 °C min<sup>-1</sup>. The difference in the amount of biochar was due to the heat transfer and reaction time at different heating rates. For a higher heating rate, to reach a target temperature (900°C), the time required was far lower than for a low heating rate (residence time: 60 min for 15 °C min<sup>-1</sup> and 450 min for 2°C min<sup>-1</sup>). Hence, at a lower heating rate, more than sufficient reaction time was available for the structural decomposition of the biomass (cellulose, hemicellulose and lignin) compared to a high heating rate for the same feedstock at the same temperature. At lower heating rate, it gets more residence time so that temperature can reach to the core of the biomass to decompose, including secondary pyrolysis reactions of tar/gas with char. Therefore, the solid remained was lowest at 2°C/min compare to other heating rate. This observation can be confirmed from the DTG plot, which shows the temperature required for the decomposition of the material per minute was quite high at 15 °C min<sup>-1</sup> (17.7°C min<sup>-1</sup>) and vice versa for the 2°C min<sup>-1</sup> (2.2 °C min<sup>-1</sup>). At a low heating rate, nitrogen gas took a long time to reach equilibrium with the furnace temperature and, due to the long reaction

time available; pyrolysis reaction was completed and yielded almost negligible biochar. These conclusions were completely aligned with those in the literature (Mehrabian et al., 2012; Salin & Seferis, 1993).

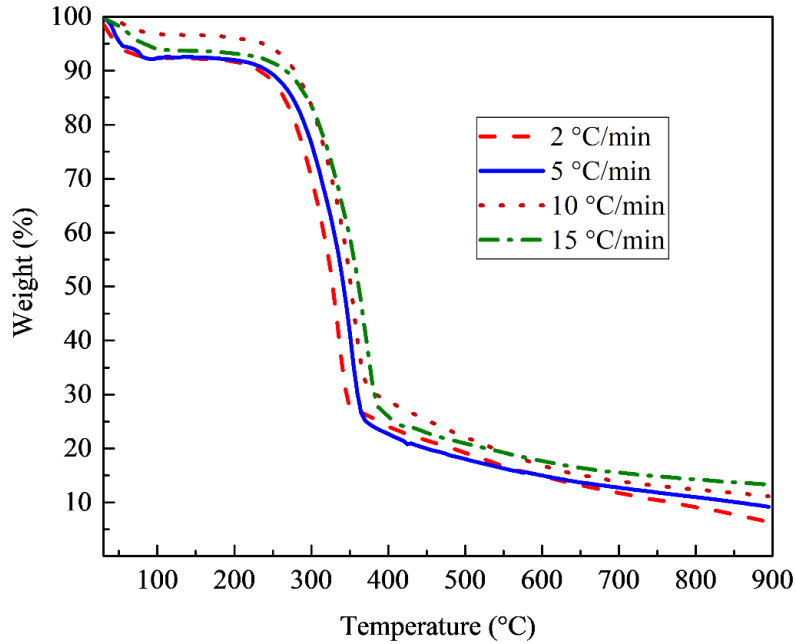


**Figure 3.6. TGA curves of spruce at four different heating rates**

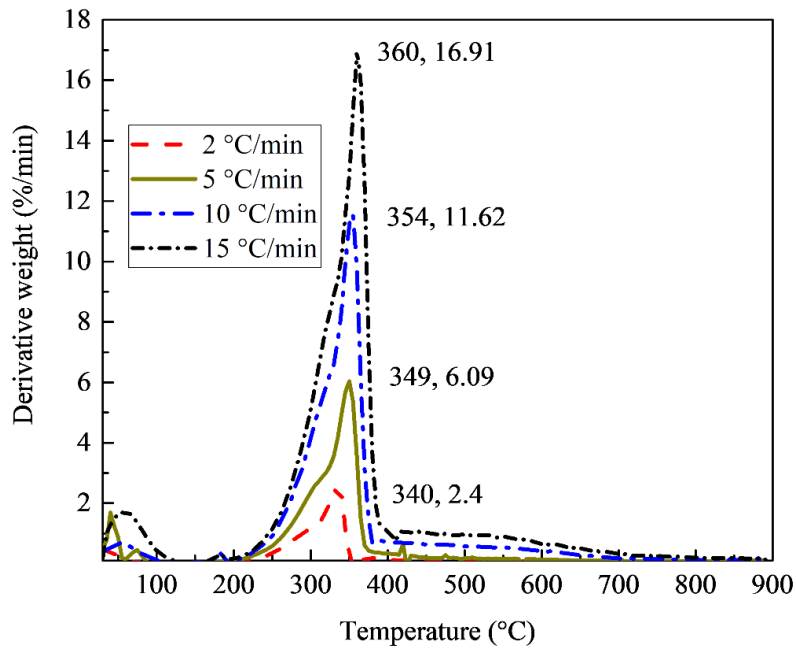


**Figure 3.7. DTG curves of spruce at four different heating rates**

### 3.4.1.3 Pyrolysis kinetics from TGA

The kinetic parameters from the TGA were estimated for each biomass sample using the model-free FWO method. Figure 3.8 shows the FWO plot of spruce hardwood at different conversion. The trends of the other biomass samples were similar to those of spruce for this method.  $E_a$  and  $A$  were estimated from the slope and intercepts of the FWO plot respectively. Figure 3.9 shows the variation of  $E_a$  with conversion for all the biomass feedstocks.

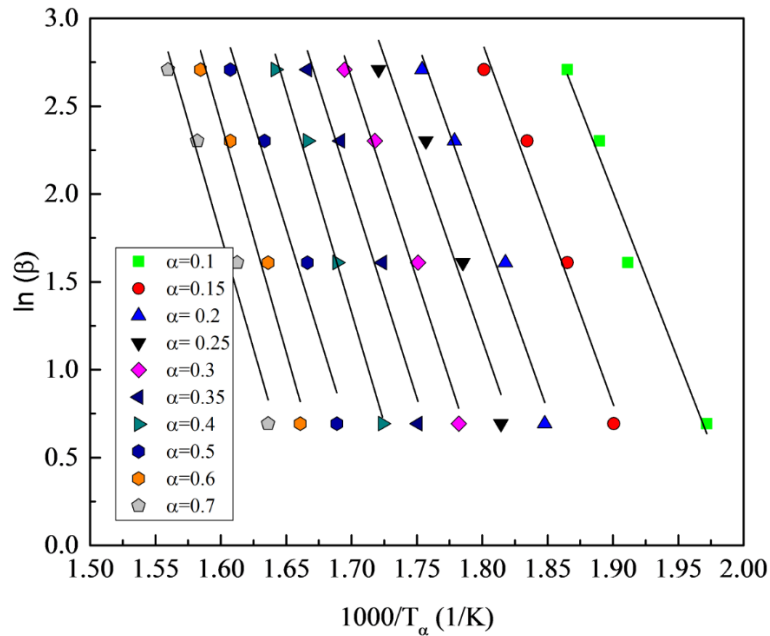
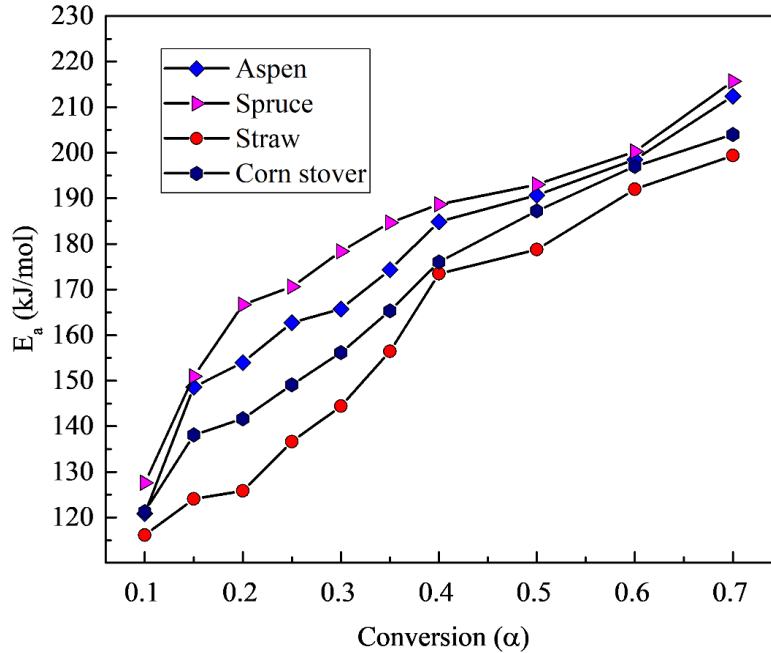


Figure 3.8. FWO plot of spruce hardwood for a range of conversions



**Figure 3.9. Variation of  $E_a$  with conversion using FWO method**

Kinetic parameters were estimated from the FWO method for all the biomass samples using Equation (9) for a particular value of conversion,  $\alpha$ . From Figure 3.9 it can be observed that the activation energy is monotonously increasing with conversion (120-220 kJ mol<sup>-1</sup>). Therefore, it can be predicted that the remaining biomass becomes more refractory (harder to decompose) with pyrolysis at different conversions. This agrees with the fact that lower  $E_a$  is required for decomposition of cellulose and hemicellulose than lignin (Quan et al., 2016; Slopiecka et al., 2012). The calculated average squares of the correlation coefficients,  $R^2$ , were higher for all the cases and were from 0.98 -0.99. For all the feedstocks, Arrhenius constant varied between 1E+7 min<sup>-1</sup> – 3E+12 min<sup>-1</sup>.

From Figure 3.9, it can be noted that the  $E_a$  of the feedstocks lies in the range of 110 -215 kJ mol<sup>-1</sup>. The  $E_a$  for the woody biomass is found to be higher than the agricultural residues (herbaceous biomass). The variation of  $E_a$  for different biomasses is related to the chemical composition in terms of cellulose, lignin, and hemicellulose. The woody biomass feedstocks have higher lignin

content and lignin is a complex and high molecular weight molecule, it needs high  $E_a$  to decompose (Burhenne et al., 2013). Huang et al. (1998) studied the thermal degradation of cellulose and Lv et al. (2010) investigated the kinetics of hemicellulose present in biomass. They reported that the  $E_a$  required to decompose these materials depends on the quantity and molecular structure of the material present in the biomass. As wheat straw contains less cellulose than woody biomass and corn stover, the required  $E_a$  is lower than in the aforementioned feedstocks.

### 3.4.2 *Fast Pyrolysis in Fluidized Bed*

#### 3.4.2.1 *Biomass conversion with temperature and particle size*

The effects of temperature and particle size distribution on the decomposition of biomass to solid residue were studied in a fluidized bed reactor for several lignocellulosic Canadian biomass feedstocks. Figure 3.10 shows ranges of biomass conversion with temperature for all the feedstocks at a fixed particle size of 0.425 – 1mm. The selected temperature range was 400 - 520°C was for all the feedstocks. Particle size distribution was also tested for each feedstock at 490°C and is shown in Figure 3.11 for the conversion of biomass. When the temperature increases, the decomposition of biomass to volatiles starts and biochar is obtained as the leftover. At 400°C, biomass conversion by weight was 57%, 56%, 51%, and 50% for aspen, spruce, corn stover, and wheat straw, respectively. Biomass conversion was low due to insufficient  $E_a$  at low temperatures and with a further increase in temperature, all the volatiles came out. The highest biomass conversion by weight was 91%, 92%, 87%, and 84% for aspen, spruce, corn stover, and wheat straw, respectively. As woody biomass contains more volatiles and less ash than does agricultural residue, higher biomass conversion was achieved. The higher decomposition rate of smaller particle sizes could be attributed to their larger surface area and thus higher heating rates. The variation of biomass conversion with particle size was between 2-4 wt% for all the feedstocks which had significantly less effect on the estimation of kinetic parameter for the considered particle size distribution for the fluidized bed reactor analysis (Heidari et al., 2014; Wang et al., 2005). Of the parameters temperature and particle size, temperature had a considerable effect on biomass conversion and particle size distribution had minimal effect.

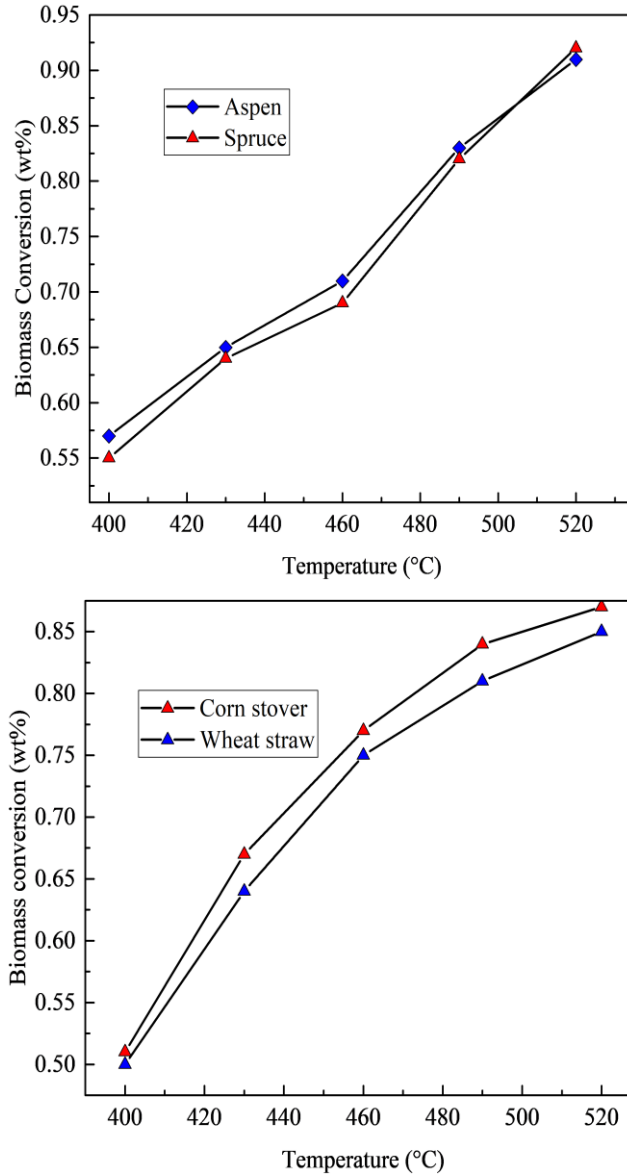


**Figure 3.10. Effects of temperature on biomass conversion in the fluidized bed reactor at a fixed particle size (0.425 – 1mm): (a) aspen and spruce and (b) corn stover and wheat straw**

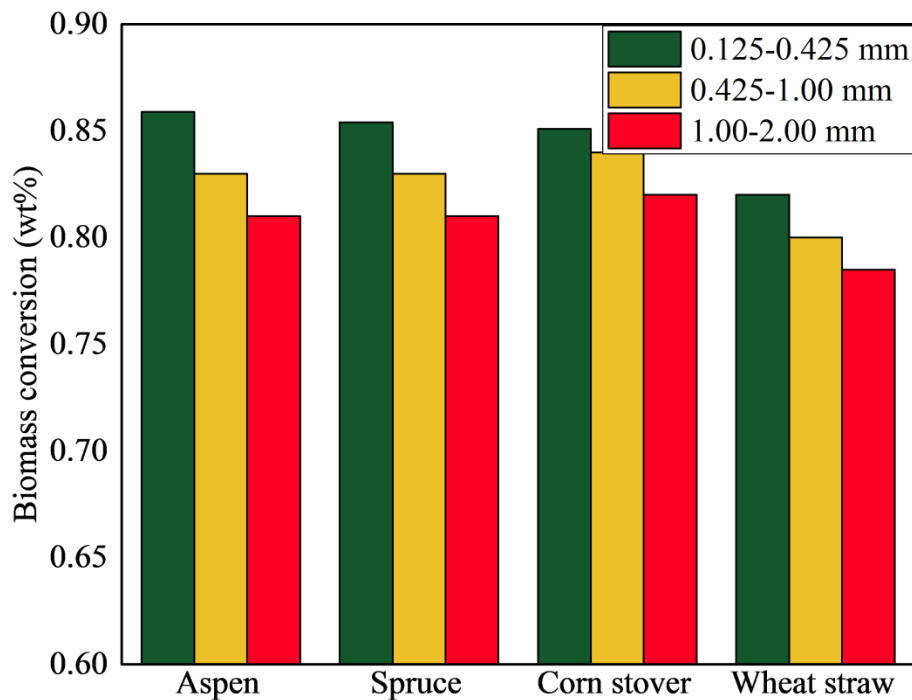


**Figure 3.11. Effects of particle size distribution on biomass conversion at 490 °C in the fluidized bed reactor**

#### 3.4.2.2 Estimation of kinetic parameters from the fluidized bed reactor

Figure 3.12 shows the plots between  $\ln(k)$  and  $1/T$  for aspen, spruce, wheat straw, and corn stover. It is interesting to observe that for all the feedstocks, this plot was a straight line.  $E_a$  was calculated from the slope and the Arrhenius constant was calculated from the intercept. Table 3.4 compares the global  $E_a$  from both the fluidized bed reactor and the TGA analysis and shows that the difference in  $E_a$  was within 7 – 12 kJ mol<sup>-1</sup>. The expected global  $E_a$  required in fluidized bed reactor was lower than the TGA due to high heating rate, method used for kinetic analysis and biomass conversion. An increase and decrease in particle size had small effect on biomass conversion (within 2-4% of the conversion) (see Figure 3.11). Heidari et al., (2014) investigated variations of pyrolysis products for three average particle sizes – 1.5, 2.4 and 3.5 mm – at 450°C and reported that biomass conversion decreased from 87 to 83 wt% with an increase in particle size. Wang et al.,(2005) also studied the effect of particle size distribution on biochar yield for a wide range, from 0.4 mm to 17 mm. They also concluded that biochar yield increased with an increase in particle size. The variation in yield was significant after an average diameter of 2mm, but for a lower average particle size of less than 2 mm, the change in yield was minimal, as reported by

Heidari et al, (2014). For this study, the selected average particle diameter ranges were 0.27 – 1.5 mm and biomass conversion was between 2 and 4 wt%, which is in good agreement with the literature. As kinetic parameters are a function of temperature and conversion, the selected range of particle sizes did not affect the  $E_a$  significantly.

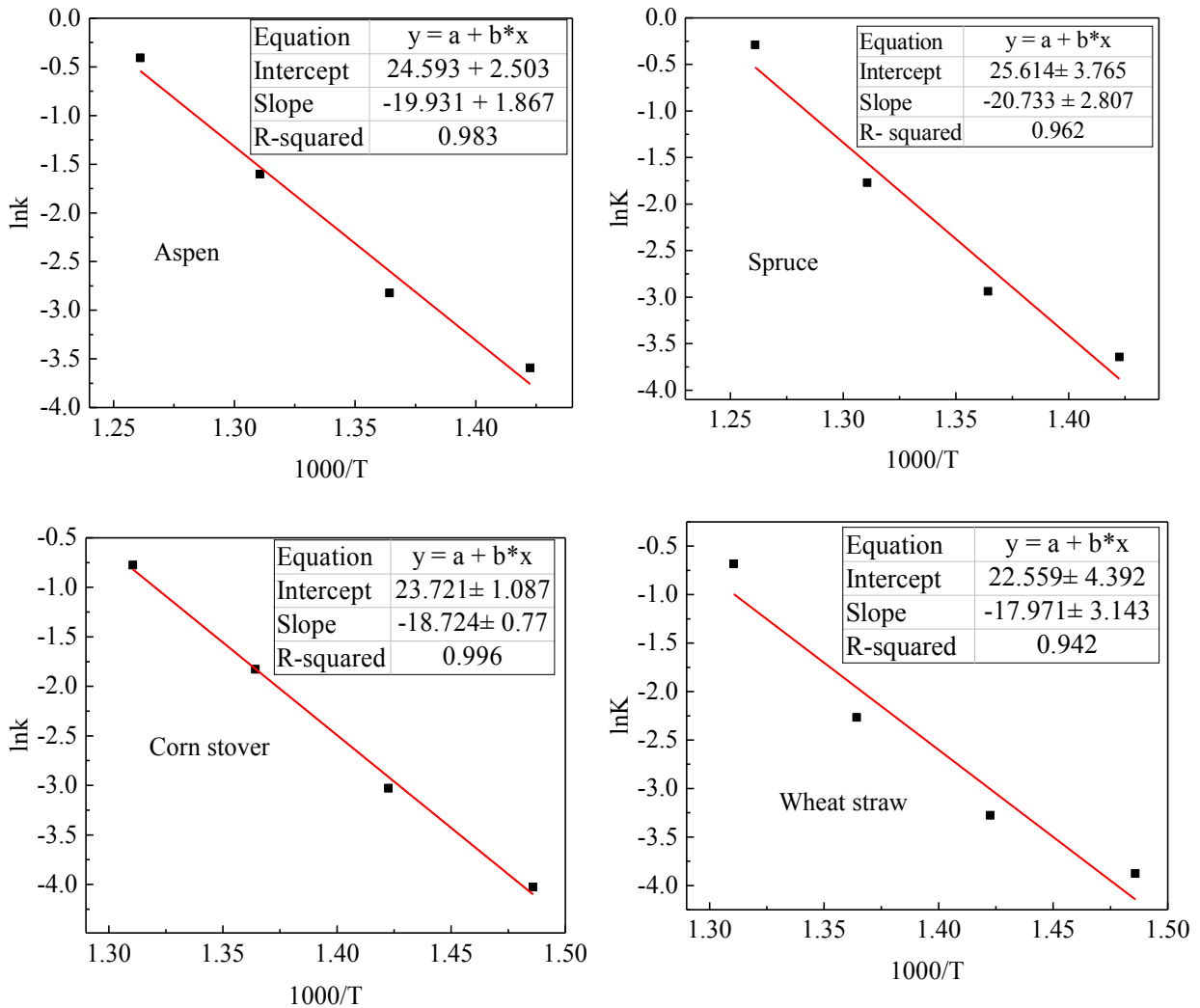


**Figure 3.12. Prediction of  $E_a$  from the fluidized bed reactor for (a) aspen, (b) spruce, (c) corn stover, and (d) straw**

**Table 3-4. Comparison of  $E_a$  from the TGA and fluidized bed reactor**

Feedstock	$E_a$ (kJ mol <sup>-1</sup> )	
	FWO method	Fluidized bed kinetics
Spruce	180.4	168.8
Aspen	173.2	160.1
Wheat straw	158.7.	150.6
Corn stover	164.5	157.3

### **3.5 Comparison of Predicted Biomass Conversion in Fluidized Experiments Using Kinetics from the TGA**

The global kinetic parameters obtained from the TGA estimated from FWO method (average of all parameters from complete pyrolysis). These kinetic parameters were applied to the fluidized bed data to calculate biomass conversion at different temperatures and predicted conversions were compared with the actual biomass conversion in the fluidized bed data. Figure 3.13 compares the predicted biomass conversion with the experimental (fluidized bed). It fitted well at high temperatures for the estimation of biomass conversion. This is because biomass conversion at high temperatures in fluidized bed was close to the conversions in TGA. At lower temperatures, predicted biomass conversion was low compared to the experimental results. The reason is that the  $E_a$  at lower conversion is lower (as shown in Figure 3.9) from iso-conversional kinetics according to the FWO method. The prediction of the biomass conversions in fluidized bed at lower temperatures were improved significantly, when  $E_a$  from the FWO method (shown in Figure 3.9) corresponding to lower conversions from fluidized bed were used. The variation between experimental and corrected predicted biomass conversion was less than 4% by weight. For aspen feedstock, this variation was around 10% by weight at 430°C.

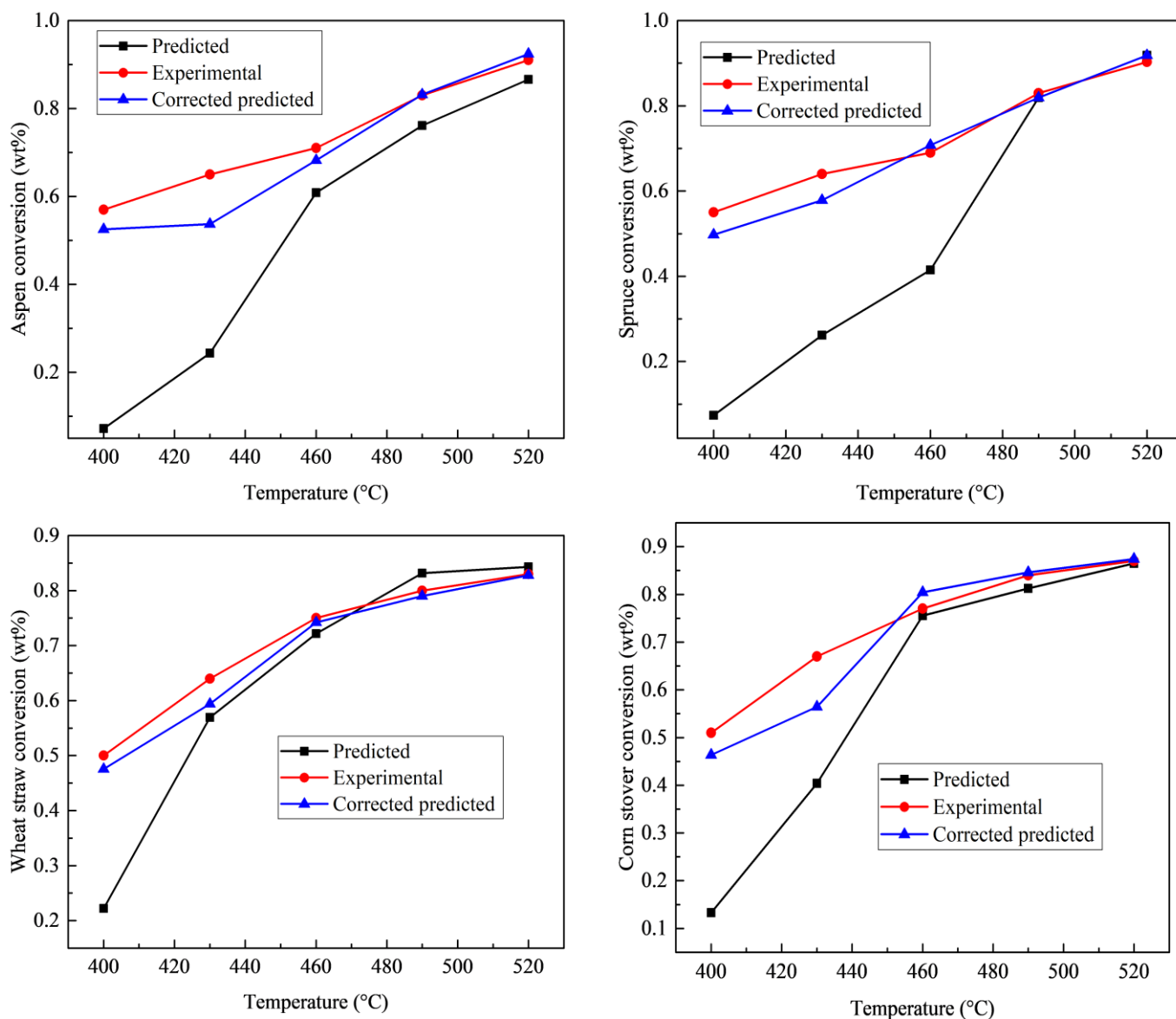


**Figure 3.13. Predicted, experimental, and corrected predicted biomass conversion for (a) aspen, (b) spruce, (c) straw, and (d) corn stover.**

### 3.6 Comparison with Other Kinetic Studies in the Literature

In the literature,  $E_a$  is calculated by other researchers in different experimental conditions and for different varieties of feedstock.  $E_a$  varies from one study to the next (see Table 3.5). The reason is differences in percentages of chemical composition (of cellulose, hemicellulose, and lignin),

experimental environment (gas type, temperature, heating rate, and particle size), and kinetic methods. For the same feedstock,  $E_a$  varies depending on the experimental conditions and the method used to calculate kinetic parameters. Therefore, studying the kinetic properties of different individual feedstocks is essential.

**Table 3-5. Comparison of  $E_a$  results from the literature**

<b>Feedstock</b>	<b>Method</b>	$E_a$ (kJ mol <sup>-1</sup> )	<b>Reference</b>
Corn stover and wheat straw	Integral iso-conversional method	182 -273.6 180.8 -287	(Wu et al., 2014)
Hybrid poplar	Kissinger, KAS, and FWO	158	(Slopiecka et al., 2012)
Woodchip	Iso-conversional method	190 -217	(Gasparovic et al., 2010)
Natural fibre	Kissinger, Friedman, FWO, and modified Coats-Redfern methods	150 – 220	(Yao et al., 2008)
Aspen	FWO	138-213	
Spruce	FWO	150-220	This study
Corn stover	FWO	110-210	
Wheat straw	FWO	116-207	

### 3.7 Conclusions

This study investigated the thermal decomposition characteristics and kinetic parameters of four different types of lignocellulosic biomass available in Canada – aspen hardwood, spruce softwood, wheat straw, and corn stover – using both a TGA and a fluidized bed reactor. The TGA experiments were performed under an inert nitrogen atmosphere from room temperature to 900 °C for four heating rates (15 °C min<sup>-1</sup>, 10 °C min<sup>-1</sup>, 5 °C min<sup>-1</sup>, and 2 °C min<sup>-1</sup>). In the fluidized bed reactor, biomass pyrolysis was carried out at 400-520 °C.

The iso-conversional activation energy,  $E_a$ , was calculated from the TGA using FWO method. The kinetic parameters were also calculated from the fluidized bed reactor data using Arrhenius model. Then the global kinetic parameters from the TGA were used to predict the decomposition of biomass to biochar and the results were compared with the experimental biochar left in the fluidized bed reactor at different temperatures. The major conclusions drawn from this study are listed below.

- The activation energy increased with conversion levels for all the biomasses from the TGA using isoconversional FWO method.
- It was observed that the difference in global  $E_a$  from the TGA for complete conversion and  $E_a$  from the fluidized bed reactor were between 7-12  $\text{kJ mol}^{-1}$ .
- The global kinetic parameters obtained from overall TGA data accurately predicted biochar yield at higher fluidizing temperatures, i.e., above 460 °C. The variation in biomass conversion was less than 1 wt% and was not the same as conversions at lower temperatures.
- At lower fluidization temperatures (i.e., below 460 °C), the kinetic parameters obtained by the FWO method (with TGA data) with corresponding lower conversion levels, the biomass conversion in the fluidized bed was predicted within 2-3%.
- The particle size distribution tested (0.125-2.0mm) resulted in variation within 4-5% of the biomass conversion.

This study helped fill the connection between the TGA and fluidized bed experiments in terms of the analysis of kinetic parameters. In this study, we concluded that information from TGA can be useful to predict the useful kinetic parameters for the biochar yields in fluidized bed experiments within the ranges of parameters (ie particle size distribution and temperature) investigated. This is useful to decide the temperature range, and corresponding biomass conversion which can be further help

## References

- Abdelouahed, L., Leveneur, S., Vernieres-Hassimi, L., Balland, L., Taouk, B. 2017. Comparative investigation for the determination of kinetic parameters for biomass pyrolysis by thermogravimetric analysis. *Journal of Thermal Analysis and Calorimetry*, **129**(2), 1201-1213.
- Bilba, K., Savastano Junior, H., Ghavami, K. 2013. Treatments of non-wood plant fibres used as reinforcement in composite materials. *Materials Research*, **16**(4), 903-923.
- Burhenne, L., Messmer, J., Aicher, T., Laborie, M.-P. 2013. The effect of the biomass components lignin, cellulose and hemicellulose on TGA and fixed bed pyrolysis. *Journal of Analytical and Applied Pyrolysis*, **101**, 177-184.
- Burton, A., Wu, H. 2017. Influence of biomass particle size on bed agglomeration during biomass pyrolysis in fluidised bed. *Proceedings of the Combustion Institute*, **36**(2), 2199-2205.
- Ceylan, S., Topçu, Y. 2014. Pyrolysis kinetics of hazelnut husk using thermogravimetric analysis. *Bioresource Technology*, **156**, 182-188.
- Chandrasekaran, A., Ramachandran, S., Subbiah, S. 2017. Determination of kinetic parameters in the pyrolysis operation and thermal behavior of *Prosopis juliflora* using thermogravimetric analysis. *Bioresource Technology*, **233**(Supplement C), 413-422.
- Choi, J.H., Kim, S.-S., Ly, H.V., Kim, J., Woo, H.C. 2017. Effects of water-washing *Saccharina japonica* on fast pyrolysis in a bubbling fluidized-bed reactor. *Biomass and Bioenergy*, **98**, 112-123.
- Damartzis, T., Vamvuka, D., Sfakiotakis, S., Zabaniotou, A. 2011. Thermal degradation studies and kinetic modeling of cardoon (*Cynara cardunculus*) pyrolysis using thermogravimetric analysis (TGA). *Bioresource Technology*, **102**(10), 6230-6238.
- Demirbaş, A. 1997. Calculation of higher heating values of biomass fuels. *Fuel*, **76**(5), 431-434.
- Flynn, J.H., Wall, L.A. 1966. A Quick Direct Method for Determination of Activation Energy from Thermogravimetric Data. *Journal of Polymer Science Part B-Polymer Letters*, **4**(5pb), 323-&.
- Garcia-Maraver, A., Salvachúa, D., Martínez, M.J., Diaz, L.F., Zamorano, M. 2013. Analysis of the relation between the cellulose, hemicellulose and lignin content and the thermal behavior of residual biomass from olive trees. *Waste Management*, **33**(11), 2245-2249.

- Gasparovic, L., Korenova, Z., Jelemensky, L. 2010. Kinetic study of wood chips decomposition by TGA. *Chemical Papers*, **64**(2), 174-181.
- Goyal, H.B., Seal, D., Saxena, R.C. 2008. Bio-fuels from thermochemical conversion of renewable resources: A review. *Renewable and Sustainable Energy Reviews*, **12**(2), 504-517.
- Harun, N.Y., Afzal, M.T. 2010. Thermal decomposition kinetics of forest residue. *Journal of Applied Sciences*, **10**(12), 1122-1127.
- Heidari, A., Stahl, R., Younesi, H., Rashidi, A., Troeger, N., Ghoreyshi, A.A. 2014. Effect of process conditions on product yield and composition of fast pyrolysis of *Eucalyptus grandis* in fluidized bed reactor. *Journal of Industrial and Engineering Chemistry*, **20**(4), 2594-2602.
- Hu, M., Chen, Z., Wang, S., Guo, D., Ma, C., Zhou, Y., Chen, J., Laghari, M., Fazal, S., Xiao, B., Zhang, B., Ma, S. 2016. Thermogravimetric kinetics of lignocellulosic biomass slow pyrolysis using distributed activation energy model, Fraser–Suzuki deconvolution, and iso-conversional method. *Energy Conversion and Management*, **118**(Supplement C), 1-11.
- Hu, S., Jess, A., Xu, M. 2007. Kinetic study of Chinese biomass slow pyrolysis: Comparison of different kinetic models. *Fuel*, **86**(17), 2778-2788.
- Huang, M.R., Li, X.G. 1998. Thermal degradation of cellulose and cellulose esters. *Journal of Applied Polymer Science*, **68**(2), 293-304.
- Huang, X., Cao, J.-P., Zhao, X.-Y., Wang, J.-X., Fan, X., Zhao, Y.-P., Wei, X.-Y. 2016. Pyrolysis kinetics of soybean straw using thermogravimetric analysis. *Fuel*, **169**(Supplement C), 93-98.
- Kantarelis, E., Yang, W., Blasiak, W., Forsgren, C., Zabaniotou, A. 2011. Thermochemical treatment of E-waste from small household appliances using highly pre-heated nitrogen-thermogravimetric investigation and pyrolysis kinetics. *Applied Energy*, **88**(3), 922-929.
- Li, C., Suzuki, K. 2009. Kinetic analyses of biomass tar pyrolysis using the distributed activation energy model by TG/DTA technique. *Journal of Thermal Analysis and Calorimetry*, **98**(1), 261.
- Lopez-Velazquez, M.A., Santes, V., Balmaseda, J., Torres-Garcia, E. 2013. Pyrolysis of orange waste: A thermo-kinetic study. *Journal of Analytical and Applied Pyrolysis*, **99**, 170-177.
- Lv, G.J., Wu, S.B., Lou, R.I. 2010. Kinetic Study of the Thermal Decomposition of Hemicellulose Isolated from Corn Stalk. *Bioresources*, **5**(2), 1281-1291.

- Maia, A.A.D., de Morais, L.C. 2016. Kinetic parameters of red pepper waste as biomass to solid biofuel. *Bioresource Technology*, **204**(Supplement C), 157-163.
- Mani, T., Murugan, P., Abedi, J., Mahinpey, N. 2010. Pyrolysis of wheat straw in a thermogravimetric analyzer: effect of particle size and heating rate on devolatilization and estimation of global kinetics. *Chemical engineering research and design*, **88**(8), 952-958.
- Mehrabian, R., Scharler, R., Obernberger, I. 2012. Effects of pyrolysis conditions on the heating rate in biomass particles and applicability of TGA kinetic parameters in particle thermal conversion modelling. *Fuel*, **93**, 567-575.
- Mishra, G., Kumar, J., Bhaskar, T. 2015. Kinetic studies on the pyrolysis of pinewood. *Bioresource technology*, **182**, 282-288.
- Morin, M., Pécate, S., Hémati, M., Kara, Y. 2016. Pyrolysis of biomass in a batch fluidized bed reactor: Effect of the pyrolysis conditions and the nature of the biomass on the physicochemical properties and the reactivity of char. *Journal of Analytical and Applied Pyrolysis*, **122**, 511-523.
- Muktham, R., Ball, A.S., Bhargava, S.K., Bankupalli, S. 2016. Study of thermal behavior of deoiled karanja seed cake biomass: thermogravimetric analysis and pyrolysis kinetics. *Energy Science & Engineering*, **4**(1), 86-95.
- Öhgren, K., Bura, R., Lesnicki, G., Saddler, J., Zacchi, G. 2007. A comparison between simultaneous saccharification and fermentation and separate hydrolysis and fermentation using steam-pretreated corn stover. *Process Biochemistry*, **42**(5), 834-839.
- Ozawa, T. 1965. A New Method of Analyzing Thermogravimetric Data. *Bulletin of the Chemical Society of Japan*, **38**(11), 1881-+.
- Parikka, M. 2004. Global biomass fuel resources. *Biomass and Bioenergy*, **27**(6), 613-620.
- Patel, M., Kumar, A. 2016. Production of renewable diesel through the hydroprocessing of lignocellulosic biomass-derived bio-oil: A review. *Renewable and Sustainable Energy Reviews*, **58**, 1293-1307.
- Patel, M., Oyedun, A.O., Kumar, A., Gupta, R. 2018. A Techno-Economic Assessment of Renewable Diesel and Gasoline Production from Aspen Hardwood. *Waste and Biomass Valorization*.

- Patel, M., Zhang, X., Kumar, A. 2016. Techno-economic and life cycle assessment on lignocellulosic biomass thermochemical conversion technologies: A review. *Renewable and Sustainable Energy Reviews*, **53**, 1486-1499.
- Pettersen, R.C. 1984. The chemical composition of wood. *The chemistry of solid wood*, **207**, 57-126.
- Polat, S., Apaydin-Varol, E., Pütün, A.E. 2016. Thermal decomposition behavior of tobacco stem Part II: Kinetic analysis. *Energy Sources, Part A: Recovery, Utilization, and Environmental Effects*, **38**(20), 3073-3080.
- Quan, C., Gao, N., Song, Q. 2016. Pyrolysis of biomass components in a TGA and a fixed-bed reactor: Thermochemical behaviors, kinetics, and product characterization. *Journal of Analytical and Applied Pyrolysis*, **121**(Supplement C), 84-92.
- Rosselló, T.M., Li, J., Lue, L. 2016. Kinetic models for biomass pyrolysis. *Archives of Industrial Biotechnology*, **1**(1).
- Salin, I.M., Seferis, J.C. 1993. Kinetic analysis of high-resolution TGA variable heating rate data. *Journal of Applied Polymer Science*, **47**(5), 847-856.
- Slopiecka, K., Bartocci, P., Fantozzi, F. 2012. Thermogravimetric analysis and kinetic study of poplar wood pyrolysis. *Applied Energy*, **97**, 491-497.
- Soria-Verdugo, A., Morato-Godino, A., Garcia-Gutierrez, L.M., Garcia-Hernando, N. 2017. Pyrolysis of sewage sludge in a fixed and a bubbling fluidized bed – Estimation and experimental validation of the pyrolysis time. *Energy Conversion and Management*, **144**, 235-242.
- Várhegyi, G., Antal, M.J., Jakab, E., Szabó, P. 1997. Kinetic modeling of biomass pyrolysis. *Journal of Analytical and Applied Pyrolysis*, **42**(1), 73-87.
- Varma, A.K., Mondal, P. 2016. Physicochemical characterization and pyrolysis kinetic study of sugarcane bagasse using thermogravimetric analysis. *Journal of Energy Resources Technology*, **138**(5), 052205.
- Venkatesh, M., Ravi, P., Tewari, S.P. 2013. Isoconversional Kinetic Analysis of Decomposition of Nitroimidazoles: Friedman method vs Flynn-Wall-Ozawa Method. *Journal of Physical Chemistry A*, **117**(40), 10162-10169.
- Vyazovkin, S., Wight, C.A. 1999. Model-free and model-fitting approaches to kinetic analysis of isothermal and nonisothermal data. *Thermochimica Acta*, **340-341**(Supplement C), 53-68.

- Wang, X., Kersten, S.R., Prins, W., van Swaaij, W.P. 2005. Biomass pyrolysis in a fluidized bed reactor. Part 2: Experimental validation of model results. *Industrial & engineering chemistry research*, **44**(23), 8786-8795.
- Warnecke, R. 2000. Gasification of biomass: comparison of fixed bed and fluidized bed gasifier. *Biomass and Bioenergy*, **18**(6), 489-497.
- Wen, C., Yu, Y. 1966. A generalized method for predicting the minimum fluidization velocity. *AIChE Journal*, **12**(3), 610-612.
- Wu, W.X., Mei, Y.F., Zhang, L., Liu, R.H., Cai, J.M. 2014. Effective Activation Energies of Lignocellulosic Biomass Pyrolysis. *Energy & Fuels*, **28**(6), 3916-3923.
- Yao, F., Wu, Q., Lei, Y., Guo, W., Xu, Y. 2008. Thermal decomposition kinetics of natural fibers: Activation energy with dynamic thermogravimetric analysis. *Polymer Degradation and Stability*, **93**(1), 90-98.
- Yildiz, S., Gezer, E.D., Yildiz, U.C. 2006. Mechanical and chemical behavior of spruce wood modified by heat. *Building and Environment*, **41**(12), 1762-1766.
- Zhang, H., Shao, S., Jiang, Y., Vitidsant, T., Reubroycharoen, P., Xiao, R. 2017. Improving hydrocarbon yield by two-step pyrolysis of pinewood in a fluidized-bed reactor. *Fuel Processing Technology*, **159**, 19-26.
- Zhu, Z.G., Sathitsuksanoh, N., Vinzant, T., Schell, D.J., McMillan, J.D., Zhang, Y.H.P. 2009. Comparative Study of Corn Stover Pretreated by Dilute Acid and Cellulose Solvent-Based Lignocellulose Fractionation: Enzymatic Hydrolysis, Supramolecular Structure, and Substrate Accessibility. *Biotechnology and Bioengineering*, **103**(4), 715-724.

## **Chapter 4: A Techno-Economic Assessment of Renewable Diesel and Gasoline Production from Aspen Hardwood<sup>4</sup>**

### **4.1 Introduction**

Biomass is a renewable resource that can be used in place of petroleum-based liquid-fuels, providing it is processed and upgraded using appropriate technology (Shashikantha, 2008). Currently, biomass contributes a mere 3% to the world's energy sector (Ladanai & Vinterback, 2011). According to the World Bioenergy Association, lignocellulosic biomass is underused and can be exploited and increase the bioenergy contribution to 20% by 2020 (Ladanai & Vinterback, 2011). Twenty-four percent of the world's boreal forest, is in Canada and is emerging as the future source for bioenergy (Natural Resources Canada, 2014).

Renewable diesel and biodiesel are the two transportation fuel alternatives that satisfy current regulations and policies, according to Natural Resources Canada (Ecoresources Consultants, 2012b). These biofuels have significantly different processing technologies and chemical compositions. Biodiesel is produced through the transesterification of vegetable oils from grain feedstock in the presence of catalysts (Verma et al., 2016). Biodiesel emits fewer greenhouse gas

---

<sup>4</sup> A version of this chapter has been published in *Journal of Waste and Biomass Valorization*: Patel M, Oyedun A, Kumar A, Gupta R. A techno-economic assessment of renewable diesel and gasoline production from aspen hardwood, **Waste Biomass Valorization**, 2018. 9(48) 1-16

emissions than conventional petro-fuels and has a low sulfur content; in addition, it is miscible with hydrocarbons and nontoxic, which makes it a strong contender for biofuels. However, it performs poorly at low temperatures, which limits its use in cold countries like Canada (Miller & Kumar, 2014). Renewable diesel, however, can handle the cold and is thus superior to biodiesel. Renewable diesel is produced from grains-based vegetable oil [6] as well as lignocellulosic biomass. Lignocellulosic biomass can be converted to renewable diesel through fast pyrolysis and hydroprocessing (Patel & Kumar, 2016; Wright et al., 2010; Zhang et al., 2005). Renewable diesel have similar properties to petro-diesel in terms of density, flash point, kinematic viscosity and other important fuel properties. The comparison between biodiesel, renewable diesel and petro-diesel has been previously highlighted by the same author (Patel & Kumar, 2016). Lignocellulosic biomass is a type of biomass that includes agricultural waste, forest residues, whole trees, and energy crops.

In fast pyrolysis, lignocellulosic biomass is heated to 450-600°C in a pyrolyzer in the absence of oxygen and at atmospheric pressure for a residence time of less than 2 s to produce bio-oil in a fixed bed or fluidized bed reactor (Bridgwater et al., 1999; Kim et al., 2013; Peters et al., 2014). A fluidized bed reactor is more preferred because of its better temperature distribution, low capital investment and maintenance cost, good gas-solid contact, low residence time, high heating rates, and ability to handle varieties of feedstock with wide particle size distribution (Bridgwater et al., 1999; Bridgwater, 2012; Ringer et al., 2006). Bio-oil produced from this process, in addition to being unsuitable to Canada's climate, is by nature highly viscous, acidic, and contains many oxygenated compounds, all of which makes it unsuitable either as a transportation fuel or a blend with crude oil (Chiaramonti et al., 2003). Hence this bio-oil is further treated to produce renewable diesel, through catalytic hydroprocessing, a chemical process (hydrodeoxygenation) in which oxygenated compounds are reacted with hydrogen in the presence of catalysts to produce hydrocarbons (Brown et al., 2013). The composition of renewable diesel is similar to that of petro-diesel and its cloud point can go as low as -25°C (Miller & Kumar, 2014). Existing refinery upgrading units, used for hydrodesulfurization (HDS), can be used to upgrade bio-oil to renewable diesel. These units can also be used for hydrodeoxygenation (HDO) with little modification as bio-

oil is acidic and corrosive. Therefore renewable diesel is better than biodiesel (Ecoresources Consultants, 2012a).

Techno-economic studies reflect the economic features of an entire pathway from, in this case, biomass harvesting to transportation fuel production. This pathway has two operations: the conversion of biomass to bio-oil and upgrading. There are several techno-economic assessments of bio-oil production through fast pyrolysis (Gregoire & Bain, 1994; LaClaire et al., 2004; Patel et al., 2016; Ringer et al., 2006; Rogers & Brammer, 2012), but very limited on upgrading bio-oil to transportation fuels. Bio-oil production costs depend on several factors such as feedstock type, plant capacity, reactor type, operating conditions, and vapor residence time. Different researchers have used various feedstock (wood chips, corn stover, rice straw, energy crops, etc.) and reported bio-oil production costs from 0.1 to 0.6 \$ L<sup>-1</sup> depending on operating conditions (Gregoire & Bain, 1994; LaClaire et al., 2004; Patel et al., 2016; Ringer et al., 2006; Rogers & Brammer, 2012). In this study, the suitability of Canadian aspen woodchips for bio-oil production is considered using a lab-scale fluidized bed reactor followed by process modelling and techno-economic analysis using Aspen Plus<sup>®</sup> (Aspentech, 2014; Plus<sup>®</sup>, 2015), none of which has been done to date.

Upgrading bio-oil to a transportation fuel can be carried out through hydroprocessing, a well-established technology in the refinery industry (Ward, 1993). Hydroprocessing involves two steps: hydrotreating and hydrocracking. Hydroprocessing of bio-oil is still in the demonstration stage and not yet commercialized. Limited data are available in the literature on this topic. Wright et al. conducted a techno-economic analysis on upgrading bio-oil through the fast pyrolysis of corn stover to naphtha and diesel (Wright et al., 2010). They investigated two different scenarios, one in which the hydrogen is purchased and the other in which the hydrogen is produced, and concluded that transportation fuel production is cheaper in the hydrogen purchased scenario than the hydrogen production scenario (Wright et al., 2010). Brown et al. (2013) expanded Wright et al. (2010)'s study by incorporating recent literature data in a techno-economic analysis of fast pyrolysis and hydroprocessing the same corn stover feedstock. The authors considered a 2000 t d<sup>-1</sup> facility that converted corn stover to gasoline and diesel and concluded that the fuel produced

could be competitive with petro-fuels (Brown et al., 2013). Zhang et al. (2013) investigated the economic feasibility of two bio-oil upgrading pathways: two-stage hydrotreating followed by fluid catalytic cracking and single-stage hydrotreating followed by hydrocracking for a 2000 t d<sup>-1</sup> facility. They found that the facility that used hydrotreating with fluid catalytic cracking and hydrogen production via natural gas reforming generated a higher internal rate of return (IRR).

In these studies, the authors investigated costs to produce various transportation fuels from corn stover and mixed wood using different upgrading conditions for a 2000 t d<sup>-1</sup> plant capacity. However, the effect of plant capacity variation on the production cost of transportation fuel has not been reported in the literature.

To the best of our knowledge, there is no techno-economic study on the upgrading of lignocellulosic biomass-based fast pyrolysis oil through hydroprocessing in Canada. For this analysis, 2000 t d<sup>-1</sup> biomass plant capacity is considered to produce gasoline and renewable diesel through fast pyrolysis and hydroprocessing pathway and simultaneously which can be compared with limited available results (Wright et al., 2010; Zhang et al., 2013). There is very limited understanding of the scale factors for the major unit operations involved in conversion of lignocellulosic biomass to transportation fuel through the above pathway. Therefore, the main objective of this paper is to perform a detailed techno-economic analysis of renewable diesel production through fast pyrolysis of aspen woodchips and of bio-oil upgrading via hydroprocessing through development of a process model and address the gap in knowledge in this area.

The key objectives of this study are:

- ❖ To develop a techno-economic model that evaluates the costs of producing renewable diesel and gasoline from hydroprocessing 2000 t d<sup>-1</sup> aspen woodchips
- ❖ To conduct experiment to determine the properties of biomass feedstocks and produced bio-oil from aspen woodchips

- ❖ Development of scale factor for estimation of capital cost for major unit operations involved in conversion of lignocellulosic biomass to transportation fuels
- ❖ To estimate the production costs of renewable diesel and gasoline from hydroprocessing through the fast pyrolysis of aspen woodchips
- ❖ To evaluate the economic optimum production capacity for this pathway
- ❖ To conduct economic sensitivity analyses of different bio-oil yield, delivery cost, operating cost, and capital cost parameters
- ❖ To conduct an uncertainty analysis using a Monte Carlo simulation to assess the risk associated with the production cost
- ❖ To compare the results of this study with those available in the literature

The scope of this study is a dedicated pyrolysis and hydroprocessing plant of 2000 t d<sup>-1</sup> capacity to produce renewable fuels using aspen biomass feedstock operating for 20 years. The techno-economic model involves biomass feedstock preparation, fast pyrolysis unit and hydro-processing unit (see Figure 4.1).

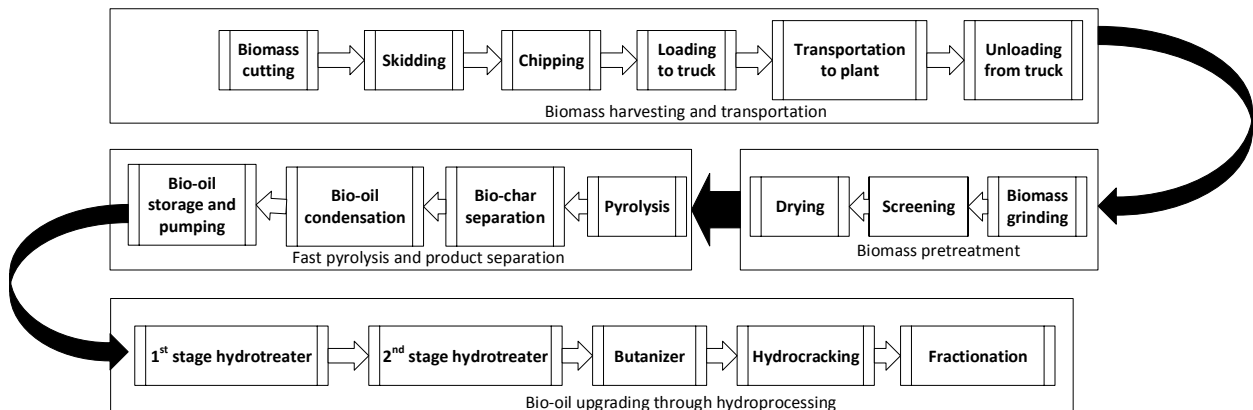


**Figure 4.1. Schematic diagram of process flow sheet for fast pyrolysis and hydroprocessing pathway**

The results of this study will help to determine the minimum production cost of transportation fuels produced from lignocellulosic biomass through hydroprocessing technology in Western Canada. In addition, the results will reflect how economically competitive this technology is with petroleum fuel.

## 4.2 Material and methods

### 4.2.1 Feedstock

Aspen woodchip (*Populus tremuloides*) is chosen as the feedstock for the fast pyrolysis process. It is supplied by a wood processing facility near Edmonton, Alberta. The woodchip's particle size is in the range of 6-10 mm. To make the feedstock suitable for pyrolysis, the feedstock is further ground to less than 2 mm using a grinder. The feedstock properties are given in the Table 4.1. A proximate analysis is conducted through thermogravimetric analysis (701, LECO, St. Joseph, MI, USA) and an ultimate analysis is carried out using an Elemental Analyzer (EA1108, Carlo Erba, Val de Reuil, France) for CHNS (carbon, hydrogen, nitrogen, and sulfur) and oxygen. All the tests are repeated three times and the average values are reported.

**Table 4-1. Proximate and ultimate analyses of aspen woodchip**

Parameter	Value
Initial moisture mass fraction (%)	50
Proximate analysis, mass fraction (%) <sup>a</sup>	
Ash	0.66
Volatile	82.97
Fixed carbon	15.96
Ultimate analysis, mass fraction (%) <sup>a</sup>	
Nitrogen	0.12
Carbon	46.97
Hydrogen	5.98
Sulfur	0
Oxygen	43.9

<sup>a</sup> All calculations are in a dry weight basis

#### 4.2.2 *Experimental set-up*

The fast pyrolysis experiments are carried out in a vertical double-valve fluidized bed reactor and the detailed about the experimental set-up is discussed in section 3.3.3 in chapter 3.

#### 4.2.3 *Characterization of products*

The main products of fast pyrolysis are bio-oil, non-condensable gases, and bio-char. Bio-oil is collected from the condensers and bio-char is collected from the cyclone and the reactor bed. The quantity of non-condensable gases is determined by subtracting the total biomass input and adding the bio-oil and bio-char. The composition of the non-condensable gases is analyzed using a micro gas chromatograph (CP 4900, Varian, CA, USA) equipped with a thermal conductivity detector (TCD). The liquid sample is analyzed using a 7890A gas chromatograph with 5975C MSD system (Aglient, CA, USA), which consists of a gas chromatograph coupled to a quadrupole mass spectrometer using a capillary column (DB-5, 30m x 0.25mm, 0.25mm, J&W Scientific, CA, USA). The composition of bio-oil and non-condensable gases is given in Table 4.2.

**Table 4-2. Composition of bio-oil and uncondensed gases from fast pyrolysis of aspen woodchip**

<b>Compound</b>	<b>Mass fraction (%)</b>
<b>Bio-oil</b>	
3-hexanone 2-methyl	2.59
3-cyclobutene 1,2 dione 3,4 dihydroxy	1.93
Phenol	8.33
2-hydroxy 3-methyl 2-cyclopenten1one	3.52
Guaiacol	8.45
1,3,5 benzenetriol	1.43
2-methoxy 4-methyl phenol	2.38
Benzoic acid	1.96
2-methoxy 4-vinyl phenol	2.06
2,6 dimethoxy phenol	8.25
Vanillin	3.14
2 methoxy 4 (1 propenyl) phenol	2.96
4 methoxy benzene ethanamine	0.75
1 (2,4,6 trihydroxyphenyl) 2-pentanone	0.88
Water	14.7
<b>Non-condensable gases</b>	
Propane	0.41
Butane	0.02
Hydrogen	0.32
Methane	2.3
Carbon monoxide	6.88
Carbon dioxide	8.64
<b>Solid</b>	
Biochar	18.1

#### 4.2.4 *Bio-oil upgrading (hydroprocessing)*

Hydroprocessing is a combination of two technologies, hydrotreating and hydrocracking, through which bio-oil is upgraded to a product similar to or better than petroleum fuels. During upgrading, the feed is initially processed in a hydrotreater unit and then the hydrotreated oil is further treated in a hydrocracker unit. Both units operate in the presence of hydrogen and catalysts. The hydrotreating unit is a primary pretreatment unit that produces stabilized bio-oil by removing heteroatoms and hydrogenates unsaturated hydrocarbons. A hydrotreater is a high pressure reactor that operates at pressures and temperatures in the range of 50-200 bar and 200-400°C, respectively (Elliott & Neuenschwander, 1997). The basic reaction in this unit is HDO as oxygen is the dominating heteroatom (compared to negligible amounts of sulfur and nitrogen atoms) in the bio-oil, which is similar to HDS in the refinery unit. In the hydrotreater, oxygen, nitrogen, and sulfur are removed in the form of water, ammonia, and hydrogen sulfide, respectively, after reacting with hydrogen in presence of a catalyst. The stabilized oil coming out of the hydrotreater is non-polar and made up of high molecular weight compounds, which need further refining. So the oil is further processed in a hydrocracker in the presence of a catalyst and hydrogen at high pressure (100-200 bar) and temperature (300-400°C) conditions. In the hydrocracker, high molecular weight compounds are broken to lower molecular weight compounds through hydrodealkylation, hydrocracking, and isomerization (Patel & Kumar, 2016). The detailed of the reaction mechanism involved in the hydroprocessing technology has been discussed in a previous study by the same author (Patel & Kumar, 2016).

In both units the catalyst plays an important role in determining the final composition of the renewable diesel. Different researchers have tried various catalysts for upgrading bio-oil ranging from transition metals to noble metals (Ardiyanti et al., 2011; Elliott et al., 2012; Gagnon & Kaliaguine, 1988; Sheu et al., 1988; Wildschut et al., 2009). A sulfided nickel molybdenum/cobalt molybdenum catalyst supported on gamma alumina is used as a benchmark catalyst for the HDO reaction as it is used in refineries for HDS to remove sulfur atoms from crude oil (Elliott & Neuenschwander, 1997; Elliott et al., 2012; Patel & Kumar, 2016; Ward, 1993). In the reported studies, the use of noble metal catalysts, ruthenium, rhodium, platinum, and palladium are widely used in hydroprocessing (Ardiyanti et al., 2011; Wildschut et al., 2009).

## 4.3 Modelling

### 4.3.1 *Process modeling*

A process model is developed using Aspen Plus<sup>®</sup> to simulate the whole pathway from biomass preparation to upgrading to the production of renewable diesel and gasoline for a 2000 dry t d<sup>-1</sup> capacity biomass facility. The developed model integrates process unit operations and economic analysis. Process modelling involves both energy and material balance between different unit operations used in the flowsheet. The property method used for this simulation is PENG ROB. The process model included equipment cost, capital cost, operating cost, and installation cost. Data for bio-oil and non-condensable gases are obtained from the lab-scale fluidized bed reactor set-up discussed in previous section. The capital costs of the equipment are extracted from Aspen Icarus and the literature (Aspentech, 2014; Peters et al., 2003; Wright et al., 2010; Zhang et al., 2013). Figure A1 to A6 in Appendix A1 show the Aspen Plus<sup>®</sup> flow diagram for fast pyrolysis and hydroprocessing technology. Finally, a sensitivity analysis is conducted to study the impact of different parameters on the production costs of renewable diesel and gasoline. The major processes considered in this model are feedstock preparation, fast pyrolysis, char collection, bio-oil condensation, and bio-oil upgrading. The block diagram of the entire process from harvesting of biomass to end products is shown in Figure 4.1 and the detailed mass flow diagram of the conversion technology (biomass pretreatment, fast pyrolysis and hydroprocessing) of prepared biomass to transportation fuels is shown in Figure 4.2 (Ward, 1993).

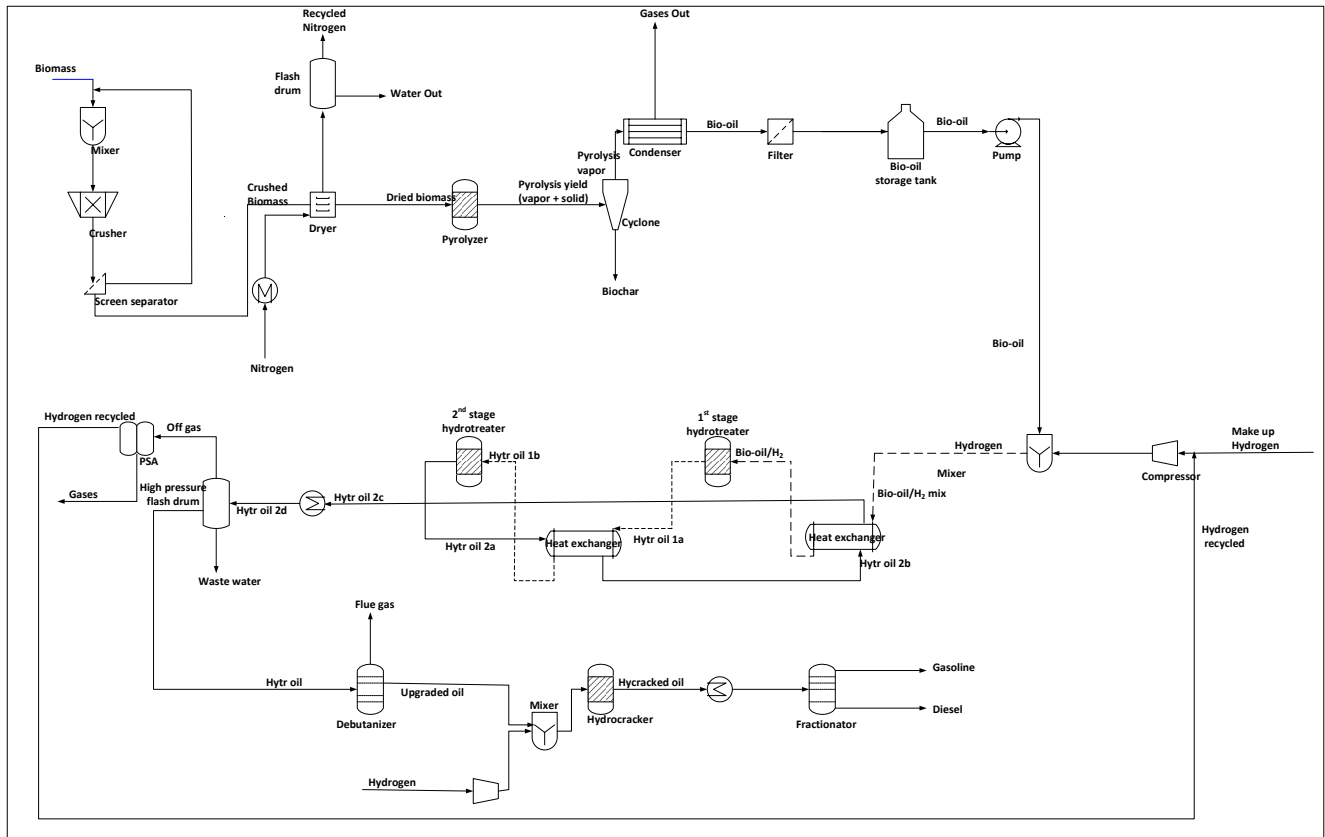


**Figure 4.2. Mass flow diagram of fast pyrolysis and hydroprocessing technology for a 2000 t d<sup>-1</sup> aspen feedstock plant**

*4.3.1.1 Feedstock preparation*

The aspen woodchips provided by the supplier are ground to meet the pyrolyzer particle size requirements. Decreasing the particle size will result in more bio-oil yield than gas and char production quantities and will also increase the required contact between sand and biomass. This process involves grinding, screening, and drying.

The as-received particle size of the aspen biomass varies from 6 to 10 mm, which is too large for fluidized bed reactor. This model employs a gyratory crusher (grinder) to grind the biomass to a particle size of less than 2 mm, which is suitable for the pyrolyzer, and any oversized biomass is passed through a rectangular screen block for further grinding.

The initial moisture mass fraction of the biomass is 50% as delivered. The moisture fraction needs to be reduced to approximately 5-7% to increase the efficiency of the pyrolyzer in terms of heat consumption and product formation. The dryer is modelled in an Rstoic block in the Aspen Plus<sup>®</sup> model and the drying takes place in presence of nitrogen .

#### *4.3.1.2 Fast pyrolysis*

Fast pyrolysis is the core of the whole pathway wherein solid feedstock is converted to a liquid product with gas and solid as byproducts. The process takes place in an atmospheric sand fluidized bed reactor at a temperature of 480°C and a low residence time, details adopted from laboratory experiments on aspen woodchips. Since the complete reaction mechanism is not available for the pyrolyzer, the Ryield reactor (this block performs the calculation based on the composition of the yield) is used to model the pyrolyzer. The composition of bio-oil, analyzed by gas chromatography-mass spectroscopy is specified in this Ryield reactor.

#### *4.3.1.3 Bio-char collection*

The vapor coming out of the pyrolyzer contains micro-sized sand and char particles that can pollute the bio-oil and affect the performance of downstream unit operations. So the outlet from the fluidized bed reactor is passed through a cyclone separator. The model employs a cyclone with 90% solid separation efficiency. The bio-char collected from the cyclone is used as the revenue in the techno-economic model. So no further modelling for bio-char is considered since no char combustor is used in the experiment. Bio-char can be further used for soil enhancement and protection of water quality in the soil, which can accordingly reduce the need for fertilizer (Canada Renewable Bioenergy Corp, 2012).

#### *4.3.1.4 Bio-oil condensation*

After the solids are removed from the pyrolysis vapor, the vapor is processed in a series of condensers to condense the bio-oil. The vapor, coming out of the pyrolyzer at a temperature of 480°C, is passed through three coolers to reduce the temperature to 40°C. This stream is then

processed in a flash column to separate the liquid phase from the non-condensable gases. The bio-oil is stored in a storage tank for further upgradation. Long storage time will deteriorate the properties of the bio-oil due to condensation and the polymerization that occurs in the bio-oil (Siriwardhana, 2013). Therefore, to reduce the risk of deterioration, it is assumed in the model that the pyrolysis plant and the hydroprocessing plant will be at the same location.

#### *4.3.1.5 Hydroprocessing and product separation*

The hydroprocessing units have separate unit operations for hydrotreating and hydrocracking. This technology is very well known in the crude refinery industry as a means of removing sulfur and nitrogen atoms from crude during upgrading to petro-fuels. So to upgrade bio-oil, the same technology is adapted. But very limited data are available for bio-oil hydroprocessing. In this study, to model the upgrading of bio-oil from aspen feedstock, the bio-oil is first passed through a two-stage hydrotreating unit in the presence of an excess amount of hydrogen. The first stage hydrotreater (also known as a mild hydrotreater) operates at temperature and pressure of 240°C and 150 atm to stabilize the bio-oil by removing the acidic compounds in the presence of a sulfided nickel-molybdenum catalyst (Elliott et al., 2009; Jones et al., 2013). The removal of heteroatoms, mainly oxygen, through hydrodeoxygenation takes place in the second hydrotreater unit, which operates at temperature 300°C and pressures at 170 atm in the presence of the same catalyst bed. Merchant hydrogen is used in both hydrotreaters.

The hydrotreated oil is further processed in the hydrocracker unit under temperature of 430 °C and pressure at 170 atm conditions in the presence of excess hydrogen as well as nickel-molybdenum supported on an alumina catalyst (Venderbosch et al., 2010). Hydrocracking and hydrodealkylation are the major reactions that break the high molecular weight compounds in the bio-oil to lower molecular weight compounds in the transportation fuel ranges (C<sub>6</sub>–C<sub>12</sub>). The process conditions of the hydroprocessing here are similar to those found in literature (Elliott et al., 2009). The hydrogen used for hydroprocessing is compressed to respective pressures applied in the hydroprocessing units using two-stage compressors.

The upgraded oil from the hydroprocessing is further processed through a series of columns to produce transportation fuels such as diesel and gasoline. In the model, we have incorporated a debutanizer and fractionation column. In the debutanizer, hydrotreated oil is processed before entering into the hydrocracker to separate light components (propane and butane) thereby improving the quality of the end products. Finally, hydrocracked oil is fed into the fractionation column to separate the diesel as bottom product and gasoline as overhead product.

#### 4.3.2 *Techno-economic model*

The total project investment cost of fast pyrolysis and hydroprocessing of biomass plant capacity of 2000 t d<sup>-1</sup> is developed based on the process model, as well as on assumptions from literature. It is assumed that the pyrolysis plant and the bio-oil upgrading plant at the same location to eliminate the bio-oil transportation cost and preserve the bio-oil from condensation and polymerization.

The inputs to this model for the estimation of the production cost of renewable diesel can be divided into three major categories: capital cost, feedstock cost, and operating and maintenance cost. These costs are explained in more detail in the following sections and the detailed summary of the discounted cash flow is given in Table A2 of Appendix A.

##### 4.3.2.1 *Capital cost*

The capital cost of a plant comprises building construction, equipment purchase, and equipment installation costs. Most of the equipment cost is taken from the Aspen Icarus software and some is from the literature (Aspen-Icarus, 2014; Ringer et al., 2006). The detailed equipment cost are given in the Table 4.3 (Aspen-Icarus, 2014; Ringer et al., 2006). To calculate the total project investment cost, investment factors from the literature (Peters et al., 2003) are considered. Table 4.4 shows the method for calculating the total capital cost. Plant construction time is spread over three years (see Table 4.5). The plant's lifetime is assumed to be 20 years, after which all the equipment must be replaced. The key assumptions for developing the techno-economic analysis are summarized in

Table 4.6 (Aspen-Icarus, 2014; Kumar et al., 2003; Miller & Kumar, 2014; Shahrukh et al., 2016).  
The cost numbers used in this paper are in 2016 US dollars.

**Table 4-3. Detailed equipment cost for the 2000 t d<sup>-1</sup> biomass plant**

	Original stream	New stream	Unit	Size ratio	Equipment cost for new stream	Reference
<b>Biomass pretreatment and fast pyrolysis unit</b>						
Biomass pretreatment	500	2000	t d <sup>-1</sup>	4	9,295,646	(Aspen-Icarus, 2014; Ringer et al., 2006)
Fluidized bed reactor	500	2000	t d <sup>-1</sup>	4	9,736,731	
Condensers	500	2000	t d <sup>-1</sup>	4	3,237,622	
Cyclone	500	2000	t d <sup>-1</sup>	4	4,700,000	
Product recovery and storage tank	500	2000	t d <sup>-1</sup>	4	3,022,400	
					29,992,399	
<b>Hydrotreating unit</b>						
Bio-oil pump	1000	2000	t d <sup>-1</sup>	2	133,090	Flowrate: 100 gpm Residence time: 1 h, Flow rate: 60m <sup>3</sup> /h, Material: stainless steel (Aspen-Icarus, 2014)
1 <sup>st</sup> stage hydrotreater	2000	2000	t d <sup>-1</sup>	1	3,921,000	
2 <sup>nd</sup> stage hydrotreater	2000	2000	t d <sup>-1</sup>	1	2,490,800	Residence time: 1 h, Flow rate: 60m <sup>3</sup> /h, Material: stainless steel
1st heat exchanger	2000	2000	t d <sup>-1</sup>	1	718,400	
2nd heat exchanger	2000	2000	t d <sup>-1</sup>	1	987,400	
Three phase separator	2000	2000	t d <sup>-1</sup>	1	9,556,778	Residence time: 1 h, Flow rate: 200 m <sup>3</sup> /h Material: stainless steel
PSA	2000	2000	t d <sup>-1</sup>	1	3,345,466	
H <sub>2</sub> compressor	2000	2000	t d <sup>-1</sup>	1	4,073,000	
Flash drum	2000	2000	t d <sup>-1</sup>	1	450,341	
other equipment	2000	2000	t d <sup>-1</sup>	1	903,245	

	Original stream	New stream	Unit	Size ratio	Equipment cost for new stream		Reference
					26,579,520		
<b>Hydrocracking and fractionation unit</b>							
<i>Debutanizer unit</i>							
<i>Condenser</i>	2000	2000	t d <sup>-1</sup>	1	55,000	No of trays: 16 Material: Stainless steel	(Aspen-Icarus, 2014)
<i>Reboiler</i>	2000	2000	t d <sup>-1</sup>	1	88,700		
<i>Reflux pump</i>	2000	2000	t d <sup>-1</sup>	1	6,500		
<i>Tower</i>	2000	2000	t d <sup>-1</sup>	1	9,376,700		
<i>Fractionation column</i>							
<i>Condenser</i>	2000	2000	t d <sup>-1</sup>	1	200,210	No of trays: 20 Material: Stainless steel	(Aspen-Icarus, 2014)
<i>Reboiler</i>	2000	2000	t d <sup>-1</sup>	1	52,800		
<i>Reflux pump</i>	2000	2000	t d <sup>-1</sup>	1	127,500		
<i>Tower</i>	2000	2000	t d <sup>-1</sup>	1	10,256,500		
Hydrocracker unit	2000	2000	t d <sup>-1</sup>	1	7,684,900	Residence time: 1 h, Flow rate: 40m <sup>3</sup> /h, Material: stainless steel	
H <sub>2</sub> compressor	2000	2000	t d <sup>-1</sup>	1	3,876,345		
Other equipment	2000	2000	t d <sup>-1</sup>	1	94,987		
					31,820,142		

**Table 4-4. Methodology for estimating plant capital cost**

<b>Parameter</b>	<b>Value</b>
Total purchase equipment cost (TPEC)	100% TPEC
Total installed cost (TIC)	302% TPEC
Indirect cost (IC)	89% TPEC
Total direct and indirect cost (TDIC)	TIC + IC
Contingency	20% TDIC
Fixed capital investment (FCI)	TDIC + Contingency
Location factor (LF)	10% FCI
Total capital cost	FCI + LF

**Table 4-5. Key assumptions for the development of the techno-economic model**

<b>Parameter</b>	<b>Value</b>	<b>Reference</b>
Plant lifetime (y)	20	
Escalation rate of different components		
General & administrative	3.5%	
Project capital	5%	
Products	5%	(Aspen-Icarus,
Raw Material	3.5%	2014)
Operating and maintenance labor	3%	
Utilities	3%	
IRR	10%	
Base year	2016	
Dollar used	US	
Plant start-up factor		
Year 0	0.7	
year 1	0.8	(Kumar et al.,
Year 2+	0.85	2003; Miller &
		Kumar, 2014;
		Shahrukh et al.,
		2016)
Spread of construction cost		
Year -3	20%	
Year -2	35%	(Miller & Kumar,
Year -1	45%	2014)

#### 4.3.2.2 Feedstock cost and camping cost

Feedstock cost, also known as feedstock delivery cost in this study, includes the cost from cultivation to the transportation of the feedstock to the plant gate (see Figure 4.1). Once the biomass is cut by feller bencher, it is dragged to the nearby tertiary road using a skidder where it is chopped. Then the chopped biomass is loaded in to a truck and transported to the plant where it is processed to its end products. To calculate the feedstock cost, a number of components are considered: harvesting cost, transportation cost, silviculture cost, tertiary road construction cost, nutrient spreading cost, and the premium above the cost of fuel that is paid to the owners which are given in Table 4.6 (Kumar et al., 2003). For a 2000 t d<sup>-1</sup> capacity plant, the delivery cost is estimated to be 48 \$ t<sup>-1</sup>. The approach used by Shahrukh et al. (2016) and Agbor et al. (2016) is adopted here in estimating the delivery cost of biomass. As biomass harvesting is carried out in the remote location of forest where accessibility and communication are very limited, a camping cost of 5% of total investment cost is considered in the analysis. In this study, we assume that the pyrolysis and hydroprocessing plants are situated at same location; therefore, the cost to transport bio-oil to the upgrading unit is not incorporated into the model.

**Table 4-6. Components of feedstock cost**

<b>Components</b>	<b>\$ t<sup>-1</sup></b>
Feller bencher cost	9.96
Skidding cost	8.91
Chipping cost	8.22
Road construction and infrastructure cost	0.06
Silviculture cost	1.88
Royalty/Premium fee	5.98
Loading, unloading and transportation cost	13.00
<b>Delivered biomass cost</b>	<b>48.01</b>

#### 4.3.2.3 Operating and maintenance cost

The operating costs used in this analysis come from the use of electricity, nitrogen, and hydrogen, which is assessed from the energy and material balances of the process model, and sand quantity, which is estimated from the experimental set-up. The unit costs for electricity, nitrogen, hydrogen, and sand are given in Table 4.7 (EPCOR, 2016; Kaycircle, 2016; Miller & Kumar, 2014; Sil Industrial Minerals, 2016). In our model, only the hydrogen purchased scenario is explored to calculate production cost of diesel and gasoline. The labor cost is developed based on the process model and the average Canadian labor wage is considered (Canadavisa, 2016). To operate a 2000 t d<sup>-1</sup> plant, 12 operators and 1 supervisor per shift are considered. The maintenance cost is assumed to be 3% of the capital cost (Kumar et al., 2003). The plant operating charge is considered to be 25% of the operating labor cost, and plant overhead is 50% of the total operating and maintenance cost. The catalyst cost is an important factor as it is used during hydroprocessing. Although sulfided nickel-molybdenum (a transition metal catalyst and not expensive compared to noble metal catalysts) supported on alumina is used (Patel & Kumar, 2016; Wright et al., 2010), more of this catalyst is required for the reactors than of noble metals. The ratio of catalyst to bio-oil is assumed to be 1:1 (Jantaraksa et al., 2015). However, the catalyst activity decreases with time (Patel & Kumar, 2016). For this study, the catalyst lifetime is considered to be one year. The annual catalyst replacement cost is considered to be 2.03 M \$ y<sup>-1</sup> (Wright et al., 2010).

**Table 4-7. Unit price of components used in the model**

Components	Cost	Reference
Electricity	0.04 \$ kWh <sup>-1</sup>	(EPCOR, 2016)
Nitrogen	0.04/100 \$ g <sup>-1</sup>	(Kaycircle, 2016)
Hydrogen	0.72 \$ kg <sup>-1</sup>	(Miller & Kumar, 2014)
Sand	7.8 \$ t <sup>-1</sup>	(Sil Industrial Minerals, 2016)

As hydrodeoxygenation is the dominating reaction in the hydrotreater, a sustainable quantity of waste water is produced, which needs to be disposed of in the waste water disposal plant. The waste water disposal cost is 0.0058 \$ L<sup>-1</sup> (Department, 2016).

#### 4.3.2.4 Product

Gasoline and renewable diesel are the final products of hydroprocessing technology analyzed through the process model. Gasoline and diesel are separated from the hydrotreated and hydrocracked bio-oil in a series of distillation columns. To estimate the cost of transportation fuels separately, in the analysis it is assumed that cost of diesel as the function of gasoline (diesel cost = gasoline cost + 0.05 \$ L<sup>-1</sup>) for the specific location which is taken from the Natural Resources Canada (Natural Resources Canada, 2016b). Bio-char produced from the pyrolysis plant is also considered as a byproduct and it can be further used to nourish soil.

#### 4.3.2.5 Sensitivity analysis

A sensitivity analysis is conducted on a series of process-sensitive parameters to see the impact on the transportation fuel value. Capital cost and bio-oil yield have the largest impact on the selling price of transportation fuel. There are currently no commercial- or demonstration-scale plants of 2000 t d<sup>-1</sup> of aspen feedstock in operation. So the estimated total plant capital cost is associated with uncertainties due to lack of information. Bio-oil yield in the pyrolyzer is another sensitive parameter as it is directly related to the production of diesel and gasoline from hydroprocessing technology.

## 4.4 Results and Discussion

### 4.4.1 Process Model Results for 2000 dry t d<sup>-1</sup> Plant Capacity

The energy and material balance of the fast pyrolysis and hydroprocessing of plant capacity 2000 dry t d<sup>-1</sup> is summarized in Table A1 in the appendix A based on the Figure 4.2. The moisture content in the raw biomass is 50% by wt which is reduced to around 10 % using nitrogen as the drying medium. After fast pyrolysis, the dried biomass produces 63% of bio-oil with 18% of biochar and 18% uncondensable gases. The intermediate, bio-oil in the present form is highly unstable and corrosive due to the high oxygen content which is further treated in the two stage hydrotreater. In the first stage hydrotreater, acid and ketone compounds are converted to small acid and alcohol intermediates with some lighter gases compounds (CH<sub>4</sub>, ethane) due to partial

hydrodeoxygenation. The lighter compounds are formed due to the Decarbonylation and methanation reaction. In the second hydrotreater, all the aldehydes and acid intermediates, alcohol, guaiacol, phenol etc. are converted to paraffin, aromatics, naphtha compounds, indene, C<sub>6</sub>-C<sub>12</sub> compounds with lighter gaseous compounds. In the second stage hydrotreater, complete hydrodeoxygenation reaction takes place in presence of hydrogen. According to the process model, hydrotreated oil is 51% of the bio-oil with 39% of waste water and 20% of lighter gases. Hydrogen is extracted from the gas stream using pressure swing adsorption method. In the hydrocracker, the high molecular weight compound are broken to gasoline and diesel range hydrocarbons through hydroalkylation, hydrocracking and isomerization. In this model, hydrocracker is considered as RYield reactor where the final products content maximum of C<sub>10</sub> hydrocarbons. At the end, the hydrocracked oil is passed into a fractionation column to produce diesel and gasoline which are 29.7% and 19.8% by weight respectively of bio-oil.

#### 4.4.2 Economic study on the base case of a 2000 t d<sup>-1</sup> aspen woodchip plant

Table 4.8 summarizes this study's important outcomes. In this study, merchant hydrogen is used for bio-oil hydroprocessing. The breakdown of installed costs for this plant is shown in the Figure 4.3. The installed cost for the hydrocracking unit is higher than the other sub-unit costs as it comes with a fractionation column. The total installed cost for this plant is 265 M \$.

**Table 4-8. Summary of key results from the techno-economic study**

<b>Parameters</b>	<b>Value</b>
Installed capital cost (M \$)	265.81
Fixed capital investment (M \$)	412.99
Annual operating cost (\$ y <sup>-1</sup> )	140.71
Renewable diesel yield (M L)	148.80
Gasoline yield (M L)	99.20
Cost of renewable diesel (\$ L <sup>-1</sup> )	1.09
Cost of gasoline (\$ L <sup>-1</sup> )	1.04

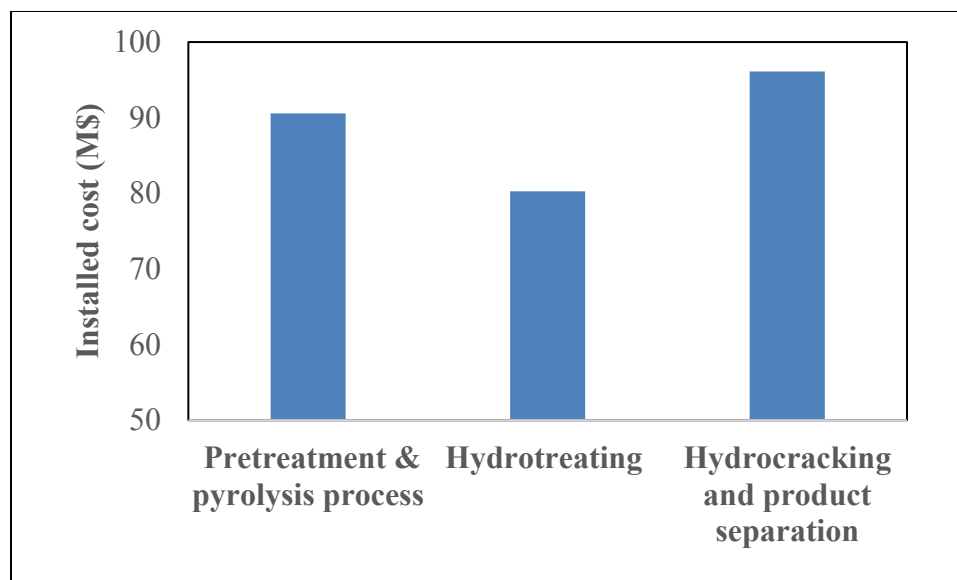


**Figure 4.3. Breakdown of installed cost of 2000 t d<sup>-1</sup> capacity aspen plant**

For the fast pyrolysis process, the total yields of bio-oil and bio-char are 541 M L y<sup>-1</sup> and 164.45 kt y<sup>-1</sup>, representing 63 wt% and 18 wt% of dried aspen feedstock, respectively. The amount of hydrogen required to upgrade the bio-oil is taken from literature (Wright et al., 2010) and is in a 30:1 mass ratio of bio-oil to hydrogen. The estimated production costs of renewable diesel and gasoline are 1.09 \$ L<sup>-1</sup> and 1.04 \$ L<sup>-1</sup>, respectively. The annual operating cost for a 2000 t d<sup>-1</sup> capacity plant is estimated to be 140 M \$. This cost is from the labor and electricity consumption. Electricity consumption is estimated from the developed process model to be 3533 kW h<sup>-1</sup>. For labor, it is assumed that the plant runs three shifts per day with one supervisor and 12 operators in each shift.

Figure 4.4 shows the total cost breakdown. Raw material cost is a major contributor followed by capital cost, maintenance cost, and camping cost. Loading, unloading, and transportation of raw material from forest to plant make up most of the raw material cost. Operating labor cost is comparatively lower because most of the machines can be operated automatically. The production cost of renewable diesel and gasoline can be reduced by optimizing the transportation distance and reducing plant maintenance costs.

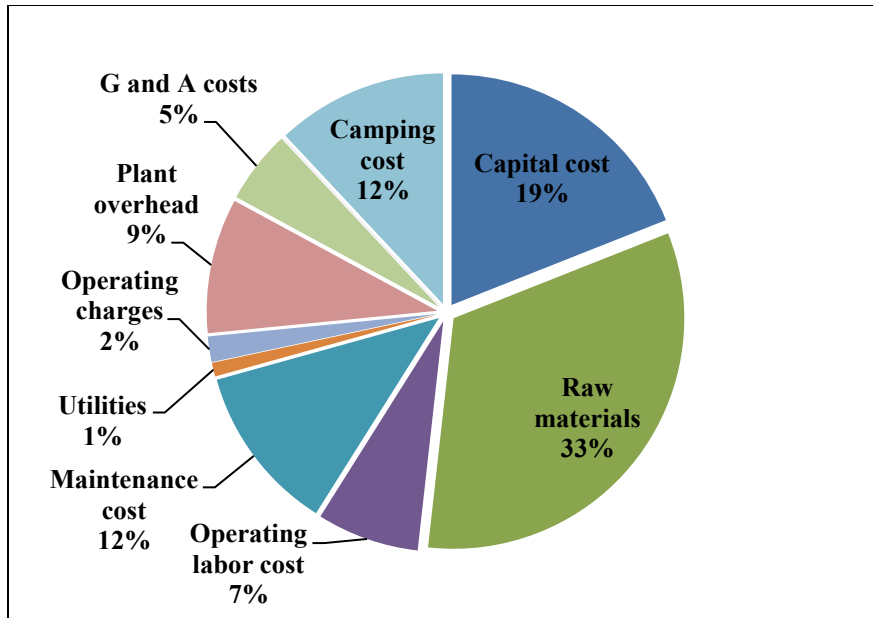


**Figure 4.4. Cost distribution for 2000 t d-1 capacity plant**

#### 4.4.3 Influence of plant size on production cost

##### 4.4.3.1 Scale factor

In this study, renewable diesel and gasoline production cost variation with plant capacity has been investigated. The equipment cost is estimated from the process model and follows investment factors from literature to calculate the total project investment cost (Peters et al., 2003). Figure 4.5 shows the variation of total project investment cost with capacity. The developed scale factor for the plant is calculated from this fig. is 0.71, and tells us that capital cost increases slower than the capacity, which assures higher return.

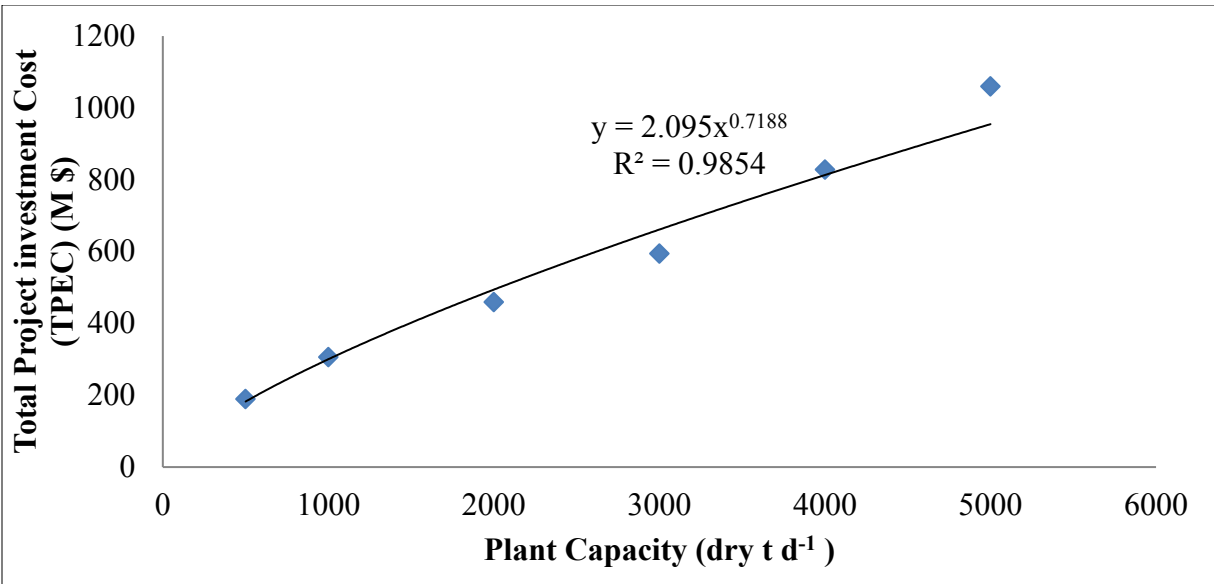


**Figure 4.5. Variation of total project investment cost with capacity**

#### 4.4.3.2 Profile of capacity with renewable diesel and gasoline

The difference in production cost vs. plant capacity shows a decreasing trend followed by a plateau (see Figure 4.6). This distinct curve is due to the trade-off between mainly two parameters: capital cost and delivered raw material cost. The curve is there because with the increase in plant capacity, fuel production costs decrease due to trade-off between decreasing capital cost unit due to economy of scale benefits and the delivered cost of raw material which increases due to increase in size of the plant. The production costs decreases with the increase in the capacity of the plant and reaches a minimum at 3000 t d<sup>-1</sup>. Beyond this capacity, transportation cost (one component of delivery cost) of biomass plays a major role as this cost increases with the square root of the plant capacity (Kumar et al., 2003).

The production cost of renewable diesel and gasoline decreases to a plant capacity of 3000 t d<sup>-1</sup>, after which it levels out. The leveling indicates that the production cost of the diesel and gasoline does not change with the increase in capacity as transportation cost is counterbalanced by the economy of scale of the project's total capital investment per unit output. Generally, transportation

cost has two components, loading and unloading costs (considered fixed costs) and variable costs that vary with the distance travelled. Therefore, the optimum plant capacity is a trade-off between the capital cost per unit output and the transportation cost. In this case, the economic optimum production size is 3000 t d<sup>-1</sup> aspen woodchips and the production costs of renewable diesel and gasoline are 1.007 \$ L<sup>-1</sup> and 0.95 \$ L<sup>-1</sup>, respectively.

Figure 4.7 shows the impact of different parameters on renewable diesel production costs for 500 and 5000 t d<sup>-1</sup> plant capacities. The most influential factors are raw material cost, operating labor cost, and plant overhead. As the capacity of the plant increases, the cost of raw material increases from 19% to 37% due to biomass transportation, but the labor cost drops from 17% to 3% through economies of scale. Plant overhead decreases with capacity as it is a percentage of labor cost. Therefore, selecting the appropriate plant capacity significantly depends on the availability and handling of raw material in the geographic location. It can be observed that the capital cost and labor cost are not affected significantly with changes capacity. So selecting the optimum plant capacity will depend on the availability of capital investment, labor, and biomass in the region.

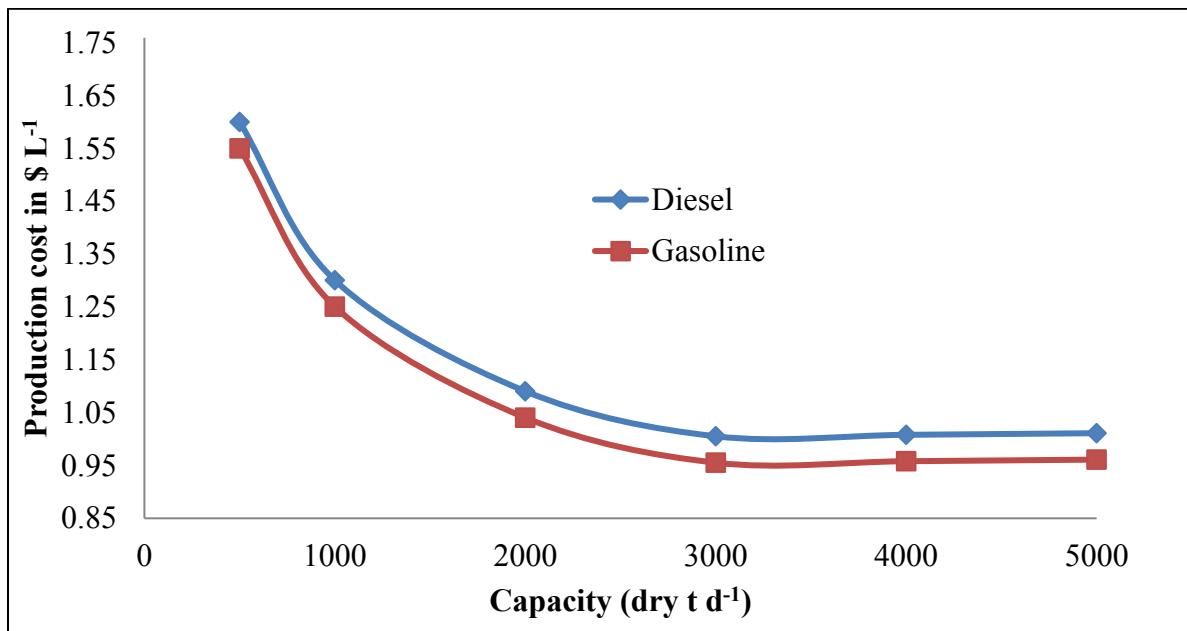


**Figure 4.6. Renewable diesel and gasoline production cost with different capacities**

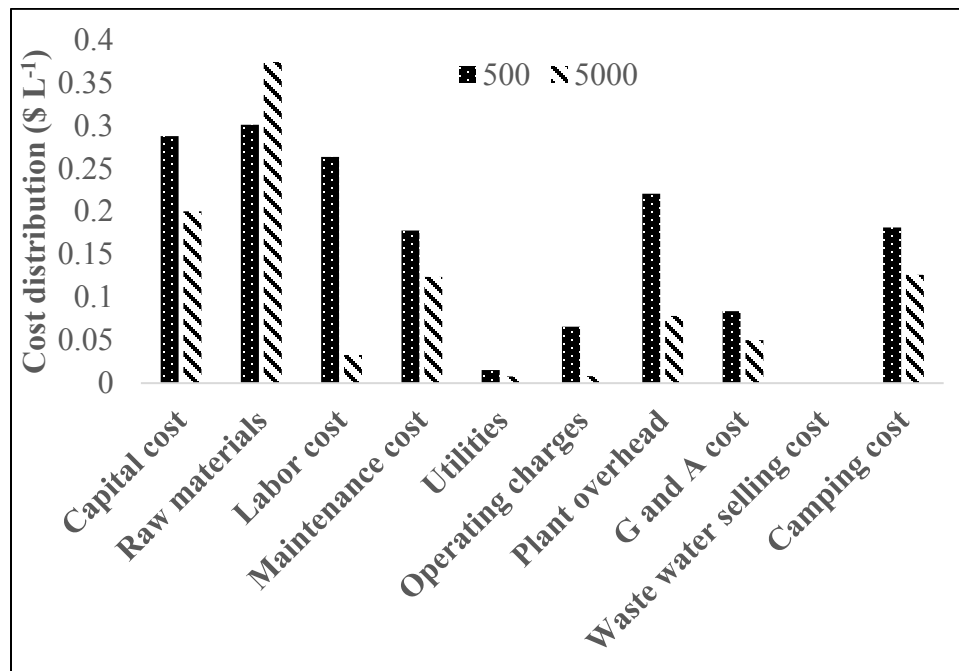


**Figure 4.7. Cost distribution for 500 t d<sup>-1</sup> and 5000 t d<sup>-1</sup> capacity plant**

#### 4.4.4 *Comparison production cost of transportation fuels with published results and actual petro-fuel production*

Currently, there is no commercial facility with a hydroprocessing unit for bio-oil upgrading operating anywhere in the world. There has been some work on a lab-scale for the hydroprocessing of corn stover and mixed wood feedstock (Jones et al., 2013). Transportation fuel production costs through this technology range from 0.6-1.25 \$ L<sup>-1</sup> (Anex et al., 2010; Brown et al., 2013; Hu et al., 2016; Jones et al., 2009; Shemfe et al., 2015; Wright et al., 2010). The production cost is somewhat location-specific, so the cost varies from location to location.

The production cost of renewable diesel and gasoline estimated from this study is compared with the production cost for the fossil diesel and gasoline and it is observed that these numbers are higher than the conventional fuel. The production costs of petro-diesel have changed drastically in

last decade. From October 2015 –October 2016, the monthly average wholesale rack price of diesel in Calgary, AB, was approximately ranged between 0.0.49 – 0.7 \$ L<sup>-1</sup> after deducting the federal and provincial taxes, profit margin and marketing cost (Natural Resources Canada, 2016a; Natural Resources Canada, 2016b). The production cost of renewable diesel and gasoline are higher than the conventional diesel because of the raw material cost. But biomass (known as carbon neutral source) has the potential to reduce the greenhouse gases emission which is lacking from conventional petro-fuel, Because of this, it is gaining interest and these costs can be further reduced, though more intensive research on the technical aspects of hydroprocessing and fast pyrolysis technology.

#### 4.4.5 *Sensitivity study*

A sensitivity analysis has been carried out on the base case (2000 t d<sup>-1</sup>) to understand the influence of different variables on the production costs of diesel and gasoline. Figure 4.8 shows the sensitivity analysis of different process parameters by varying the cost parameters by ± 20%.

Production costs of renewable diesel and gasoline are more sensitive to bio-oil yield . The production costs of renewable diesel and gasoline range from 0.91 -1.35 \$ L<sup>-1</sup> and 0.86 -1.30 \$ L<sup>-1</sup>, respectively, with a change of ±20%. These ranges show that more bio-oil yield can increase fuel yield and vice versa. So bio-oil yield can be improved by optimizing the process operating conditions of the fluidized bed reactor during fast pyrolysis operation and also modifying the process. The internal rate of return (IRR) is also sensitive to the production costs of renewable diesel and gasoline and ranges from 0.98-1.19 \$ L<sup>-1</sup> for diesel and 0.93-1.14 \$ L<sup>-1</sup> for gasoline.

The high sensitivity of production cost to bio-oil suggests that further experimentation is required to optimize the reactor design and process conditions (pressure, temperature, nitrogen flow rate, and particle size of biomass and sand). This high sensitivity also implies that high quality feedstock with low ash content will yield more bio-oil than bio-char and non-condensable gases. The IRR is

an important parameter that helps make budget decisions for new facilities. The project with a higher IRR is preferred.

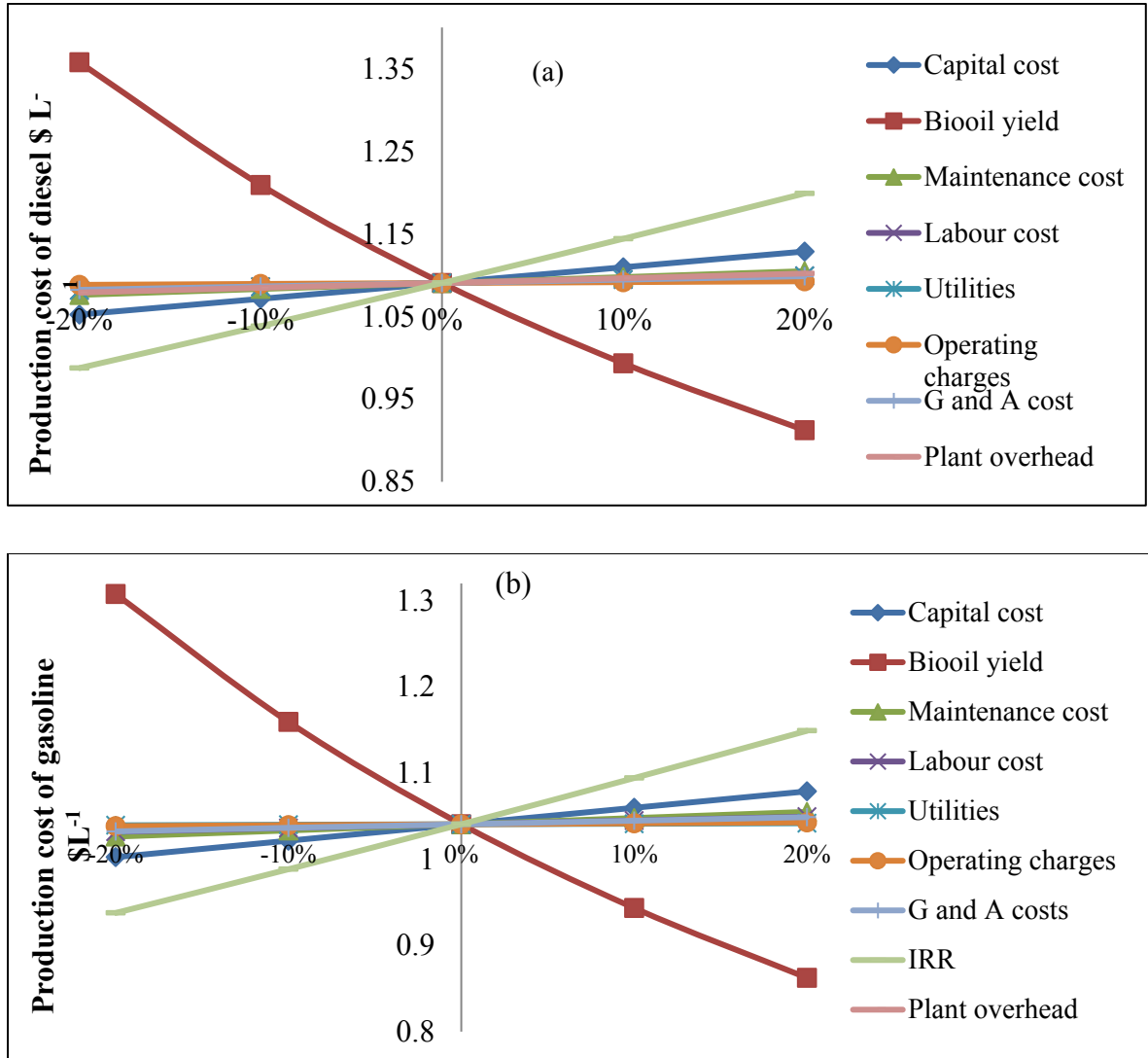
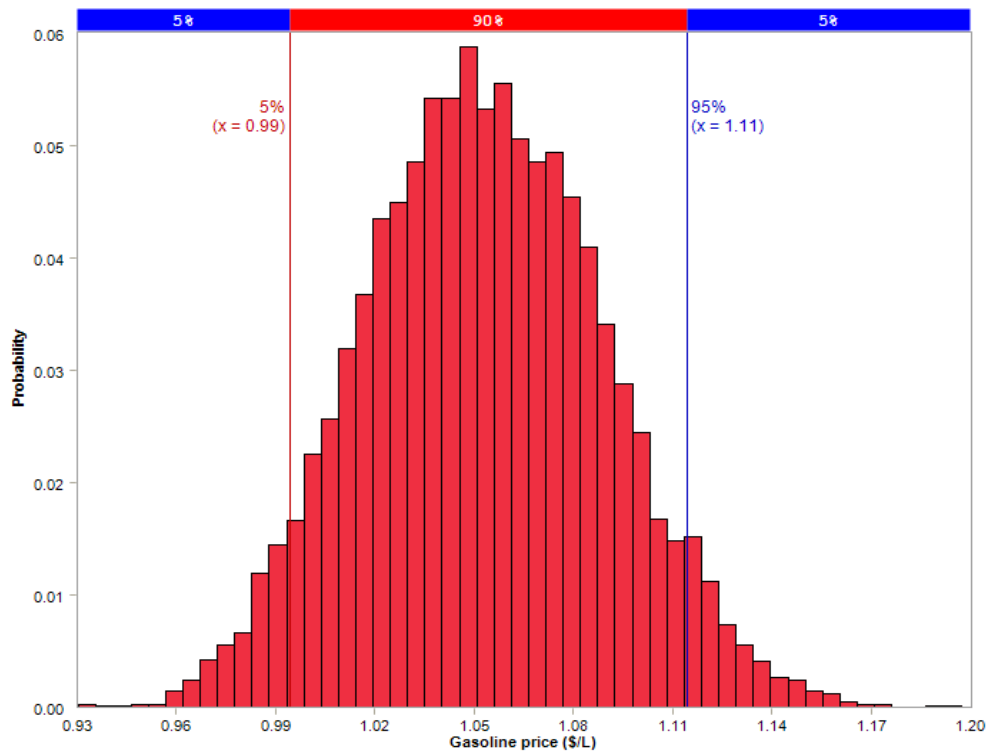
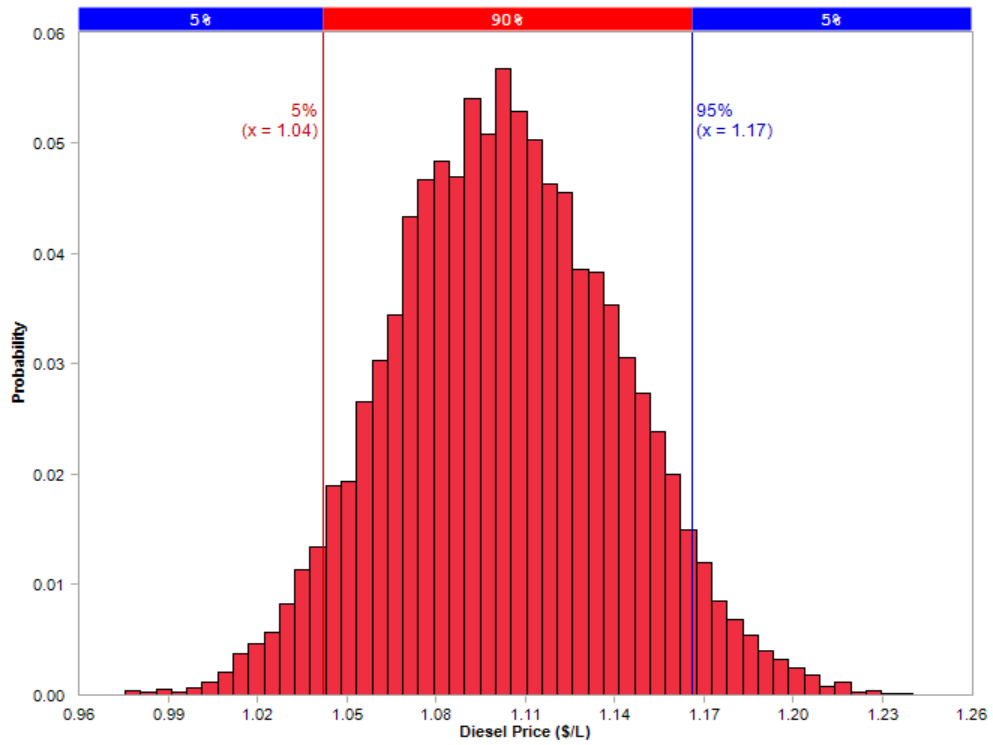


Figure 4.8. Sensitivity of renewable diesel and gasoline production cost

#### 4.4.6 *Uncertainty analysis*

The above-mentioned sensitivity analysis considered only single point variation of a parameter on the production cost of renewable diesel and gasoline whereas other parameters are assumed to be constant at that time of analysis. To understand the variation of more than one parameters at a point in time and simultaneously to handle some cost components which are highly uncertain and volatiles (unavailability of field data), an uncertainty analysis has been conducted to understand the impact of risk and uncertainty in the production costs of diesel and gasoline. The uncertainty issues come up when we try to develop a model that takes some assumptions with the real data. To perform the uncertainty analysis, we ran a Monte Carlo simulation using ModelRisk software (Vosesoftware, 2015). In a Monte Carlo simulation, random values are chosen, in this case from all the parameters that have an impact on the production costs of renewable diesel and gasoline (based on the range of the cost components), and the software iterates a number of times by using a probability function to give a range for the production costs.

The Monte Carlo simulation is performed for the base case 2000 t d<sup>-1</sup> aspen wood based plant with the most volatile cost components, and the uncertainty is quantified in the final products with 10,000 iterations. The input costs for the simulation considered are capital cost, biomass cost, maintenance cost, labor cost, utilities, operating charges, general and administrative costs, and plant overhead. Uncertainties considered for these above mentioned inputs are 85 -125%, 80-125%, 90 -115%, 75 -125%, 90 -110%, 90 -115%, 90 -110% and 90% -115% ,respectively, based on the sensitivity analysis. The production costs generated from this simulation for the renewable diesel and gasoline are shown in Figure 4.9. For the base case scenario, the production costs of diesel and gasoline are calculated to be  $1.10 \pm 0.038$  \$ L<sup>-1</sup> and  $1.05 \pm 0.036$  \$ L<sup>-1</sup>, respectively, at 95% confidence. From the Monte Carlo simulation, it can be concluded that production costs of transportation fuels depend more on the technical cost inputs than the market conditions. Controlling these parameters will make this pathway economic and competitive with petro-fuels.



**Figure 4.9. Uncertainty analysis of diesel and gasoline production cost**

## 4.5 Conclusions

This study developed a process model to conduct a techno-economic assessment of fast pyrolysis and upgrading through the hydroprocessing of aspen wood feedstock for production of renewable diesel and gasoline. A detailed study of a 2000 t d<sup>-1</sup> plant was carried out to investigate the production costs of renewable diesel and gasoline through this pathway using merchant hydrogen and sulfided nickel-molybdenum supported on an alumina catalyst. The production costs of renewable diesel and gasoline are 1.09 \$ L<sup>-1</sup> and 1.04 \$ L<sup>-1</sup>, respectively, for a 2000 t d<sup>-1</sup> capacity biomass plant. To understand the variations in transportation fuel production costs at various capacities, a wide range of production capacities is considered (from 500 to 5000 t d<sup>-1</sup>). The optimum size was found to be 3000 t d<sup>-1</sup> with a renewable diesel price of 1.007 \$ L<sup>-1</sup> at which the cost of production is minimum. When the capacity is increased, raw material delivered costs increase significantly however the capital cost per unit output decreases. Scale factor of the lignocellulosic biomass-based renewable diesel production was developed to be 0.71 using the developed process model.

A sensitivity analysis was done to determine the influence of different process parameters on the final outputs. The results show that production cost of liquid fuels is most sensitive to bio-oil yield and IRR with a variation of ±20%. A Monte Carlo simulation showed variations in the production cost of diesel and gasoline from 1.10 ± 0.038 \$ L<sup>-1</sup> and 1.05 ± 0.036 \$ L<sup>-1</sup>, respectively, at a 95% confidence level.

The results of this techno-economic assessment provide insights on the economic competitiveness of producing HDRD from bio conventional mass via fast pyrolysis and hydroprocessing.

## References

- Agbor, E., Oyedun, A.O., Zhang, X., Kumar, A. 2016. Integrated techno-economic and environmental assessments of sixty scenarios for co-firing biomass with coal and natural gas. *Applied Energy*, **169**, 433-449.
- Anex, R.P., Aden, A., Kazi, F.K., Fortman, J., Swanson, R.M., Wright, M.M., Satrio, J.A., Brown, R.C., Daugaard, D.E., Platon, A. 2010. Techno-economic comparison of biomass-to-transportation fuels via pyrolysis, gasification, and biochemical pathways. *Fuel*, **89**, S29-S35.
- Ardiyanti, A.R., Gutierrez, A., Honkela, M.L., Krause, A.O.I., Heeres, H.J. 2011. Hydrotreatment of wood-based pyrolysis oil using zirconia-supported mono- and bimetallic (Pt, Pd, Rh) catalysts. *Applied Catalysis A: General*, **407**(1–2), 56-66.
- Aspen-Icarus. 2014. Aspen process economic analyzer, available at <https://www.aspentech.com/Company/About-AspenTech/>.
- Aspentech. 2014. Aspen process economic analyzer, available at <https://www.aspentech.com/Company/About-AspenTech/>. Accessed on 23 September 2015.
- Bridgwater, A., Meier, D., Radlein, D. 1999. An overview of fast pyrolysis of biomass. *Organic geochemistry*, **30**(12), 1479-1493.
- Bridgwater, A.V. 2012. Review of fast pyrolysis of biomass and product upgrading. *Biomass and bioenergy*, **38**, 68-94.
- Brown, T.R., Thilakaratne, R., Brown, R.C., Hu, G. 2013. Techno-economic analysis of biomass to transportation fuels and electricity via fast pyrolysis and hydroprocessing. *Fuel*, **106**, 463-469.
- Canada Renewable Bioenergy Corp. 2012. Pyrolysis project, available at [http://canadarenewablebioenergy.com/project/pyrolysis\\_technology/](http://canadarenewablebioenergy.com/project/pyrolysis_technology/). Accessed on 17 August 2017.
- Canadavisa. 2016. Canada salary calculator, available at <https://www.canadavisa.com/canada-salary-wizard.html>, Accessed on 22nd October 2016.
- Chiaramonti, D., Bonini, M., Fratini, E., Tondi, G., Gartner, K., Bridgwater, A.V., Grimm, H.P., Soldaini, I., Webster, A., Baglioni, P. 2003. Development of emulsions from biomass

- pyrolysis liquid and diesel and their use in engines—Part 1 : emulsion production. *Biomass and Bioenergy*, **25**(1), 85-99.
- Department, W.a.W. 2016. Hauled wastewater program, available at <http://winnipeg.ca/waterandwaste/sewage/hauledWastewater.stm>. .
- Ecoresources Consultants. 2012a. Study of hydrogenation derived renewable diesel as a renewable fuel option in North America, available at [http://www.nrcan.gc.ca/sites/www.nrcan.gc.ca/files/oeefiles/pdf/transportation/alternative-fuels/resources/pdf/HDRD\\_Final\\_Report\\_eng.pdf](http://www.nrcan.gc.ca/sites/www.nrcan.gc.ca/files/oeefiles/pdf/transportation/alternative-fuels/resources/pdf/HDRD_Final_Report_eng.pdf). Accessed on 06 September 2017.
- Ecoresources Consultants. 2012b. An update on renewable diesel infrastructure in Canada, available at [http://www.nrcan.gc.ca/sites/www.nrcan.gc.ca/files/oeefiles/pdf/transportation/alternative-fuels/resources/pdf/Infrastructure\\_update\\_final\\_report\\_eng.pdf](http://www.nrcan.gc.ca/sites/www.nrcan.gc.ca/files/oeefiles/pdf/transportation/alternative-fuels/resources/pdf/Infrastructure_update_final_report_eng.pdf). Accessed on 17 August 2017.
- Elliott, D., Neuenschwander, G. 1997. Liquid fuels by low-severity hydrotreating of biocrude. in: *Developments in thermochemical biomass conversion*, Springer, pp. 611-621.
- Elliott, D.C., Hart, T.R., Neuenschwander, G.G., Rotness, L.J., Olarte, M.V., Zacher, A.H., Solantausta, Y. 2012. Catalytic hydroprocessing of fast pyrolysis bio-oil from pine sawdust. *Energy & Fuels*, **26**(6), 3891-3896.
- Elliott, D.C., Hart, T.R., Neuenschwander, G.G., Rotness, L.J., Zacher, A.H. 2009. Catalytic hydroprocessing of biomass fast pyrolysis bio-oil to produce hydrocarbon products. *Environmental Progress & Sustainable Energy*, **28**(3), 441-449.
- EPCOR. 2016. Commercial rates and fees, available at <http://www.epcor.com/power-natural-gas/regulated-rate-option/commercial-customers/Pages/commercial-rates.aspx>. .
- Gagnon, J., Kaliaguine, S. 1988. Catalytic hydrotreatment of vacuum pyrolysis oils from wood. *Industrial & engineering chemistry research*, **27**(10), 1783-1788.
- Gregoire, C.E., Bain, R.L. 1994. Technoeconomic analysis of the production of biocrude from wood. *Biomass and Bioenergy*, **7**(1), 275-283.
- Hu, W., Dang, Q., Rover, M., Brown, R.C., Wright, M.M. 2016. Comparative techno-economic analysis of advanced biofuels, biochemicals, and hydrocarbon chemicals via the fast pyrolysis platform. *Biofuels*, **7**(1), 57-67.

- Jantaraksa, N., Prasassarakich, P., Reubroycharoen, P., Hinchiranan, N. 2015. Cleaner alternative liquid fuels derived from the hydrodesulfurization of waste tire pyrolysis oil. *Energy Conversion and Management*, **95**, 424-434.
- Jones, S., Meyer, P., Snowden-Swan, S., Padmaperuma, A., Tan, E., Dutta, A., Jacobson, J., Cafferty, K. 2013. Process design and economics for the conversion of lignocellulosic biomass to hydrocarbon fuels. PNNL-23053, NREL/TP-5100-61178.
- Jones, S.B., Holladay, J.E., Valkenburg, C., Stevens, D.J., Walton, C.W., Kinchin, C., Elliott, D.C., Czernik, S. 2009. Production of gasoline and diesel from biomass via fast pyrolysis, hydrotreating and hydrocracking: a design case.
- Kaycircle. 2016. What is the average cost of nitrogen gas per gram/pound/cubic foot? Average nitrogen price, available at <http://www.kaycircle.com/What-Is-The-Average-Cost-Of-Nitrogen-Gas-Per-Gram-Pound-Cubic-Foot-Average-Nitrogen-Price>. Accessed on 17 August 2017.
- Kim, K.H., Kim, T.-S., Lee, S.-M., Choi, D., Yeo, H., Choi, I.-G., Choi, J.W. 2013. Comparison of physicochemical features of biooils and biochars produced from various woody biomasses by fast pyrolysis. *Renewable Energy*, **50**, 188-195.
- Kumar, A., Cameron, J.B., Flynn, P.C. 2003. Biomass power cost and optimum plant size in western Canada. *Biomass and Bioenergy*, **24**(6), 445-464.
- LaClaire, C.E., Barrett, C.J., Hall, K. 2004. Technical, environmental and economic feasibility of bio-oil in new hampshire's north country. *Durham, NH: University of New Hampshire*.
- Ladanai, S., Vinterback, J. 2011. Global potential of sustainable biomass for energy, available at [http://pub.epsilon.slu.se/5586/1/ladanai\\_s\\_etal\\_110120\\_4.pdf](http://pub.epsilon.slu.se/5586/1/ladanai_s_etal_110120_4.pdf).
- Miller, P., Kumar, A. 2014. Techno-economic assessment of hydrogenation-derived renewable diesel production from canola and camelina. *Sustainable Energy Technologies and Assessments*, **6**, 105-115.
- Natural Resources Canada. 2016a. Average retail fuel prices in calgary, available at [http://www2.nrcan.gc.ca/eneene/sources/pripri/prices\\_byfuel\\_e.cfm?locationName=Calgary#priceGraph](http://www2.nrcan.gc.ca/eneene/sources/pripri/prices_byfuel_e.cfm?locationName=Calgary#priceGraph). Accessed on 17 August 2017.
- Natural Resources Canada. 2016b. Daily Average Wholesale (Rack) Prices for Diesel (Rack) in 2014, available at [http://www2.nrcan.gc.ca/eneene/sources/pripri/wholesale\\_bycity\\_e.cfm?PriceYear=2014](http://www2.nrcan.gc.ca/eneene/sources/pripri/wholesale_bycity_e.cfm?PriceYear=2014)

- &ProductID=13&LocationID=66,8,39,17&Average=3&dummy=#PriceGraph. Accessed on 02 October 2017.
- Natural Resources Canada. 2014. The state of Canada's forests annual report, available at <http://cfs.nrcan.gc.ca/pubwarehouse/pdfs/35713.pdf>. Accessed on 17 August 2017.
- Patel, M., Kumar, A. 2016. Production of renewable diesel through the hydroprocessing of lignocellulosic biomass-derived bio-oil: A review. *Renewable and Sustainable Energy Reviews*, **58**, 1293-1307.
- Patel, M., Zhang, X., Kumar, A. 2016. Techno-economic and life cycle assessment on lignocellulosic biomass thermochemical conversion technologies: A review. *Renewable and Sustainable Energy Reviews*, **53**, 1486-1499.
- Peters, J.F., Petrakopoulou, F., Dufour, J. 2014. Exergetic analysis of a fast pyrolysis process for bio-oil production. *Fuel Processing Technology*, **119**, 245-255.
- Peters, M., Timmerhaus, K., West, R. 2003. *Plant Design and Economics for Chemical Engineers*. 5th ed. McGraw-Hill Education.
- Plus®, A. 2015. Jump Start: Getting Started with Aspen Plus® V8.4.
- Ringer, M., Putsche, V., Scahill, J. 2006. Large-scale pyrolysis oil production: a technology assessment and economic analysis. National Renewable Energy Laboratory (NREL), Golden, CO.
- Rogers, J., Brammer, J. 2012. Estimation of the production cost of fast pyrolysis bio-oil. *Biomass and bioenergy*, **36**, 208-217.
- Shahrukh, H., Oyedun, A.O., Kumar, A., Ghiasi, B., Kumar, L., Sokhansanj, S. 2016. Techno-economic assessment of pellets produced from steam pretreated biomass feedstock. *Biomass and Bioenergy*, **87**, 131-143.
- Shashikantha. 2008. Biomass – a substitute for fossil fuels?, available at [https://www.pssurvival.com/PS/Gasifiers/Biomass\\_A\\_Substitute\\_For\\_Fossil\\_Fuels\\_2008.pdf](https://www.pssurvival.com/PS/Gasifiers/Biomass_A_Substitute_For_Fossil_Fuels_2008.pdf).
- Shemfe, M.B., Gu, S., Ranganathan, P. 2015. Techno-economic performance analysis of biofuel production and miniature electric power generation from biomass fast pyrolysis and bio-oil upgrading. *Fuel*, **143**, 361-372.
- Sheu, Y.-H.E., Anthony, R.G., Soltes, E.J. 1988. Kinetic studies of upgrading pine pyrolytic oil by hydrotreatment. *Fuel Processing Technology*, **19**(1), 31-50.

- Sil Industrial Minerals. 2016. Other industrial sands, available at <http://www.sil.ab.ca/>. Accessed on 17 August 2017.
- Siriwardhana, A. 2013. Aging and Stabilization of Pyrolytic Bio-Oils and Model Compounds.
- Venderbosch, R., Ardiyanti, A., Wildschut, J., Oasmaa, A., Heeres, H. 2010. Stabilization of biomass-derived pyrolysis oils. *Journal of chemical technology and biotechnology*, **85**(5), 674-686.
- Verma, P., Sharma, M.P., Dwivedi, G. 2016. Impact of alcohol on biodiesel production and properties. *Renewable and Sustainable Energy Reviews*, **56**, 319-333.
- Vosesoftware. 2015. Model Risk, Monte Carlo Simulation, available at <http://www.vosesoftware.com/contactus.php>.
- Ward, J.W. 1993. Hydrocracking processes and catalysts. *Fuel Processing Technology*, **35**(1), 55-85.
- Wildschut, J., Mahfud, F.H., Venderbosch, R.H., Heeres, H.J. 2009. Hydrotreatment of fast pyrolysis oil using heterogeneous noble-metal catalysts. *Industrial & Engineering Chemistry Research*, **48**(23), 10324-10334.
- Wright, M.M., Daugaard, D.E., Satrio, J.A., Brown, R.C. 2010. Techno-economic analysis of biomass fast pyrolysis to transportation fuels. *Fuel*, **89**, S2-S10.
- Zhang, S., Yan, Y., Li, T., Ren, Z. 2005. Upgrading of liquid fuel from the pyrolysis of biomass. *Bioresource Technology*, **96**(5), 545-550.
- Zhang, Y., Brown, T.R., Hu, G., Brown, R.C. 2013. Techno-economic analysis of two bio-oil upgrading pathways. *Chemical Engineering Journal*, **225**, 895-904

# **Chapter 5: What Is the Production Cost of Renewable Diesel from Woody Biomass and Agricultural Residue Based on Experimentation? A Comparative Assessment<sup>5</sup>**

## **5.1 Introduction**

According to Canada's federal and provincial governments, the addition of 2% renewable diesel to petro-diesel is mandatory to reduce greenhouse gas emissions from the transportation sector, a sector that contributes around 25% to global emissions (Government of Canada, 2017). Of the renewable resources, biomass is the only one that can be directly converted to a liquid renewable fuel to replace fossil fuel. 9% of the world's boreal forests are found in Canada, and 94% of them are owned by the Government of Canada and most of this has been leased to the private companies (Govenment of Canada, 2017). With proper harvesting practices and land-use planning, this feedstock (the forests) can be used as a resource for biofuels. In addition, in Western Canada, about 27 million tons of agricultural residue is available after the considering its use for soil conservation and livestock (Sokhansanj et al., 2006). These lignocellulosic feedstocks are also good candidates for biofuel production.

---

<sup>5</sup> A version of this chapter is submitted to fuel Processing Technology as Patel M, Oyedun A, Kumar A, Gupta R. What Is The Production Cost of Renewable Diesel from Woody Biomass and Agricultural Residue Based on Experimentation? A Comparative Assessment, 2018 (submitted)

Fast pyrolysis is a well-known thermochemical conversion technology that can convert solid biomass to an intermediate liquid product (bio-oil), gas, and biochar in the absence of oxygen and at a high heating rate. The bio-oil can be further upgraded to a transportation fuel through hydroprocessing technology to produce renewable diesel and gasoline. The properties of renewable diesel from biomass are similar to those of petro-diesel (Patel & Kumar, 2016). Many studies are available on the conversion of biomass to bio-oil through fast pyrolysis (Bridgwater et al., 1999; Gable & Brown, 2016; Jeong et al., 2016; Kan et al., 2016; Patel et al., 2016; Torri et al., 2016). These studies found that bio-oil quality and quantity are a function of feedstock type, pyrolysis reactor, heating rate, and particle size distribution of the feed. Bio-oil yield varies by feedstock because of the differences in the chemical and elemental composition of biomass.

Researchers have studied various pyrolysis reactors such as fixed bed, bubbling bed, fluidized bed, cyclone bed, vacuum reactor, etc. (Bridgwater et al., 1999; Patel et al., 2016). Of the reactors, the fluidized bed reactor yields the most bio-oil because it allows for the right contact between biomass and the fluidizing medium.

As fast pyrolysis is well understood and commercially viable process, many studies have carried out techno-economic analyses of bio-oil production from different biomass feedstocks. The production cost of bio-oil is between 0.13 \$ L<sup>-1</sup> and 0.65 \$ L<sup>-1</sup> (Islam & Ani, 2000; LaClaire et al., 2004; Ringer et al., 2006; Sarkar & Kumar, 2010). The reported total capital cost is between 40 M\$ and 150 M\$ for a 1000 dry tonne/day pyrolysis plant (Gregoire & Bain, 1994; Solantausta et al., 1992). The differences in bio-oil production cost are due to feedstock type, biomass cost (harvesting and transportation cost), bio-oil yield, and pyrolysis plant capital cost. Biomass cost is location-specific and depends on yield, cultivation method, and transportation cost.

To upgrade bio-oil to renewable diesel, hydroprocessing technology is generally used; it is well established in the petroleum industry. Hydrogen (H<sub>2</sub>) is used to upgrade the bio-oil to the hydrocarbon range by removing the oxygen in the form of water. A few techno-economic studies

are available on the upgrading pathway from bio-oil, which acts as an intermediate. Wright et al. (2010) determined the H<sub>2</sub> production costs of naphtha and diesel through the fast pyrolysis and hydroprocessing of corn stover in the United States for a 2000 dry t d<sup>-1</sup> plant; the costs are 0.94 \$ L<sup>-1</sup> and 0.64 \$ L<sup>-1</sup> in the H<sub>2</sub> production and the purchase scenarios, respectively. In 2010 in the United States, Brown et al. (2013) explored the fast pyrolysis and hydroprocessing technology for corn stover to the gasoline and diesel range for the same plant capacity and reported the production cost to be 0.79 \$ L<sup>-1</sup>. Their study included a 90 M \$ boiler and a 30 M \$ turbine to produce electricity, which raised the capital costs to 492 M \$. Shemfe et al. (2015) investigated the production of gasoline and diesel through fast pyrolysis and hydroprocessing technology in a 72 t d<sup>-1</sup> plant from pine wood in the United Kingdom. The estimated cost was 2.17 \$ L<sup>-1</sup> gasoline equivalent; their figure is very high because the plant they considered had a low capacity (72 t d<sup>-1</sup>). There are a few more studies that investigate different end products through fast pyrolysis and the upgrading process (Anex et al., 2010; Jones et al., 2013a; Jones et al., 2013b; Jones et al., 2009; Zhu et al., 2014).

The above-mentioned studies focus on a single feedstock in techno-economic assessments of transportation fuels. In a recent publication by the authors, we estimated the production cost of renewable diesel from the Canadian aspen hardwood for hydrogen purchase scenario (Patel et al., 2018). The current study focuses on the comparative experimental and techno-economic assessment of woody biomass and agricultural residues used to produce renewable diesel. These assessments are essential to ultimately determine which feedstock is the best to use for the production of renewable diesel under the same process conditions. In addition, the studies cited above were conducted in different jurisdictions and are based on the authors' assumptions, and so the renewable fuel costs vary widely. As mentioned earlier, the pyrolysis plant location (which affects biomass transportation cost) and the feedstock itself significantly affect the production cost of the transportation fuel. To the best of the authors' knowledge, there is no study on process modelling nor a techno-economic analysis of the fast pyrolysis and hydroprocessing of Canadian lignocellulosic biomass to produce renewable diesel and gasoline. In addition, it is important to explore the variation production cost of renewable diesel as a function of biochar selling price to improve the applicability of pyrolysis process. In addition to process modeling for techno-

economic assessment, experiments were conducted to investigate the effects of process parameters on bio-oil yield in a fluidized bed reactor for three Canadian biomass feedstocks (spruce, corn stover, and wheat straw). The effects of byproduct (biochar) selling price on the production cost of renewable diesel for all the feedstocks in two scenarios, hydrogen production and purchase, were also investigated.

This study is a assessment of the production of renewable diesel and gasoline through fast pyrolysis and hydroprocessing technology for a plant capacity of 2000 t d<sup>-1</sup> from Canadian feedstocks. A process model was developed using predominantly the experimental data. The fast pyrolysis experiments were carried out in a lab-scale fluidized bed reactor at different process conditions to achieve high quantities of high-quality bio-oil. The specific objectives are:

1. To characterize the physical and chemical properties of three Canadian biomass feedstocks (spruce hardwood, corn stover, and wheat straw);
2. To perform fast pyrolysis experiments using a fluidized bed reactor at temperatures of 400-550°C and for three particle size distributions (0.125-0.425 mm, 0.425-1 mm and 1-2 mm);
3. To develop a detailed process model for fast pyrolysis and the hydroprocessing unit for a plant capacity of 2000 dry t d<sup>-1</sup>;
4. To develop capital cost estimates for the developed process model to determine renewable diesel and gasoline costs;
5. To estimate the production cost of renewable diesel and gasoline through two scenarios:
  - a. The hydrogen production scenario: H<sub>2</sub> used for hydroprocessing is produced through steam reforming the non-condensable gases. This scenario includes a power generation unit.
  - b. The hydrogen purchase scenario: H<sub>2</sub> used for hydroprocessing is purchased from outside sources.
6. To analyze the effects of byproduct costs (biochar selling price) on the renewable diesel cost for all three feedstocks
7. To estimate the net energy ratio, it is necessary to understand the production of useful sustainable renewable energy with respect to the consumption of fossil fuel input on the overall process, from harvesting to renewable fuel production
8. To carry out a case study on Canadian forest and agriculture resources.

## 5.2 Materials and method

### 5.2.1 Feedstock preparation

Three lignocellulosic biomass feedstocks – spruce, wheat straw, and corn stover – were selected for this study. Spruce (*Picea abies*) wood chips, corn stover (*Zea mays* ssp. *mays* L.), and wheat straw (*Triticum aestivum* L.) were collected from Weyerhaeuser in Drayton Valley, from southern Alberta, and from northern Alberta, Canada, respectively. The feedstock particle sizes supplied were inappropriate for the fast pyrolysis experiments and were ground to less than 2 mm and dried in an oven at 100°C. The samples were then classified into three size distributions (0.125-0.425 mm, 0.425-1 mm, and 1-2 mm) using screens. To avoid contact with atmospheric moisture, the prepared samples were stored in properly sealed plastic bags.

Table 5.1 summarizes the biomass properties of the feedstocks (Burhenne et al., 2013; Demirbaş, 1997; Öhgren et al., 2007; Zhu et al., 2009). A proximate analysis of the biomass was conducted in LECO TGA 701 to determine the percentages of moisture, volatile, fixed carbon, and ash using ASTM d7582, and an ultimate analysis was carried out in a Carlo Erba EA1108 Elemental Analyzer for CHNS (carbon, hydrogen, nitrogen, and sulphur) and oxygen. For accuracy, both analyses were done three times. The average values are reported in the Table 5.1.

**Table 5-1. Typical chemical analysis of biomass samples**

<b>Chemical analysis (wt% on a dry basis)</b>			
	<b>Spruce</b>	<b>Corn stover</b>	<b>Wheat straw</b>
Cellulose	40-50	40-50	25-35
Hemicellulose	20-30	28-32	40-45
Lignin	25-35	12-20	15-22
Ash	0.5-1	4-8	5-12
Source	(Burhenne et al., 2013; Demirbaş, 1997)	(Burhenne et al., 2013; Demirbaş, 1997)	(Demirbaş, 1997; Öhgren et al., 2007; Zhu et al., 2009)
<b>Proximate analysis (wt% on a dry basis)</b>			
Ash	0.45	6.06	6.3
Volatile	79.5	76.32	75.4
Moisture	3.9	6.15	4.1
Fixed carbon	16.15	17.62	18.3
<b>Ultimate analysis (wt% on a dry basis)</b>			
Nitrogen	0.18	1.2	0.76
Carbon	47.48	41.5	42.24
Hydrogen	6.44	5.6	5.69
Sulfur	0	0.05	0.03
Oxygen	45.90	50.25	51.08

### 5.2.2 *Experimental set-up*

Fast pyrolysis experiments of three Canadian feedstocks – spruce, corn stover and wheat straw were conducted in a laboratory-scale batch fluidized bed reactor which is described in section 3.3.3 of chapter 3.

### 5.2.3 *Product characterization*

An Agilent 7890A gas chromatograph-mass spectrometer (GC/MS) was used to analyze bio-oil samples of different biomass feedstocks. The GC/MS consists of a gas chromatograph coupled to a quadrupole mass spectrometer with a capillary column (J&W Scientific DB-5, 30mx0.25mm, 0.25mm). A micro gas chromatograph (Varian CP 4900) equipped with a thermal conductivity detector (TCD) was used to analyze the composition of the non-condensable gaseous samples. The analyzed compositions were used as yield data in the process model for the reactor design and subsequently in the economic analyzer to estimate renewable diesel production cost. Figure 5.1 shows experimental procedure to produce bio-oil through fast pyrolysis process in a fluidized bed reactor.

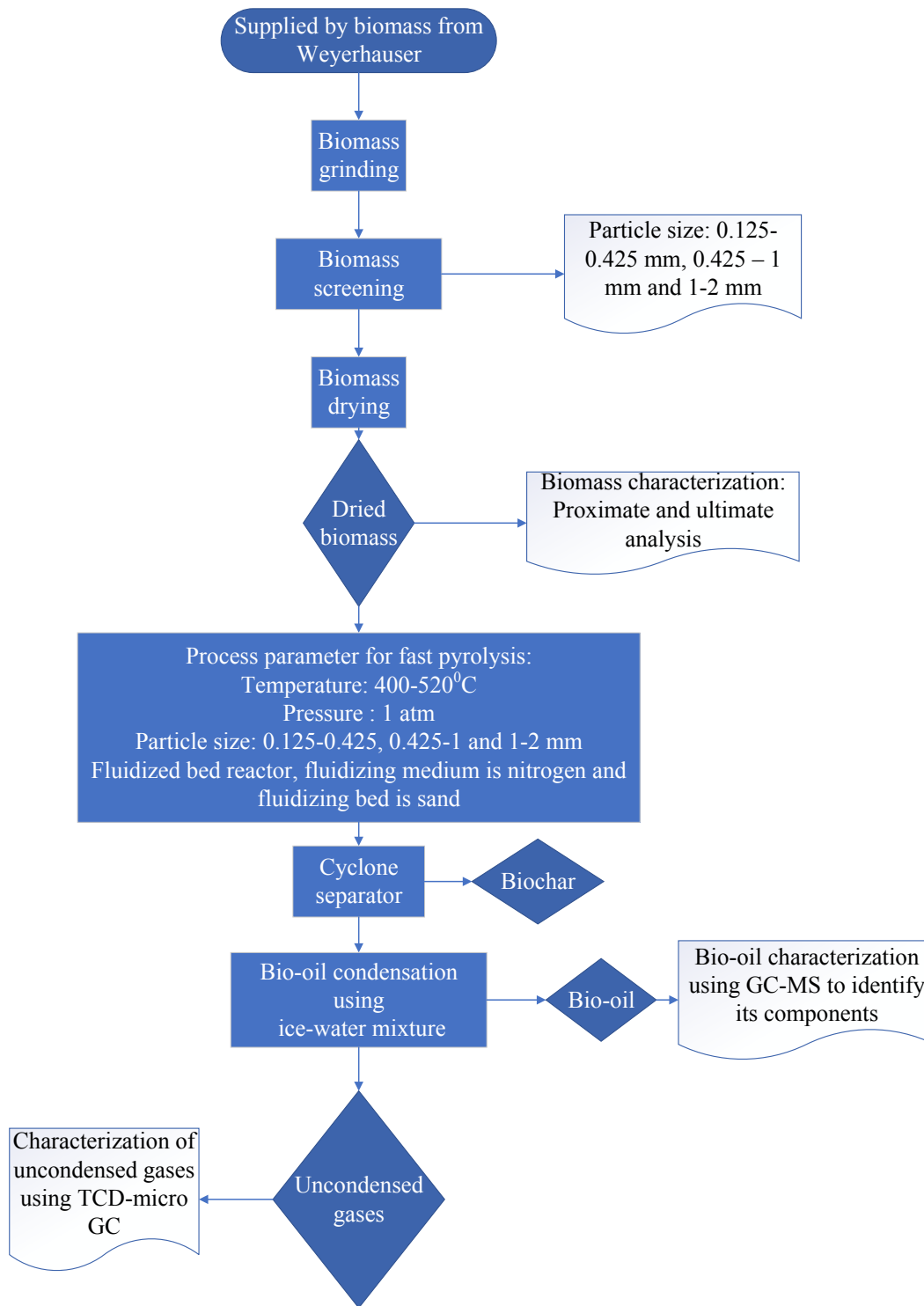


**Figure 5.1. Experimental methodology for fast pyrolysis process**

## 5.3 Modelling

### 5.3.1 Process modelling

Figure 5.2 is the process flow diagram of biomass feedstock conversion to transportation fuel and. The conversion has five major unit operations: the biomass pre-treatment, the pyrolysis and product separation, the hydroprocessing and fractionation, the steam reforming, and the power production. Aspen Plus<sup>®</sup> software was used to model these processes and the developed flow diagrams are given in Figure A1 to A6 in Appendix A1, and the process conditions are summarized in Table 5.2 (Elliott et al., 2009; Jones et al., 2013b; Patel et al., 2018; Wright et al., 2010).

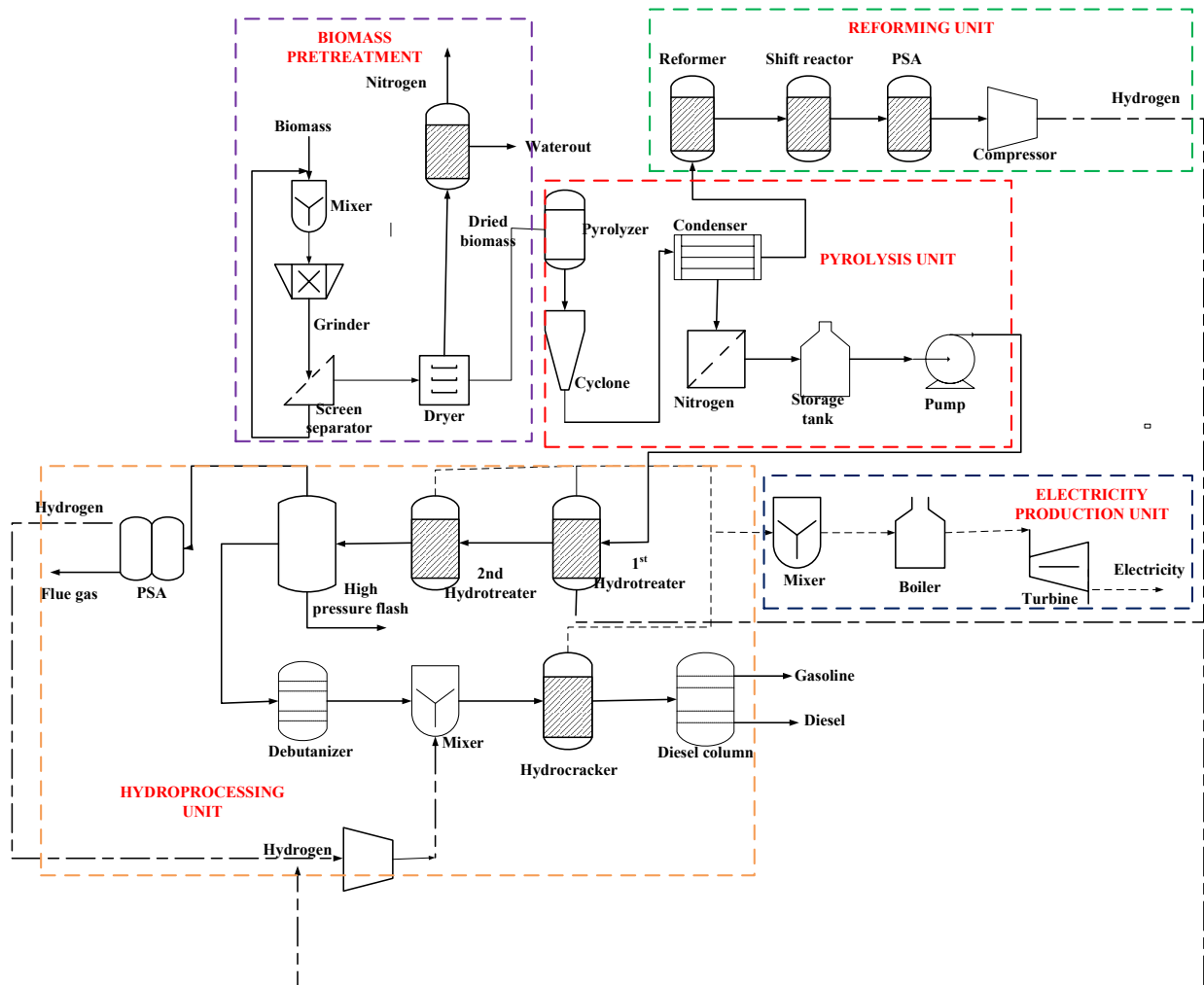


Figure 5.2. Schematic process diagram of fast pyrolysis and hydroprocessing technology

**Table 5-2. Process conditions and model details for the equipment used in the process simulation**

<b>Equipment</b>	<b>Aspen plus model</b>	<b>Process conditions</b>
Dryer	RStoic reactor	In the block, temperature is 100°C and nitrogen is the drying medium.
Screen	Rectangular vibrating screen	Particle size distribution: 90% for 0.1-1mm and 10% for 1-2 mm
Grinder	Gyratory crusher	This block crushes the biomass from as received (6-10mm) to less than 2 mm.
Pyrolyzer	RYield reactor	Pyrolyzer is maintained at 450-500°C depending the feedstock type and pressure at 1 atmosphere. The composition and quantity of the bio-oil, non-condensable gases, and biochar are given.
Cyclone	Solid cyclone separator	The assumed efficiency of cyclone is 90%.
Condenser	Heat exchangers	Water is used as the cooling medium and reduced the temperature to less than 0°C. Three coolers are used.
1 <sup>st</sup> stage hydrotreater	RYield reactor	Temperature is 240 °C and pressure is 100 bar.
2 <sup>nd</sup> stage hydrotreater	RYield reactor	Temperature is 340 °C and pressure is 120 bar.
Hydrocracker	RYield reactor	Temperature is 540 °C and pressure is 100 bar.
Fractionator	Radfrac column	It is a distillation column of 20 trays, and kettle type reboiler is used.
Steam reformer for gases	RGibb reactor	Non-condensable gases from the pyrolyzer are used as the feed, the reformer temperature is 800°C, and the pressure at 25 bar in presence of high-pressure steam.
WGS reactor	REquil reactor	Temperature and pressure are 370 °C and 25 bar.
Combustor	RGibb reactor	The off-gases from the hydroprocessing unit are burned in presence of air to produce high-pressure steam at a pressure of 50 bar.
Turbine electricity generation	for Turbine	The turbine is operated at 90% isentropic efficiency and 95% mechanical efficiency.

The biomass pre-treatment unit consists of a grinder, dryer, and screen separator. The biomass as received from the supplier is not appropriate for pyrolysis because of the particle size and moisture content. Therefore, the biomass, supplied at a particle size 6-10 mm, is fed into a crusher to reduce it to less than 2 mm and from there to a screen separator to remove the oversized from the required undersized feed. The oversized are returned to the crusher for further grinding. The final undersized feed is dried in a rotary dryer to lower the moisture content to 7 wt%. The initial moisture content of spruce, corn stover, and straw biomass as received was 50%, 25% and 14%, respectively, by weight. After this pre-treatment, the processed feed is sent to the fluidized bed pyrolyzer.

The pyrolysis unit consists of a fluidized bed reactor, a cyclone separation unit, a condenser, and a bio-oil storage tank. In the pyrolyzer, biomass is rapidly heated to 450-550 °C (depending on the feedstock) and atmosphere pressure to yield bio-oil, gases, and biochar. Biochar is separated in the cyclone separator. The efficiency of the cyclone is assumed to be 95%. After separation of the solids, the pyrolysis vapor is sent to a series of condensers to get the liquid products and non-condensable gases that are used in the hydrogen generation unit to produce H<sub>2</sub>.

The hydroprocessing unit has three stages: first stage hydrotreating, second stage hydrotreating, and hydrocracking. As the names suggest, all three processes are done in a H<sub>2</sub>-rich atmosphere. Hydrotreating is also known as a low-temperature hydrogenation process and is done in a fixed bed reactor at a temperature and pressure between 180-250 °C and 100-150 bar, respectively (Elliott & Neuenschwander, 1997). The treated oil is further upgraded at an extremely high temperature (300-400 °C) and pressure (100-200 bar) in the second stage hydrotreater. In both stages, sulfided nickel-molybdenum is used as the catalyst bed. In the first stage hydrotreater, the raw bio-oil is stabilized by removing the acidic compounds such as acetic acid, benzoic acid, etc., and in the second stage, mainly heteroatoms such as oxygen are eliminated in the form of water through the hydrodeoxygenation reaction in presence of the H<sub>2</sub> and the catalyst. Finally, upgraded oil from the second stage hydrotreater is passed to the hydrocracking unit, which is operated between 400 and 500 °C and a pressure around 150 bar in the presence of the same sulfided nickel-molybdenum

catalyst (Patel et al., 2018; Wright et al., 2010). Hydrocracking, hydrodealkylation, depolymerisation, and deoxygenation are the major reactions in the hydrocracker that break the high molecular weight compounds in the hydrotreated oil to low molecular weight compounds in diesel and gasoline ranges. The off-gases from both the hydrotreater and hydrocracker units are sent to the power generation unit and the hydrocracked oil is processed in the fractionation unit to produce gasoline and diesel fuel (Miller & Kumar, 2013; Zhu et al., 2013).

For this modelling, two H<sub>2</sub> scenarios are considered, merchant hydrogen and hydrogen production (at the plant site). For the merchant scenario, H<sub>2</sub> is purchased from an external source at a cost of 0.73 \$ kg<sup>-1</sup> (Miller & Kumar, 2014). For the H<sub>2</sub> production scenario, H<sub>2</sub> is produced on site through steam reforming of non-condensable gases from pyrolysis in a fixed bed reformer. In the reformer, temperature and pressure are maintained at 800-850°C and 20-25 bar in the presence of a noble metal Pt/Al<sub>2</sub>O<sub>3</sub> catalyst (Cortright et al., 2002). This catalyst activates the reforming reaction to enhance H<sub>2</sub> production over carbon monoxide (CO). Before entering the reformer, the reactants (both the non-condensable gases and steam) are compressed to a pressure of 23-30 bar. Then the products from the reformer are sent to a high temperature water gas shift (WGS) reactor to convert the CO to H<sub>2</sub> in the presence of water. In the WGS reactor, carbon monoxide reacts with water to form H<sub>2</sub> and carbon dioxide at a temperature of 300-450°C in presence of an iron oxide catalyst (FeO) (Newsome, 1980).

Electricity is generated in the plant by combusting the off-gases from the hydroprocessing unit. The combustion of off-gases takes place in the presence of water and air to produce high-pressure steam (50 bar), and the generated steam is used in the single-stage turbine to produce electricity for the facility.

### 5.3.2 *Economic parameters*

The equipment cost for fast pyrolysis and upgrading technology is estimated through the Aspen Process Economic Analyzer (APEA). First the complete process model is developed in the Aspen

Plus<sup>®</sup> platform using both experimental and literature data. Once the process model is successfully analyzed, it is used to estimate the equipment cost for the entire process. In techno-economic model, each piece of equipment is mapped and sized to the actual design parameter. The design parameters were obtained from the literature and vendor data. To estimate the total plant investment cost, Peters and Timmerhaus's method (Peters & Timmerhaus, 1991) was used and is summarized in Table 5.3. Once equipment is purchased, it is installed at a cost of 3.02 times the total purchased equipment cost; these are the project's direct costs. Installation costs include piping, electrical, yard improvement, building, equipment, installation, etc. (Peters & Timmerhaus, 1991). The indirect cost is 0.89 times the total equipment purchase cost and is made up of the contractor's fee, legal expenses, construction expenses, and engineering and supervision costs (Peters & Timmerhaus, 1991). The direct and indirect costs, combined with contingency and location factor, form the capital cost for the pyrolysis and hydroprocessing units. It is assumed that the pyrolysis and hydroprocessing plants are situated at the same place to avoid bio-oil transportation costs and that the hypothetical plant is located in the Western Canada. The cost model uses regional labor, supervisor, and utility rates. The feedstocks considered in the analysis are locally available biomass.

**Table 5-3. Method for the estimation of plant capital cost**

<b>Parameter</b>	<b>Value</b>
Total purchase equipment cost (TPEC)	100% TPEC
Total installed cost (TIC)	302% TPEC
Indirect cost (IC)	89% TPEC
Total direct and indirect cost (TDIC)	TIC + IC
Contingency	20% TDIC
Fixed capital investment (FCI)	TDIC + Contingency
Location factor (LF)	10% FCI
Total project investment (TPI)	FCI + LF

**Table 5-4. Key assumptions for techno-economic model development**

<b>Parameters</b>	<b>Values/Comments</b>	<b>Reference</b>
Plant lifetime	20 years	This study
IRR	10%	
Escalation rate (inflation factor)		
General & administrative	3.50%	(Patel et al., 2018)
Products	5%	
Raw Material	3.50%	
Operating and Maintenance		
Labor	3%	
Utilities	3%	
Base year	2016	
Dollar used	USD	
Plant start-up factor		
Year 0	0.7	(Miller & Kumar, 2014; Patel et al., 2018).
Year 1	0.8	
Year 2+	0.85	
Spread of construction cost		
Year 3	20%	(Agbor et al., 2016; Miller & Kumar, 2014; Patel et al., 2018).
Year 2	35%	
Year 1	45%	
Maintenance cost	3% of TPI	(Patel et al., 2018)
Operating charges	25% of the operating labor cost	(Oyedun et al., 2018; Patel et al., 2018)
Plant overhead	50% of total operating labor cost and the maintenance cost	
Total operating cost	Sum of operating labor cost, maintenance cost, utility cost and raw material cost	
General & administrative cost (G&A)	8% of total operating cost	

Table 5.4 summarizes the key characteristics of the plant assumed for this analysis; the same approach was used recently by Agbor et al. (Agbor et al., 2016). The plant lifetime is assumed to be 20 years with plant construction beginning three years before start-up. The plant construction cost distribution is 20%, 45%, and 35%, respectively, for years 3, 2 and 1 (Miller & Kumar, 2014; Patel et al., 2018). The efficiency of the plant is assumed to be 70% in the first year, 80% in the

second, and 85% in the third year and beyond. Plant maintenance costs are assumed to be 3% of the total project investment cost. A location factor of 10% of the total fixed investment is considered to accommodate jurisdictional requirements (Miller & Kumar, 2014; Patel et al., 2018). A camping cost of 5% of the total project investment is considered for the spruce hardwood because it is assumed that harvesting takes place in a remote forest location where accessibility and communication is difficult (Oyedun et al., 2018). No camping cost is considered for the agricultural residues (Patel et al., 2018) because of the easy access to the harvesting area. To estimate the present production cost of the renewable diesel and gasoline, a discounted cash flow (DCF) analysis was developed with an internal rate of return of 10% for a 20-year plant life. Table 5.3 includes the inflation factor used for the different cost components.

After capital cost, operating cost plays an important role in the analysis. Variable operating costs include raw material cost, maintenance cost, operating labor cost, plant overhead cost, general and administrative costs, operating charges, water disposal cost, and utilities. In the H<sub>2</sub> purchase scenario, raw materials include biomass, H<sub>2</sub>, nitrogen, sand, and catalysts, and in the H<sub>2</sub> production scenario, raw materials include all of these except H<sub>2</sub> and reformer catalysts. So, the raw material cost for the H<sub>2</sub> purchase scenario is higher than in the H<sub>2</sub> production scenario. For the H<sub>2</sub> purchase scenario, the H<sub>2</sub> purchase cost is included. Table 5.5 lists biomass yield and delivery costs. The biomass delivery cost has two components, field cost and biomass transportation cost. The harvesting method is different for woody biomass than for agricultural residue and is described in detail elsewhere (Agbor et al., 2016; Kumar et al., 2003). Of the feedstocks considered, harvesting costs are lowest for woody biomass because of the high yield per hectare, and yield is lowest for wheat straw. The lower yield raised the transportation cost.

**Table 5-5. Input data on biomass yield and delivery cost for the techno-economic model**

<b>Feedstock</b>	<b>Biomass yield (t ha<sup>-1</sup>)</b>	<b>Biomass delivered cost (\$ t<sup>-1</sup>)</b>	<b>Field cost (\$ t<sup>-1</sup>)</b>	<b>Transportation cost (\$ t<sup>-1</sup>)</b>
Spruce	84	40.74	28.87	11,87
Wheat straw	0.41	72.66	37.23	40.43
Corn stover	3.75	55.99	36.74	19.25

In the H<sub>2</sub> production scenario, there is a cost for the catalyst used in the hydrotreaters, hydrocracker, reformer, and shift reactors; in the H<sub>2</sub> purchase scenario, however, the reforming catalyst cost is excluded. The lifetime of the catalyst is considered to be 1 year; after that, it is replaced. The catalyst costs used in the hydroprocessing unit were derived from Wright et al. (Wright et al., 2010) and in the reformer from Zhu et al. (Zhu et al., 2013). The costs of electricity, nitrogen, H<sub>2</sub>, and sand used in our cost analysis are, respectively, 0.056 \$ kWh<sup>-1</sup> (EPCOR, 2017), 0.04/100 \$ g<sup>-1</sup> (Kaycircel, 2017), 0.74 \$ kg<sup>-1</sup> (Miller & Kumar, 2014), and 7.8 \$ t<sup>-1</sup> (Minerals, 2017).

To run a 2000 t d<sup>-1</sup> capacity plant continuously, the number of employees (including laborers and supervisor) is assumed to be 13 and 18, respectively, per shift, for the H<sub>2</sub> purchase and production scenarios, and three shifts per day are assumed. Operating charges for the plant are assumed to be 25 % of the total labor cost and plant overhead to be 50 % of the sum of the operating and the maintenance costs. (Oyedun et al., 2018; Patel et al., 2018) Table 5.4 lists the operating charges included in the analysis. All cost are reported in 2016 US dollars.

For the analysis, renewable diesel and gasoline are considered the main products with biochar as the byproduct. Diesel and gasoline are separated in a fraction column after the hydroprocessing operation. To estimate the production cost of individual renewable fuels, we assumed that diesel cost was a function of gasoline cost (diesel cost = gasoline cost + 0.05 \$ L<sup>-1</sup>) for the specific

location (Natural resources Canada, 2017). We also assumed that the biochar can be sold at a price of 100 \$ t<sup>-1</sup> on a dry basis (Shabangu et al., 2014).

## 5.4 Result and discussion

### 5.4.1 *Results of Experimental work on fast pyrolysis in fluidized bed reactor*

#### 5.4.1.1 *Experimental results on the effects of temperature on pyrolysis yield*

Figure 5.3 (a), (b), and (c) show the influence of temperature on the fast pyrolysis yield of spruce, corn stover, and wheat straw, respectively, in a fluidized bed reactor. As each figure shows, bio-oil yield increases with increases in temperature and, at a certain point, decreases. The temperature at which maximum bio-oil yield is achieved differs by feedstock. The temperatures are 490°C, 460°C, and 460°C and the maximum bio-oil yields are 64%, 49%, and 55% by weight for spruce, wheat straw, and corn stover, respectively. Gas yield increases and biochar yield decreases with increases in temperature for all the feedstocks. The product distribution trends for all the feedstocks are similar; this is because they share the same biomass decomposition kinetics. At low temperatures, activation energy is not sufficient to break the solid feedstock to pyrolysis vapor. Thus, biochar yield is highest at low temperatures and some unconverted biomass is found with the biochar. However, with increases in temperature, bio-oil yield increases because of increased volatile compounds in the pyrolysis vapor from the fast pyrolysis process. With further increases in temperature (for spruce, to 490 °C, and for corn stover and wheat straw, to 460°C), bio-oil yield decreases because of the secondary cracking reaction of the pyrolysis vapor, which forms more low molecular weight non-condensable gases (see Figure 5.3). The bio-oil yield for wheat straw is lowest because of its low carbon content and high oxygen percentage. These same product distribution trends have been reported by other researchers (Garcia-Perez et al., 2008; Ji-lu, 2007; Liu et al., 2009; Meibod, 2013).

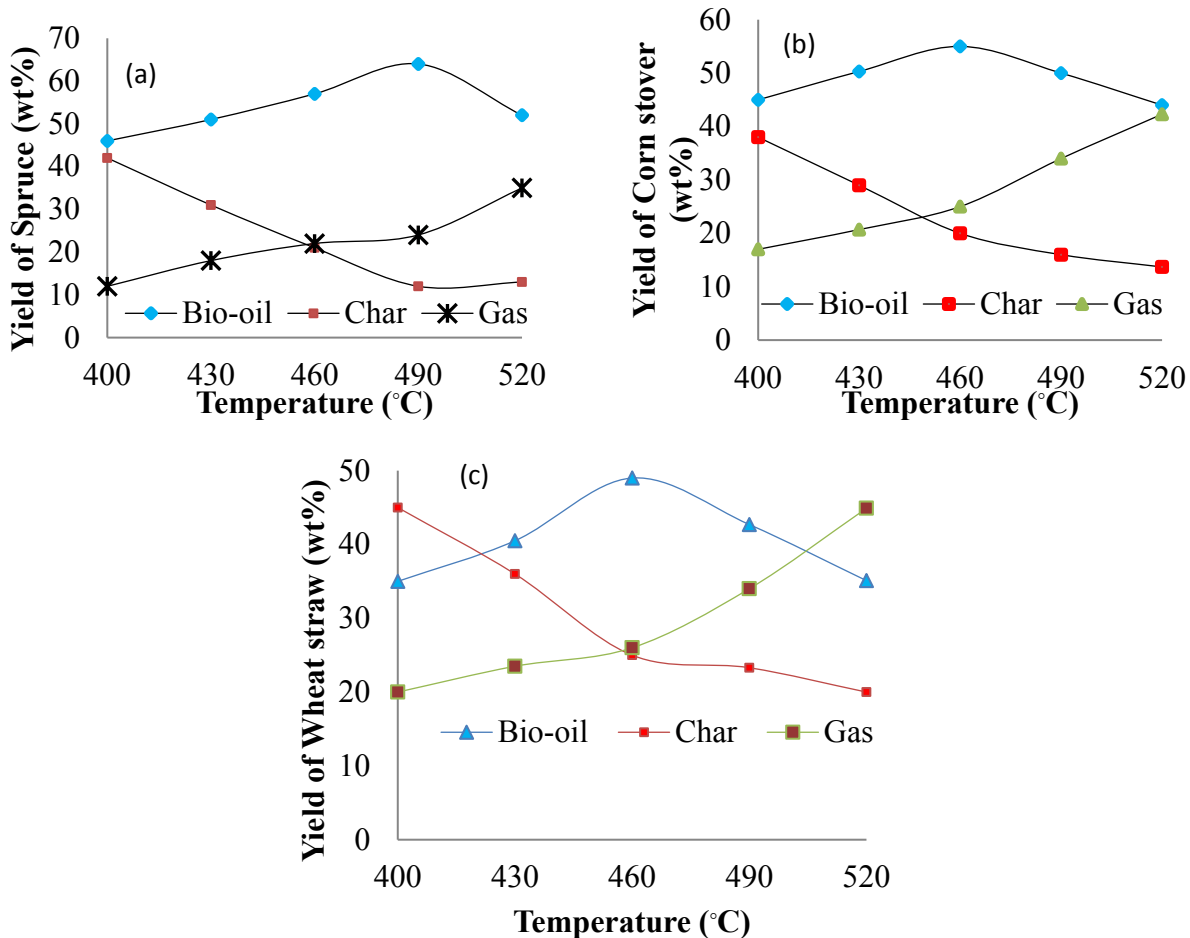


**Figure 5.3. Effects of temperature on product distribution for fast pyrolysis of biomass with (a) spruce, (b) corn stover, and (c) wheat straw**

#### 5.4.1.2 Experimental results on the effects of particle size on pyrolysis yield

The effects of particle size distribution on bio-oil yield were also studied for each feedstock at a particular temperature. The temperatures were selected based on the highest bio-oil yield and for corn stover and wheat straw was 460°C and for spruce was 490°C. Three particle size distributions were selected: 0.125-0.425 mm, 0.425-1 mm, and 1-2 mm. The average diameter of the smaller particles (0.275 mm) is one-fifth the size of the larger ones (1.5 mm). Figure 5.4 shows the variations in bio-oil and biochar yield with changes in particle size distribution. At a low particle size, maximum bio-oil yield was attained, and, with increases in particle size, the weight of the bio-oil yield dropped. The drop in yield with increased particle size is related to heat transfer

conditions during the pyrolysis process. The energy required to heat the entire biomass particle in a particular time is related to its heat transfer coefficient, which is related to particle thickness. The smaller particles easily convert to pyrolysis vapor but the pyrolysis vapor yield is lower for the large particles. Bio-oil yield for spruce, corn stover, and wheat straw decreased from 67% to 59%, 57.5% to 49%, and 52% to 44.3% by weight with particle size increases of 0.125-0.425 mm, 0.425-1 mm and 1-2 mm, respectively (Greenhalf et al., 2013; Ringer et al., 2006; Shen et al., 2009). It takes more time for heat to transfer from the particle surface to the center for big particles than for small ones, and since fast pyrolysis has a very short residence time, solid biomass cannot decompose to gas in that time. Bio-char yield thus increased with increased particle size, as shown Figure 5.4, and is highest for large particles.

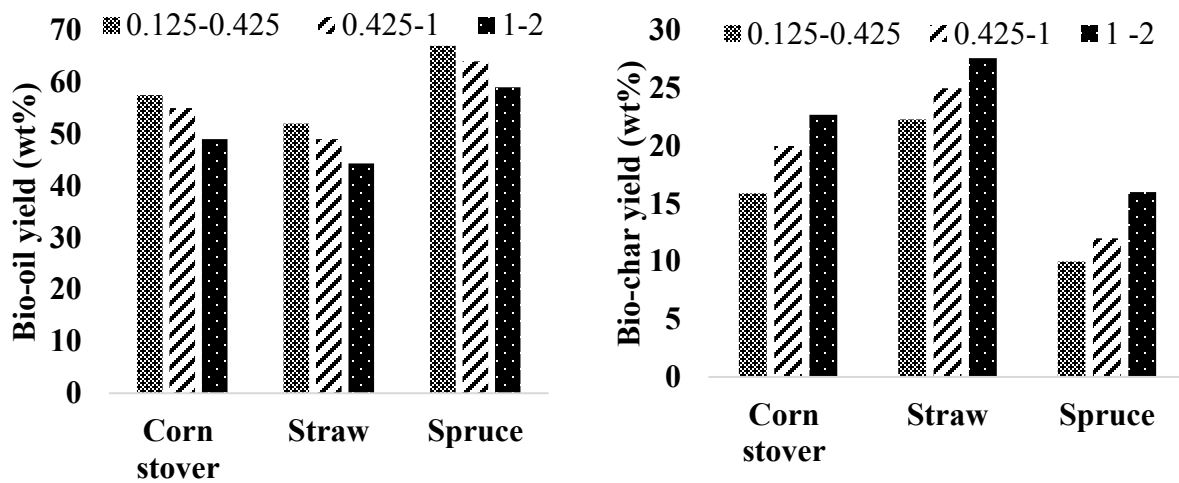


**Figure 5.4. Effects of particle size distribution on bio-oil and biochar yield at 460°C for corn stover and wheat straw and at 490°C for spruce in an inert nitrogen atmosphere**

#### *5.4.1.3 Experimental results on the bio-oil characterization*

Bio-oil is a complex mixture of organic compounds, mainly acids, alcohols, aldehydes, esters, ketones, sugars, phenols, phenol derivatives, etc., that are formed by the decomposition of cellulose, hemicellulose, and lignin. Table 5.6 shows the percentage of different compounds identified by the GC/MS in the bio-oil from different biomass feedstocks (spruce at 490°C and corn stover and wheat straw at 460 °C); these figures were used for the process simulation. The main acid compounds identified are acetic acid and carboxylic acid. Phenol and phenol-derived compounds are present in large portions compared to other organic compounds. These compounds are formed by depolymerization of the lignin compounds, which present in a ring form. Generally, cellulose decomposes to form mainly ketones and aldehyde through condensation reactions (Russell et al., 1983). The amounts of organic compounds vary depending on the percentages of cellulose, hemicellulose, and lignin content in the feedstock.

**Table 5-6. Experimental results on the composition of bio-oil by feedstock**

<b>Spruce</b>	<b>Wt%</b>	<b>Corn stover</b>	<b>Wt%</b>	<b>Wheat straw</b>	<b>Wt%</b>
1,3-Cyclopentanedione	4.46%	Cyclohexanone	1.28%	Guaiacol	7.24%
3-Hexanone	0.92%	1,2 Cyclohexane dimethanol	2.76%	P-cresol	0.95%
2,5-Piperazinedione	2.95%	Phenol	4.85%	2-ethyl-2-hexenal	1.27%
Phenol, 2-methoxy-	6.55%	2-cyclopentone, 2,3 dimethyl	5.80%	4-methyl-2- methoxyphenol	1.64%
Maltol	1.59%	Mequinol	7.02%	5-ethylguaiacol	1.60%
Phenol, 2-methoxy-4-methyl-	5.10%	2-ethyl phenol	1.15%	2-Methoxy-4- vinylphenol	2.24%
Phenol, 4-ethyl-2-methoxy-	2.79%	Benzofuran 2,3 dihydro	7.76%	Syringol	4.27%
Eugenol	2.06%	1,2 benzenediol 3-methoxy	1.62%	Vanillin	2.19%
Vanillin	5.40%	Benzene	2.87%	Phenol	3.36%
Phenol, 2-methoxy-4-(1- propenyl)-,	4.55%	Octanoic acid	0.94%	2-ethylbiphenyl	1.15%
Homovanillyl alcohol	2.85%	Vanillin	1.96%	1,2,4-trimethoxybenzene	1.47%
Ethanone, 1-(4-hydroxy-3- methoxyphenyl	1.83%	Acetic acid	1.89%	Benzaldehyde	1.25%
Benzoic acid, 4-hydroxy-3- methoxy-	1.13%	Ethanone	1.21%	1-monobenzyl glycerol	2.25%
Acetic acid	3.11%	Diphenyl	0.88%	Acetic acid	3.20%
3-Acetyl-6- methoxybenzaldehyde	8.71%				

## 5.4.2 *Techno-economic model*

### 5.4.2.1 *Renewable diesel and gasoline production costs*

Table 5.7 lists the main costs in the production of transportation fuel through fast pyrolysis and hydroprocessing technology from three biomass feedstocks (spruce, corn stover, and wheat straw) for a plant capacity of 2000 t d<sup>-1</sup>. All three feedstocks were assessed in the H<sub>2</sub> production scenario; however, only spruce hardwood was assessed in the H<sub>2</sub> purchase scenario. The installed equipment cost for H<sub>2</sub> production unit in the H<sub>2</sub> production scenario is almost 100 M\$ more than in the H<sub>2</sub> purchase scenario.

In the spruce hardwood hydrogen production scenario, the pretreatment and pyrolysis unit, hydrotreating unit, hydrocracking and fractionation unit, electricity generation unit, and H<sub>2</sub>

production unit make up 19%, 18%, 32%, 15%, and 15%, respectively, of the total purchased equipment cost which is shown in Figure 5.5. The hydrocracking and fractionation unit cost is highest because this unit consists of one hydrocracker and several fractionation columns to separate the flue gas, diesel, and gasoline.

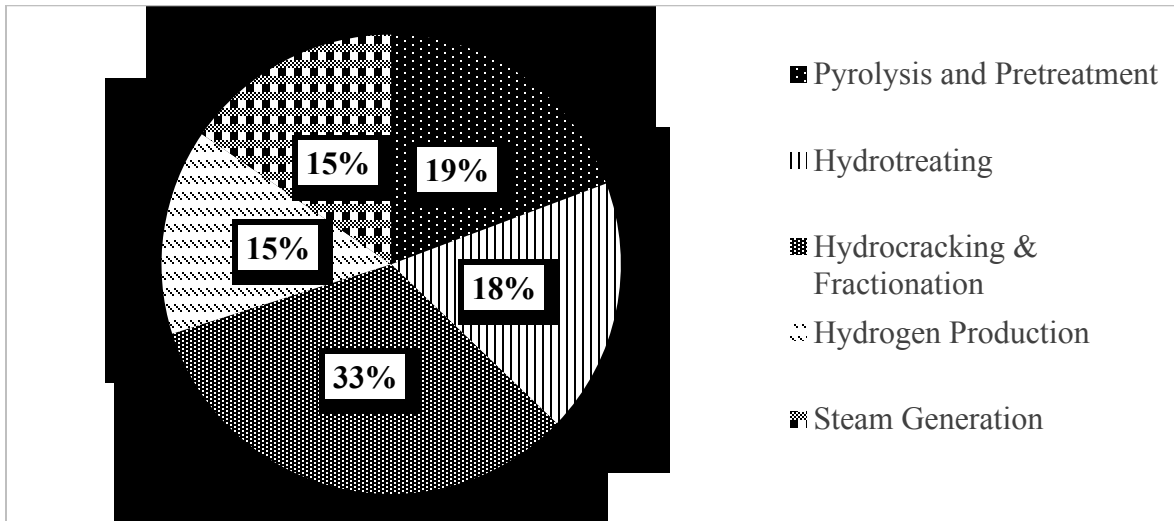


**Figure 5.5. Distribution of purchased equipment cost for hydrogen production scenario for spruce wood**

In the H<sub>2</sub> purchase scenario analysis, electricity production and H<sub>2</sub> production unit costs are not considered; the total equipment cost thus falls by 30%, thereby reducing capital costs and renewable production cost from 1.11 \$ L<sup>-1</sup> (in the H<sub>2</sub> production scenario) to 0.98 \$ L<sup>-1</sup> for spruce.

The installed capital costs are 322.7 M\$ and 300.6 M\$, respectively, for corn stover and wheat straw for the H<sub>2</sub> production scenario for a 2000 dry tonne/day plant and the corresponding renewable diesel production costs are 1.19 \$ L<sup>-1</sup> and 1.27 \$ L<sup>-1</sup>. Fast pyrolysis and hydroprocessing plant capital costs are lower for agricultural residues than for woody biomass for two reasons. The first is that agricultural residue feedstock has low moisture content and so less feedstock is handled in the biomass pretreatment unit. The second reason is a lower bio-oil yield from the pyrolyzer for

agricultural residues. The lower capital cost lowered the cost of the hydrotreaters, hydrocracker, and fractionation columns because they handle lower capacities of bio-oil than generated from spruce hardwood. Annual operating costs are 170.6 M\$, 133 M\$, and 123 M\$, respectively, for spruce, corn stover, and straw in the H<sub>2</sub> production scenario.

**Table 5-7. Summary of main cost estimates for a size of 2000 dry t d<sup>-1</sup> plant**

Parameter	Spruce		Corn stover	Wheat straw
	Merchant H <sub>2</sub>	H <sub>2</sub> production	H <sub>2</sub> production	H <sub>2</sub> production
Installed capital cost (M\$)	247.3	347.8	322.7	300.6
Total project investment cost (M\$)	422.6	594.5	551.5	513.8
Annual operating cost (M\$ y <sup>-1</sup> )	157.3	170.6	133.0	123.4
Cost of renewable diesel (\$ L <sup>-1</sup> )	0.98	1.11	1.19	1.27
Cost of gasoline (\$ L <sup>-1</sup> )	0.93	1.06	1.14	1.22

#### 5.4.2.2 Cost distribution

Figure 5.6 shows the operating cost distribution of renewable diesel for spruce (H<sub>2</sub> purchase and production scenarios), corn stover (H<sub>2</sub> production scenario), and wheat straw (H<sub>2</sub> production scenario) for a plant capacity of 2000 t d<sup>-1</sup>. Renewable diesel production costs for spruce hardwood are 1.11 \$ L<sup>-1</sup> and 0.98 \$ L<sup>-1</sup>, respectively, in the H<sub>2</sub> production and purchase scenarios. In both scenarios, raw material cost contributed significantly to cost of renewable diesel, followed by capital cost, maintenance cost, utility cost, and camping cost. Raw material costs are 0.52 \$ L<sup>-1</sup> and 0.49 \$ L<sup>-1</sup> in the H<sub>2</sub> purchase and the H<sub>2</sub> production scenarios, respectively. In the H<sub>2</sub> production scenario, the raw material cost is low because there are no H<sub>2</sub> purchase costs, but capital costs are high because of the costs to install a H<sub>2</sub> reforming plant and an electricity generation plant. The capital costs are 0.15 \$ L<sup>-1</sup> and 0.10 \$ L<sup>-1</sup>, respectively, in the H<sub>2</sub> production and the purchase scenarios. The utility cost is significantly lower in the H<sub>2</sub> purchase scenario (0.05 \$ L<sup>-1</sup>) than in the H<sub>2</sub> production scenario (0.09 \$ L<sup>-1</sup>) because less equipment is needed. For this analysis, the biochar produced in the fast pyrolysis process is considered revenue instead of an energy

source; in other words, the electricity produced in the power generation unit is consumed in the plant and there is no excess for revenue. Plant maintenance and overhead costs are high in the H<sub>2</sub> production scenario because more equipment is needed during operation.

For corn stover and wheat straw, the renewable diesel production cost present values are 1.19 \$ L<sup>-1</sup> and 1.27 \$ L<sup>-1</sup>, respectively, in the hydrogen production scenario. Both are higher than the renewable diesel production costs in both spruce scenarios because of the higher transportation fuel yield. For corn stover and wheat straw, the raw material cost makes up a significant portion of the renewable diesel production cost, 0.47 \$ L<sup>-1</sup> and 0.56 \$ L<sup>-1</sup>, respectively. These costs are higher than for spruce wood because of the lower agricultural residue yield per hectare than woody biomass (see Table 5.4). As stated earlier, there is no camping cost in agricultural residue harvesting as the fields are easily accessible. Capital costs are 0.19 \$ L<sup>-1</sup> and 0.21 \$ L<sup>-1</sup> and maintenance costs are 0.12 \$ L<sup>-1</sup> and 0.13 \$ L<sup>-1</sup>, respectively, for corn stover and straw. Cost ranges are explained in more detail in the sensitivity analysis.

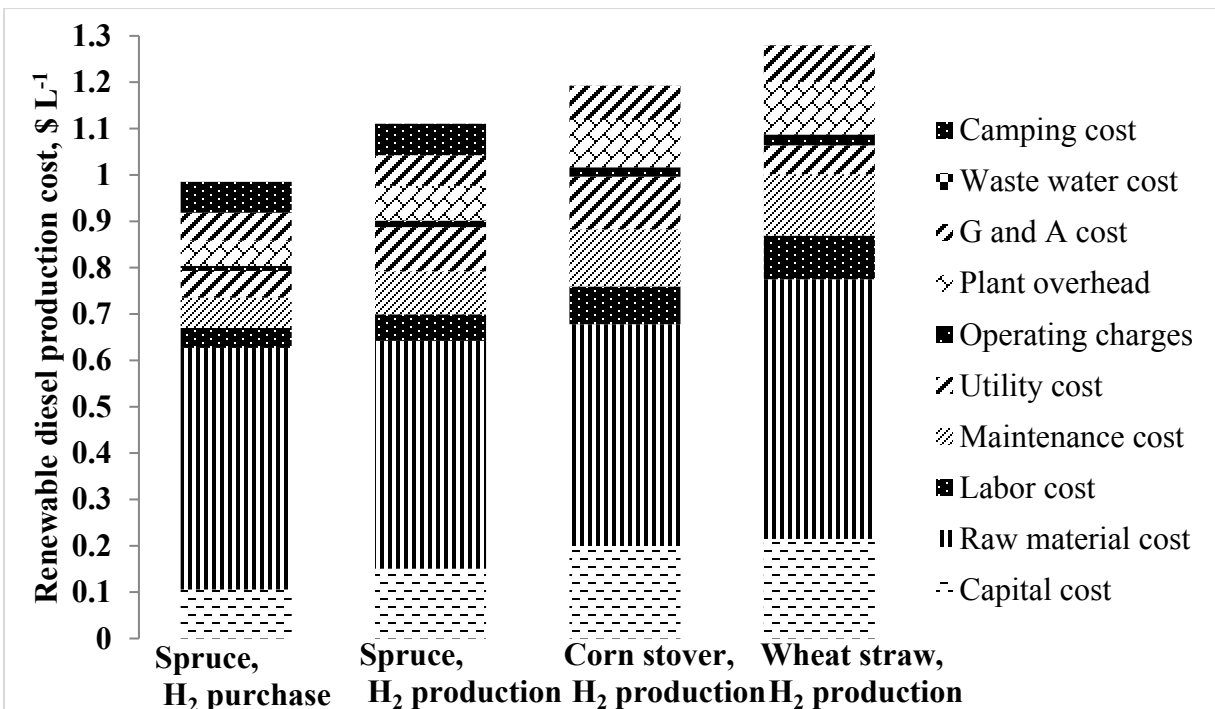


**Figure 5.6. Distribution of operating cost on present worth of renewable diesel for a plant capacity of 2000 t d<sup>-1</sup> based on techno-economic model**

#### 5.4.2.3 Effects of byproduct cost on renewable diesel production cost

To make pyrolysis process competitive with conventional fossil fuel technologies, it is required to identify the value of biochar as a by product and making it marketable will enhance feasibility of this process. In this study, an attempt was made to understand the effects of byproduct costs on the production cost of renewable diesel. Figure 5.7 (a) and Table 5.8 show variation in renewable diesel cost with a biochar selling price of 0 to 500 \$ t<sup>-1</sup> on a dry basis (Shabangu et al., 2014). The diesel production cost decreases with increases in the selling price of biochar. For both the hydrogen production and purchase scenarios of spruce wood, the renewable diesel cost fell by almost 15% when biochar cost increased from 0 to 500 \$ t<sup>-1</sup>. However, for wheat straw and corn stover, renewable diesel costs fell by 29.7% and 23.3%, respectively, when biochar cost increased from 0 to 500 \$ t<sup>-1</sup> as agricultural residues produced more biochar than woody biomass, which increased the biochar revenue and which was reflected in the renewable diesel cost. Therefore, the byproduct cost has a significant effect on the production cost of the main products.

**Table 5-8. Variation of renewable production cost as a function of biochar selling price**

Biochar cost (\$ t <sup>-1</sup> )	Renewable diesel cost (\$ L <sup>-1</sup> )			
	selling Spruce (H <sub>2</sub> prod)	Spruce (H <sub>2</sub> purchase)	Wheat straw (H <sub>2</sub> prod)	Corn stover (H <sub>2</sub> prod)
0	1.143	1.017	1.361	1.251
50	1.126	1.001	1.320	1.222
100	1.110	0.985	1.280	1.193
150	1.094	0.969	1.239	1.163
250	1.062	0.936	1.158	1.105
350	1.029	0.904	1.077	1.047
400	1.013	0.888	1.037	1.018
500	0.981	0.855	0.955	0.959

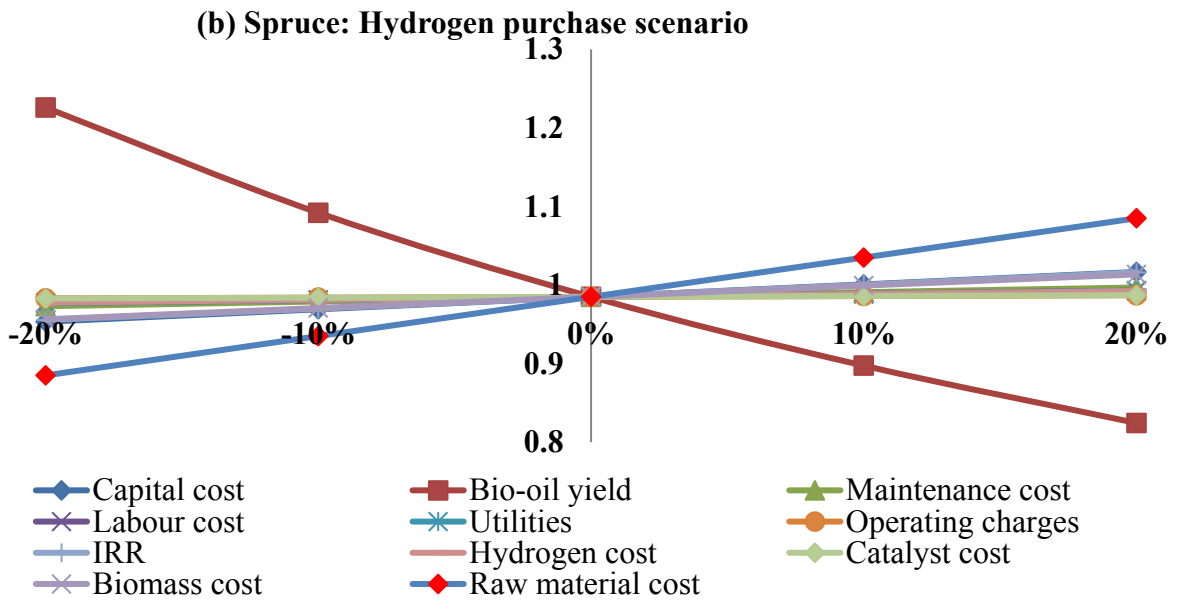
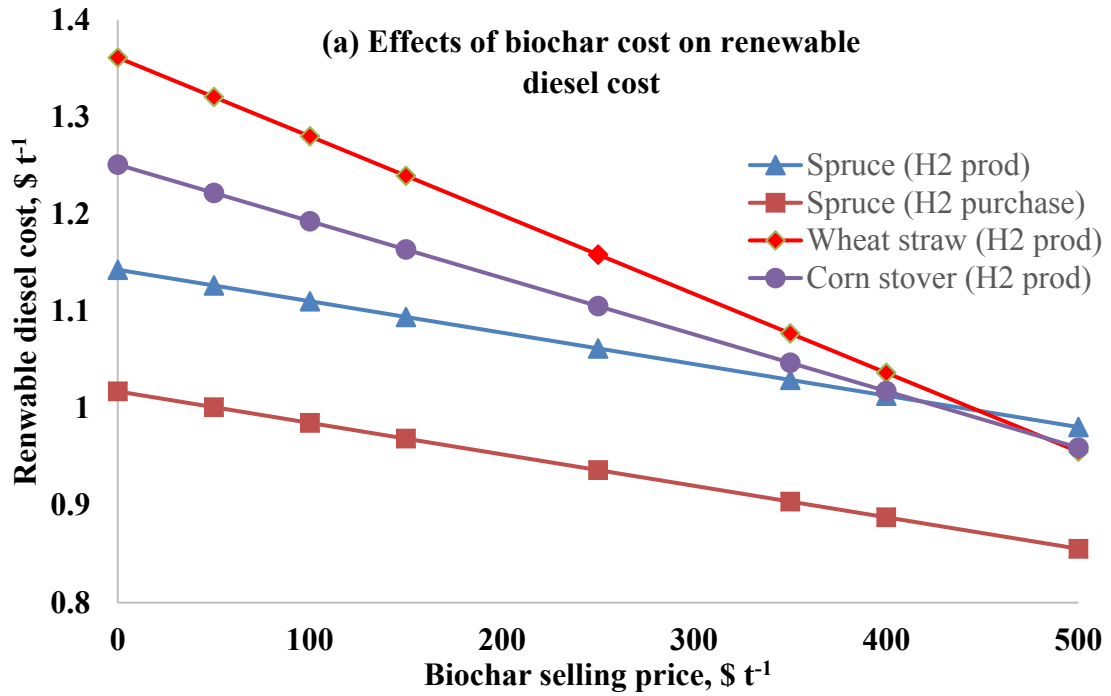
#### 5.4.2.4 Sensitivity analysis

Figure 5.7 (b), (c), (d), and (e) show the economic and process parameter sensitivities of spruce (in the H<sub>2</sub> production and purchase scenarios) and of agricultural residues (in the H<sub>2</sub> production scenario) on the production cost of renewable diesel in terms of present worth. All the parameters

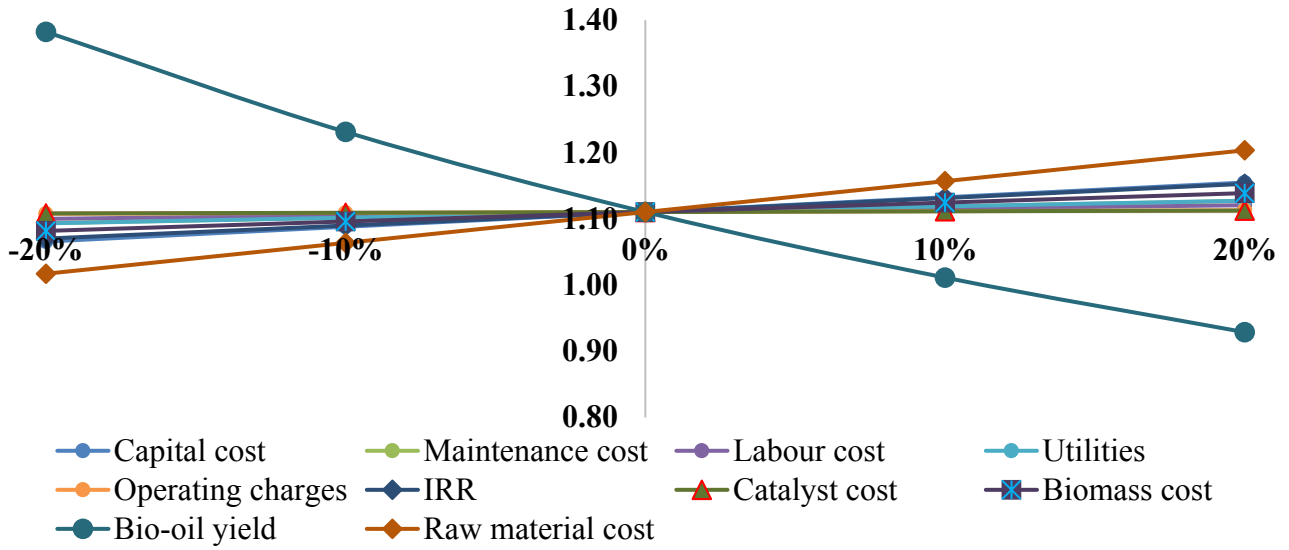
were varied by  $\pm 20\%$ . The cost of renewable diesel in  $\$ \text{L}^{-1}$  changed from 0.82-1.22, 0.93-1.38, 0.99-1.48, and 1.07-1.59, respectively, in the spruce  $\text{H}_2$  purchase scenario, the spruce  $\text{H}_2$  production scenario, the corn stover  $\text{H}_2$  production scenario, and the wheat straw  $\text{H}_2$  production scenario. Of all the parameters, bio-oil yield is most sensitive to the production cost of the renewable diesel for all the feedstocks for both the  $\text{H}_2$  production and the purchase scenario. Optimizing process conditions (i.e., reactor design, temperature, and particle size) could increase the bio-oil yield, which further reduces production costs. The diesel cost fell to  $0.82 \text{ \$ L}^{-1}$  from  $1.22 \text{ \$ L}^{-1}$  and  $0.99 \text{ \$ L}^{-1}$  from  $1.38 \text{ \$ L}^{-1}$  in the  $\text{H}_2$  purchase and the production scenarios, respectively, when bio-oil yield was increased by 20% for spruce feedstock. When bio-oil yields for corn stover and wheat straw were increased by 20%, the renewable diesel costs fell from 1.19 to  $0.99 \text{ \$ L}^{-1}$  and 1.27 to  $1.07 \text{ \$ L}^{-1}$ , respectively.

After bio-oil yield, raw material cost is the most influential parameter. When raw material costs were increased by 20%, diesel costs increased from 0.98 to  $1.08 \text{ \$ L}^{-1}$  and 1.11 to  $1.20 \text{ \$ L}^{-1}$ , respectively, for the spruce feedstock  $\text{H}_2$  purchase and the  $\text{H}_2$  production scenarios. For corn stover and straw, renewable diesel cost also increases with an increase in raw material cost.

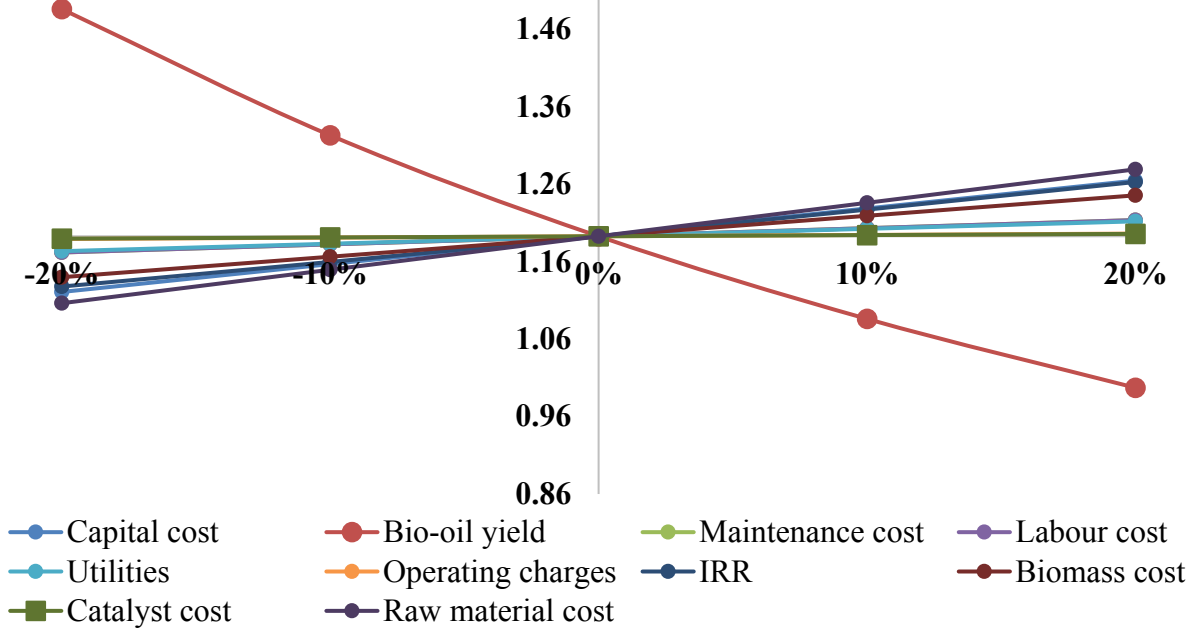
The other influential parameters are the internal rate of return (IRR) and capital cost. The cost of renewable diesel increases with an increase in these parameters. By increasing the IRR by 20%, the  $\text{ \$ L}^{-1}$  cost of renewable diesel increases by 3%, 4%, 5.4%, and 5%, respectively, in the spruce  $\text{H}_2$  purchase scenario, the spruce  $\text{H}_2$  production scenario, the corn stover  $\text{H}_2$  production scenario, and the wheat straw  $\text{H}_2$  production scenario. Capital cost and renewable diesel cost are directly proportional to each other.



(c) Spruce: Hydrogen production scenario



(d) Corn stover: Hydrogen production scenario



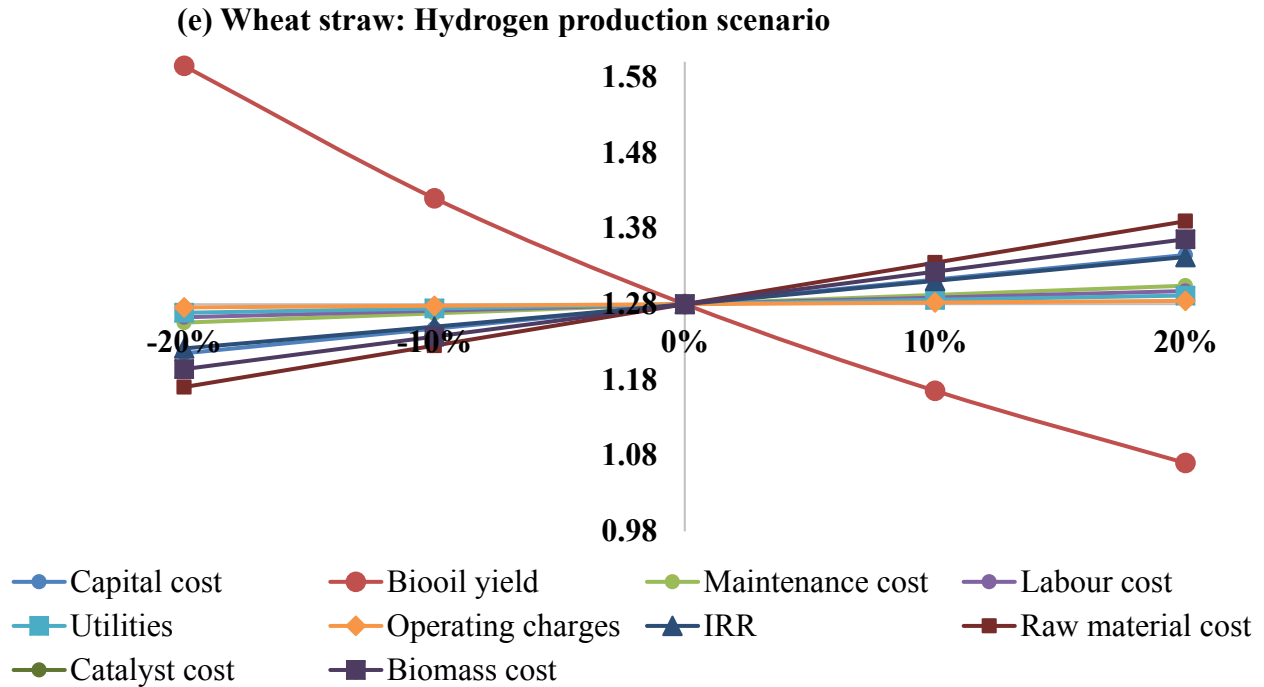


**Figure 5.7. Sensitivity analysis for renewable diesel from (e) Effects of biochar selling price on renewable diesel cost, (b) Spruce: H<sub>2</sub> purchase, (c) Spruce: H<sub>2</sub> production (d) Corn stover: H<sub>2</sub> production, and (e) Wheat straw: H<sub>2</sub> production**

#### 5.4.2.5 Net energy ratio analysis

By definition, the net energy ratio (NER) is the ratio between the energy output in terms of renewable energy to the energy input from non-renewable resources (Burgess & Fernández-Velasco, 2007; Miller & Kumar, 2013; Shahrukh et al., 2016; Shahrukh et al., 2015). To calculate the NER for fast pyrolysis and hydroprocessing technology, the following operations are considered: biomass cultivation, harvesting, biomass transportation to the plant, the fast pyrolysis process, the reforming, power generation, and hydroprocessing. In the H<sub>2</sub> purchase scenario, H<sub>2</sub> reforming and the power generation unit are not included. The NER is the ratio of efficient renewable energy production to the consumption of energy from a fossil fuel. For this analysis, diesel and electricity are assumed as the energy input from conventional sources. By definition, if the NER of a process is greater than 1, then the process is considered energy efficient. Specifically,

for new technology for renewable resources, which are economically very demanding, an NER greater than one is required to see any energy and emissions benefits.

In this study, the NERs for spruce, corn stover and wheat straw were estimated to be 2.16, 1.5, and 1.16, respectively, for fast pyrolysis and hydroprocessing technology in the H<sub>2</sub> production scenario. For all the feedstocks, the NER shows that less fossil fuel is consumed than the energy produced through renewable energy. Of all the biomass considered, spruce was found to have highest NER; this is because of the high transportation fuel yield and lower diesel consumption during harvesting than agricultural feedstock. These NER numbers were compared with published results for similar pathways and different feedstocks and are in good agreement. For example, Miller and Kumar (Miller & Kumar, 2013) (analyzed the NER for canola and camelina feedstock for the production of renewable diesel and reported an NER from 1 to 2.3. The NER ranges are a result of feedstock type, oil extraction method, and upgrading technology. Wong et al. (Wong et al., 2016) also did an NER analysis for renewable diesel production and reported NER values of 1.55 to 1.9 depending on the feedstock type. The output energy from biomass feedstock fast pyrolysis and upgrading technology is higher than the fossil fuel energy input, which helps to reduce greenhouse gas emissions.

#### *5.4.2.6 Comparison of renewable diesel production costs with published values*

Because of their lower costs and availability, petro-fuels from crude oil are more attractive than renewable diesel to investors and end users. Renewable diesel from fast pyrolysis and hydroprocessing technology has a comparatively higher capital cost than conventional methods. Further research and development and potential government support is needed for large commercial scale development of the technology.

Production costs of transportation fuels from fast pyrolysis and hydroprocessing reported in the literature range from 0.64-1.3 \$ L<sup>-1</sup>, depending on the biomass (Patel & Kumar, 2016; Shemfe et al., 2015). Recently, Li et al. (2017) studied different fractions of bio-oil and upgraded that to

gasoline and diesel fractions through hydroprocessing for red oak feedstock and reported a production cost of 0.8 \$ L<sup>-1</sup>. Following their sensitivity study, they found that feedstock cost, capital cost, and product yield are more sensitive than other factors to transportation cost. Differences in the production cost of the upgraded biofuel are due to location factor and product yield. To the best of our knowledge, there is no Canadian study on techno-economic assessment of upgrading bio-oil from different feedstocks and comparing the production costs of the end products. In this study, we looked at the three different Canadian biomass feedstocks and two different scenarios (H<sub>2</sub> purchase and production) to estimate the present value of the renewable diesel and gasoline. The production costs of renewable diesel are 0.98 \$ L<sup>-1</sup>, 1.11 \$ L<sup>-1</sup>, 1.19 \$ L<sup>-1</sup>, and 1.27 \$ L<sup>-1</sup>, respectively, for the spruce H<sub>2</sub> purchase scenario, the spruce H<sub>2</sub> production scenario, the corn stover H<sub>2</sub> production scenario, and the wheat straw H<sub>2</sub> production scenario for a plant capacity of 2000 dry t d<sup>-1</sup>.

Finally, the production cost of renewable diesel found in this analysis was compared with the production cost of conventional diesel. After provincial taxes and the market margin are deducted from the rack price, the production costs of petro-diesel and gasoline were calculated to be 0.48-0.68 \$ L<sup>-1</sup> and 0.43-0.6 \$ L<sup>-1</sup>, respectively, from January 2017 to November 2017 (Natural resources Canada, 2017). The price of conventional fuel changed considerably due to market conditions and was highly unpredictable. The cost calculated for renewable diesel in this study is higher than the conventional diesel cost. But the cost of renewable diesel from the spruce H<sub>2</sub> purchase scenario is at the higher end of the petro-diesel cost. This analysis considered a standalone pyrolysis and hydroprocessing unit. The cost of renewable fuel could be reduced if this unit can be combined with an existing refinery where a H<sub>2</sub> production unit is already established. This option can be explored and more research is required in the technical aspects of the hydroprocessing technology to make this process real.

## 5.5 Conclusion

This study performed experimental work on production of bio-oil from three different biomass feedstocks in Canada. The experimental data along data from literature were used to develop

techno-economic models for the use of three Canadian biomass feedstocks to produce renewable diesel and gasoline through fast pyrolysis and hydroprocessing technology for a plant capacity of 2000 t d<sup>-1</sup>. The production cost of renewable diesel cost ranges from 0.98 – 1.27 \$ L<sup>-1</sup> depending on the feedstocks type and hydrogen production scenarios. The sensitivity analysis showed that bio-oil yield is most sensitive to renewable diesel production cost, followed by raw material cost, capital cost, and IRR. The raw material cost is approximately 53% of total production cost for spruce hydrogen purchase scenario, whereas for hydrogen production scenario, raw material cost varies between 40-44% of total production cost of renewable diesel for all the feedstocks. To make the process cost competitive with existing refinery technology, more attention should be paid to reducing both biomass feedstock and capital costs of the whole pathway. The plant location and collaboration with an existing refinery could help to commercialize this technology.

In this study, an attempt was made to investigate the variation in the production cost of renewable diesel as a function of selling price of biochar, ranges from 0 to 500 \$ t<sup>-1</sup> on the dry basis. With increase in selling price of biochar, the renewable diesel cost decreases significantly. With increase in cost from 0 to 500 \$ t<sup>-1</sup>, the renewable diesel cost reduces from 1.02 to 0.85, 1.14 to 0.98, 1.25 to 0.95 and 1.36 to 0.95 \$ L<sup>-1</sup>, respectively, for spruce hydrogen purchase scenario, spruce hydrogen production scenario, corn stover hydrogen production scenario and wheat straw hydrogen production scenario. Therefore, consideration of biochar as byproduct could be improve the economic feasibility of the pyrolysis and hydroprocessing technology.

## References

- Agbor, E., Oyedun, A.O., Zhang, X., Kumar, A. 2016. Integrated techno-economic and environmental assessments of sixty scenarios for co-firing biomass with coal and natural gas. *Applied Energy*, **169**(Supplement C), 433-449.
- Anex, R.P., Aden, A., Kazi, F.K., Fortman, J., Swanson, R.M., Wright, M.M., Satrio, J.A., Brown, R.C., Daugaard, D.E., Platon, A., Kothandaraman, G., Hsu, D.D., Dutta, A. 2010. Techno-economic comparison of biomass-to-transportation fuels via pyrolysis, gasification, and biochemical pathways. *Fuel*, **89**, S29-S35.
- Bridgwater, A.V., Meier, D., Radlein, D. 1999. An overview of fast pyrolysis of biomass. *Organic Geochemistry*, **30**(12), 1479-1493.
- Brown, T.R., Thilakaratne, R., Brown, R.C., Hu, G. 2013. Techno-economic analysis of biomass to transportation fuels and electricity via fast pyrolysis and hydroprocessing. *Fuel*, **106**(Supplement C), 463-469.
- Burgess, G., Fernández-Velasco, J.G. 2007. Materials, operational energy inputs, and net energy ratio for photobiological hydrogen production. *International Journal of Hydrogen Energy*, **32**(9), 1225-1234.
- Burhenne, L., Messmer, J., Aicher, T., Laborie, M.-P. 2013. The effect of the biomass components lignin, cellulose and hemicellulose on TGA and fixed bed pyrolysis. *Journal of Analytical and Applied Pyrolysis*, **101**, 177-184.
- Cortright, R.D., Davda, R.R., Dumesic, J.A. 2002. Hydrogen from catalytic reforming of biomass-derived hydrocarbons in liquid water. *Nature*, **418**(6901), 964-967.
- Demirbaş, A. 1997. Calculation of higher heating values of biomass fuels. *Fuel*, **76**(5), 431-434.
- Elliott, D., Neuenschwander, G. 1997. Liquid fuels by low-severity hydrotreating of biocrude. in: *Developments in thermochemical biomass conversion*, Springer, pp. 611-621.
- Elliott, D.C., Hart, T.R., Neuenschwander, G.G., Rotness, L.J., Zacher, A.H. 2009. Catalytic hydroprocessing of biomass fast pyrolysis bio- oil to produce hydrocarbon products. *Environmental Progress & Sustainable Energy: An Official Publication of the American Institute of Chemical Engineers*, **28**(3), 441-449.
- EPCOR. 2017. Rate, tariffs and fee, available at <https://www.epcor.com/products-services/power/rates-tariffs-fees/Pages/default.aspx>. Accessed on 26th Spetember 2017.

- Gable, P., Brown, R.C. 2016. Effect of biomass heating time on bio-oil yields in a free fall fast pyrolysis reactor. *Fuel*, **166**(Supplement C), 361-366.
- Garcia-Perez, M., Wang, X.S., Shen, J., Rhodes, M.J., Tian, F., Lee, W.-J., Wu, H., Li, C.-Z. 2008. Fast Pyrolysis of Oil Mallee Woody Biomass: Effect of Temperature on the Yield and Quality of Pyrolysis Products. *Industrial & Engineering Chemistry Research*, **47**(6), 1846-1854.
- Government of Canada. 2017. How much forest does Canada have?, available at <http://www.nrcan.gc.ca/forests/report/area/17601>. Accessed on 7th November 2017.
- Government of Canada. 2017. Greenhouse gas emissions by Canadian economic sector, available at <https://www.canada.ca/en/environment-climate-change/services/environmental-indicators/greenhouse-gas-emissions/canadian-economic-sector.html>. Accessed on 7th November, 2017.
- Greenhalf, C.E., Nowakowski, D.J., Harms, A.B., Titiloye, J.O., Bridgwater, A.V. 2013. A comparative study of straw, perennial grasses and hardwoods in terms of fast pyrolysis products. *Fuel*, **108**, 216-230.
- Gregoire, C.E., Bain, R.L. 1994. Technoeconomic analysis of the production of biocrude from wood. *Biomass and Bioenergy*, **7**(1), 275-283.
- Islam, M.N., Ani, F.N. 2000. Techno-economics of rice husk pyrolysis, conversion with catalytic treatment to produce liquid fuel. *Bioresource Technology*, **73**(1), 67-75.
- Jeong, J.-Y., Lee, U.-D., Chang, W.-S., Jeong, S.-H. 2016. Production of bio-oil rich in acetic acid and phenol from fast pyrolysis of palm residues using a fluidized bed reactor: Influence of activated carbons. *Bioresource Technology*, **219**(Supplement C), 357-364.
- Ji-lu, Z. 2007. Bio-oil from fast pyrolysis of rice husk: Yields and related properties and improvement of the pyrolysis system. *Journal of Analytical and Applied Pyrolysis*, **80**(1), 30-35.
- Jones, S.B., Meyer, P.A., Snowden-Swan, L.J., Padmaperuma, A.B., Tan, E., Dutta, A., Jacobson, J., Cafferty, K. 2013a. Process Design and Economics for the Conversion of Lignocellulosic Biomass to Hydrocarbon Fuels: Fast Pyrolysis and Hydrotreating Bio-Oil Pathway. ; Pacific Northwest National Lab. (PNNL), Richland, WA (United States). PNNL--23053; NREL/TP--5100-61178; Other: BM0101010 United States 10.2172/1115839 Other: BM0101010 PNNL English.

- Jones, S.B., Meyer, P.A., Snowden-Swan, L.J., Padmaperuma, A.B., Tan, E., Dutta, A., Jacobson, J., Cafferty, K. 2013b. Process design and economics for the conversion of lignocellulosic biomass to hydrocarbon fuels: fast pyrolysis and hydrotreating bio-oil pathway. Pacific Northwest National Lab.(PNNL), Richland, WA (United States).
- Jones, S.B., Valkenburt, C., Walton, C.W., Elliott, D.C., Holladay, J.E., Stevens, D.J., Kinchin, C., Czernik, S. 2009. Production of gasoline and diesel from biomass via fast pyrolysis, hydrotreating and hydrocracking: a design case. Pacific Northwest National Laboratory (PNNL), Richland, WA (US).
- Kan, T., Strezov, V., Evans, T.J. 2016. Lignocellulosic biomass pyrolysis: A review of product properties and effects of pyrolysis parameters. *Renewable and Sustainable Energy Reviews*, **57**(Supplement C), 1126-1140.
- Kaycircle. 2017. Average nitrogen price, available at <http://www.kaycircle.com/What-Is-The-Average-Cost-Of-Nitrogen-Gas-Per-Gram-Pound-Cubic-Foot-Average-Nitrogen-Price>. Accessed on 26th September 2017.
- Kumar, A., Cameron, J.B., Flynn, P.C. 2003. Biomass power cost and optimum plant size in western Canada. *Biomass and Bioenergy*, **24**(6), 445-464.
- LaClaire, C.E., Barrett, C.J., Hall, K. 2004. Technical, environmental and economic feasibility of bio-oil in new hampshire's north country. *Durham, NH: University of New Hampshire*.
- Li, W., Dang, Q., Smith, R., Brown, R.C., M. Wright, M. 2017. Techno-Economic Analysis of the Stabilization of Bio-Oil Fractions for Insertion into Petroleum Refineries. *ACS Sustainable Chemistry & Engineering*, **5**(2), 1528-1537.
- Liu, R., Deng, C., Wang, J. 2009. Fast Pyrolysis of Corn Straw for Bio-oil Production in a Bench-scale Fluidized Bed Reactor. *Energy Sources, Part A: Recovery, Utilization, and Environmental Effects*, **32**(1), 10-19.
- Meibod, M.P. 2013. Bio-oil from wheat straw and hydrogen from aqueous phase of bio-oil. in: *Department of Chemical and Petroleum Engineering*, Vol. Master of science, University of Alberta.
- Miller, P., Kumar, A. 2013. Development of emission parameters and net energy ratio for renewable diesel from Canola and Camelina. *Energy*, **58**(Supplement C), 426-437.

- Miller, P., Kumar, A. 2014. Techno-economic assessment of hydrogenation-derived renewable diesel production from canola and camelina. *Sustainable Energy Technologies and Assessments*, **6**, 105-115.
- Minerals, S.I. 2017. Industrial sands, available at <http://sil.ab.ca/sil-filter-sand/>. Accessed on 28th Spetember 2017.
- Natural resources Canada. 2017. Diesel price, available at <http://www.nrcan.gc.ca/energy/fuel-prices/4797>. Accessed on 14th November 2017
- Newsome, D.S. 1980. The Water-Gas Shift Reaction. *Catalysis Reviews*, **21**(2), 275-318.
- Öhgren, K., Bura, R., Lesnicki, G., Saddler, J., Zacchi, G. 2007. A comparison between simultaneous saccharification and fermentation and separate hydrolysis and fermentation using steam-pretreated corn stover. *Process Biochemistry*, **42**(5), 834-839.
- Oyedun, A.O., Kumar, A., Oestreich, D., Arnold, U., Sauer, J. 2018. The development of the production cost of oxymethylene ethers as diesel additives from biomass. *Biofuels, Bioproducts and Biorefining*, **12**(4), 694-710.
- Patel, M., Kumar, A. 2016. Production of renewable diesel through the hydroprocessing of lignocellulosic biomass-derived bio-oil: A review. *Renewable and Sustainable Energy Reviews*, **58**, 1293-1307.
- Patel, M., Oyedun, A.O., Kumar, A., Gupta, R. 2018. A Techno-Economic Assessment of Renewable Diesel and Gasoline Production from Aspen Hardwood. *Waste and Biomass Valorization*.
- Patel, M., Zhang, X., Kumar, A. 2016. Techno-economic and life cycle assessment on lignocellulosic biomass thermochemical conversion technologies: A review. *Renewable and Sustainable Energy Reviews*, **53**(Supplement C), 1486-1499.
- Peters, M.S., Timmerhaus, K.L. 1991. *plant design and economics for chemical engineers. fourth ed.* McGraw-Hill, Inc.
- Ringer, M., Putsche, V., Scahill, J. 2006. Large-scale pyrolysis oil production: a technology assessment and economic analysis. National Renewable Energy Laboratory (NREL), Golden, CO.
- Russell, J.A., Miller, R.K., Molton, P.M. 1983. Formation of aromatic compounds from condensation reactions of cellulose degradation products. *Biomass*, **3**(1), 43-57.

- Sarkar, S., Kumar, A. 2010. Large-scale biohydrogen production from bio-oil. *Bioresource Technology*, **101**(19), 7350-7361.
- Shabangu, S., Woolf, D., Fisher, E.M., Angenent, L.T., Lehmann, J. 2014. Techno-economic assessment of biomass slow pyrolysis into different biochar and methanol concepts. *Fuel*, **117**, 742-748.
- Shahrukh, H., Oyedun, A.O., Kumar, A., Ghiasi, B., Kumar, L., Sokhansanj, S. 2016. Comparative net energy ratio analysis of pellet produced from steam pretreated biomass from agricultural residues and energy crops. *Biomass and Bioenergy*, **90**, 50-59.
- Shahrukh, H., Oyedun, A.O., Kumar, A., Ghiasi, B., Kumar, L., Sokhansanj, S. 2015. Net energy ratio for the production of steam pretreated biomass-based pellets. *Biomass and Bioenergy*, **80**, 286-297.
- Shemfe, M.B., Gu, S., Ranganathan, P. 2015. Techno-economic performance analysis of biofuel production and miniature electric power generation from biomass fast pyrolysis and bio-oil upgrading. *Fuel*, **143**(Supplement C), 361-372.
- Shen, J., Wang, X.-S., Garcia-Perez, M., Mourant, D., Rhodes, M.J., Li, C.-Z. 2009. Effects of particle size on the fast pyrolysis of oil mallee woody biomass. *Fuel*, **88**(10), 1810-1817.
- Sokhansanj, S., Mani, S., Stumborg, M., Samson, R., Fenton, J. 2006. Production and distribution of cereal straw on the Canadian prairies. *Canadian Biosystems Engineering*, **48**, 3.
- Solantausta, Y., Beckman, D., Bridgwater, A., Diebold, J., Elliott, D. 1992. Assessment of liquefaction and pyrolysis systems. *Biomass and Bioenergy*, **2**(1-6), 279-297.
- Torri, I.D.V., Paasikallio, V., Faccini, C.S., Huff, R., Caramão, E.B., Sacon, V., Oasmaa, A., Zini, C.A. 2016. Bio-oil production of softwood and hardwood forest industry residues through fast and intermediate pyrolysis and its chromatographic characterization. *Bioresource Technology*, **200**(Supplement C), 680-690.
- Wong, A., Zhang, H., Kumar, A. 2016. Life cycle assessment of renewable diesel production from lignocellulosic biomass. *The International Journal of Life Cycle Assessment*, **21**(10), 1404-1424.
- Wright, M.M., Daugaard, D.E., Satrio, J.A., Brown, R.C. 2010. Techno-economic analysis of biomass fast pyrolysis to transportation fuels. *Fuel*, **89**(Supplement 1), S2-S10.

- Zhu, Y., Albrecht, K.O., Elliott, D.C., Hallen, R.T., Jones, S.B. 2013. Development of hydrothermal liquefaction and upgrading technologies for lipid-extracted algae conversion to liquid fuels. *Algal Research*, **2**(4), 455-464.
- Zhu, Y., Bidy, M.J., Jones, S.B., Elliott, D.C., Schmidt, A.J. 2014. Techno-economic analysis of liquid fuel production from woody biomass via hydrothermal liquefaction (HTL) and upgrading. *Applied Energy*, **129**(Supplement C), 384-394.
- Zhu, Z., Sathitsuksanoh, N., Vinzant, T., Schell, D.J., McMillan, J.D., Zhang, Y.H.P. 2009. Comparative study of corn stover pretreated by dilute acid and cellulose solvent- based lignocellulose fractionation: Enzymatic hydrolysis, supramolecular structure, and substrate accessibility. *Biotechnology and bioengineering*, **103**(4), 715-724.

## **Chapter 6: Development of Cost Model of Supply Chain Network for Two Scenarios of Decentralized pyrolysis system to Produce Bio-oil<sup>6</sup>**

### **6.1 Introduction**

Greenhouse gases (GHG) emission and associated global warming due to fossil fuel use, sustainability of biomass (consider as carbon neutral) and availability of local biomass are the main reasons for the growing interest in bioenergy and biofuels.

In North America, there is growing interest in biofuel as a transportation fuel replacement (World Energy Council, 2017). Canada has 347 million hectares of forest, an estimated 9% of the world's forests (Natural Resources Canada, 2017). In the last several decades, biomass has been used primarily in the pulp and paper industry, but due to the popularity and adoption of electronic media, demand for pulp and paper is shrinking which was using about 57% of biomass energy (Bradburn, 2014; Canada, 2008; Historica Canada, 2017).

Governments around the world support bioenergy sector and are encouraging use of biomass resources for the production of biofuels and chemicals (Demirbas & Balat, 2006; Guo et al., 2015;

---

<sup>6</sup> A version of this chapter is submitted to Biomass and Bioenergy as Patel M, Oyedun A, Kumar A, Doucette J. Economic feasibility and model development for the bio-oil production from hardwood for two configurations of mobile pyrolysis system (MPS), 2018 (submitted)

Lynd et al., 2011). Fast pyrolysis is a well-investigated commercial technology for the conversion of biomass to liquid fuels in a centralized plant. Fast pyrolysis takes place in a pyrolyzer in the absence of oxygen at 400-600 °C and at atmospheric pressure (Bridgwater, 2012; Patel et al., 2018). The outputs from this process are bio-oil, gas, and biochar. Generally, the bio-oil yields vary from 50-75 wt% depending on the feedstock and process parameters (Bridgwater & Peacocke, 2000; Patel et al., 2016). Bio-oil is considered an intermediate for transportation fuel and can be further upgraded through hydroprocessing technology to produce a petro-fuel equivalent (Bridgwater, 1999; Patel & Kumar, 2016).

In general, centralized plants are used for conventional fuels such as coal and natural gas because of economies of scale benefits in capital cost at higher capacities. Usually biomass is transported from the nearest forest to a centralized pyrolysis plant to produce biofuel. An economy of scale concept is also true for biomass (Kumar et al., 2003). Kumar et al. investigated the production costs of electricity from biomass for different plant capacities (Kumar et al., 2003). They found that electricity costs initially decreased with an increase in capacity as the economy of scale benefits outweighs the increase in the biomass transportation cost, and reaches a minimum. With further increase in plant capacity, electricity cost increases. This is because of increase in biomass transportation costs which outweighs the benefits from the economy of scale in capital cost. Another study by Kumar et al. (Kumar et al., 2008) also estimated cost of power generation from combustion of Canadian mountain pine infested wood for a range of plant capacity from 50 to 450 MW and observed the cost of power production was highest at low capacity and with increased in plant capacity, the cost reached the lowest value. But with further increased in plant capacity, it maintained a flat trend. The reason was aligned with their previous study (Kumar et al., 2003). Other key challenges for a large capacity centralized pyrolysis plant are the feedstock availability and large capital investment. These challenges might be overcome by using mobile pyrolysis system (Sorenson, 2010).

The concept of the decentralized or MPS is to reduce the raw biomass handling and transportation costs compared to centralized pyrolysis plants. The characteristics and advantages of an MPS over a centralized plant are portability, mobility, simplicity, and adaptability to regions and weather.

The technical and economic aspects of mobile pyrolysis system are studied by a few researchers in the literature (Badger et al., 2010; Badger & Fransham, 2006; Brown et al., 2011; Brown et al., 2013; Ha et al., 2010; Palma et al., 2011; Wright et al., 2008). Brown et al. (Brown et al., 2011) investigated economic feasibility of two capacities of MPS units: 10 and 50 dry t d<sup>-1</sup> for small diameter conifer trees available in northern New Mexico forests. Simultaneously, a series of experiments were performed to enhance the yield of pyrolysis oil in the remote condition. They concluded that larger capacity of MPS unit is more cost effective and the cost of bio-oil can be optimized by reducing labor cost and increased utilization of fixed cost utilization such as suppliers for pre-chipped or pre-sized biomass. Another study in 2013 focused on two distributed mobile conversion facilities (fast pyrolysis and torrefication process) of 50 dry t d<sup>-1</sup> biomass plant capacity to convert forest residue to higher energy density material which can be further processed in biofuel facility and compared the levelized cost of delivery cost for these pathways. Badger and Fransham (2006) conducted a very preliminary techno-economic analysis to estimate the capital cost including installation cost of a bio-oil handling system for a mobile pyrolysis system and concluded that the estimated capital cost was comparable to the 50 MWe biomass handling system at the power plant. A techno-economic assessment of 100 dry tonne/day southern pine wood chip transportable pyrolysis system has been studied by Badger et al. (2010) using life cycle operating cost provided by Renewable Oil International (ROI) LLC. To produce Fischer Tropsch fuel in a centralized catalytic synthesis facility, Wright et al. (2008) compared two pathways: one is traditional centralized biomass gasification and Fischer Tropsch synthesis and second is distributed pyrolysis system to produce bio-oil followed by bio-oil gasification and Fischer Tropsch synthesis. For distributed pyrolysis, they considered three biomass facilities: on farm pyrolyzer, small cooperative pyrolyzer and large cooperative pyrolyzer. Few researchers have used geographic information system (GIS) to optimize the path and move of the distributed pyrolysis system to reduce the biomass transportation cost based on the feedstock availability and subsequently cost of bio-oil (Ha et al., 2010; Palma et al., 2011)

All the above studies are basically focused on the technical and economic feasibility of mobile pyrolysis system to produce bio-oil. But there is no study available in the literatures which describe the model development of supply chain network for the allocation of MPS units during the lifetime of the operation. These models take account of five different capacity of MPS units (10, 20, 40, 50 and 100 dry t d<sup>-1</sup>) and four relocation time (yearly, biyearly, quarterly and monthly) for estimation of bio-oil production cost. Relocation time stands for the frequency that a decentralized unit is moving in a year (such as biyearly relocation means that MPS unit will move 2 times in a year). To create framework for the distributed pyrolysis system, two configurations are considered which are shown in the Figure 6.1 and results are compared with the centralized pyrolysis facility.

The key objectives of this study are:

- Development of supply chain networks to evaluate the distributed mobile pyrolysis system to produce bio-oil through pyrolysis process using Canadian hardwood as the feedstock for a base case plant capacity of 2000 dry t d<sup>-1</sup>,
- Development of techno-economic models for each configuration (radial and square) of MPS to assess its economic feasibility,
- Comparison of bio-oil production cost from both centralized and distributed pyrolysis system for the base case capacity of 2000 dry t d<sup>-1</sup>,
- Evaluation of optimum plant capacity for each configuration where they intersect with the centralized system.

In this study, the term scenario and configuration are used interchangeably and also the term decentralized and mobile pyrolysis system is used interchangeably.

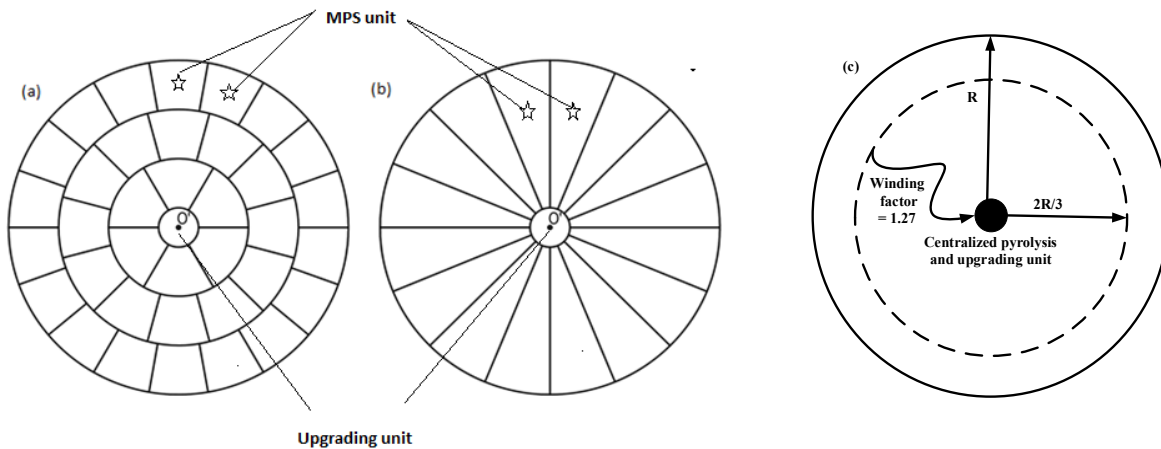


**Figure 6.1. Two MPS allocation configurations: (a) truncated and (b) radial and (c) centralized unit**

## 6.2 Method

### 6.2.1 *Centralized pyrolysis plant*

A centralized pyrolysis plant handles the large-scale production of bio-oil from whole tree biomass feedstock at one facility (a fixed facility where biomass is brought from nearby) which is shown by Figure 6.1 (c). A centralized facility is located at the center of the circular area and biomass is transported to the plant gate for processing. The biomass is harvested, chipped, and then trucked to the plant gate. The chipped biomass is then ground to a particle size less than 2 mm and dried to a moisture content less than 10 wt%, which is suitable for the pyrolyzer (Patel et al., 2018). Biomass pyrolysis takes place in a fluidized bed reactor in the absence of oxygen with nitrogen as the fluidizing gas to produce vapor and biochar. Biochar is separated through a cyclone and combusted to generate energy. The pyrolysis vapor is quenched in a series of condensers to produce bio-oil. For the centralized plant, it was assumed that the pyrolysis unit and upgrading unit are located at the same place, so the bio-oil transportation cost was not considered in the analysis. The detailed process and operating conditions of a centralized plant are further explained by Sarkar and Kumar (2010).

### 6.2.2 Mobile pyrolysis system

As a mobile pyrolysis plant is convenient, easy to assemble and use, and portable, it is considered a strong alternative to a centralized plant. An MPS unit is loaded on a trailer that is attached to a truck or tractor. The unit can be moved to a remote area where feedstock is available and the produced bio-oil can be transported to an upgrading facility. As the density of bio-oil ( $1.2\text{-}1.3 \text{ kg L}^{-1}$ ) is almost three times more than the density of raw biomass, transportation costs are low (Sarkar & Kumar, 2010). An MPS unit consists of a dryer, grinder, biomass feeder, auger screw feeder, auger reactor, cyclone separator, condenser, biochar collector, and bio-oil collection chamber (see Figure 6.2). Each MPS unit requires a biomass field storage area.

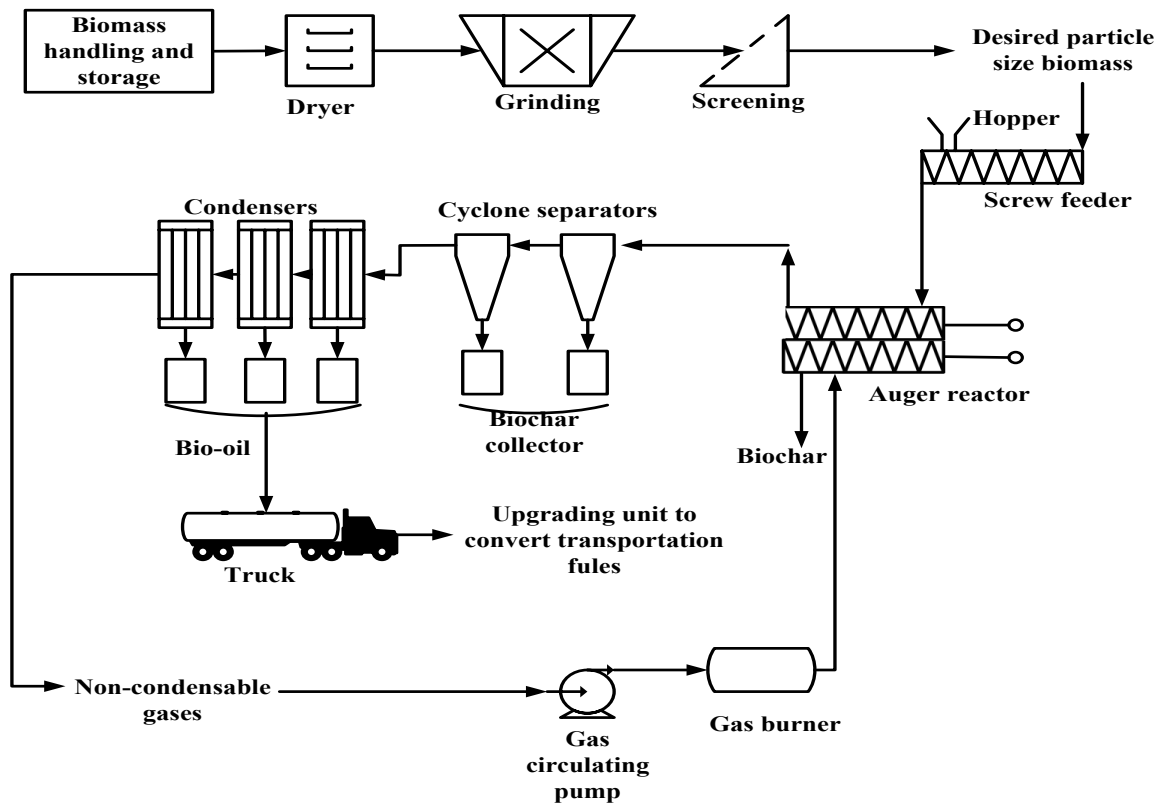


Figure 6.2. Schematic of an MPS unit

Auger pyrolysis technology was developed by ABRI-Tech (Marshall, 2013). The reactor mechanically mixes the biomass and uses a heat transfer medium. In the pyrolysis system, two independent rotating devices rotate inside the horizontal auger reactor; the reactor does not self-

rotate (Brown et al., 2011; Sorenson, 2010). The heating medium is heated prior to pyrolysis, so no fluidizing medium is required, thereby further increasing the efficiency of the condensers as they handle only the pyrolysis vapor. Biochar is collected from two places: at the end of the reactor and from the cyclone char collector. In this study, non-condensable gases are assumed as the heating carrier for the reactor. The pyrolysis vapor products are separated from the reactor due to the pressure difference and passed through the cyclone and a series of condensers where the bio-oil is collected and non-condensable gases are combusted to produce heat (and used as the heating carrier). As the MPS unit is located in the forest, part of bio-oil is used to produce electricity using a flex fuel generator (Sorenson, 2010).

The main objective of this paper is to develop generic models to investigate the technical and economic feasibility of bio-oil production from the two MPS configurations. A base case of a 2000 dry tonnes/day biomass facility was considered and Canadian whole trees were assumed as feedstock. The capacity of an MPS unit is from 10 to 100 dry t d<sup>-1</sup>, thus many units are required to achieve the target base case capacity. The actual number of units required is higher than expected because part of the produced bio-oil is used to produce electricity, which affects the overall revenue. For each MPS, a restricted area is assigned for the lifetime of the harvesting operation so that no two MPSs intersect. In this study, five MPS capacities (10, 20, 40, 50, and 100 dry t d<sup>-1</sup>) and four relocation times (yearly, biyearly, quarterly, and monthly) were considered. Two scenarios (configurations) were assumed in the allocation of harvesting areas, truncated and radial; they are shown in Figure 6.2. Two generic equations were developed to estimate bio-oil production costs for the two configurations, and the results were compared with those reported by Sarkar et al. (2010) for a centralized pyrolysis system.

### **6.3 Generic model development for an MPS**

Figure 6.1 shows two MPS scenarios in which all the units operate simultaneously to achieve the target base case plant capacity. To derive generalized equations, each parameter is considered as a variable that can be changed depending on the requirements. It is assumed that a centralized plant of  $A$  dry t d<sup>-1</sup> capacity produces  $A_1$  dry tonnes of bio-oil each day. One MPS unit of  $B$  dry t d<sup>-1</sup>

capacity yields  $B_1$  dry tonnes of bio-oil each day. Because an MPS operates in a remote location, part of the produced bio-oil,  $z$  tonnes of bio-oil per day, is used to generate electricity. To ensure equal amounts of bio-oil from each framework (centralized and MPS) for comparison,  $N$  numbers of MPS units are required and can be calculated from Equation (1):

$$N = \frac{A_1}{B_1 - z} \quad (1)$$

The required biomass area for one MPS in each relocation time is  $M$  ha (represent by  $A_s$ ) and the lifetime of each MPS is  $T$  years. It is important to note that the area required for each MPS for the lifetime of the operation is assigned at the beginning of the operation to avoid overlapping between MPS units. In addition to  $M$  ha area, each MPS requires  $\frac{3}{4}$  acre (0.3035 ha) for its set up (Palma et al., 2011). Therefore, the total area required by each MPS is  $M + 0.3035$  ha. For example, in the yearly relocation scenario, the MPS requires  $M$  ha/year, and the total area required for a 10-year MPS lifetime is  $10*(M + 0.3035)$  ha. The same area is required by each MPS.

The total area  $A'$  required for  $N$  MPS units for the lifetime of the operation for both scenarios can be estimated using Equation (2):

$$A' = (M + 0.3035) * N * T * m \quad (2)$$

where  $m$  is the number of MPS relocations in a year (e.g.,  $m = 1, 2, 4,$  and  $12$  for yearly, biyearly, quarterly, and monthly relocation, respectively).

The total area required for the lifetime of all MPSs is considered to be circular because for the centralized plant, it is also assumed that the total area is circular and the plant is situated at the center of the region. The radius of the circular area  $R$  is calculated using Equation (3):

$$R = \left(\frac{2}{3}\right) * 1.27 * \sqrt{\frac{(M + 0.3035) * N * T * m}{\pi}} \quad (3)$$

$R$  is constant for the two MPS scenarios (truncated and radial), but the calculations for the other parameters, such as biomass transportation distance to the MPS unit, bio-oil transportation distance from the MPS to the bio-oil processing facility, and relocation distance, are, as explained in the subsequent section. In Eqn. 3, 1.27 is the winding factor to account the winding of the roads in the remote area and  $2/3$  is the average transportation displacement of the biomass collection area (Wong et al., 2016).

### 6.3.1 *Scenario 1- Truncated*

In the truncated scenario, the total circular area of radius  $R$  is divided into rings (see Figure 6.1 [a]) and each MPS is placed in the truncated -like  $d$  segment. The upgrading unit be located at the center  $O'$  of the circular area of radius  $R$ . Therefore, the number of truncated  $d$  segments in the inner most ring do not touch the center (still it will be a truncated area). The section framed by the letters  $A, B, F, C, D,$  and  $E$  is the location area,  $A_s$ , for one MPS for a particular relocation time in which  $AD = BC = EOF = d$ , as shown in Figure 6.3. In the segment, the MPS unit is located at the center  $O$  of the polygon  $ABFCDEA$ . Equation (4) is the derived expression of  $A_s$  to calculate  $d$ . The detailed calculation steps are given in Appendix B.

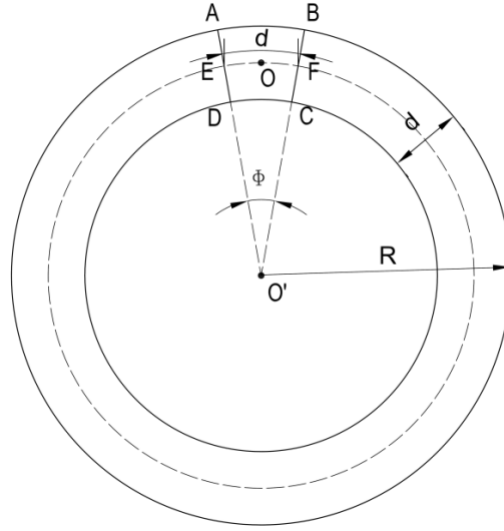


**Figure 6.3. MPS allocation in area  $A_s$  for scenario 1: Truncated**

$$A_s = \frac{2\pi R d - \pi d^2}{2\pi} * \frac{d}{\left(R - \frac{d}{2}\right)} = d^2 \quad (4)$$

From Equation (4) the distance  $d$  can be calculated using Equation (5):

$$d = \sqrt{(M + 0.3035)} \quad (5)$$

#### 6.3.1.1 Bio-oil transportation distance

The bio-oil transportation distance is the distance bio-oil is transported from the MPS unit to the central bio-oil processing facility at the center  $O'$  (see Figure 6.4[a]). It is important to estimate the number of relocations ( $A_s$ ) by the  $N$  MPS units and allocate the position of each MPS so that the MPS units do not interact with each other during the lifetime of each plant. Figure 6.4 shows the formation of rings and the division of each ring location area ( $A_s$ ) for each MPS unit and ‘•’ shows the position of the MPS units in the  $A_s$  area. The inner most circular area is for the upgrading unit to process the bio-oil to produce renewable diesel.

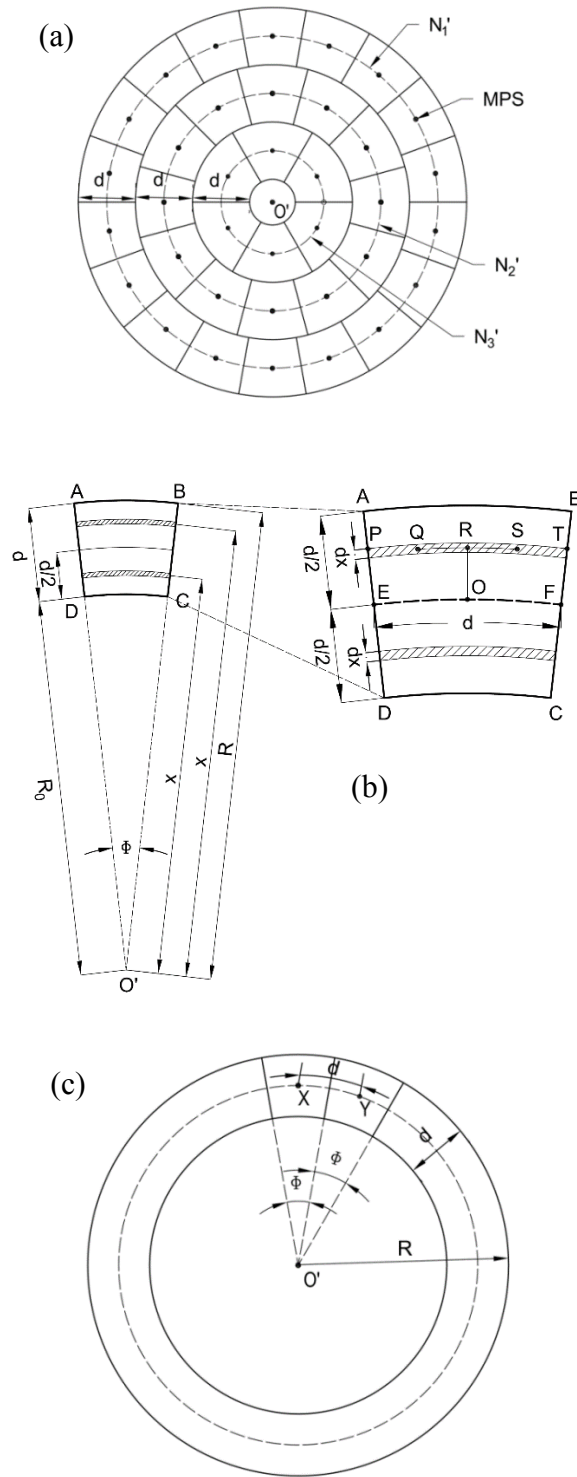


**Figure 6.4 Bio-oil transportation distance (a), biomass transportation distance (b) and MPS relocation distance (c) for the truncated scenario**

The number of rings ( $N'$ ) can be calculated from Equation (6):

$$N' = \frac{R}{d} \quad (6)$$

The number of  $A_s$  in the circle with the radius  $R$  ( $N_{N'}$ ) can be calculated using Equation (7), which is the sum of the all the  $A_s$  in all the rings.

$$N_{i'} = \sum_{i=1}^{N'} \frac{\text{Perimeter of dotted circle } N_i'}{d} \quad (7)$$

$$= \sum_1^{N'} \frac{2\pi \left( R - \frac{(2i-1)d}{2} \right)}{d}$$

where  $i = 1, 2, 3, \dots, N'$

The bio-oil produced in the MPS needs to be transported to a bio-oil processing facility. Bio-oil transportation distances vary with the location of the MPS.

Equation (8) is the generalized expression for the bio-oil transportation distance for all  $A_s$  located in the  $N'$  rings.  $D_N$  is the total bio-oil transportation distance for  $N$  MPS units for the entire lifetime of the plant for different relocations. The distance covered each year can be calculated by taking 1/10 of the  $D_i$  since 10 years is considered the MPS lifetime in this study.

$$\begin{aligned}
D_N &= \sum_{i=1}^{N'} N'_i * \left( R - \frac{(2i-1)d}{2} \right) \\
&= \sum_{i=1}^{N'} \frac{2\pi \left( R - \frac{(2i-1)d}{2} \right)}{d} * \left( R - \frac{(2i-1)d}{2} \right) \\
&= \sum_{i=1}^{N'} \frac{2\pi \left( R - \frac{(2i-1)d}{2} \right)^2}{d}
\end{aligned} \tag{8}$$

### 6.3.1.2 Biomass transportation distance

Biomass transportation distance varies with relocation time and MPS capacity. In each  $A_s$ , the MPS is located at the center ( $O$ ) and biomass is transported from the surrounding area, as shown in Figure 6.4(b). To estimate average biomass transportation distance  $D$  for a relocation period, the truncated area  $ABFCDEA$  is divided into two segments: one is  $ABFEA$  (outer arc to MPS) and the second is  $EFCD E$  (MPS to inside arc). To estimate the average biomass transportation distance, a small strip of area  $dx$  is located at a distance of  $x$  from the center  $O'$  is considered for both segments as shown in the Figure 6.4(b). The small area  $dx$  known as  $PQRST$  is divided into two equal polygons,  $PQR$  and  $RST$ .  $Q$  and  $S$  are the biomass collection centers following harvesting, skidding, and chipping. A 10 dry tonne capacity truck per trip is used to deliver the feedstock to the MPS from the biomass collection point (Mahmudi & Flynn, 2006). Generally for centralized plant, 20- 40 dry tonne/day (20 dry t d<sup>-1</sup>) to transport the biomass from the road side to the plant gate (Thompson et al., 2012). But the decentralized plant, biomass need to be transported from in the remote forest location to the MPS unit. Therefore, in this study, a small capacity truck capacity of 10 dry t d<sup>-1</sup> is considered (Mahmudi & Flynn, 2006; Thompson et al., 2012; Wong et al., 2016). The path followed will be  $QR$  and  $RO$  for the small polygon  $PQR$  and  $RS$  and  $RO$  for the other side of the polygon  $RST$ . The average biomass transportation distance for the truncated area  $ABFCDEA$  is given in Equation (9). The detailed derivation steps are given in Appendix B.

$$D = \frac{7d^3}{10(d + 2R_0)^2} [13d^2 + 40dR_0 + 36R_0^2] + \frac{7d^3}{5(d + 2R_0)} \left[ \frac{d}{2} + 3R_0 \right] \tag{9}$$

### 6.3.1.3 Relocation distance

Relocation distance refers to the distance travelled by the MPS between two consecutive allocated points where it settles down to operate for a particular time and is shown in Figure 6.4(c).  $X$  and  $Y$  represent the MPS locations for the respective relocation times. The distance travelled by the MPS from point  $X$  to point  $Y$  is  $d$ .

### 6.3.2 Scenario 2 – Radial

Figure 6.1 (b) shows the radial configuration for MPS operations. For this scenario, the number of MPSs required and the radius of the circular area are estimated through Eqn. 1 and Eqn. 3, respectively. BO'C is the area required by one MPS throughout its lifetime which is shown in the Figure 6.5.

Figure 6.5 shows the distribution of an MPS unit's area into subsectors based on relocation frequency. An MPS will relocate with time in the assigned area. In each relocation, the MPS settles in the centroid position (the average distance from every point in a specified area) to minimize biomass and bio-oil transportation distance. In this configuration, each sector is assigned by dividing the total angle ( $2\pi$ ) with the number of MPS units and relocation frequencies. The angle  $\beta$  is subtended by each sector and can be calculated by Equation (10).

$$\beta = \frac{2\pi}{Nm} \tag{10}$$

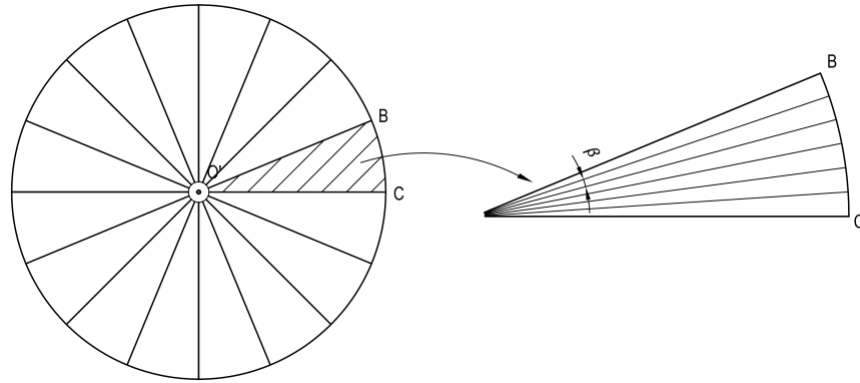


**Figure 6.5. Distribution areas into subsectors, radial scenario**

*6.3.2.1 Bio-oil transportation distance*

The bio-oil produced from each MPS is transported to the bio-oil upgrading facility, as shown in Figure 6.6(a). In sector PO'Q, the MPS is situated at the centroid ( $O$ ) before being moved. Therefore, the bio-oil transportation distance,  $O'O$ , is two-thirds of the radius of the entire area, as shown in Equation (11).

$$O'O = R' = \frac{2R}{3} \quad (11)$$

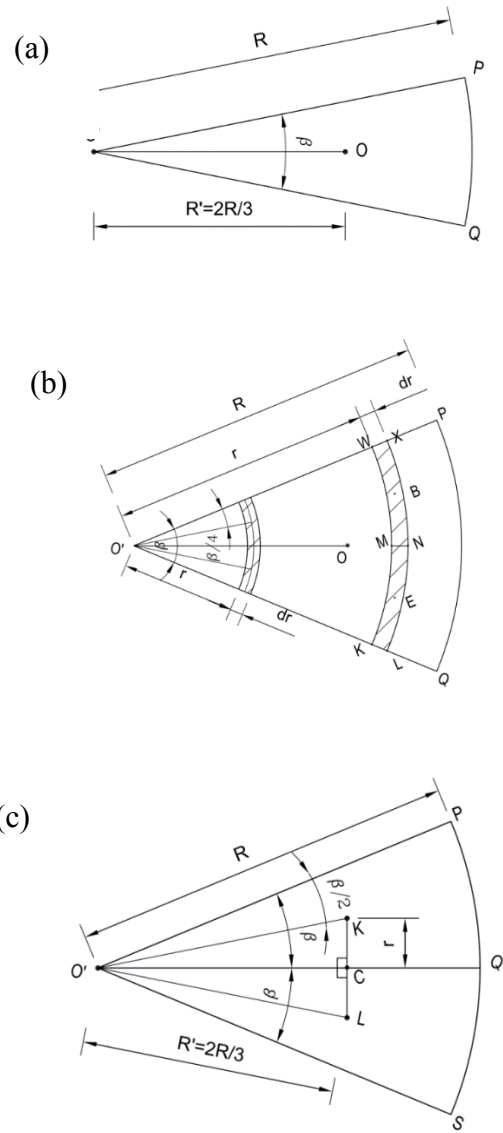


**Figure 6.6. Bio-oil transportation distance (a), biomass transportation distance (b) and MPS relocation distance (c) for the radial scenario**

### 6.3.2.2 Biomass transportation distance

Figure 6.6(b) shows the biomass transportation distance in the radial configuration for a subsector at a particular relocation period. For the transportation distance, the sector  $PO'Q$  is divided into two segments: one is from the center  $O'$  to the centroid and the second is from the centroid to the end of sector  $PO'Q$ . To calculate the average biomass transportation distance, a small strip of area

$dr$  is considered in both segments, shown in Figure 6.9. The small area  $dr$  known as polygon  $WXBNELKMW$  is located at distance  $r$  from the center. The biomass in the area  $dr$  is divided into two equal polygons,  $WXBNMW$  and  $MNELKM$ .  $B$  and  $E$  are the biomass collection centers following harvesting, skidding, and chipping. A 10 dry tonne capacity truck is used to deliver the feedstock to the MPS from the biomass collection points. The total average distance travelled by truck can be estimated by summing the two integrations for the sector  $PO'Q$ , which are estimated in Equation (12). The detailed calculation is given in Appendix B.

$$D = \frac{2 * 84 * 2\pi}{20 * Nm} * \frac{R^3}{27} \left[ \left( \frac{9 * 2\pi}{4Nm} \right) + \frac{8}{3} \right] \quad (12)$$

### 6.3.2.3 Relocation distance

Figure 6.6(c) shows the two adjacent segments  $PO'Q$  and  $QO'S$ , where one MPS unit is moved following the completion of a harvest. The relocation distance from  $PO'Q$  to  $QO'S$  is the sum of  $KC$  and  $CL$  and is represented by Equation (13). We assumed that  $O'CK$  and  $O'CL$  are a right-angled triangle.

$$\begin{aligned} \text{MPS Relocation distance} = X = KC + CL = 2r = 2d \sin\left(\frac{\beta}{2}\right) \\ = 2d \sin\left(\frac{2\pi}{2Nm}\right) = 2 * R' * \sin\left(\frac{2\pi}{2Nm}\right) \end{aligned} \quad (13)$$

## 6.4 Description of economic parameters

This section describes the techno-economic parameters used in the MPS analysis. All the cost numbers are reported in 2017 US dollars (1 USD = 1.33 CAD). Biomass properties are given in Table 6.1. The cost model inputs used to estimate bio-oil production costs from the MPS are shown in Tables 2 and 3. The characteristics of the centralized 2000 dry t d<sup>-1</sup> plant were taken from Sarkar and Kumar (Sarkar & Kumar, 2010).

**Table 6-1. Whole tree biomass properties**

<b>Parameters</b>	<b>Value</b>	<b>Reference/Comments</b>
Feedstock type	Hard wood	This study
Moisture content (%)	50	(Kumar et al., 2003)
Heating value (MJ kg <sup>-1</sup> , HHV)	20	(Kumar et al., 2003)
Fuel density (kg m <sup>-3</sup> )	486	(Krajnc, 2015)
Biomass yield (dry t gross ha <sup>-1</sup> )	84	(Kumar et al., 2003)

#### 6.4.1 *Field cost*

The field cost includes harvesting (cutting, skidding, and chipping), the premium paid to the land owner, road construction cost, and silviculture cost (Shahrukh et al., 2016). In this study, it was assumed that harvesting equipment (such as a feller bencher for cutting, a skidder to skid whole trees, and a chipper for making chips) is rented and was considered operating cost. A premium of 5.26 \$ dry t<sup>-1</sup> of feedstock is paid above the forest biomass cost for the collection and use of the forest biomass (Agbor et al., 2016). The silviculture cost is the cost to cultivate and grow new trees after harvesting and is \$119.04 \$ ha<sup>-1</sup> (Agbor et al., 2016). Road construction costs are the costs to build a tertiary road network that can be used during harvesting and for truck capacities of 10 dry tonnes (Agbor et al., 2016; Mahbub et al., 2017). The details of these costs are listed in Table 6.2.

**Table 6-2. Field cost, transportation cost, and storage cost for an MPS unit**

<b>Parameters</b>	<b>Value</b>	<b>Reference/Comments</b>
<b>Field cost</b>		
Harvesting cost (cutting, chipping, and skidding) (\$ dry t <sup>-1</sup> )	24.42	(Agbor et al., 2016; Shahrukh et al., 2016)
Premium paid to the land owner (\$ dry t <sup>-1</sup> )	5.26	(Agbor et al., 2016; Kumar et al., 2003)
Road construction and infrastructure cost (\$ ha <sup>-1</sup> )	3.68	(Agbor et al., 2016; Kumar et al., 2003)
Silviculture cost (\$ ha <sup>-1</sup> )	119.04	(Agbor et al., 2016; Kumar et al., 2003)
<b>Transportation cost</b>		
Biochar transportation cost (\$ dry t <sup>-1</sup> of biochar)	4.5	(Kumar, 2013)
Biomass transportation cost (\$ m <sup>-3</sup> )	2.35 + 0.03 <i>D</i>	<i>D</i> is the round-trip distance travelled by the truck from the forest to the plant gate. (Agbor et al., 2016; Badger & Fransham, 2006; Kumar et al., 2003)
Truck capacity for the transportation of biomass dry tonne	10	(Mahmudi & Flynn, 2006) (Kumar et al., 2004)
Bio-oil transportation cost (\$ m <sup>-3</sup> )	6.824 + 0.0060 <i>D</i>	<i>D</i> is the round-trip distance travelled by the liquid tank truck from the MPS point to the bio-oil processing plant. (Pootakham & Kumar, 2010)
Capacity of liquid tank truck (m <sup>3</sup> )	30	(Pootakham & Kumar, 2010)
<b>Storage system</b>		
Biomass storage type		(Agbor et al., 2016) On-field storage
Biomass storage cost (\$ dry t <sup>-1</sup> )	1.1	(Agbor et al., 2016)
No. of biomass storage days	15	Assumed
Bio-oil storage capacity (m <sup>3</sup> )	100	This study
Cost of storage tank for bio-oil (\$)	137,689.02	(Badger & Fransham, 2006; Pootakham & Kumar, 2010)
Material type for bio-oil storage tank	Stainless steel	(Pootakham & Kumar, 2010)
No. of days bio-oil can be stored	2-3	(Pootakham & Kumar, 2010)

#### 6.4.2 *Biomass and bio-oil transportation cost*

Biomass and bio-oil transportation costs comprise two components, the fixed cost for loading and unloading and the variable cost for the round trip transportation of biomass and bio-oil (Shahrukh et al., 2016). The variable cost is a function of plant capacity. In both scenarios, both biomass and bio-oil transportation distance were shown to be a function of the radius of the whole circular area. The radius depends on the yield of the biomass as a higher yield reduces the area required for the plant.

#### 6.4.3 *Capital cost*

The capital cost is the investment to fabricate an MPS unit to produce bio-oil in a remote location. For this analysis, five capacities are considered: 10, 20, 40, 50, and 100 dry t d<sup>-1</sup>. Capital cost data were drawn from publications and industrial reports (Marshall et al., 2014; Palma et al., 2011; Sorenson, 2010). From the available data, a scale factor was derived to calculate the capital cost at various capacities. As the MPS concept is new and operation is available only on a small scale in a laboratory setting, there is very limited published research available. The MPS unit characteristics and cost inputs are given in Table 6.3.

**Table 6-3. MPS plant characteristics and cost input**

<b>Parameters</b>	<b>Value</b>	<b>Reference/Comments</b>
<b><i>MPS characteristics</i></b>		
MPS capacity (dry t d <sup>-1</sup> )	10,20, 40, 50 &100	
Lifetime of plant (years)	10	
Running time of MPS (days)	273	Assumed for this study
Use rate (%)	90	
Finalcial analysis method	Discounted cash flow	
Internal rate of return (%)	10	
No. of shifts per day	3	(Sorenson, 2010)
No. of employees per shift	2 or 3	(Brown et al., 2011)
Adminstarative staff	1	Assumed
Employee salary including benefits (\$ h <sup>-1</sup> )	30	(Kumar et al., 2003; Sarkar & Kumar, 2010; Sorenson, 2010)
Scale factor for MPS capacity from 10 to 100 dry t d <sup>-1</sup>	0.61	Calculated. The details are included in section 3.2.
Maintanance costs	3% of initial capital investment	(Kumar et al., 2003)
Relocation frequency	Yearly, biyearly, quarterly, and monthly	Assumed.
<b><i>Fast pyrolysis results (wt%)</i></b>		
Bio-oil	57%	(Sorenson, 2010)
Biochar	27%	
Noncondensable gases	16%	
<b><i>Energy used in MPS</i></b>		
Bio-oil used to produce electricity (wt <sup>0</sup> )	11% of the bio-oil yield	This reduces the bio-oil yield to 50% from 57% by weight.
<b><i>Thermal energy</i></b>		
Propane	25%	(Sorenson, 2010)
Noncondensable gases	75%	
Propane cost (\$ L <sup>-1</sup> )	0.456	

#### 6.4.4 *Operational cost*

The operational cost includes labor, maintenance, energy, and relocation costs. Each MPS unit operates continuously for 24 hours per day. There are 3 eight-hour shifts and each is run by 2 employees (one for controlling and one for fuel handling) for MPS capacity from 10 to 50 dry t d<sup>-1</sup>, and one administrative staff is assigned to each MPS. But for 100 dry t d<sup>-1</sup> MPS unit, one extra employee is provided per shift which increases number of employees to 3 (one for controlling and two for fuel handling). An average wage of 30 \$ h<sup>-1</sup> is assumed; this includes benefits (Kumar et al., 2003; Sarkar & Kumar, 2010; Sorenson, 2010). The maintenance cost is assumed to be 3% of the initial capital cost investment including all the MPSs (equivalent to a base case capacity of 2000 dry t d<sup>-1</sup>) (Kumar et al., 2003). The relocation cost is the cost to move an MPS unit from one point to another by two rental trucks. Relocation involves three activities: dismantling, moving the unit to the next processing point, and reassembling. It is assumed that it takes 6 hours for dismantling the unit, 5 hours to move it, and 6 hours to reassemble the unit, or 17 hours altogether (Sorenson, 2010). The rental truck charge is considered to be 78 \$ h<sup>-1</sup>. Electricity from bio-oil, noncondensable gases, and propane are used as the energy in the plant. Thermal energy for pyrolysis is provided by the non-condensable gases and propane in the ratio of 3:1, respectively. The details of the operating costs are in Table 6.3.

#### 6.4.5 *Biomass and bio-oil storage costs*

It is assumed that biomass is stored for at least 15 days. On-field storage costs are 1.1 \$ dry t<sup>-1</sup> (Agbor et al., 2016). The bio-oil produced from the MPS unit is stored on site for 2-3 days in a 100 m<sup>3</sup> capacity stainless steel tank and then transported to the bio-oil processing plant in a 30 m<sup>3</sup> (Pootakham & Kumar, 2010) capacity liquid tank. Storage cost details are provided in Table 6.2.

#### 6.4.6 *Biochar transportation cost*

The biochar produced during pyrolysis is spread out in the harvested area to preserve soil nutrients for reforestation (Laird et al., 2017). Costs to transport the biochar from the plant gate to the field are 4.5 \$ dry t<sup>-1</sup> of biochar (Kumar, 2013).

#### 6.4.7 *Product cost*

Although bio-oil is ultimately the source of revenue from the MPS unit, some of it is used to produce electricity for the portable pyrolysis unit. The bio-oil production cost is calculated using a discounted cash flow method.

#### 6.4.8 *Uncertainty analysis*

In this study, a detailed robust approach has been employed to estimate bio-oil production cost from two configurations of distributed pyrolysis facility. But as we know, mobile pyrolysis process is an emerging technology and not yet commercialized, a certain degree of uncertainties is associated with the field cost and operating parameters of MPS unit. Therefore, to reduce the uncertainties and risk associated with the input parameters, a uncertainty analysis has been performed using Monte Carlo application (VoseSoftware, 2018) on the base case plant capacity of 2000 dry t d<sup>-1</sup>. The idea behind this simulation is to use the randomness of the input variables to obtain the accurate result without propagating the errors. Each variable is varied in a range depending on their sensitiveness on the output and large numbers of iteration are used to produce accurate results.

### 6.5 **Results and discussion**

This study develops techno-economic models to investigate the economic and technical feasibility of replacing centralized pyrolysis plants with a decentralized system. A centralized plant benefits from economies of scale, but mobile pyrolysis, because it can reduce biomass transportation costs and improve accessibility in remote locations and in extreme weather conditions, is gaining some

interest. For the base case comparison, a centralized plant with a capacity of 2000 dry t d<sup>-1</sup> producing 72% by weight of bio-oil was assumed (Sarkar & Kumar, 2010). To produce a comparable amount of bio-oil per day from MPS, several units operating simultaneously are required.

### 6.5.1 *Estimate of the number of MPS units required for different capacities*

Figure 6.7 shows the number of MPS units required with variations in plant capacity. Both scenarios require the same number regardless of plant capacity. A significant part of the bio-oil produced is used to generate electricity for biomass pretreatment in the MPS. 31.25 gallons of bio-oil produces 0.75 MM BTU of electricity per hour (Sorenson, 2010). This reduces the bio-oil revenue from 57% to 50% by weight for each MPS. Therefore the actual number of MPS units required for the various capacities is not an exact divisible relation to the base capacity of 2000 dry t d<sup>-1</sup>. When the MPS capacity increases, the required number of MPS units decreases.

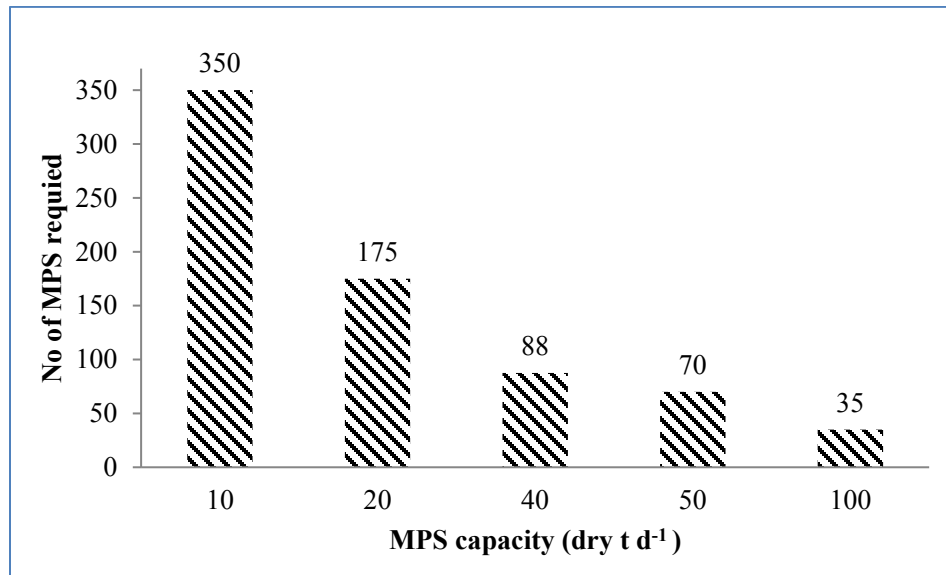


**Figure 6.7. Change in the number of MPS units with plant capacity**

### 6.5.2 MPS capital costs

Few studies are available on the mobile pyrolysis process. To develop a scale factor to calculate the capital cost of an MPS unit, a curve was plotted showing the capital cost and MPS capacity using data from the literature (Badger et al., 2010; Marshall et al., 2014; Sorenson, 2010) (see Figure 6.8). The calculated scale factor is 0.61 with an  $R^2$  value of 0.993 and indicates that capital cost increases at a slower rate than it should with an increase in capacity. Figure 6.8 shows the capital cost for different capacities of MPS units. The capital cost is the cost for the biomass pretreatment unit, the pyrolysis unit, and the bio-oil condensing and bio-oil storage unit.

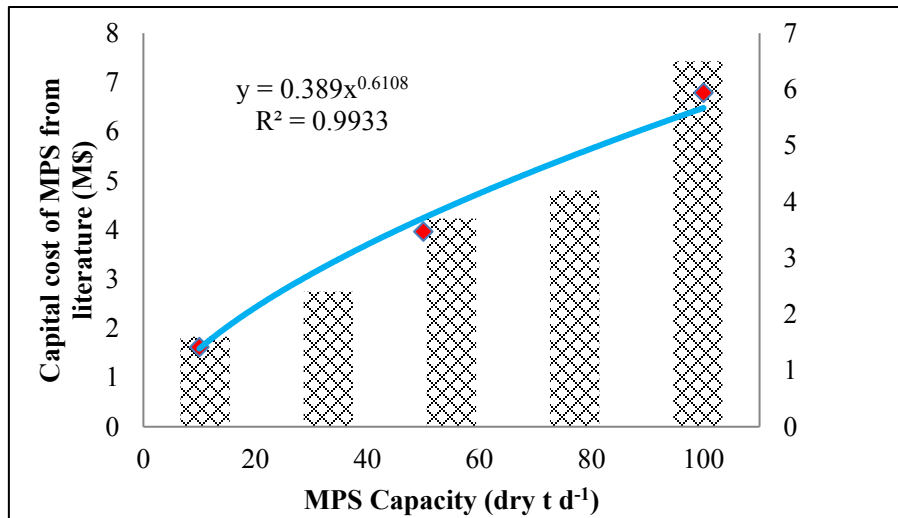


**Figure 6.8. The development of the scale factor for an MPS plant and Changes in capital cost with MPS capacity**

### 6.5.3 Biomass transportation distance in scenarios 1 and 2

In the two configurations (truncated and radial), the MPS unit is treated like a centralized unit for the specific times. In this study, four relocation times are considered: yearly, bi-yearly, quarterly, and monthly. For the specific relocation time, biomass is transported to the MPS by 10 dry t d<sup>-1</sup> capacity trucks. As stated earlier, the average transportation distance for the two scenarios depends

on the MPS area. The MPS area varies with MPS capacity and relocation time. Figure 6.9 (a) and (b) shows the biomass transportation distance for the truncated and radial scenarios, respectively. In both scenarios, biomass transportation distance increases with increases in capacity and relocation time. This distance is significantly higher in the radial scenario than in the truncated scenario. For a yearly relocation for a 100 dry tonnes/day MPS capacity, transportation distance is 129 km for the radial scenario and 30 km for the truncated scenario. This is due to the nature of the assigned area. In the radial scenario, MPSs are located at the centroid of each sector and the centroid is located two-thirds the distance of the radius. But in the truncated scenario, the MPS is located in the center of the truncated d-segment, thus the transportation distance is considerably smaller than in the radial scenario.

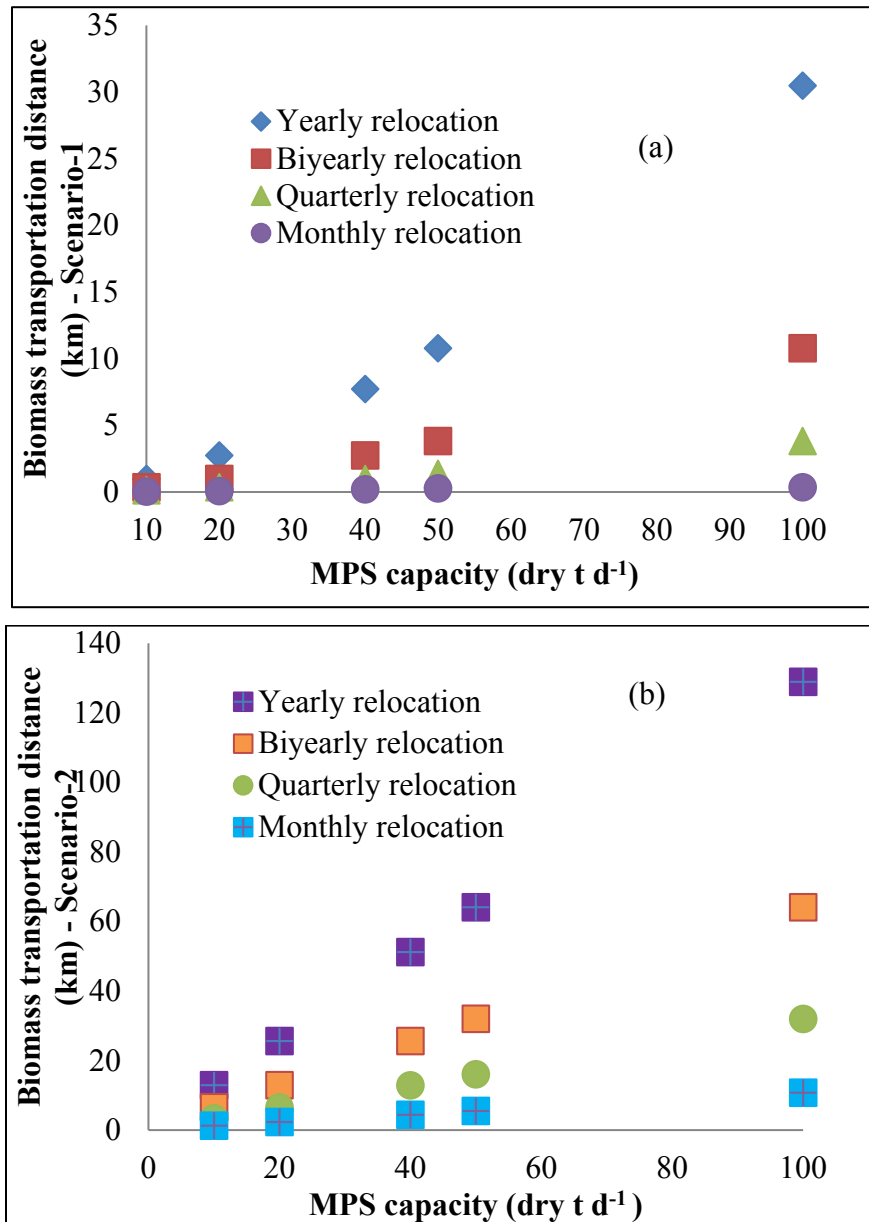


**Figure 6.9. Biomass transportation distance with variations in MPS capacity: (a) truncated and (b) radial configurations**

#### 6.5.4 *Bio-oil transportation distance in scenarios 1 and 2*

After the pyrolysis operation, bio-oil is transported to the upgrading facility in the center of the harvest area. The transportation distance varies with the MPS allocation configuration, as explained earlier. Figure 6.10 (a) and (b) shows the average bio-oil transportation distance for both scenarios. In both cases, with changes in relocation time, a small change in bio-oil transportation distance is observed, in the range of 0.5 to 1 km. With variations in relocation frequency from yearly to monthly for a 100 dry t d<sup>-1</sup> MPS capacity, the transportation distance changes from 10.80 to 10.90 km for both scenarios, which is insignificant. However, the change is somewhat significant at lower capacities. This is because the number of units increases the radius of the circle a little due to the addition of the settle down area for each MPS. At lower capacities, the number of MPS units is comparatively higher than at higher capacities, and thus the bio-oil transportation distance increases slightly with the additional settle down areas.

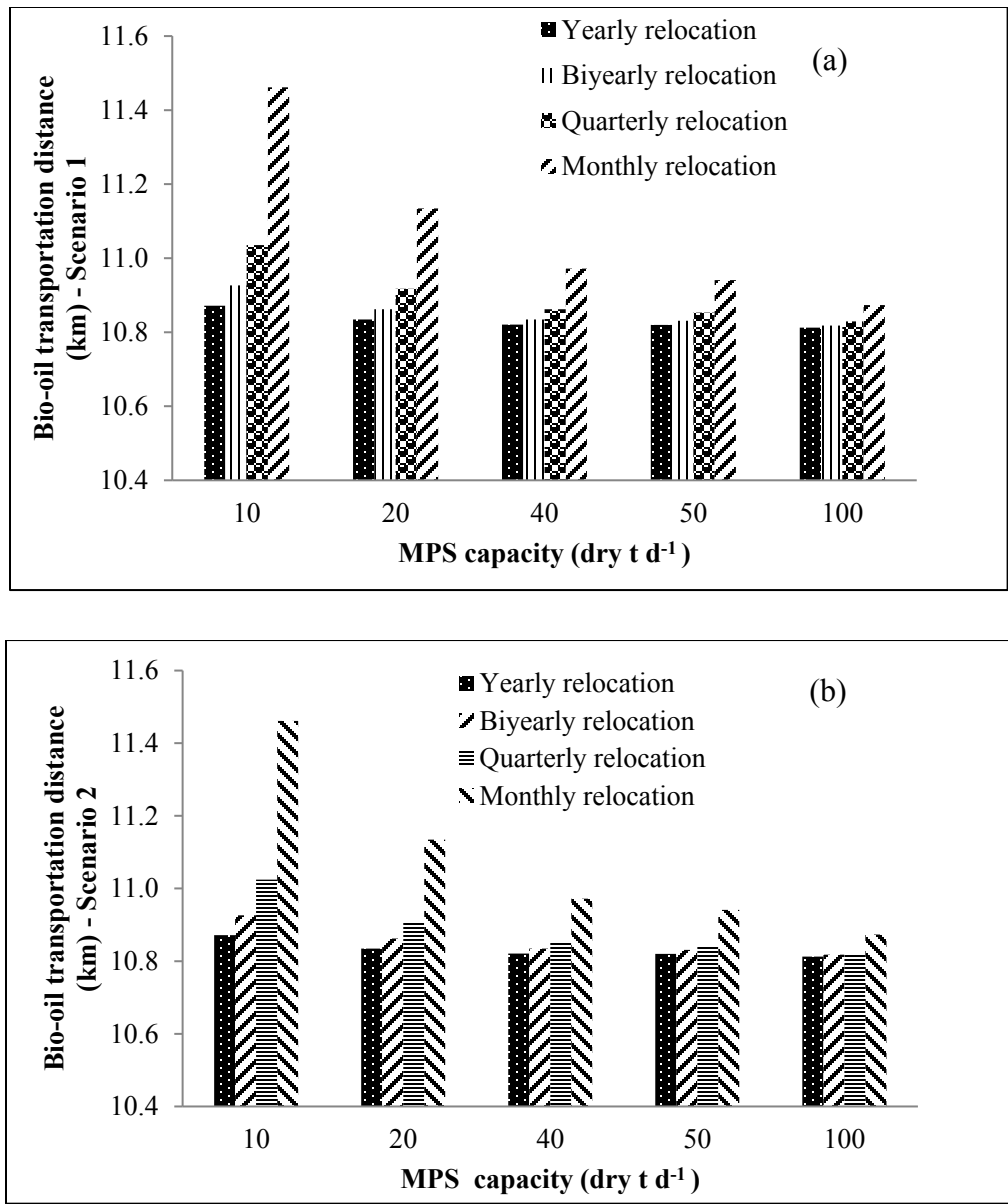


**Figure 6.10. Bio-oil transportation distance with variations in MPS capacity: (a) truncated and (b) radial configurations**

**6.5.5 Relocation distance**

The relocation distances for scenarios 1 and 2 for different MPS capacities with different relocation times are shown in Figure 6.11 (a) and (b). In both scenarios, the relocation distance is less than 2 km. The relocation distance is highest for the 100 dry t d<sup>-1</sup> capacity yearly relocation for both

scenarios. Because many MPSs work concurrently to achieve the base case target of 2000 dry t d<sup>-1</sup> in a circular area, the relocation distance is significantly lower at that capacity for both scenarios. Therefore the relocation cost is considered an operating cost. To disassemble, relocate, and reassemble every MPS unit, 17 hours of labor are required. Hence with an increase in the number of MPS units and relocation frequency comes an increase in relocation cost.

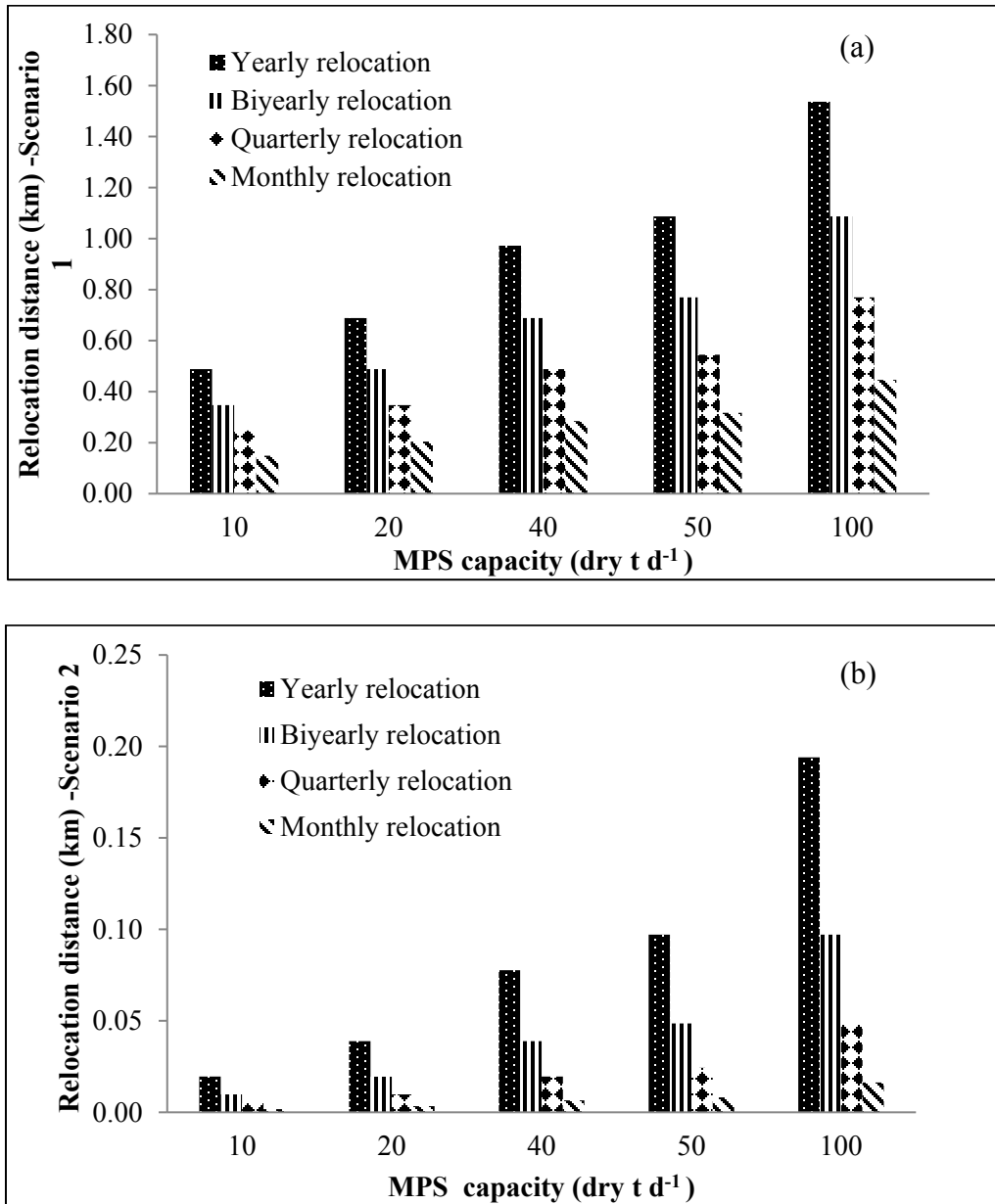


Figure 6.11. MPS relocation distance with variations in MPS capacity: (a) truncated and (b) radial configurations

### 6.5.6 *Bio-oil production cost*

This study investigates the bio-oil production costs of a 2000 dry t d<sup>-1</sup> biomass plant for a mobile pyrolysis system and compares them with results for a centralized plant from work by Sarkar and Kumar (Sarkar & Kumar, 2010). The results are summarized in the Table 6.4. Bio-oil produced in an MPS costs significantly more than bio-oil produced in a centralized plant due to economies of scale.

Of the two MPS scenarios, the truncated scenario shows better results than the radial scenario. Bio-oil production costs are drastically higher for low-capacity MPS units and decrease with increases in plant capacity for both MPS scenarios. The reason behind this is the labor cost. Even if the MPS capacity size changes, two employees are required to run the unit in each shift. Therefore, for lower capacity mobile units, far more units are required than for a higher capacity MPS unit. In a centralized unit, however, labor cost is not a significant component because of fixed facility.

**Table 6-4. Bio-oil production costs in two frameworks, centralized and MPS**

Bio-oil production cost (\$ L <sup>-1</sup> ) for 2000 dry tonnes/day									
Capacity of MPS (dry t d <sup>-1</sup> )	Yearly relocation		Biyearly relocation		Quarterly relocation		Monthly relocation		Centralized plant (Sarkar & Kumar, 2010)
	Truncated	Radial	Truncated	Radial	Truncated	Radial	Truncated	Radial	
10	1.455	1.462	1.459	1.461	1.466	1.466	1.496	1.500	
20	0.828	0.841	0.830	0.838	0.834	0.841	0.854	0.864	<b>0.241</b>
40	0.502	0.528	0.503	0.523	0.506	0.526	0.520	0.543	
50	0.432	0.467	0.436	0.461	0.438	0.464	0.451	0.480	
100	<b>0.349</b>	<b>0.407</b>	<b>0.345</b>	<b>0.398</b>	<b>0.345</b>	<b>0.400</b>	<b>0.353</b>	<b>0.414</b>	

Table 6.5 shows the distribution of bio-oil production cost components for the radial and truncated scenarios for yearly relocations of a 2000 dry t d<sup>-1</sup> plant. Of all the cost components, capital, labor, harvesting, and biomass transportation cost have a significant effect on the bio-oil production cost. With an increase in MPS capacity, labor costs fall from 76% to 46% and 75% to 39%, respectively, for the truncated and radial scenarios. For a 10 dry t d<sup>-1</sup> MPS unit, 350 units are active at one time. Each unit is operated by 2 employees per shift, which increases the labor cost significantly, resulting in very high labor costs compared to other cost components. Harvesting and biomass transportation costs increase with the increase in MPS capacity. For the harvesting cost, as the MPS capacity increases, it can handle more biomass than a lower capacity MPS. Therefore it requires more biomass as feed, which increases the harvesting cost. In the case of biomass transportation costs, a 100 dry t d<sup>-1</sup> MPS unit has a greater transportation distance than the 10 dry t d<sup>-1</sup> unit. But the biomass transportation distance is 12% for the truncated scenario and 23% for the radial scenario. The overall bio-oil production costs are lower for a 100 dry t d<sup>-1</sup> plant with yearly relocation: 0.294 \$ L<sup>-1</sup> and 0.334 \$ L<sup>-1</sup> for the truncated and radial scenarios.

**Table 6-5. Cost distribution of bio-oil production costs for an MPS**

	Cost distribution of bio-oil production costs (\$/L) for a 2000 dry t d <sup>-1</sup> plant					
	Yearly relocation- truncated			Yearly relocation- radial		
	10 dry t d <sup>-1</sup>	50 dry t d <sup>-1</sup>	100 dry t d <sup>-1</sup>	10 dry t d <sup>-1</sup>	50 dry t d <sup>-1</sup>	100 dry t d <sup>-1</sup>
Capital cost	10.19%	18.73%	17.79%	10.14%	17.39%	15.12%
Labor and overhead cost	75.31%	51.87%	46.10%	74.94%	48.17%	39.20%
Harvesting cost	3.22%	11.10%	13.81%	3.21%	10.31%	11.74%
Transportation cost of biomass to MPS	1.68%	7.18%	12.46%	2.16%	13.79%	25.57%
Maintenance cost	2.04%	3.75%	3.56%	2.03%	3.48%	3.02%
Bio-oil transportation cost	0.58%	1.99%	2.48%	0.58%	1.85%	2.11%
Propane cost	5.73%	3.94%	2.45%	5.70%	3.66%	2.09%
Relocation cost	0.00%	0.00%	0.00%	0.00%	0.00%	0.00%
Bio-oil storage cost	0.17%	0.12%	0.07%	0.17%	0.11%	0.06%
Biomass storage cost	0.88%	0.61%	0.38%	0.88%	0.56%	0.32%
Biochar transportation cost	0.00%	0.00%	0.00%	0.00%	0.00%	0.00%
Bio-oil production cost (\$ L <sup>-1</sup> )	<b>1.45</b>	<b>0.43</b>	<b>0.35</b>	<b>1.46</b>	<b>0.47</b>	<b>0.41</b>

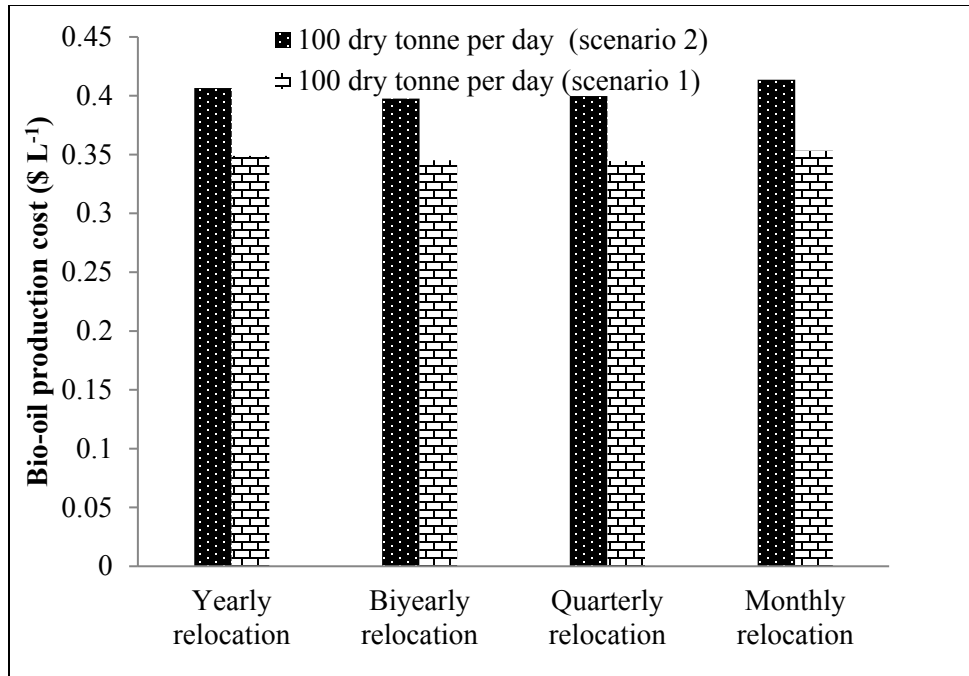


**Figure 6.12. Bio-oil production costs for a 100 dry t d<sup>-1</sup> MPS plant in the truncated and radial configurations**

Bio-oil production costs in the decentralized scenarios for a 100 dry t d<sup>-1</sup> capacity in four relocation time are shown in Figure 6.12. The trend of bio-oil production cost decreases by varying the relocation time from yearly to biyearly and with further reducing the location time from biyearly to quarterly and monthly, the bio-oil production starts to increase. The cost distributions of different components are given in Table 6.6.

**Table 6-6. Cost distribution of 100 dry t d<sup>-1</sup> for four different relocation scenarios**

	Scenario 1: Truncated 100 dry t d <sup>-1</sup>			
	Monthly	Quarterly	Biyearly	Yearly
Capital cost	16.7%	17.2%	17.1%	17.8%
Labour and overhead cost	46.0%	47.2%	47.1%	46.1%
Harvesting cost	13.8%	14.1%	14.1%	13.8%
Transportation cost of biomass to MPS	8.6%	10.0%	11.1%	12.5%
Maintenance cost	3.5%	3.6%	3.6%	3.6%
Bio-oil transportation cost	6.8%	3.8%	2.9%	2.5%
Propane cost	2.4%	2.5%	2.5%	2.5%
Relocation cost	0.0%	0.0%	0.0%	0.0%
Storage cost of bio-oil	0.9%	0.3%	0.1%	0.1%
Storage cost of biomass	0.4%	0.4%	0.4%	0.4%
Biochar transportation cost	0.0%	0.0%	0.0%	0.0%
Bio-oil production cost	0.9%	0.9%	0.9%	0.9%
	Scenario 2: Radial 100 dry t d <sup>-1</sup>			
	Monthly	Quarterly	Biyearly	Yearly
Capital cost	13.7%	15.4%	14.7%	15.1%
Labour and overhead cost	49.9%	39.8%	40.5%	39.2%
Harvesting cost	9.9%	11.1%	11.3%	11.7%
Transportation cost of biomass to MPS	11.1%	24.0%	24.5%	25.6%
Maintenance cost	3.6%	3.1%	3.1%	3.0%
Bio-oil transportation cost	5.3%	3.2%	2.5%	2.1%
Propane cost	3.8%	2.1%	2.2%	2.1%
Relocation cost	0.0%	0.0%	0.0%	0.0%
Storage cost of bio-oil	1.4%	0.3%	0.1%	0.1%
Storage cost of biomass	0.6%	0.3%	0.3%	0.3%
Biochar transportation cost	0.0%	0.0%	0.0%	0.0%
Bio-oil production cost	0.7%	0.8%	0.8%	0.8%

### 6.5.7 *Bio-oil cost variations with changing centralized plant capacity*

Figure 6.13 shows the variations in bio-oil production cost in the mobile pyrolysis system (100 dry t d<sup>-1</sup> for yearly relocation) and the centralized system. It is interesting to observe that at lower capacities (less than 500 dry t d<sup>-1</sup>), both MPS scenarios perform better than the centralized facility. With increases in plant capacity in the centralized plant, bio-oil production costs decrease due to economies of scale. But for the mobile system, the results are quite different. In the radial configuration, bio-oil production costs increase with an increase in base case plant capacity, and

in the truncated configuration, production costs are almost constant with variations in plant capacity. The plot of the centralized plant intersects the radial and truncated scenarios at 410 and 500 dry t d<sup>-1</sup>, respectively.

From this assessment it is reasonable to conclude that at lower capacities, it is good to adopt the MPS to produce bio-oil. In general, plant capacity in a region depends on the availability of biomass and the accessibility of the trees. If biomass resources are limited, it is better to use a mobile pyrolysis plant. And of the two MPS configurations considered, the truncated scenario is economically more attractive.

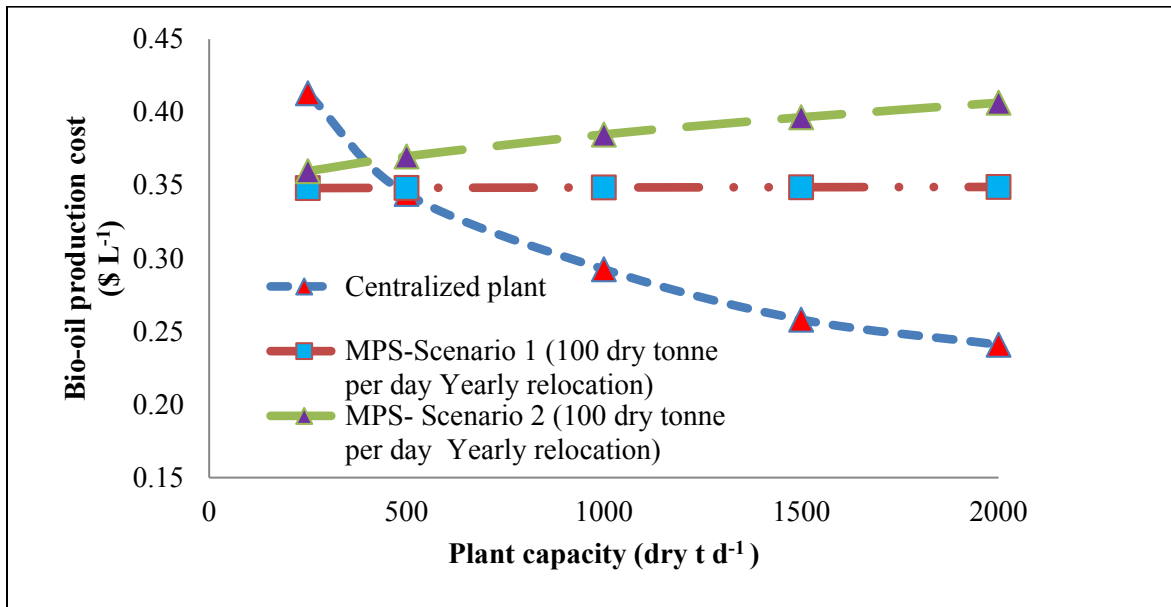


**Figure 6.13. Bio-oil production costs for centralized and decentralized pyrolysis plants**

### 6.5.8 Uncertainty analysis

The Monte Carlo analysis was performed on the 100 dry t d<sup>-1</sup> MPS unit for yearly relocation for the two configurations where bio-oil production cost was optimum. For these analysis, 10,000 iterations were considered and triangular distribution was used. The input parameters were

considered were capital cost, labor and overhead cost, harvesting cost, transportation cost of biomass to MPS, maintenance cost, bio-oil transportation cost, propane cost, relocation cost, bio-oil storage cost, biomass storage cost and biochar transportation cost. The uncertainties considered for these variables were between 70 -130%. The production cost of bio-oil was to be  $0.41 \pm 0.0198$   $\$ L^{-1}$  and  $0.35 \pm 0.0189$   $\$ L^{-1}$  at 95% confidence, respectively, for radial and truncated configuration of 100 dry  $t d^{-1}$  MPS unit for yearly relocation which is shown in Figure 6.14. The uncertainty associated with radial configuration was little higher than the truncated which can be reflected from the higher standard deviation associated with the cost at 95% confidence.

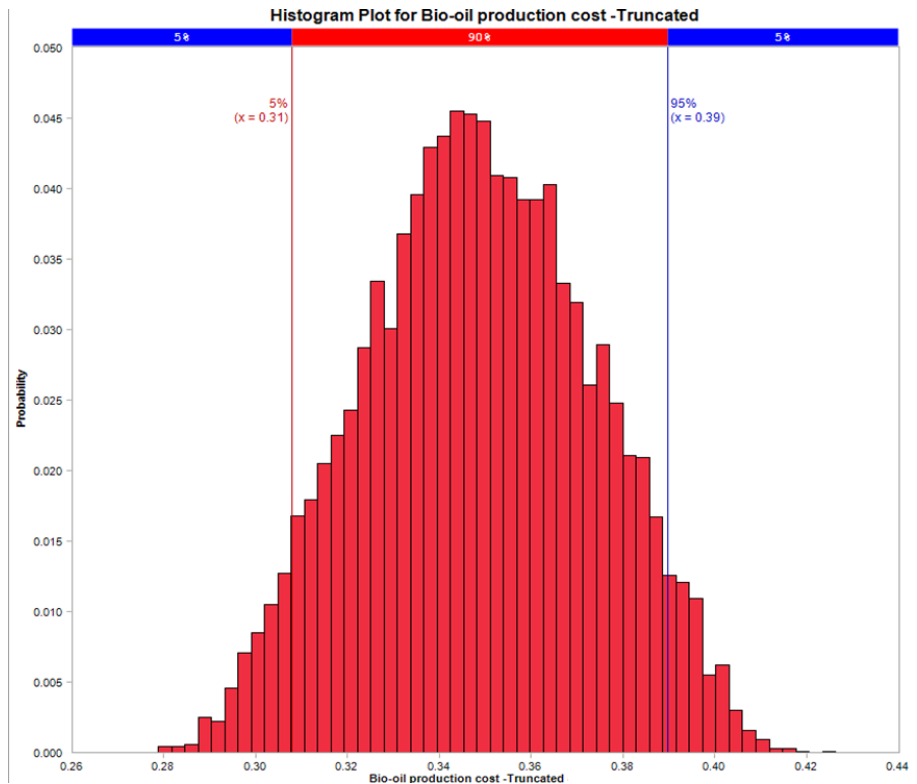
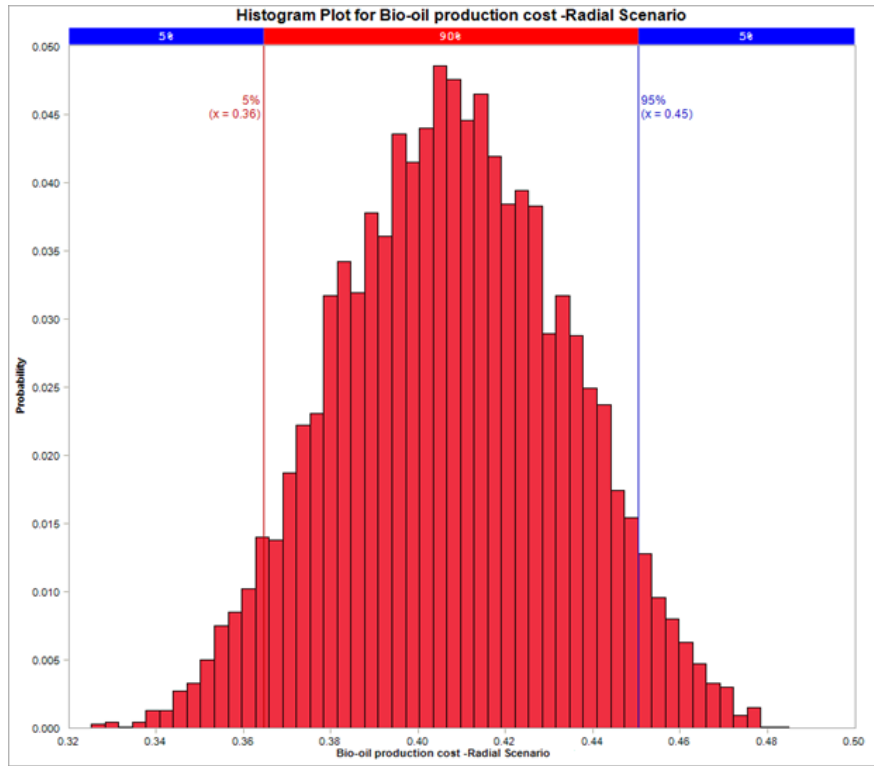


**Figure 6.14. Uncertainty analysis for bio-oil production cost for 100 dry t d<sup>-1</sup> capacity**

## 6.6 Conclusions

Bio-oil can be produced from both the centralized and decentralized pyrolysis plants and be further processed to produce transportation fuel. In this study, two supply chain networks were explored (radial and square) to allocate number of decentralized units which were working simultaneously. From the cost distribution it was determined that by reducing the MPS capacity from 100 to 10 dry t d<sup>-1</sup>, labor costs increase around from 40% to 75%. This is because with the decrease in capacity, the number of MPS units required increases, which increases labor costs. Of the two MPS scenarios, the truncated scenario is more economical than the radial scenario because it has a shorter biomass transportation distance.

Bio-oil production costs of the centralized and mobile frameworks were compared. For higher plant capacities, the centralized plant performs better due to economies of scale. For a 2000 dry tonnes/day biomass plant, bio-oil production costs are 0.24 \$ L<sup>-1</sup>, 0.35 \$ L<sup>-1</sup>, and 0.41 \$ L<sup>-1</sup> for a centralized plant, an MPS unit in the truncated scenario (100 dry t d<sup>-1</sup> unit, yearly relocation), and an MPS unit in the radial scenario (100 dry t d<sup>-1</sup> unit, yearly relocation), respectively. For plant capacities below or equal to 500 dry t d<sup>-1</sup>, an MPS performs better than a centralized plant. At low capacities, the capital and administrative costs in a centralized plant are significantly higher than those for an MPS. Therefore, at lower base case plant capacities, an MPS is recommended as it is movable, provides access to remote locations, and tolerates extreme weather conditions.

In addition, decentralized unit has other benefits which are listed below:

- Farmers can produce bio-oil from the agricultural residues which can be sold and biochar can be used for soil neutralizer
- Municipal waste can be reduced by processing it in this unit. No cost for incineration, therefore no environmental pollution
- Generation of employment at local level.
- Wildfire can be controlled and mitigated based on the availability of the biomass.

- As capital cost is low for the decentralized unit, renewable energy could be available at local point which further reduces the dependence on the fossil fuel.

A centralized plant performs better at higher capacities, but it might not be preferred due to limited availability of large amounts of biomass feedstock. Biomass availability is the driver for the selection of the pyrolysis framework.

The results of this study will help researchers, investors, and governments to understand the advantages of a decentralized system over a centralized one as well as how the allocation of harvesting areas can affect bio-oil production. The outcomes from this paper can also be used to encourage local government to provide decentralized unit to farmers, municipalities and forest communities to divert waste and woody biomass to valuable products and generate employment at small scale pyrolysis unit.

## References

- Agbor, E., Oyedun, A.O., Zhang, X., Kumar, A. 2016. Integrated techno-economic and environmental assessments of sixty scenarios for co-firing biomass with coal and natural gas. *Applied Energy*, **169**, 433-449.
- Badger, P., Badger, S., Puettmann, M., Steele, P., Cooper, J. 2010. Techno-economic analysis: Preliminary assessment of pyrolysis oil production costs and material energy balance associated with a transportable fast pyrolysis system. *BioResources*, **6**(1), 34-47.
- Badger, P.C., Fransham, P. 2006. Use of mobile fast pyrolysis plants to densify biomass and reduce biomass handling costs—A preliminary assessment. *Biomass and Bioenergy*, **30**(4), 321-325.
- Bradburn, K. 2014. 2014 CanBio Report on the Status of Bioenergy in Canada , available at [http://www.fpac.ca/wp-content/uploads/2014\\_CanBio\\_Report.pdf](http://www.fpac.ca/wp-content/uploads/2014_CanBio_Report.pdf). Accessed on 8 June 2018
- Bridgwater, A.V. 1999. Principles and practice of biomass fast pyrolysis processes for liquids. *Journal of Analytical and Applied Pyrolysis*, **51**(1), 3-22.
- Bridgwater, A.V. 2012. Review of fast pyrolysis of biomass and product upgrading. *Biomass and Bioenergy*, **38**, 68-94.
- Bridgwater, A.V., Peacocke, G.V.C. 2000. Fast pyrolysis processes for biomass. *Renewable and Sustainable Energy Reviews*, **4**(1), 1-73.
- Brown, A.L., Brady, P.D., Mowry, C.D., Borek, T.T. 2011. An economic analysis of mobile pyrolysis for Northern New Mexico forests. *Report no. SAND2011-9317. Sandia National Laboratories, US Department of Energy, Albuquerque, New Mexico.*
- Brown, D., Rowe, A., Wild, P. 2013. A techno-economic analysis of using mobile distributed pyrolysis facilities to deliver a forest residue resource. *Bioresource technology*, **150**, 367-376.
- Canada, N.R. 2008. Benchmarking energy use in canadian pulp and paper mills, available at <https://www.nrcan.gc.ca/sites/www.nrcan.gc.ca/files/oeo/pdf/industrial/technical-info/benchmarking/pulp-paper/pdf/benchmark-pulp-paper-e.pdf>. Accessed on 8 June 2018.

- Demirbas, M.F., Balat, M. 2006. Recent advances on the production and utilization trends of bio-fuels: A global perspective. *Energy Conversion and Management*, **47**(15), 2371-2381.
- Guo, M., Song, W., Buhain, J. 2015. Bioenergy and biofuels: History, status, and perspective. *Renewable and Sustainable Energy Reviews*, **42**, 712-725.
- Ha, M., Bumguardner, M.L., Munster, C.L., Vietor, D.M., Capareda, S., Palma, M.A., Provin, T. 2010. Optimizing the logistics of a mobile fast pyrolysis system for sustainable bio-crude oil production. *2010 Pittsburgh, Pennsylvania, June 20-June 23, 2010*. American Society of Agricultural and Biological Engineers. pp. 1.
- Historica Canada. 2017. pulp and paper industry, available at <http://www.thecanadianencyclopedia.ca/en/article/pulp-and-paper-industry/>. Accessed on 22 May 2017.
- Krajnc, N. 2015. Wood fuels handbook, available at <http://www.fao.org/3/a-i4441e.pdf>. Accessed on 1 June 2017.
- Kumar, A. 2013. Techno-economic assessment of biochar production for carbon sequestration, available at [http://albertabiochar.ca/wp-content/uploads/2013/05/A\\_Kumar.pdf](http://albertabiochar.ca/wp-content/uploads/2013/05/A_Kumar.pdf). Accessed on 8 June 2017.
- Kumar, A., Cameron, J.B., Flynn, P.C. 2003. Biomass power cost and optimum plant size in western Canada. *Biomass and Bioenergy*, **24**(6), 445-464.
- Kumar, A., Cameron, J.B., Flynn, P.C. 2004. Pipeline transport of biomass. *Proceedings of the Twenty-Fifth Symposium on Biotechnology for Fuels and Chemicals Held May 4-7, 2003, in Breckenridge, CO*. Springer. pp. 27-39.
- Kumar, A., Flynn, P., Sokhansanj, S. 2008. Biopower generation from mountain pine infested wood in Canada: An economical opportunity for greenhouse gas mitigation. *Renewable Energy*, **33**(6), 1354-1363.
- Laird, D.A., Novak, J.M., Collins, H.P., Ippolito, J.A., Karlen, D.L., Lentz, R.D., Sistani, K.R., Spokas, K., Van Pelt, R.S. 2017. Multi-year and multi-location soil quality and crop biomass yield responses to hardwood fast pyrolysis biochar. *Geoderma*, **289**, 46-53.
- Lynd, L.R., Aziz, R.A., de Brito Cruz, C.H., Chimphango, A.F.A., Cortez, L.A.B., Faaij, A., Greene, N., Keller, M., Osseweijer, P., Richard, T.L., Sheehan, J., Chugh, A., van der Wielen, L., Woods, J., van Zyl, W.H. 2011. A global conversation about energy from

- biomass: the continental conventions of the global sustainable bioenergy project. *Interface Focus*.
- Mahbub, N., Oyedun, A.O., Kumar, A., Oestreich, D., Arnold, U., Sauer, J. 2017. A life cycle assessment of oxymethylene ether synthesis from biomass-derived syngas as a diesel additive. *Journal of Cleaner Production*, **165**, 1249-1262.
- Mahmudi, H., Flynn, P.C. 2006. Rail vs truck transport of biomass. *Twenty-Seventh Symposium on Biotechnology for Fuels and Chemicals*. Springer. pp. 88-103.
- Marshall, A.S.J. 2013. Commercial application of pyrolysis technology in agriculture, available at <https://ofa.on.ca/uploads/userfiles/files/pyrolysis%20report%20final.pdf>. Accessed on 22 May 2017.
- Marshall, A.S.J., Wu, P.F., Mun, S.H., Lalonde, C. 2014. Commercial application of pyrolysis technology in agriculture. *2014 Montreal, Quebec Canada July 13–July 16, 2014*. American Society of Agricultural and Biological Engineers. pp. 1.
- Natural Resources Canada. 2017. How much forest does Canada have?, available at <http://www.nrcan.gc.ca/forests/report/area/17601>. Accessed on 23 May 2017.
- Palma, M.A., Richardson, J.W., Roberson, B.E., Ribera, L.A., Outlaw, J., Munster, C. 2011. Economic feasibility of a mobile fast pyrolysis system for sustainable bio-crude oil production. *International Food and Agribusiness Management Review*, **14**(3).
- Patel, M., Kumar, A. 2016. Production of renewable diesel through the hydroprocessing of lignocellulosic biomass-derived bio-oil: A review. *Renewable and Sustainable Energy Reviews*, **58**, 1293-1307.
- Patel, M., Oyedun, A.O., Kumar, A., Gupta, R. 2018. A Techno-Economic Assessment of Renewable Diesel and Gasoline Production from Aspen Hardwood. *Waste and Biomass Valorization*.
- Patel, M., Zhang, X., Kumar, A. 2016. Techno-economic and life cycle assessment on lignocellulosic biomass thermochemical conversion technologies: A review. *Renewable and Sustainable Energy Reviews*, **53**, 1486-1499.
- Pootakham, T., Kumar, A. 2010. Bio-oil transport by pipeline: A techno-economic assessment. *Bioresource Technology*, **101**(18), 7137-7143.
- Sarkar, S., Kumar, A. 2010. Large-scale biohydrogen production from bio-oil. *Bioresource Technology*, **101**(19), 7350-7361.

- Shahrukh, H., Oyedun, A.O., Kumar, A., Ghiasi, B., Kumar, L., Sokhansanj, S. 2016. Techno-economic assessment of pellets produced from steam pretreated biomass feedstock. *Biomass and Bioenergy*, **87**, 131-143.
- Sorenson, C.B. 2010. A comparative financial analysis of fast pyrolysis plants in Southwest Oregon.
- Thompson, J.D., Klepac, J., Sprinkle, W. 2012. Trucking characteristics for an in-woods biomass chipping operation. *Proceedings of the 2012 Council on Forest Engineering Annual Meeting: Engineering New Solutions for Energy Supply and Demand*.
- VoseSoftware. 2018. Model Risk – Monte Carlo Simulation, available at <https://www.vosesoftware.com/index.php>. Accessed on 12 February 2018.
- Wong, A., Zhang, H., Kumar, A. 2016. Life cycle assessment of renewable diesel production from lignocellulosic biomass. *The International Journal of Life Cycle Assessment*, **21**(10), 1404-1424.
- World Energy Council. 2017. World energy resources bioenergy 2016, available at [https://www.worldenergy.org/wp-content/uploads/2017/03/WEResources\\_Bioenergy\\_2016.pdf](https://www.worldenergy.org/wp-content/uploads/2017/03/WEResources_Bioenergy_2016.pdf). Accessed on 29 July 2017.
- Wright, M.M., Brown, R.C., Boateng, A.A. 2008. Distributed processing of biomass to bio-oil for subsequent production of Fischer-Tropsch liquids. *Biofuels, bioproducts and biorefining*, **2**(3), 229-238.

## **Chapter 7: Conclusions and Recommendations**

### **7.1 Conclusions**

The contribution of this study is in the understanding of the technology used to produce renewable fuels from available local lignocellulosic biomass in order to reduce dependence on petro-fuels and mitigate GHG emissions. To produce renewable diesel from biomass feedstocks, centralized fast pyrolysis and hydroprocessing technology was chosen. Of all the thermochemical processes, fast pyrolysis produces the highest yield of liquid intermediates, known as bio-oil, which can be further upgraded through hydroprocessing, a mature and well understood technology in the petroleum industry. This study involved experimental work, detailed process simulation, and techno-economic analysis of four selected Canadian feedstocks, aspen hardwood, spruce softwood, corn stover, and wheat straw. To produce bio-oil, fast pyrolysis experiments were carried out in a tubular fluidized bed reactor using pretreated dried biomass feedstock. Then, a detailed process model and techno-economic models were developed, respectively, for each feedstock to establish the energy and material balances and to calculate the production costs of renewable diesel and gasoline for a centralized pyrolysis system. Generally, a centralized system favours plants with higher capacity feedstock because of economies of scale. But in the case of biomass conversion at large scales, the economies of scale benefits are undermined by the cost of transporting large amounts of biomass to a centralized plant. Therefore, in this thesis, a decentralized mobile pyrolysis system, where bio-oil, instead of biomass, is transported, was also investigated. The density of bio-oil is three times higher than that of raw biomass. Hence, a supply chain configuration network framework was developed for the decentralized system and two allocation scenarios were investigated (radial and truncated).

### 7.1.1 *Status of fast pyrolysis and hydroprocessing technology*

A detailed review was done on the technical and economic feasibility of fast pyrolysis and hydroprocessing technology for the conversion of lignocellulosic biomass to renewable diesel. The first review focused on the production of bio-oil, an intermediate for renewable diesel, through fast pyrolysis. There are many papers published on the production of bio-oil through fast pyrolysis from a range of biomass. The technology is well understood technically. The production cost of bio-oil varies with the feedstock, reactor type, process conditions in the pyrolyzer, the particle size, etc. There is no techno-economic analysis in the literature on bio-oil production from Canadian biomass feedstocks through fast pyrolysis and hydroprocessing. Moreover, harvesting is different for different biomass and needs to be studied.

Further review of literature mainly focused on the properties of bio-oil produced through fast pyrolysis from various sources of biomass, insight into hydroprocessing technology, operating conditions and catalyst for hydroprocessing, and finally a cost comparison with various thermochemical conversions of lignocellulosic biomass to various end products. Figure 7.1 summarizes the reaction mechanism for the hydroprocessing of bio-oil to produce transportation fuels to replace petrofuels. To study the production of bio-oil from biomass, we chose fast pyrolysis because it is well understood. The bio-oil produced through fast pyrolysis is highly unstable, acidic, viscous, polar, and immiscible with hydrocarbons because of the high oxygen content in the form of organic compounds. Therefore, for the upgrading of this bio-oil, hydroprocessing technology was chosen because it is mature and well established in refineries. Broadly speaking, hydroprocessing technology has two steps, hydrotreating and hydrocracking. In hydrotreating, hydrodeoxygenation occurs and removes the oxygen in the form of water and in the presence of hydrogen and a catalyst. Then, the hydrotreated product is treated in the hydrocracker to form products in the diesel and gasoline range. In this research, the detailed reaction mechanism of the hydrodeoxygenation of fast pyrolysis oil and its significant model compounds are discussed. Then, the effects of process parameters (i.e., temperature, biomass feedstock, catalyst, and catalyst deactivation) on the properties of renewable diesel were studied. But this technology is still immature given the limited understanding of cost. In this thesis, an effort was made to address this

cost gap through a detailed understanding of both hydrotreating and hydrocracking processes for Canadian lignocellulosic biomass feedstocks.

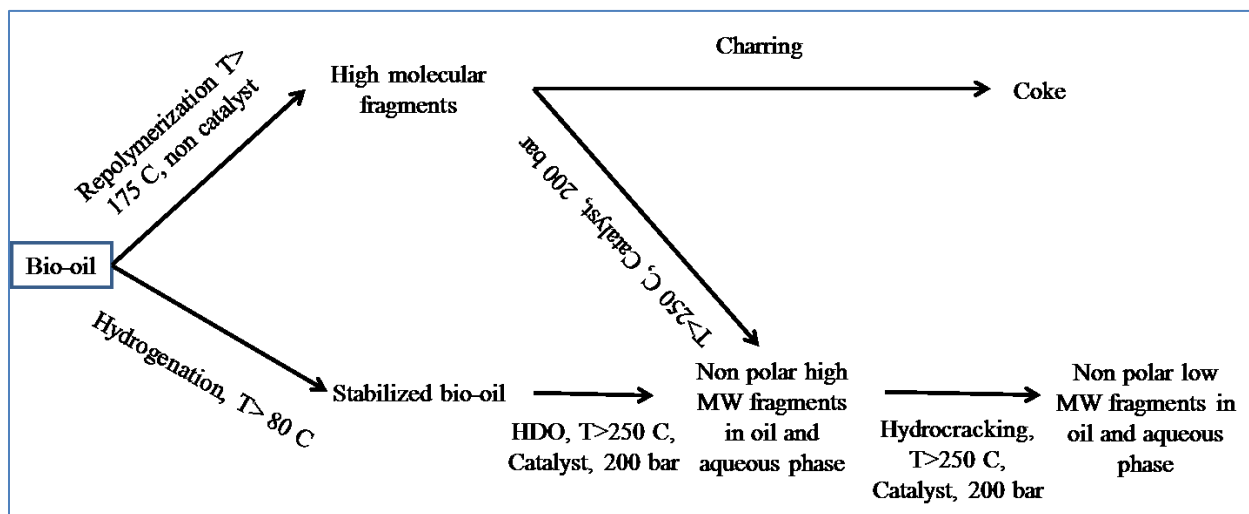
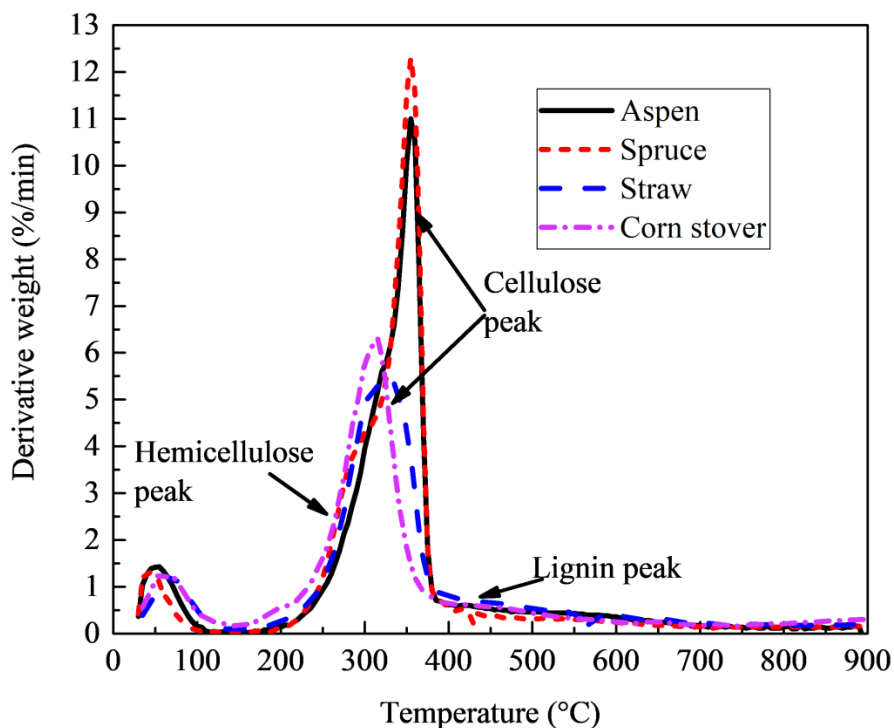


Figure 7.1. Reaction mechanism for the hydroprocessing of bio-oil

### 7.1.2 Identification of Canadian biomass and its pyrolysis kinetics using TGA and fluidized bed reactor

Understanding the pyrolysis kinetics and thermal degradation profile of lignocellulosic biomass is vital to design the process parameters for fast pyrolysis. A detailed kinetic study was carried out for the selected biomass feedstock using thermogravimetric analysis. These feedstocks were assessed with a thermogravimetric analyzer at four heating rates ( $2\text{ }^{\circ}\text{Cmin}^{-1}$ ,  $5\text{ }^{\circ}\text{C min}^{-1}$ ,  $10\text{ }^{\circ}\text{C min}^{-1}$  and  $15\text{ }^{\circ}\text{C min}^{-1}$ ) in an inert nitrogen atmosphere; the temperatures used for the decomposition study range from room temperature to  $900\text{ }^{\circ}\text{C}$ . Figure 7.2 shows the derivative thermogravimetric (DTG) curves for a heating rate of  $10\text{ }^{\circ}\text{C min}^{-1}$  in a nitrogen-controlled atmosphere for woody biomass (spruce and aspen) and agricultural residues (wheat straw and corn stover). DTG plot is the quantitative representation of TGA thermograms in terms of decomposition rate, pyrolysis zones with peak, peak temperature and the temperature ranges for the corresponding pyrolysis zone.



**Figure 7.2. Detailed DTG curves of spruce and aspen as a function of temperature at a heating rate of 10 °C min<sup>-1</sup> in nitrogen atmosphere**

The activation parameters for lignocellulosic biomass were estimated using the model-free (Kissinger, Flynn-Wall-Ozawa [FWO], and Kissinger-Akahira-Sonuse [KAS]) methods. The model-free method predicts activation energies as a function of conversion. The average activation energies are 180.4 kJ mol<sup>-1</sup>, 173.2 kJ mol<sup>-1</sup>, 158.7 kJ mol<sup>-1</sup>, and 164.5 kJ mol<sup>-1</sup>, respectively, for spruce, aspen, wheat straw, and corn stover. These feedstocks were pyrolyzed in a fluidized bed reactor at 400-520°C at three particle size distributions of feed (0.125-0.425 mm, 0.425-1 mm and 1-2 mm) to estimate the kinetic parameters using a simple Arrhenius model. The average activation obtained in this method was 150-168 kJmol<sup>-1</sup>, which was comparable to the TGA results. Then, an attempt was made to apply the kinetic parameters obtained from the TGA study to the experimental fluidized bed reactor to estimate the biomass conversion in order to compare the accuracy between two methods which is shown in Figure 7.3. The average kinetic parameters obtained from the TGA

were well fitted only at high temperatures (450-520°C) and the difference in the predicted biomass conversion was within 4 wt% of the experimental results. However, for the lower fluidization temperatures, when the kinetic parameters from the TGA for the corresponding biomass conversion were used, the predicted conversions were in good agreement with the experimental data.

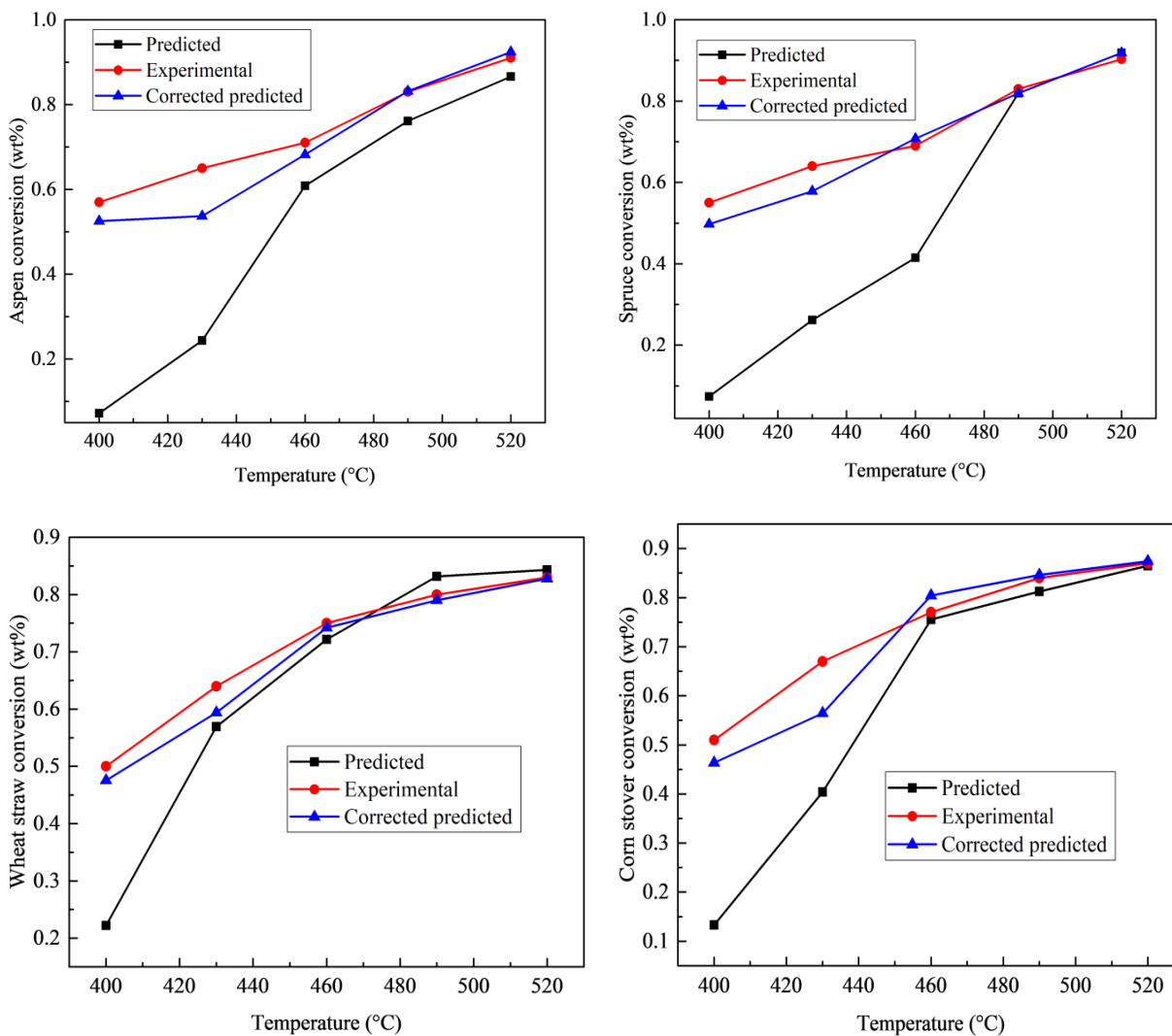


**Figure 7.3. Predicted, experimental, and corrected predicted biomass conversion for (a) aspen, (b) spruce, (c) straw, and (d) corn stover.**

### ***7.1.3 Process modelling and techno-economic assessment of the centralized fast pyrolysis and hydroprocessing technology***

A base case process model was developed on a process simulation platform for Canadian biomass feedstock (aspen wood, spruce wood, wheat straw, and corn stover) to produce renewable diesel and gasoline through fast pyrolysis and hydroprocessing technology in a centralized plant capacity of 2000 t d<sup>-1</sup> plant capacity. The model was developed with both experimental and literature data.

Detailed fast pyrolysis experiments were carried out in a tubular fluidized bed reactor for different temperatures (430°C, 460°C, 490°C, and 520°C) and particle size distribution (0.125-0.425 mm, 0.425-1 mm and 1-2 mm) which is shown in Figure 7.4. The yield of bio-oil through fast pyrolysis depends on feedstock type, temperature, and particle size distribution.

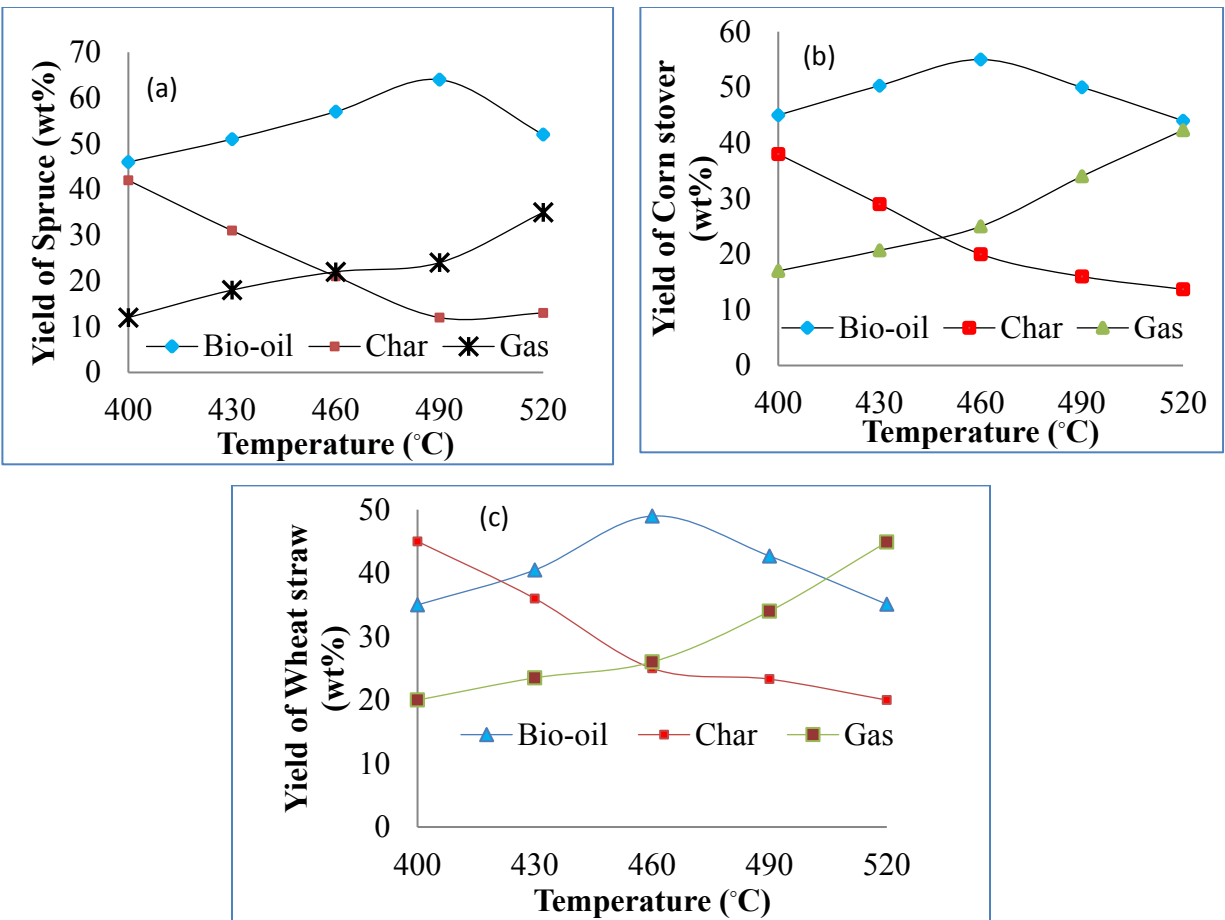


**Figure 7.4. Effects of temperature on product distribution for fast pyrolysis of biomass with (a) spruce, (b) corn stover, and (c) wheat straw**

Bio-oil yield from woody biomass was higher than from agricultural residue because of the lower lignin content and higher cellulosic fraction content in woody biomass. The bio-oil produced from woody biomass was more than 60% by weight and less than 55% by weight from agricultural residues. With an increase in temperature, bio-oil yield increased because of the high formation of volatiles (organic compounds in vapor form). But with a further rise in temperature, volatile compounds were broken into smaller molecular weight compounds, which improved the yield of non-condensable gases. Particle size distribution was also critical to the end products of the pyrolysis process because of the heat transfer between the fluidizing medium (sand) and biomass particle. In this study, three particle size distributions (0.125-0.425 mm, 0.425-1 mm and 1-2 mm) were tested and the highest bio-oil yield was obtained with the 0.125-0.425 mm range because of

better contact between sand and biomass. However, small particles were entrained in the bio-oil. Thus, the 0.425-1 mm particle size distribution range was selected for the analysis.

A process model was developed to establish the energy and mass balances to produce renewable diesel from lignocellulosic biomass. The process model was developed for two scenarios, hydrogen production and merchant hydrogen. The model included a biomass pretreatment unit, a fast pyrolysis unit, a hydrotreating and hydrocracking unit, hydrogen generation, and a power production unit. From material balance, it was confirmed that the renewable diesel produced depended on the quantity and quality of the bio-oil obtained from pyrolysis. Hence, woody biomass produced more renewable diesel than the agricultural residues did.

A data-intensive techno-economic assessment was conducted to estimate the production cost of renewable diesel from various lignocellulosic biomasses. To estimate the renewable diesel production cost, several costs (biomass harvesting and transportation, camping, energy, labor, raw material, catalyst, plant capital cost, etc.) and revenue (renewable diesel, gasoline, and biochar) were used. For a 2000 t d<sup>-1</sup> plant capacity, the renewable diesel production cost was 0.98 \$ L<sup>-1</sup>, 1.11 \$ L<sup>-1</sup>, 1.04 \$ L<sup>-1</sup>, 1.19 \$ L<sup>-1</sup>, and 1.27 \$ L<sup>-1</sup> for the spruce hydrogen purchase, spruce hydrogen production, aspen hydrogen purchase, corn stover hydrogen production, and wheat straw hydrogen production scenarios, respectively. Figure 7.5 shows the distribution of purchased equipment cost for hydrogen production scenario for spruce wood. A large portion of cost is for the hydrocracking and product recovery units followed by fast pyrolysis and biomass pretreatment, hydrotreating units. In total, steam generation and hydrogen generation units contribute 30% of total purchase equipment cost. Therefore, the production cost was lower for the hydrogen purchase scenario because it had lower equipment costs than the hydrogen production scenario. From the sensitivity analysis, it was concluded that the production cost of renewable diesel was most sensitive to bio-oil yield, followed by raw material cost, capital cost, and internal rate of return (IRR), with fluctuations of ±20%. To understand the differences in renewable diesel production cost at various capacities, a wide range of production capacities was considered (from 500 to 5000 t d<sup>-1</sup>) which is shown in Figure 7.6. The optimum size at which the production cost is lowest was found to be

3000 t d<sup>-1</sup> with a renewable diesel price of 1.007 \$ L<sup>-1</sup>. When the capacity increased, raw material delivered costs increased significantly; however, the capital cost per unit output decreased. The scale factor of lignocellulosic biomass-based renewable diesel production was determined to be 0.71 through the developed process model. For all feedstocks, the NER was more than 1, which indicates that the useful sustainable energy coming from the overall process is more than the energy input from the fossil fuel. In other words, this pathway is environmentally friendly.

In this study, an attempt was made to investigate the variation in the production cost of renewable diesel as a function of selling price of biochar, ranges from 0 to 500 \$ t<sup>-1</sup> on the dry basis. With increase in selling price of biochar, the renewable diesel cost decreases significantly. With increase in cost from 0 to 500 \$ t<sup>-1</sup>, the renewable diesel cost reduces from 1.02 to 0.85, 1.14 to 0.98, 1.25 to 0.95 and 1.36 to 0.95 \$ L<sup>-1</sup>, respectively, for spruce hydrogen purchase scenario, spruce hydrogen production scenario, corn stover hydrogen production scenario and wheat straw hydrogen production scenario. Therefore, consideration of biochar as byproduct could be improved the economic feasibility of fast pyrolysis and hydroprocessing technology.

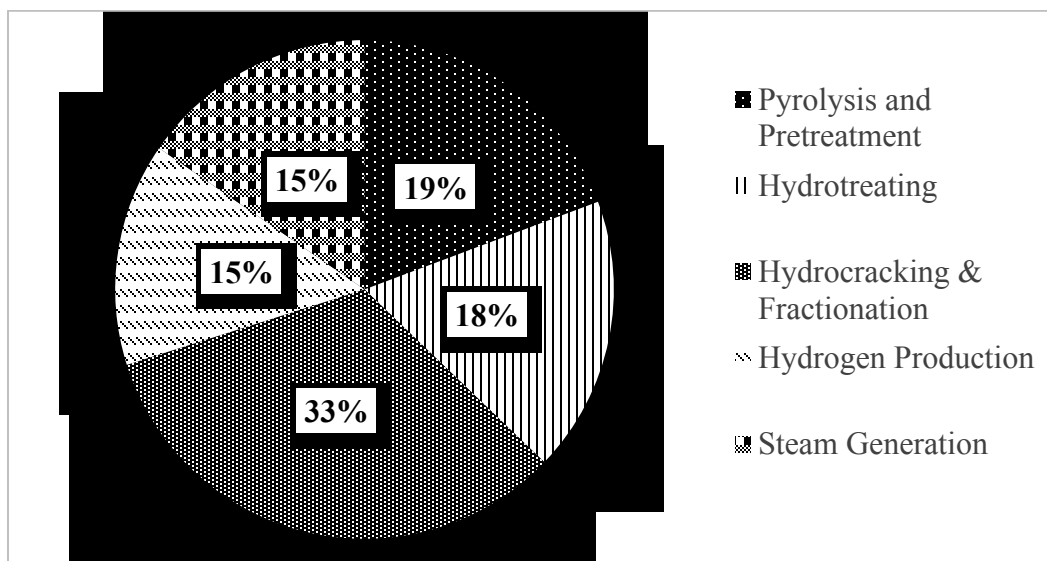


**Figure 7.5. Distribution of purchased equipment cost for hydrogen production scenario for spruce wood**

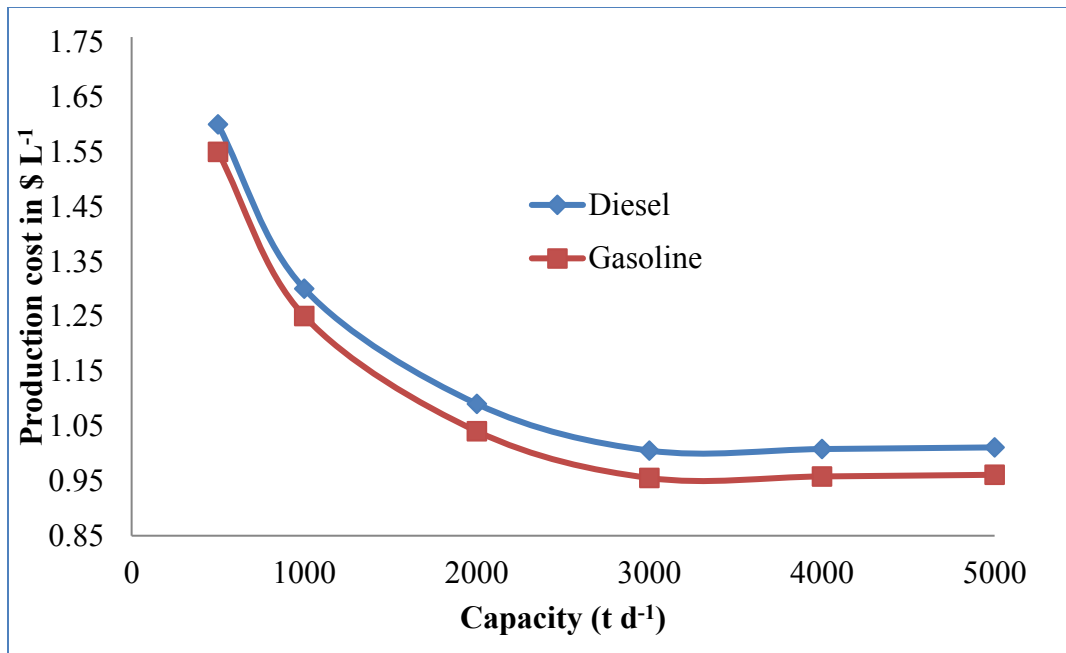


Figure 7.6. Renewable diesel and gasoline production cost with different capacities

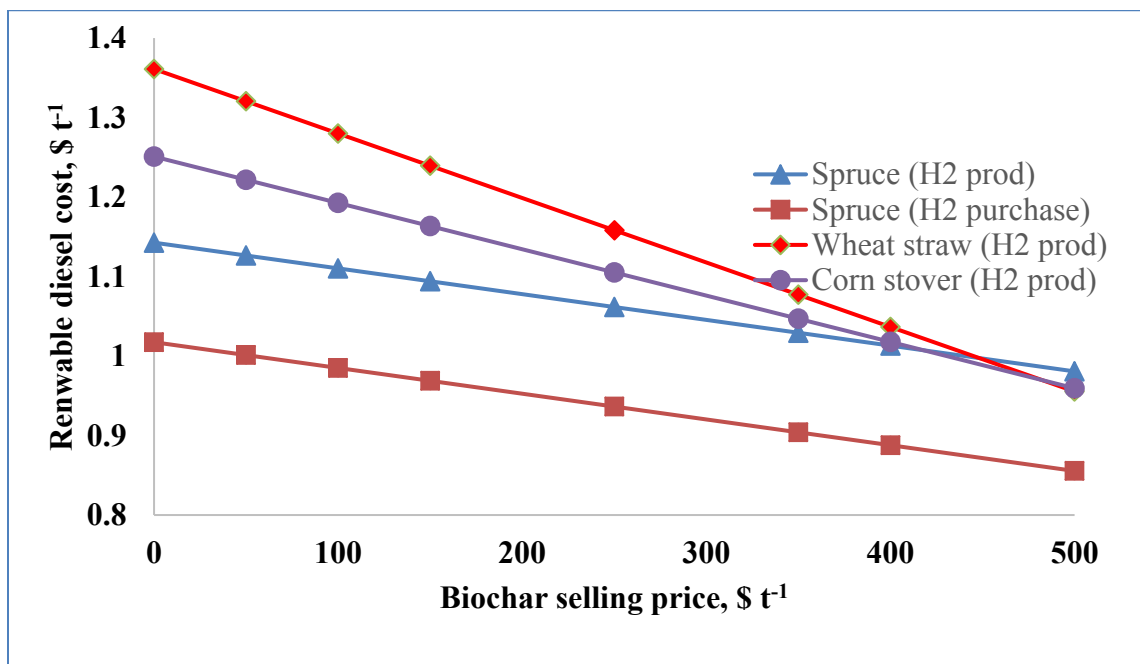


Figure 7.7. Effects of biochar cost on renewable diesel cost

#### 7.1.4 *Development of the supply chain networks for the decentralized pyrolysis system*

Fast pyrolysis process can be performed using either a centralized or decentralized mobile pyrolysis system to produce bio-oil from biomass feedstock. In a centralized system, biomass is transported to a plant to produce bio-oil, which is upgraded in the same unit, while in a mobile pyrolysis system (MPS), the mobile plant is moved to the forest to produce bio-oil, which is transported to an upgrading facility. The main challenges for a large capacity centralized pyrolysis plant include feedstock availability, and high capital investment. These challenges might be overcome by using a mobile pyrolysis system.

In this study, supply chain networks were developed to evaluate the use of a distributed mobile pyrolysis system to produce bio-oil through pyrolysis using Canadian whole trees as the feedstock; in addition, a techno-economic assessment was conducted for each MPS configuration (radial and square) to assess its economic feasibility. For the analysis, five MPS capacities (10, 20, 40, 50, and 100 dry tonnes/day) and four relocation times (yearly, biyearly, quarterly, and monthly) were considered to estimate bio-oil production costs for a base case plant capacity of 2000 dry tonnes/day. For both the truncated and the radial scenarios, the 100 dry tonnes/day MPS performed better than the MPSs at other capacities. When the MPS capacity is decreased from 100 to 10 dry t d<sup>-1</sup>, the labor cost increased from 38% to 78% because more MPS units at lower capacity are required. The detailed cost distribution of bio-oil production from decentralized system is summarized in the Table 7.1. Of the two configurations, the truncated scenario is more economical than the radial scenario because it has a shorter biomass transportation distance. The bio-oil production costs of the centralized and decentralized mobile systems were compared. For a 2000 dry t d<sup>-1</sup> biomass plant capacity, bio-oil production costs are 0.241\$ L<sup>-1</sup>, \$0.294\$ L<sup>-1</sup>, and 0.334 t d<sup>-1</sup> for a centralized plant, an MPS unit in the truncated scenario (100 dry t d<sup>-1</sup> unit, yearly relocation), and an MPS unit in the radial scenario (100 t d<sup>-1</sup> unit, yearly relocation), respectively. For plant capacities below 1000 dry t d<sup>-1</sup>, an MPS performs better than a centralized plant which is shown in Figure 7.8. Therefore, at lower base case plant capacities, an MPS is recommended as it is movable, provides access to remote locations, and tolerates extreme weather conditions. A centralized plant performs better at higher capacities, but it is less preferable because of the limited

availability of large amounts of biomass feedstock. Biomass availability is the driver for the selection of the pyrolysis framework.

**Table 7-1. Cost distribution of bio-oil production costs for an MPS**

<b>Cost distribution of bio-oil production costs (\$ L<sup>-1</sup>) for a 2000 dry t d<sup>-1</sup> plant</b>						
	<b>Yearly relocation- Scenario 1:truncated</b>			<b>Yearly relocation- Scenario 2:radial</b>		
	<b>10 dry t d<sup>-1</sup></b>	<b>50 dry t d<sup>-1</sup></b>	<b>100 dry t d<sup>-1</sup></b>	<b>10 dry t d<sup>-1</sup></b>	<b>50 dry t d<sup>-1</sup></b>	<b>100 dry t d<sup>-1</sup></b>
Capital cost	10.19%	18.73%	17.79%	10.14%	17.39%	15.12%
Labor and overhead cost	75.31%	51.87%	46.10%	74.94%	48.17%	39.20%
Harvesting cost	3.22%	11.10%	13.81%	3.21%	10.31%	11.74%
Transportation cost of biomass to MPS	1.68%	7.18%	12.46%	2.16%	13.79%	25.57%
Maintenance cost	2.04%	3.75%	3.56%	2.03%	3.48%	3.02%
Bio-oil transportation cost	0.58%	1.99%	2.48%	0.58%	1.85%	2.11%
Propane cost	5.73%	3.94%	2.45%	5.70%	3.66%	2.09%
Relocation cost	0.00%	0.00%	0.00%	0.00%	0.00%	0.00%
Bio-oil storage cost	0.17%	0.12%	0.07%	0.17%	0.11%	0.06%
Biomass storage cost	0.88%	0.61%	0.38%	0.88%	0.56%	0.32%
Biochar transportation cost	0.00%	0.00%	0.00%	0.00%	0.00%	0.00%
Bio-oil production cost (\$ L <sup>-1</sup> )	<b>1.45</b>	<b>0.43</b>	<b>0.35</b>	<b>1.46</b>	<b>0.47</b>	<b>0.41</b>

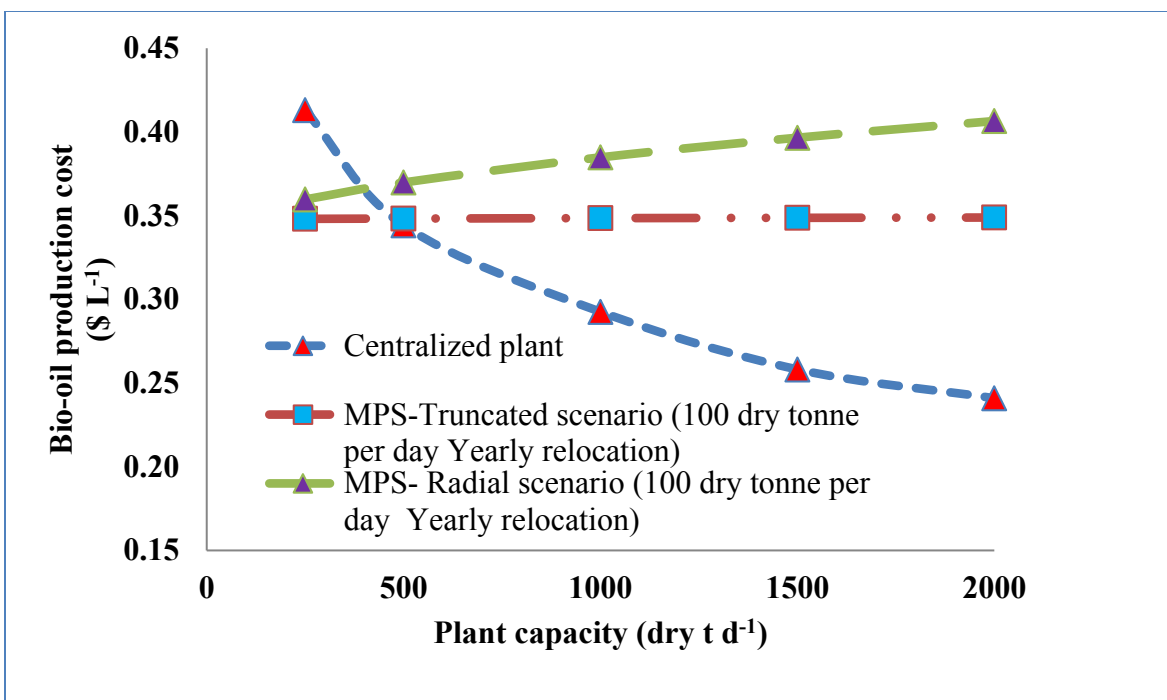


**Figure 7.8. Bio-oil production costs for centralized and decentralized pyrolysis plant**

## 7.2 Recommendation for future work

This study focused on the production of renewable diesel and gasoline through fast pyrolysis and hydroprocessing technology from several Canadian lignocellulosic biomasses.

Recommendations for future work from this research study:

- To identify and explore Canadian feedstocks other than woody biomass and agricultural residues, such as municipal waste, organic waste, algal feedstock, etc. In this study, we considered Western Canadian feedstocks; other kinds of biomass feedstocks need to be considered.
- In this study, fast pyrolysis was carried out experimentally to convert lignocellulosic biomass to bio-oil in a fluidized bed reactor. In the same reactor, the catalytic pyrolysis

could be tried with little modification to the reactor bed. This approach would help to reduce the oxygen content in the bio-oil, which could further reduce upgrading cost.

- Detailed experiments should be carried out for the upgrading of the bio-oil through a high pressure hydrogen reactor. In hydroprocessing, hydrogen is an important and expensive reactant that should be optimized based on the operating conditions of the upgrading process. Simultaneously, it is equally important to investigate the detailed reaction mechanism experimentally for the hydrodeoxygenation reaction of the bio-oil to hydrocarbon products.
- The design and characterization of the catalyst should be considered in both catalytic fast pyrolysis and upgrading (hydrotreating and hydrocracking) operations to enhance the final end products. The catalyst plays a key role in improving the selectivity of the end products. Therefore, significant attention should be paid to understand and prepare the catalysts for the fast pyrolysis and upgrading process.
- In this study, renewable diesel and gasoline as the end products have been considered. Other end products such as jet fuel, hydrogen, kerosene, etc., should be considered through the same process. Therefore, a detailed process model and techno-assessment model need to be developed for the each end product.
- For a decentralized optimization framework, two allocation configurations were considered for the mobile pyrolysis system for woody biomass. Other configurations to optimize the biomass transportation and bio-oil transportation distances should be explored. Moreover, for a case study, it is important to incorporate a GIS-based optimization approach to determine the location of decentralized units for the production of bio-oil.
- Finally, the production of transportation fuels from thermochemical conversion technologies other than fast pyrolysis such as intermediate pyrolysis, and hydrothermal liquefaction and co-processing of bio-oil with conventional transportation fuels should be explored and assessed.

# Bibliography

- Abdelouahed, L., Leveneur, S., Vernieres-Hassimi, L., Balland, L., Taouk, B. 2017. Comparative investigation for the determination of kinetic parameters for biomass pyrolysis by thermogravimetric analysis. *Journal of Thermal Analysis and Calorimetry*, 129(2), 1201-1213.
- Agbor, E., Oyedun, A.O., Zhang, X., Kumar, A. 2016. Integrated techno-economic and environmental assessments of sixty scenarios for co-firing biomass with coal and natural gas. *Applied Energy*, 169(Supplement C), 433-449.
- Ahmad, M.M., Nordin, M.F., Azizan, M.T. 2010. Upgrading of bio-oil into high-value hydrocarbons via hydrodeoxygenation. *American Journal of Applied Sciences*, 7(6), 746-755.
- Alberta Environment and Parks. 2018. Renewable Fuels Standard, available at <http://aep.alberta.ca/climate-change/programs-and-services/renewable-fuels-standard/default.aspx>. Accessed on 7 May 2018
- Anex, R.P., Aden, A., Kazi, F.K., Fortman, J., Swanson, R.M., Wright, M.M., Satrio, J.A., Brown, R.C., Daugaard, D.E., Platon, A., Kothandaraman, G., Hsu, D.D., Dutta, A. 2010. Techno-economic comparison of biomass-to-transportation fuels via pyrolysis, gasification, and biochemical pathways. *Fuel*, 89, S29-S35.
- Antizar-Ladislao, B., Turrion-Gomez, J.L. 2008. Second-generation biofuels and local bioenergy systems. *Biofuels Bioproducts & Biorefining-Biofpr*, 2(5), 455-469.
- Ardiyanti, A.R., Gutierrez, A., Honkela, M.L., Krause, A.O.I., Heeres, H.J. 2011. Hydrotreatment of wood-based pyrolysis oil using zirconia-supported mono- and bimetallic (Pt, Pd, Rh) catalysts. *Applied Catalysis A: General*, 407(1–2), 56-66.
- Ardiyanti, A.R., Khromova, S.A., Venderbosch, R.H., Yakovlev, V.A., Heeres, H.J. 2012a. Catalytic hydrotreatment of fast-pyrolysis oil using non-sulfided bimetallic Ni-Cu catalysts on a  $\delta$ -Al<sub>2</sub>O<sub>3</sub> support. *Applied Catalysis B: Environmental*, 117–118(0), 105-117.
- Ardiyanti, A.R., Khromova, S.A., Venderbosch, R.H., Yakovlev, V.A., Melián-Cabrera, I.V., Heeres, H.J. 2012b. Catalytic hydrotreatment of fast pyrolysis oil using bimetallic Ni–Cu catalysts on various supports. *Applied Catalysis A: General*, 449(0), 121-130.

- Aspen-Icarus. 2014. Aspen process economic analyzer, available at <https://www.aspentech.com/Company/About-AspenTech/>.
- Aspentech. 2014. Aspen process economic analyzer, available at <https://www.aspentech.com/Company/About-AspenTech/>. Accessed on 23 September 2015.
- Azargohar, R., Jacobson, K.L., Powell, E.E., Dalai, A.K. 2013. Evaluation of properties of fast pyrolysis products obtained, from Canadian waste biomass. *Journal of Analytical and Applied Pyrolysis*, 104(0), 330-340.
- Badger, P., Badger, S., Puettmann, M., Steele, P., Cooper, J. 2010. Techno-economic analysis: Preliminary assessment of pyrolysis oil production costs and material energy balance associated with a transportable fast pyrolysis system. *BioResources*, 6(1), 34-47.
- Badger, P.C., Fransham, P. 2006. Use of mobile fast pyrolysis plants to densify biomass and reduce biomass handling costs—A preliminary assessment. *Biomass and Bioenergy*, 30(4), 321-325.
- Baldauf, W., Balfanz, U., Rupp, M. 1994. Upgrading of flash pyrolysis oil and utilization in refineries. *Biomass and Bioenergy*, 7(1-6), 237-244.
- Bartholomew, C.H. 2001. Mechanisms of catalyst deactivation. *Applied Catalysis A: General*, 212(1-2), 17-60.
- Berkeley Biodiesel. Advantages and Disadvantages of Biodiesel Fuel, <http://www.berkeleybiodiesel.org/advantages-and-disadvantages-of-biodiesel.html>, Accessed: September 2013.
- Bezergianni, S., Dimitriadis, A. 2013. Comparison between different types of renewable diesel. *Renewable and Sustainable Energy Reviews*, 21(0), 110-116.
- Bilba, K., Savastano Junior, H., Ghavami, K. 2013. Treatments of non-wood plant fibres used as reinforcement in composite materials. *Materials Research*, 16(4), 903-923.
- BiofuelsDigest. The lowdown on making jet fuel and diesel from biomass, <http://www.biofuelsdigest.com/bdigest/2012/08/31/the-lowdown-on-making-jet-fuel-and-diesel-from-biomass/>. Accessed: October 2013.
- Bothast, R.J., Schlicher, M.A. 2005. Biotechnological processes for conversion of corn into ethanol. *Applied Microbiology and Biotechnology*, 67(1), 19-25.

- BP Statistical Review of World Energy. 2017, available at <https://www.bp.com/content/dam/bp/en/corporate/pdf/energy-economics/statistical-review-2017/bp-statistical-review-of-world-energy-2017-full-report.pdf>. Accessed on 7 May 2018.
- BP. Biofuels, <http://www.bp.com/sectiongenericarticle.do?categoryId=9026466&contentId=7048815>. Accessed: October 2013.
- Bradburn, K. 2014. 2014 CanBio Report on the Status of Bioenergy in Canada , available at [http://www.fpac.ca/wp-content/uploads/2014\\_CanBio\\_Report.pdf](http://www.fpac.ca/wp-content/uploads/2014_CanBio_Report.pdf). Accessed on 8 June 2018
- Bridgwater, A., Meier, D., Radlein, D. 1999. An overview of fast pyrolysis of biomass. *Organic geochemistry*, 30(12), 1479-1493.
- Bridgwater, A.V. 1999. Principles and practice of biomass fast pyrolysis processes for liquids. *Journal of Analytical and Applied Pyrolysis*, 51(1), 3-22.
- Bridgwater, A.V. 2003. Renewable fuels and chemicals by thermal processing of biomass. *Chemical Engineering Journal*, 91(2-3), 87-102.
- Bridgwater, A.V. 2012. Review of fast pyrolysis of biomass and product upgrading. *Biomass and Bioenergy*, 38(0), 68-94.
- Bridgwater, A.V., Meier, D., Radlein, D. 1999. An overview of fast pyrolysis of biomass. *Organic Geochemistry*, 30(12), 1479-1493.
- Bridgwater, A.V., Peacocke, G.V.C. 2000. Fast pyrolysis processes for biomass. *Renewable and Sustainable Energy Reviews*, 4(1), 1-73.
- Brown, A.L., Brady, P.D., Mowry, C.D., Borek, T.T. 2011. An economic analysis of mobile pyrolysis for Northern New Mexico forests. Report no. SAND2011-9317. Sandia National Laboratories, US Department of Energy, Albuquerque, New Mexico.
- Brown, D., Rowe, A., Wild, P. 2013. A techno-economic analysis of using mobile distributed pyrolysis facilities to deliver a forest residue resource. *Bioresource technology*, 150, 367-376.
- Brown, T.R., Thilakaratne, R., Brown, R.C., Hu, G. 2013. Techno-economic analysis of biomass to transportation fuels and electricity via fast pyrolysis and hydroprocessing. *Fuel*, 106(Supplement C), 463-469.

- Bu, Q., Lei, H., Zacher, A.H., Wang, L., Ren, S., Liang, J., Wei, Y., Liu, Y., Tang, J., Zhang, Q., Ruan, R. 2012. A review of catalytic hydrodeoxygenation of lignin-derived phenols from biomass pyrolysis. *Bioresource Technology*, 124(0), 470-477.
- Bui, V.N., Laurenti, D., Afanasiev, P., Geantet, C. 2011a. Hydrodeoxygenation of guaiacol with CoMo catalysts. Part I: Promoting effect of cobalt on HDO selectivity and activity. *Applied Catalysis B-Environmental*, 101(3-4), 239-245.
- Bui, V.N., Laurenti, D., Delichere, P., Geantet, C. 2011b. Hydrodeoxygenation of guaiacol Part II: Support effect for CoMoS catalysts on HDO activity and selectivity. *Applied Catalysis B-Environmental*, 101(3-4), 246-255.
- Bunch, A.Y., Wang, X., Ozkan, U.S. 2007. Hydrodeoxygenation of benzofuran over sulfided and reduced Ni-Mo/ $\gamma$ -Al<sub>2</sub>O<sub>3</sub> catalysts: Effect of H<sub>2</sub>S. *Journal of Molecular Catalysis A: Chemical*, 270(1-2), 264-272.
- Burgess, G., Fernández-Velasco, J.G. 2007. Materials, operational energy inputs, and net energy ratio for photobiological hydrogen production. *International Journal of Hydrogen Energy*, 32(9), 1225-1234.
- Burhenne, L., Messmer, J., Aicher, T., Laborie, M.-P. 2013. The effect of the biomass components lignin, cellulose and hemicellulose on TGA and fixed bed pyrolysis. *Journal of Analytical and Applied Pyrolysis*, 101, 177-184.
- Burton, A., Wu, H. 2017. Influence of biomass particle size on bed agglomeration during biomass pyrolysis in fluidised bed. *Proceedings of the Combustion Institute*, 36(2), 2199-2205.
- Canada Renewable Bioenergy Corp. 2012. Pyrolysis project, available at [http://canadarenewablebioenergy.com/project/pyrolysis\\_technology/](http://canadarenewablebioenergy.com/project/pyrolysis_technology/). Accessed on 17 August 2017.
- Canada, N.R. 2008. Benchmarking energy use in canadian pulp and paper mills, available at <https://www.nrcan.gc.ca/sites/www.nrcan.gc.ca/files/oe/pdf/industrial/technical-info/benchmarking/pulp-paper/pdf/benchmark-pulp-paper-e.pdf>. Accessed on 8 June 2018.
- Canadavisa. 2016. Canada salary calculator, available at <https://www.canadavisa.com/canada-salary-wizard.html>, Accessed on 22nd October 2016.
- Canadian Renewable Fuels Association. Federal Programs, <http://www.greenfuels.org/en/public-policy/federal-programs.aspx>, Accessed: September 2013.

- CBCnews. Researcher aims to create biofuel from pulp waste, <http://www.cbc.ca/news/canada/thunder-bay/researcher-aims-to-create-biofuel-from-pulp-waste-1.1197581>. Accessed: October 2013.
- Centeno, A., Laurent, E., Delmon, B. 1995. Influence of the Support of CoMo Sulfide Catalysts and of the Addition of Potassium and Platinum on the Catalytic Performances for the Hydrodeoxygenation of Carbonyl, Carboxyl, and Guaiacol-Type Molecules. *Journal of Catalysis*, 154(2), 288-298.
- Ceylan, S., Topçu, Y. 2014. Pyrolysis kinetics of hazelnut husk using thermogravimetric analysis. *Bioresource Technology*, 156, 182-188.
- Chandrasekaran, A., Ramachandran, S., Subbiah, S. 2017. Determination of kinetic parameters in the pyrolysis operation and thermal behavior of *Prosopis juliflora* using thermogravimetric analysis. *Bioresource Technology*, 233(Supplement C), 413-422.
- Chiaramonti, D., Bonini, M., Fratini, E., Tondi, G., Gartner, K., Bridgwater, A.V., Grimm, H.P., Soldaini, I., Webster, A., Baglioni, P. 2003. Development of emulsions from biomass pyrolysis liquid and diesel and their use in engines—Part 1 : emulsion production. *Biomass and Bioenergy*, 25(1), 85-99.
- Choi, J.H., Kim, S.-S., Ly, H.V., Kim, J., Woo, H.C. 2017. Effects of water-washing *Saccharina japonica* on fast pyrolysis in a bubbling fluidized-bed reactor. *Biomass and Bioenergy*, 98, 112-123.
- Climate Change Connection. 2013. GHG Emissions - Canada, available at <http://climatechangeconnection.org/emissions/ghg-emissions-canada/canada-emissions-by-sector/>. Accessed on 7 May 2018.
- ConocoPhillips. Who We Are, <http://www.conocophillips.com/who-we-are/our-legacy/history/Pages/1990-Present.aspx>. Accessed: September 2013.
- Cortright, R.D., Davda, R.R., Dumesic, J.A. 2002. Hydrogen from catalytic reforming of biomass-derived hydrocarbons in liquid water. *Nature*, 418(6901), 964-967.
- Cottam, M.L., Bridgwater, A.V. 1994. Techno-economic modelling of biomass flash pyrolysis and upgrading systems. *Biomass and Bioenergy*, 7(1–6), 267-273.
- Czernik, S., Bridgwater, A.V. 2004. Overview of Applications of Biomass Fast Pyrolysis Oil. *Energy & Fuels*, 18(2), 590-598.

- Dakar, M. Challenges of Ethanol Lignocellulosic Production from Biomass, <http://www.katzen.com/ethanol101/Lignocellulosic%20Biomass.pdf>. Accessed: October 2013.
- Damartzis, T., Vamvuka, D., Sfakiotakis, S., Zabaniotou, A. 2011. Thermal degradation studies and kinetic modeling of cardoon (*Cynara cardunculus*) pyrolysis using thermogravimetric analysis (TGA). *Bioresource Technology*, 102(10), 6230-6238.
- de la Puente, G., Gil, A., Pis, J.J., Grange, P. 1999. Effects of support surface chemistry in hydrodeoxygenation reactions over CoMo/activated carbon sulfided catalysts. *Langmuir*, 15(18), 5800-5806.
- Decanio, E.C., Edwards, J.C., Scalzo, T.R., Storm, D.A., Bruno, J.W. 1991. FT-IR and solid-state NMR investigation of phosphorus promoted hydrotreating catalyst precursors. *Journal of Catalysis*, 132(2), 498-511.
- Demirbaş, A. 1997. Calculation of higher heating values of biomass fuels. *Fuel*, 76(5), 431-434.
- Demirbaş, A. 2001. Biomass resource facilities and biomass conversion processing for fuels and chemicals. *Energy Conversion and Management*, 42(11), 1357-1378.
- Demirbas, M.F., Balat, M. 2006. Recent advances on the production and utilization trends of bio-fuels: A global perspective. *Energy Conversion and Management*, 47(15), 2371-2381.
- Department of Energy, U.S. Biodiesel, <http://www.fueleconomy.gov/feg/biodiesel.shtml>. Accessed: September 2013.
- Department, W.a.W. 2016. Hauled wastewater program, available at <http://winnipeg.ca/waterandwaste/sewage/hauledWastewater.stm>.
- Dias, M.O.S., Modesto, M., Ensinas, A.V., Nebra, S.A., Filho, R.M., Rossell, C.E.V. 2011. Improving bioethanol production from sugarcane: evaluation of distillation, thermal integration and cogeneration systems. *Energy*, 36(6), 3691-3703.
- Diffen. Hardwood vs Softwood, [http://www.diffen.com/difference/Hardwood\\_vs\\_Softwood](http://www.diffen.com/difference/Hardwood_vs_Softwood). Accessed: September 2013.
- Echeandia, S., Arias, P.L., Barrio, V.L., Pawelec, B., Fierro, J.L.G. 2010. Synergy effect in the HDO of phenol over Ni–W catalysts supported on active carbon: Effect of tungsten precursors. *Applied Catalysis B: Environmental*, 101(1–2), 1-12.
- ECN Phyllis2. ECN Phyllis classification, <https://www.ecn.nl/phyllis2/Browse/Standard/ECN-Phyllis>. Accessed: October 2013.

- Eco Resources Consultants. Study of Hydrogenation Derived Renewable Diesel as a Renewable Fuel Option in North America, [http://oee.nrcan.gc.ca/sites/oee.nrcan.gc.ca/files/files/pdf/transportation/alternative-fuels/resources/pdf/HDRD\\_Final\\_Report\\_eng.pdf](http://oee.nrcan.gc.ca/sites/oee.nrcan.gc.ca/files/files/pdf/transportation/alternative-fuels/resources/pdf/HDRD_Final_Report_eng.pdf). Accessed: October 2013.
- Ecoresources Consultants. 2012a. Study of hydrogenation derived renewable diesel as a renewable fuel option in North America, available at [http://www.nrcan.gc.ca/sites/www.nrcan.gc.ca/files/oee/files/pdf/transportation/alternative-fuels/resources/pdf/HDRD\\_Final\\_Report\\_eng.pdf](http://www.nrcan.gc.ca/sites/www.nrcan.gc.ca/files/oee/files/pdf/transportation/alternative-fuels/resources/pdf/HDRD_Final_Report_eng.pdf). Accessed on 06 September 2017.
- Ecoresources Consultants. 2012b. An update on renewable diesel infrastructure in Canada, available at [http://www.nrcan.gc.ca/sites/www.nrcan.gc.ca/files/oee/files/pdf/transportation/alternative-fuels/resources/pdf/Infrastructure\\_update\\_final\\_report\\_eng.pdf](http://www.nrcan.gc.ca/sites/www.nrcan.gc.ca/files/oee/files/pdf/transportation/alternative-fuels/resources/pdf/Infrastructure_update_final_report_eng.pdf). Accessed on 17 August 2017.
- Elliott, D., Neuenschwander, G. 1997. Liquid fuels by low-severity hydrotreating of biocrude. in: *Developments in thermochemical biomass conversion*, Springer, pp. 611-621.
- Elliott, D.C., G., N.G. 1996. *Developments in thermochemical biomass conversion*. First Edition ed. Kluwer Academic Publishers, London, UK.
- Elliott, D.C., Hart, T.R., Neuenschwander, G.G., Rotness, L.J., Olarte, M.V., Zacher, A.H., Solantausta, Y. 2012. Catalytic hydroprocessing of fast pyrolysis bio-oil from pine sawdust. *Energy & Fuels*, 26(6), 3891-3896.
- Elliott, D.C., Hart, T.R., Neuenschwander, G.G., Rotness, L.J., Zacher, A.H. 2009. Catalytic hydroprocessing of biomass fast pyrolysis bio- oil to produce hydrocarbon products. *Environmental Progress & Sustainable Energy*, 28(3), 441-449
- Elliott, D.C., Hart, T.R., Neuenschwander, G.G., Rotness, L.J., Zacher, A.H. 2009. Catalytic hydroprocessing of biomass fast pyrolysis bio- oil to produce hydrocarbon products. *Environmental Progress & Sustainable Energy: An Official Publication of the American Institute of Chemical Engineers*, 28(3), 441-449.
- Elliott, D.C., Neuenschwander, G.G. 1998. Liquid fuels by low-severity hydrotreating of biocrude. *Fuel and Energy Abstracts*, 39(4), 259.
- Elliott, D.C.a.N., G. G. 1998. Liquid fuels by low-severity hydrotreating of biocrude. *Fuel and Energy Abstracts*, 39(4), 259.

Energy Efficiency Alberta. 2018. The future is bright, available at <https://www.encyalberta.ca/>. Accessed on 15 October 2018.

Environment and Climate Change Canada. 2017. Canadian environmental sustainability indicators greenhouse gas emissions, available at [http://www.ec.gc.ca/indicateurs-indicateurs/18F3BB9C-43A1-491E-9835-76C8DB9DDFA3/GHGEmissions\\_EN.pdf](http://www.ec.gc.ca/indicateurs-indicateurs/18F3BB9C-43A1-491E-9835-76C8DB9DDFA3/GHGEmissions_EN.pdf). Accessed on 15 August 2018.

Environment Canada. Federal Renewable Fuels Regulations: Overview, <http://www.ec.gc.ca/energie-energy/default.asp?lang=En&n=828C9342-1>, Accessed: September 2013

Environment News Service. Canada Requires Two Percent Renewable Diesel Fuels 2011, <http://www.ens-newswire.com/ens/feb2011/2011-02-14-01.html>. Accessed September 2013.

Environmental Issues. What are the Drawbacks of Using Ethanol?, [http://environment.about.com/od/ethanolfaq/f/ethanol\\_problem.htm](http://environment.about.com/od/ethanolfaq/f/ethanol_problem.htm), Accessed: September 2013.

Environmental Protection Agency U.S. General Overview of What's In America's Trash, <http://www.epa.gov/osw/wycd/catbook/what.htm>. Assessed September 2013.

Environmental Protection Agency U.S. Municipal Solid Waste in the United States, <http://www.epa.gov/wastes/nonhaz/municipal/pubs/msw2009rpt.pdf>, Accessed: September 2013.

Environmental Protection Agency. 2014. Global Greenhouse Gas Emissions Data, available at <https://www.epa.gov/ghgemissions/global-greenhouse-gas-emissions-data>. Accessed on 7 May 2018.

EPCOR. 2016. Commercial rates and fees, available at <http://www.epcor.com/power-natural-gas/regulated-rate-option/commercial-customers/Pages/commercial-rates.aspx>. .

EPCOR. 2016. Rate, tariffs and fee, available at <https://www.epcor.com/products-services/power/rates-tariffs-fees/Pages/default.aspx>. Accessed on 26th Spetember 2017.

EuroBioRef. Conversion of cellulose, hemicellulose and lignin into platform molecules: biotechnological approach, [http://www.eurobioref.org/Summer\\_School/Lectures\\_Slides/day3/Lectures/L06\\_A.Frolander.pdf](http://www.eurobioref.org/Summer_School/Lectures_Slides/day3/Lectures/L06_A.Frolander.pdf). Accessed: October 2013.

- Farag, I.H., LaClaire, C.E., Barrett, C.J. 2004. Technical, environmental and economic feasibility of bio-oil in new hampshire's north country. University of New Hampshire.
- Fenwick, S. 2018. Renewable fuels for diesel applications, available at [https://cleancities.energy.gov/files/u/news\\_events/document/document\\_url/183/Fenwick\\_-\\_NBB\\_-\\_Clean\\_Cities\\_Renewable\\_Diesel.pdf](https://cleancities.energy.gov/files/u/news_events/document/document_url/183/Fenwick_-_NBB_-_Clean_Cities_Renewable_Diesel.pdf). Accessed on 7 May 2018
- Ferrari, M., Bosmans, S., Maggi, R., Delmon, B., Grange, P. 2001. CoMo/carbon hydrodeoxygenation catalysts: influence of the hydrogen sulfide partial pressure and of the sulfidation temperature. *Catalysis Today*, 65(2-4), 257-264.
- Ferrari, M., Delmon, B., Grange, P. 2002a. Influence of the active phase loading in carbon supported molybdenum-cobalt catalysts for hydrodeoxygenation reactions. *Microporous and Mesoporous Materials*, 56(3), 279-290.
- Ferrari, M., Delmon, B., Grange, P. 2002b. Influence of the impregnation order of molybdenum and cobalt in carbon-supported catalysts for hydrodeoxygenation reactions. *Carbon*, 40(4), 497-511.
- Flynn, J.H., Wall, L.A. 1966. A Quick Direct Method for Determination of Activation Energy from Thermogravimetric Data. *Journal of Polymer Science Part B-Polymer Letters*, 4(5pb), 323-&.
- Forzatti, P., Lietti, L. 1999. Catalyst deactivation. *Catalysis Today*, 52(2-3), 165-181.
- Furimsky, E. 2000. Catalytic hydrodeoxygenation. *Applied Catalysis A: General*, 199(2), 147-190.
- Gable, P., Brown, R.C. 2016. Effect of biomass heating time on bio-oil yields in a free fall fast pyrolysis reactor. *Fuel*, 166(Supplement C), 361-366.
- Gagnon, J., Kaliaguine, S. 1988. Catalytic Hydrotreatment of Vacuum Pyrolysis Oils from Wood. *Industrial & Engineering Chemistry Research*, 27(10), 1783-1788.
- Gagnon, J., Kaliaguine, S. 1988. Catalytic hydrotreatment of vacuum pyrolysis oils from wood. *Industrial & engineering chemistry research*, 27(10), 1783-1788.
- Galletti, A.M.R., Antonetti, C. Biomass pre-treatment: separation of cellulose, hemicellulose and lignin. Existing technologies and perspectives, [http://www.eurobioref.org/Summer\\_School/Lectures\\_Slides/day2/Lectures/L04\\_AG%20Raspolli.pdf](http://www.eurobioref.org/Summer_School/Lectures_Slides/day2/Lectures/L04_AG%20Raspolli.pdf). Access: October 2013.

- Gandarias, I., Barrio, V.L., Reques, J., Arias, P.L., Cambra, J.F., Güemez, M.B. 2008. From biomass to fuels: Hydrotreating of oxygenated compounds. *International Journal of Hydrogen Energy*, 33(13), 3485-3488.
- Garcia-Maraver, A., Salvachúa, D., Martínez, M.J., Diaz, L.F., Zamorano, M. 2013. Analysis of the relation between the cellulose, hemicellulose and lignin content and the thermal behavior of residual biomass from olive trees. *Waste Management*, 33(11), 2245-2249.
- Garcia-Perez, M., Wang, X.S., Shen, J., Rhodes, M.J., Tian, F., Lee, W.-J., Wu, H., Li, C.-Z. 2008. Fast Pyrolysis of Oil Mallee Woody Biomass: Effect of Temperature on the Yield and Quality of Pyrolysis Products. *Industrial & Engineering Chemistry Research*, 47(6), 1846-1854.
- Gasparovic, L., Korenova, Z., Jelemensky, L. 2010. Kinetic study of wood chips decomposition by TGA. *Chemical Papers*, 64(2), 174-181.
- Gayubo, A.G., Aguayo, A.T., Atutxa, A., Prieto, R., Bilbao, J. 2004. Deactivation of a HZSM-5 zeolite catalyst in the transformation of the aqueous fraction of biomass pyrolysis oil into hydrocarbons. *Energy & Fuels*, 18(6), 1640-1647.
- Gevert, B.S., Otterstedt, J.E., Massoth, F.E. 1987. Kinetics of the HDO of methyl-substituted phenols. *Applied Catalysis*, 31(1), 119-131.
- Gevert, S.B., Eriksson, M., Eriksson, P., Massoth, F.E. 1994. Direct hydrodeoxygenation and hydrogenation of 2,6- and 3,5-dimethylphenol over sulphided CoMo catalyst. *Applied Catalysis A, General*, 117(2), 151-162.
- Gishti, K., Iannibello, A., Marengo, S., Morelli, G., Tittarelli, P. 1984. On the role of phosphate anion in the MoO<sub>3</sub>-Al<sub>2</sub>O<sub>3</sub> based catalysts. *Applied Catalysis*, 12(4), 381-393.
- Goldemberg, J., Coelho, S.T., Guardabassi, P. 2008. The sustainability of ethanol production from sugarcane. *Energy Policy*, 36(6), 2086-2097.
- Government of Canada. 2017. How much forest does Canada have?, available at <http://www.nrcan.gc.ca/forests/report/area/17601>. Accessed on 7th November 2017.
- Government of Canada. 2017. Greenhouse gas emissions by Canadian economic sector, available at <https://www.canada.ca/en/environment-climate-change/services/environmental-indicators/greenhouse-gas-emissions/canadian-economic-sector.html>. Accessed on 7th November, 2017.

- Goyal, H.B., Seal, D., Saxena, R.C. 2008. Bio-fuels from thermochemical conversion of renewable resources: A review. *Renewable and Sustainable Energy Reviews*, 12(2), 504-517.
- Green Car Congress. ConocoPhillips Begins Production of Renewable Diesel Fuel at Whitegate Refinery at Whitegate Refinery, [http://www.greencarcongress.com/2006/12/conocophillips\\_.html](http://www.greencarcongress.com/2006/12/conocophillips_.html). Accessed: September 2013.
- Greenhalf, C.E., Nowakowski, D.J., Harms, A.B., Titiloye, J.O., Bridgwater, A.V. 2013. A comparative study of straw, perennial grasses and hardwoods in terms of fast pyrolysis products. *Fuel*, 108, 216-230.
- Greenpeace International. 2016. Carbon capture and storage a costly, risky distraction, available at <https://www.greenpeace.org/archive-international/en/campaigns/climate-change/Solutions/Reject-false-solutions/Reject-carbon-capture--storage/>. Accessed on 7 May 2018.
- Gregoire, C.E., Bain, R.L. 1994. Technoeconomic analysis of the production of biocrude from wood. *Biomass and Bioenergy*, 7(1), 275-283.
- Guo, M., Song, W., Buhain, J. 2015. Bioenergy and biofuels: History, status, and perspective. *Renewable and Sustainable Energy Reviews*, 42, 712-725.
- Gutierrez, A., Kaila, R.K., Honkela, M.L., Slioor, R., Krause, A.O.I. 2009. Hydrodeoxygenation of guaiacol on noble metal catalysts. *Catalysis Today*, 147(3-4), 239-246.
- Ha, M., Bumguardner, M.L., Munster, C.L., Vietor, D.M., Capareda, S., Palma, M.A., Provin, T. 2010. Optimizing the logistics of a mobile fast pyrolysis system for sustainable bio-crude oil production. 2010 Pittsburgh, Pennsylvania, June 20-June 23, 2010. American Society of Agricultural and Biological Engineers. pp. 1.
- Haldor Topsoe. Novel hydrotreating technology for production of green diesel. [http://www.topsoe.com/business\\_areas/refining/~media/PDF%20files/Refining/novel\\_hydrotreating\\_technology\\_for\\_production\\_of\\_green\\_diesel.ashx](http://www.topsoe.com/business_areas/refining/~media/PDF%20files/Refining/novel_hydrotreating_technology_for_production_of_green_diesel.ashx). Accessed: October 2013.
- Hamelinck, C.N., Faaij, A.P.C. 2006. Outlook for advanced biofuels. *Energy Policy*, 34(17), 3268-3283.
- Harun, N.Y., Afzal, M.T. 2010. Thermal decomposition kinetics of forest residue. *Journal of Applied Sciences*, 10(12), 1122-1127.

- Hassan, M.H., Kalam, M.A. 2013. An overview of biofuel as a renewable energy source: development and challenges. *Procedia Engineering*, 56, 39-53.
- Heidari, A., Stahl, R., Younesi, H., Rashidi, A., Troeger, N., Ghoreyshi, A.A. 2014. Effect of process conditions on product yield and composition of fast pyrolysis of *Eucalyptus grandis* in fluidized bed reactor. *Journal of Industrial and Engineering Chemistry*, 20(4), 2594-2602.
- Historica Canada. 2017. pulp and paper industry, available at <http://www.thecanadianencyclopedia.ca/en/article/pulp-and-paper-industry/>. Accessed on 22 May 2017.
- Honeywell. Honeywell Green Diesel™ To Be Produced From Bio Feedstocks In U.S. Facility, <http://honeywell.com/News/Pages/Honeywell-Green-Diesel-To-Be-Produced-From-Bio-Feedstocks-In-US-Facility.aspx>. Accessed: October 2013
- Hu, M., Chen, Z., Wang, S., Guo, D., Ma, C., Zhou, Y., Chen, J., Laghari, M., Fazal, S., Xiao, B., Zhang, B., Ma, S. 2016. Thermogravimetric kinetics of lignocellulosic biomass slow pyrolysis using distributed activation energy model, Fraser–Suzuki deconvolution, and iso-conversional method. *Energy Conversion and Management*, 118(Supplement C), 1-11.
- Hu, S., Jess, A., Xu, M. 2007. Kinetic study of Chinese biomass slow pyrolysis: Comparison of different kinetic models. *Fuel*, 86(17), 2778-2788.
- Hu, W., Dang, Q., Rover, M., Brown, R.C., Wright, M.M. 2016. Comparative techno-economic analysis of advanced biofuels, biochemicals, and hydrocarbon chemicals via the fast pyrolysis platform. *Biofuels*, 7(1), 57-67.
- Huang, M.R., Li, X.G. 1998. Thermal degradation of cellulose and cellulose esters. *Journal of Applied Polymer Science*, 68(2), 293-304.
- Huang, X., Cao, J.-P., Zhao, X.-Y., Wang, J.-X., Fan, X., Zhao, Y.-P., Wei, X.-Y. 2016. Pyrolysis kinetics of soybean straw using thermogravimetric analysis. *Fuel*, 169(Supplement C), 93-98.
- Islam, M.N., Ani, F.N. 2000. Techno-economics of rice husk pyrolysis, conversion with catalytic treatment to produce liquid fuel. *Bioresource Technology*, 73(1), 67-75.
- Jantaraksa, N., Prasassarakich, P., Reubroycharoen, P., Hinchiranan, N. 2015. Cleaner alternative liquid fuels derived from the hydrodesulfurization of waste tire pyrolysis oil. *Energy Conversion and Management*, 95, 424-434.

- Jeong, J.-Y., Lee, U.-D., Chang, W.-S., Jeong, S.-H. 2016. Production of bio-oil rich in acetic acid and phenol from fast pyrolysis of palm residues using a fluidized bed reactor: Influence of activated carbons. *Bioresource Technology*, 219(Supplement C), 357-364.
- Ji-lu, Z. 2007. Bio-oil from fast pyrolysis of rice husk: Yields and related properties and improvement of the pyrolysis system. *Journal of Analytical and Applied Pyrolysis*, 80(1), 30-35.
- Jones, S., Meyer, P., Snowden-Swan, S., Padmaperuma, A., Tan, E., Dutta, A., Jacobson, J., Cafferty, K. 2013. Process design and economics for the conversion of lignocellulosic biomass to hydrocarbon fuels. PNNL-23053, NREL/TP-5100-61178.
- Jones, S.B., Holladay, J.E., Valkenburg, C., Stevens, D.J., Walton, C.W., Kinchin, C., Elliott, D.C., Czernik, S. 2009. Production of gasoline and diesel from biomass via fast pyrolysis, hydrotreating and hydrocracking: a design case.
- Jones, S.B., Valkenburt, C., Walton, C.W., Elliott, D.C., Holladay, J.E., Stevens, D.J., Kinchin, C., Czernik, S. 2009. Production of gasoline and diesel from biomass via fast pyrolysis, hydrotreating and hydrocracking: a design case. Pacific Northwest National Laboratory (PNNL), Richland, WA (US).
- Kan, T., Strezov, V., Evans, T.J. 2016. Lignocellulosic biomass pyrolysis: A review of product properties and effects of pyrolysis parameters. *Renewable and Sustainable Energy Reviews*, 57(Supplement C), 1126-1140.
- Kantarelis, E., Yang, W., Blasiak, W., Forsgren, C., Zabaniotou, A. 2011. Thermochemical treatment of E-waste from small household appliances using highly pre-heated nitrogen-thermogravimetric investigation and pyrolysis kinetics. *Applied Energy*, 88(3), 922-929.
- Kaycircle. 2017. Average nitrogen price, available at <http://www.kaycircle.com/What-Is-The-Average-Cost-Of-Nitrogen-Gas-Per-Gram-Pound-Cubic-Foot-Average-Nitrogen-Price>. Accessed on 26th September 2017.
- Kaycircle. 2016. What is the average cost of nitrogen gas per gram/pound/cubic foot? Average nitrogen price, available at <http://www.kaycircle.com/What-Is-The-Average-Cost-Of-Nitrogen-Gas-Per-Gram-Pound-Cubic-Foot-Average-Nitrogen-Price>. Accessed on 17 August 2017.

- Kim, K.H., Kim, T.-S., Lee, S.-M., Choi, D., Yeo, H., Choi, I.-G., Choi, J.W. 2013b. Comparison of physicochemical features of biooils and biochars produced from various woody biomasses by fast pyrolysis. *Renewable Energy*, 50(0), 188-195.
- Knothe, G. 2010. Biodiesel and renewable diesel: A comparison. *Progress in Energy and Combustion Science*, 36(3), 364-373.
- Krajnc, N. 2015. Wood fuels handbook, available at <http://www.fao.org/3/a-i4441e.pdf>. Accessed on 1 June 2017.
- Krishna, M.V.S.M., Rao, V.V.R.S., Reddy, T.K.K., Murthy, P.V.K. 2014. Comparative studies on performance evaluation of DI diesel engine with high grade low heat rejection combustion chamber with carbureted alcohols and crude jatropha oil. *Renewable and Sustainable Energy Reviews*, 36, 1-19.
- Kumar, A. 2013. Techno-economic assessment of biochar production for carbon sequestration, available at [http://albertabiochar.ca/wp-content/uploads/2013/05/A\\_Kumar.pdf](http://albertabiochar.ca/wp-content/uploads/2013/05/A_Kumar.pdf). Accessed on 8 June 2017.
- Kumar, A., Cameron, J.B., Flynn, P.C. 2003. Biomass power cost and optimum plant size in western Canada. *Biomass and Bioenergy*, 24(6), 445-464.
- Kumar, A., Cameron, J.B., Flynn, P.C. 2004. Pipeline transport of biomass. *Proceedings of the Twenty-Fifth Symposium on Biotechnology for Fuels and Chemicals Held May 4–7, 2003, in Breckenridge, CO*. Springer. pp. 27-39.
- Kumar, A., Flynn, P., Sokhansanj, S. 2008. Biopower generation from mountain pine infested wood in Canada: An economical opportunity for greenhouse gas mitigation. *Renewable Energy*, 33(6), 1354-1363.
- Kuppens, T., Van Dael, M., Vanreppelen, K., Thewys, T., Yperman, J., Carleer, R., Schreurs, S., Van Passel, S. 2015. Techno-economic assessment of fast pyrolysis for the valorization of short rotation coppice cultivated for phytoextraction. *Journal of Cleaner Production*, 88, 336-344.
- LaClaire, C.E., Barrett, C.J., Hall, K. 2004. Technical, environmental and economic feasibility of bio-oil in new hampshire's north country. Durham, NH: University of New Hampshire.
- Ladanai, S., Vinterback, J. 2011. Global potential of sustainable biomass for energy, available at [http://pub.epsilon.slu.se/5586/1/ladanai\\_s\\_etal\\_110120\\_4.pdf](http://pub.epsilon.slu.se/5586/1/ladanai_s_etal_110120_4.pdf).

- Laird, D.A., Novak, J.M., Collins, H.P., Ippolito, J.A., Karlen, D.L., Lentz, R.D., Sistani, K.R., Spokas, K., Van Pelt, R.S. 2017. Multi-year and multi-location soil quality and crop biomass yield responses to hardwood fast pyrolysis biochar. *Geoderma*, 289, 46-53.
- Laurent, E., Delmon, B. 1993. Influence of Oxygen-Containing, Nitrogen-Containing, and Sulfur-Containing-Compounds on the Hydrodeoxygenation of Phenols over Sulfided CoMo/Gamma-Al<sub>2</sub>O<sub>3</sub> and NiMo/Gamma-Al<sub>2</sub>O<sub>3</sub> Catalysts. *Industrial & Engineering Chemistry Research*, 32(11), 2516-2524.
- Laurent, E., Delmon, B. 1994a. Influence of water in the deactivation of a sulfided NiMo Gamma-Al<sub>2</sub>O<sub>3</sub> catalyst during hydrodeoxygenation. *Journal of Catalysis*, 146(1), 281-291.
- Laurent, E., Delmon, B. 1994b. Study of the hydrodeoxygenation of carbonyl, carboxylic and guaiacyl groups over sulfided CoMo/Gamma-Al<sub>2</sub>O<sub>3</sub> and NiMo/Gamma-Al<sub>2</sub>O<sub>3</sub> catalyst .2. Influence of water, ammonia and hydrogen-sulfide. *Applied Catalysis a-General*, 109(1), 97-115.
- Lehto, J., Oasmaa, A., Solantausta, Y., Kyto, M., Chiaramonti, D. 2013. Fuel oil quality and combustion of fast pyrolysis bio-oils VTT Technical Research Centre of Finland.
- Li, C., Suzuki, K. 2009. Kinetic analyses of biomass tar pyrolysis using the distributed activation energy model by TG/DTA technique. *Journal of Thermal Analysis and Calorimetry*, 98(1), 261.
- Li, W., Dang, Q., Smith, R., Brown, R.C., M. Wright, M. 2017. Techno-Economic Analysis of the Stabilization of Bio-Oil Fractions for Insertion into Petroleum Refineries. *ACS Sustainable Chemistry & Engineering*, 5(2), 1528-1537.
- Liu, R., Deng, C., Wang, J. 2009. Fast Pyrolysis of Corn Straw for Bio-oil Production in a Bench-scale Fluidized Bed Reactor. *Energy Sources, Part A: Recovery, Utilization, and Environmental Effects*, 32(1), 10-19.
- Lopez-Velazquez, M.A., Santes, V., Balmaseda, J., Torres-Garcia, E. 2013. Pyrolysis of orange waste: A thermo-kinetic study. *Journal of Analytical and Applied Pyrolysis*, 99, 170-177.
- Lu, Q., Li, W.-Z., Zhu, X.-F. 2009. Overview of fuel properties of biomass fast pyrolysis oils. *Energy Conversion and Management*, 50(5), 1376-1383.
- Lu, Q., Yang, X.-l., Zhu, X.-f. 2008. Analysis on chemical and physical properties of bio-oil pyrolyzed from rice husk. *Journal of Analytical and Applied Pyrolysis*, 82(2), 191-198.

- Lv, G.J., Wu, S.B., Lou, R.I. 2010. Kinetic Study of the Thermal Decomposition of Hemicellulose Isolated from Corn Stalk. *Bioresources*, 5(2), 1281-1291.
- Lynd, L.R., Aziz, R.A., de Brito Cruz, C.H., Chimphango, A.F.A., Cortez, L.A.B., Faaij, A., Greene, N., Keller, M., Osseweijer, P., Richard, T.L., Sheehan, J., Chugh, A., van der Wielen, L., Woods, J., van Zyl, W.H. 2011. A global conversation about energy from biomass: the continental conventions of the global sustainable bioenergy project. *Interface Focus*.
- Mahbub, N., Oyedun, A.O., Kumar, A., Oestreich, D., Arnold, U., Sauer, J. 2017. A life cycle assessment of oxymethylene ether synthesis from biomass-derived syngas as a diesel additive. *Journal of Cleaner Production*, 165, 1249-1262.
- Mahmudi, H., Flynn, P.C. 2006. Rail vs truck transport of biomass. *Twenty-Seventh Symposium on Biotechnology for Fuels and Chemicals*. Springer. pp. 88-103.
- Maia, A.A.D., de Morais, L.C. 2016. Kinetic parameters of red pepper waste as biomass to solid biofuel. *Bioresource Technology*, 204(Supplement C), 157-163.
- Mani, T., Murugan, P., Abedi, J., Mahinpey, N. 2010. Pyrolysis of wheat straw in a thermogravimetric analyzer: effect of particle size and heating rate on devolatilization and estimation of global kinetics. *Chemical engineering research and design*, 88(8), 952-958.
- Marshall, A.S.J. 2013. Commercial application of pyrolysis technology in agriculture, available at <https://ofa.on.ca/uploads/userfiles/files/pyrolysis%20report%20final.pdf>. Accessed on 22 May 2017.
- Marshall, A.S.J., Wu, P.F., Mun, S.H., Lalonde, C. 2014. Commercial application of pyrolysis technology in agriculture. 2014 Montreal, Quebec Canada July 13–July 16, 2014. *American Society of Agricultural and Biological Engineers*. pp. 1.
- McKendry, P. 2002. Energy production from biomass (part 1): overview of biomass. *Bioresource Technology*, 83(1), 37-46.
- McMillan, J.D. 1994. Pretreatment of lignocellulosic biomass. *ACS symposium series*. ACS Publications. pp. 292-324.
- Mehrabian, R., Scharler, R., Obernberger, I. 2012. Effects of pyrolysis conditions on the heating rate in biomass particles and applicability of TGA kinetic parameters in particle thermal conversion modelling. *Fuel*, 93, 567-575.

- Meibod, M.P. 2013. Bio-oil from wheat straw and hydrogen from aqueous phase of bio-oil. in: Department of Chemical and Petroleum Engineering, Vol. Master of science, University of ALberta.
- Miller, P., Kumar, A. 2013. Development of emission parameters and net energy ratio for renewable diesel from Canola and Camelina. *Energy*, 58(Supplement C), 426-437.
- Miller, P., Kumar, A. 2014. Techno-economic assessment of hydrogenation-derived renewable diesel production from canola and camelina. *Sustainable Energy Technologies and Assessments*, 6, 105-115.
- Minerals, S.I. 2017. Industrial sands, available at <http://sil.ab.ca/sil-filter-sand/>. Accessed on 28th September 2017.
- Mishra, G., Kumar, J., Bhaskar, T. 2015. Kinetic studies on the pyrolysis of pinewood. *Bioresource technology*, 182, 282-288.
- Mittelbach, M. 1996. Diesel fuel derived from vegetable oils, VI: Specifications and quality control of biodiesel. *Bioresource Technology*, 56(1), 7-11.
- Morin, M., Pécate, S., Hémati, M., Kara, Y. 2016. Pyrolysis of biomass in a batch fluidized bed reactor: Effect of the pyrolysis conditions and the nature of the biomass on the physicochemical properties and the reactivity of char. *Journal of Analytical and Applied Pyrolysis*, 122, 511-523.
- Muktham, R., Ball, A.S., Bhargava, S.K., Bankupalli, S. 2016. Study of thermal behavior of deoiled karanja seed cake biomass: thermogravimetric analysis and pyrolysis kinetics. *Energy Science & Engineering*, 4(1), 86-95.
- Naik, S.N., Goud, V.V., Rout, P.K., Dalai, A.K. 2010. Production of first and second generation biofuels: A comprehensive review. *Renewable and Sustainable Energy Reviews*, 14(2), 578-597.
- Natural Resources Canada. 2014. The state of Canada's forests annual report, available at <http://cfs.nrcan.gc.ca/pubwarehouse/pdfs/35713.pdf>. Accessed on 17 August 2017.
- Natural Resources Canada. 2016a. Average retail fuel prices in calgary, available at [http://www2.nrcan.gc.ca/eneene/sources/pripri/prices\\_byfuel\\_e.cfm?locationName=Calgary#priceGraph](http://www2.nrcan.gc.ca/eneene/sources/pripri/prices_byfuel_e.cfm?locationName=Calgary#priceGraph). Accessed on 17 August 2017.
- Natural Resources Canada. 2016b. Daily Average Wholesale (Rack) Prices for Diesel (Rack) in 2014, available at

- [http://www2.nrcan.gc.ca/eneene/sources/pripri/wholesale\\_bycity\\_e.cfm?PriceYear=2014&ProductID=13&LocationID=66,8,39,17&Average=3&dummy=#PriceGraph](http://www2.nrcan.gc.ca/eneene/sources/pripri/wholesale_bycity_e.cfm?PriceYear=2014&ProductID=13&LocationID=66,8,39,17&Average=3&dummy=#PriceGraph). Accessed on 02 October 2017.
- Natural resources Canada. 2017. Diesel price, available at <http://www.nrcan.gc.ca/energy/fuel-prices/4797>. Accessed on 14th November 2017
- Natural Resources Canada. 2017. How much forest does Canada have?, available at <http://www.nrcan.gc.ca/forests/report/area/17601>. Accessed on 7 May 2018.
- Neste Oil. Neste Oil's renewable diesel plant in Rotterdam – the largest and most advanced in Europe,  
<https://www.google.ca/url?sa=t&rct=j&q=&esrc=s&source=web&cd=3&ved=0CD0QFjAC&url=http%3A%2F%2Fwww.nesteoil.com%2Fbinary.asp%3Fpath%3D1%3B41%3B540%3B2384%3B18010%3B18129%26field%3DFileAttachment&ei=Wh7CUrDDDdjm oASWjoKACQ&usg=AFQjCNEBIcF65ghlNNqdmHoFAk02aLRrQw&bvm=bv.58187178,d.cGU&cad=rja>. Accessed: September 2013.
- Neste Oil. Neste Oil's Singapore refinery – the world's largest and most advanced,  
[https://www.google.ca/url?sa=t&rct=j&q=&esrc=s&source=web&cd=4&ved=0CEMQFjAD&url=http%3A%2F%2Fwww.nesteoil.com%2Fbinary.asp%3Fpath%3D1%3B41%3B540%3B2384%3B18010%3B21058%26field%3DFileAttachment&ei=Wh7CUrDDDdjm oASWjoKACQ&usg=AFQjCNHCqV9a\\_uQc68FRDapb-1Ds89Yn3Q&bvm=bv.58187178,d.cGU&cad=rja](https://www.google.ca/url?sa=t&rct=j&q=&esrc=s&source=web&cd=4&ved=0CEMQFjAD&url=http%3A%2F%2Fwww.nesteoil.com%2Fbinary.asp%3Fpath%3D1%3B41%3B540%3B2384%3B18010%3B21058%26field%3DFileAttachment&ei=Wh7CUrDDDdjm oASWjoKACQ&usg=AFQjCNHCqV9a_uQc68FRDapb-1Ds89Yn3Q&bvm=bv.58187178,d.cGU&cad=rja). Accessed: September 2013.
- Neste Oil. Production Capacity,  
<http://www.nesteoil.com/default.asp?path=1,41,11991,22708,22720>. accessed: October 2013.
- Neste. 2016. Neste renewable diesel handbook, available at [https://www.neste.com/sites/default/files/attachments/neste\\_renewable\\_diesel\\_handbook.pdf](https://www.neste.com/sites/default/files/attachments/neste_renewable_diesel_handbook.pdf). Accessed on 7 May 2018.
- Newsome, D.S. 1980. The Water-Gas Shift Reaction. *Catalysis Reviews*, 21(2), 275-318.
- Öhgren, K., Bura, R., Lesnicki, G., Saddler, J., Zacchi, G. 2007. A comparison between simultaneous saccharification and fermentation and separate hydrolysis and fermentation using steam-pretreated corn stover. *Process Biochemistry*, 42(5), 834-839.

- Oyedun, A.O., Kumar, A., Oestreich, D., Arnold, U., Sauer, J. 2018. The development of the production cost of oxymethylene ethers as diesel additives from biomass. *Biofuels, Bioproducts and Biorefining*, 12(4), 694-710.
- Ozawa, T. 1965. A New Method of Analyzing Thermogravimetric Data. *Bulletin of the Chemical Society of Japan*, 38(11), 1881-+.
- Palma, M.A., Richardson, J.W., Roberson, B.E., Ribera, L.A., Outlaw, J., Munster, C. 2011. Economic feasibility of a mobile fast pyrolysis system for sustainable bio-crude oil production. *International Food and Agribusiness Management Review*, 14(3).
- Parikka, M. 2004. Global biomass fuel resources. *Biomass and Bioenergy*, 27(6), 613-620.
- Patel, M., Kumar, A. 2016. Production of renewable diesel through the hydroprocessing of lignocellulosic biomass-derived bio-oil: A review. *Renewable and Sustainable Energy Reviews*, 58, 1293-1307.
- Patel, M., Oyedun, A.O., Kumar, A., Gupta, R. 2018. A Techno-Economic Assessment of Renewable Diesel and Gasoline Production from Aspen Hardwood. *Waste and Biomass Valorization*.
- Patel, M., Zhang, X., Kumar, A. 2016. Techno-economic and life cycle assessment on lignocellulosic biomass thermochemical conversion technologies: A review. *Renewable and Sustainable Energy Reviews*, 53, 1486-1499.
- Peng, J., Chen, P., Lou, H., Zheng, X.M. 2008. Upgrading of bio-oil over aluminum silicate in supercritical ethanol. *Energy & Fuels*, 22(5), 3489-3492.
- Peters, J.F., Petrakopoulou, F., Dufour, J. 2014. Exergetic analysis of a fast pyrolysis process for bio-oil production. *Fuel Processing Technology*, 119(0), 245-255.
- Peters, M., Timmerhaus, K., West, R. 2003. *Plant Design and Economics for Chemical Engineers*. 5th ed. McGraw-Hill Education.
- Peters, M.S., Timmerhaus, K.L. 1991. *plant design and economics for chemical engineers*. fourth ed. McGraw-Hill, Inc.
- Pettersen, R.C. 1984. The chemical composition of wood. *The chemistry of solid wood*, 207, 57-126.
- Piskorz, J., Scott, D.S. 1987. The Composition of Oils Obtained by the Fast Pyrolysis of Different Woods. *Abstracts of Papers of the American Chemical Society*, 193, 58-Cell.
- Plus®, A. 2015. *Jump Start: Getting Started with Aspen Plus® V8.4*.

- Polat, S., Apaydin-Varol, E., Pütün, A.E. 2016. Thermal decomposition behavior of tobacco stem Part II: Kinetic analysis. *Energy Sources, Part A: Recovery, Utilization, and Environmental Effects*, 38(20), 3073-3080.
- Pootakham, T., Kumar, A. 2010. Bio-oil transport by pipeline: A techno-economic assessment. *Bioresource Technology*, 101(18), 7137-7143.
- Popoola, L.T., Adeoye, B.K., Grema, A.S., Yusuff, A.S., Adeyi, A.A. 2015. Process economic analysis of bio-oil production from wood residue using pyrolysis in South-Western Nigeria. *Journal of Applied Chemical Science International* 2(1), 12-23.
- Popov, A., Kondratieva, E., Goupil, J.M., Mariey, L., Bazin, P., Gilson, J.P., Travert, A., Mauge, F. 2010. Bio-oils hydrodeoxygenation: adsorption of phenolic molecules on oxidic catalyst supports. *Journal of Physical Chemistry C*, 114(37), 15661-15670.
- Quan, C., Gao, N., Song, Q. 2016. Pyrolysis of biomass components in a TGA and a fixed-bed reactor: Thermochemical behaviors, kinetics, and product characterization. *Journal of Analytical and Applied Pyrolysis*, 121(Supplement C), 84-92.
- Quintero, J.A., Montoya, M.I., Sánchez, O.J., Giraldo, O.H., Cardona, C.A. 2008. Fuel ethanol production from sugarcane and corn: Comparative analysis for a Colombian case. *Energy*, 33(3), 385-399.
- Richardson, A.D., Keenan, T.F., Migliavacca, M., Ryu, Y., Sonnentag, O., Toomey, M. 2013. Climate change, phenology, and phenological control of vegetation feedbacks to the climate system. *Agricultural and Forest Meteorology*, 169(0), 156-173.
- Ringer, M., Putsche, V., Scahill, J. 2006a. Large-Scale Pyrolysis Oil. Assessment.
- Ringer, M., Putsche, V., Scahill, J. 2006b. Large-scale pyrolysis oil production: A technology assessment and economic analysis. National renewable energy laboratory. NREL/TP-510-37779
- Rogers, J., Brammer, J. 2012. Estimation of the production cost of fast pyrolysis bio-oil. *Biomass and bioenergy*, 36, 208-217.
- Rogers, J.G., Brammer, J.G. 2012b. Estimation of the production cost of fast pyrolysis bio-oil. *Biomass and Bioenergy*, 36(0), 208-217.
- Romero, Y., Richard, F., Brunet, S. 2010. Hydrodeoxygenation of 2-ethylphenol as a model compound of bio-crude over sulfided Mo-based catalysts: Promoting effect and reaction mechanism. *Applied Catalysis B: Environmental*, 98(3-4), 213-223.

- Rosselló, T.M., Li, J., Lue, L. 2016. Kinetic models for biomass pyrolysis. *Archives of Industrial Biotechnology*, 1(1).
- Russell, J.A., Miller, R.K., Molton, P.M. 1983. Formation of aromatic compounds from condensation reactions of cellulose degradation products. *Biomass*, 3(1), 43-57.
- Salin, I.M., Seferis, J.C. 1993. Kinetic analysis of high-resolution TGA variable heating rate data. *Journal of Applied Polymer Science*, 47(5), 847-856.
- Sánchez, Ó.J., Cardona, C.A. 2008. Trends in biotechnological production of fuel ethanol from different feedstocks. *Bioresource Technology*, 99(13), 5270-5295.
- Saravanan, S., Nagarajan, G. 2014. Comparison of influencing factors of diesel with crude rice bran oil methyl ester in multi response optimization of NOx emission. *Ain Shams Engineering Journal*, 5(4), 1241-1248.
- Sarkar, S., Kumar, A. 2010. Large-scale biohydrogen production from bio-oil. *Bioresource Technology*, 101(19), 7350-7361.
- Senol, O.I., Viljava, T.R., Krause, A.O.I. 2005. Hydrodeoxygenation of aliphatic esters on sulphided NiMo/gamma-Al<sub>2</sub>O<sub>3</sub> and CoMo/gamma-Al<sub>2</sub>O<sub>3</sub> catalyst: The effect of water. *Catalysis Today*, 106(1-4), 186-189.
- Sepúlveda, C., Leiva, K., García, R., Radovic, L.R., Ghampson, I.T., DeSisto, W.J., Fierro, J.L.G., Escalona, N. 2011. Hydrodeoxygenation of 2-methoxyphenol over Mo<sub>2</sub>N catalysts supported on activated carbons. *Catalysis Today*, 172(1), 232-239.
- Serrano, C., Monedero, E., Lapuerta, M., Portero, H. 2011. Effect of moisture content, particle size and pine addition on quality parameters of barley straw pellets. *Fuel Processing Technology*, 92(3), 699-706.
- Shabangu, S., Woolf, D., Fisher, E.M., Angenent, L.T., Lehmann, J. 2014. Techno-economic assessment of biomass slow pyrolysis into different biochar and methanol concepts. *Fuel*, 117, 742-748.
- Shahrukh, H., Oyedun, A.O., Kumar, A., Ghiasi, B., Kumar, L., Sokhansanj, S. 2015. Net energy ratio for the production of steam pretreated biomass-based pellets. *Biomass and Bioenergy*, 80, 286-297.
- Shahrukh, H., Oyedun, A.O., Kumar, A., Ghiasi, B., Kumar, L., Sokhansanj, S. 2016. Comparative net energy ratio analysis of pellet produced from steam pretreated biomass from agricultural residues and energy crops. *Biomass and Bioenergy*, 90, 50-59.

- Shahrukh, H., Oyedun, A.O., Kumar, A., Ghiasi, B., Kumar, L., Sokhansanj, S. 2016. Techno-economic assessment of pellets produced from steam pretreated biomass feedstock. *Biomass and Bioenergy*, 87, 131-143.
- Shashikantha. 2008. Biomass – a substitute for fossil fuels?, available at [https://www.pssurvival.com/PS/Gasifiers/Biomass\\_A\\_Substitute\\_For\\_Fossil\\_Fuels\\_2008.pdf](https://www.pssurvival.com/PS/Gasifiers/Biomass_A_Substitute_For_Fossil_Fuels_2008.pdf).
- Shemfe, M.B., Gu, S., Ranganathan, P. 2015. Techno-economic performance analysis of biofuel production and miniature electric power generation from biomass fast pyrolysis and bio-oil upgrading. *Fuel*, 143, 361-372.
- Shen, J., Wang, X.-S., Garcia-Perez, M., Mourant, D., Rhodes, M.J., Li, C.-Z. 2009. Effects of particle size on the fast pyrolysis of oil mallee woody biomass. *Fuel*, 88(10), 1810-1817.
- Sheu, Y.-H.E., Anthony, R.G., Soltes, E.J. 1988. Kinetic studies of upgrading pine pyrolytic oil by hydrotreatment. *Fuel Processing Technology*, 19(1), 31-50.
- Sheu, Y.-H.E., Anthony, R.G., Soltes, E.J. 1988. Kinetic studies of upgrading pine pyrolytic oil by hydrotreatment. *Fuel Processing Technology*, 19(1), 31-50.
- Sil Industrial Minerals. 2016. Other industrial sands, available at <http://www.sil.ab.ca/>. Accessed on 17 August 2017.
- Siriwardhana, A. 2013. Aging and Stabilization of Pyrolytic Bio-Oils and Model Compounds.
- Slopiecka, K., Bartocci, P., Fantozzi, F. 2012. Thermogravimetric analysis and kinetic study of poplar wood pyrolysis. *Applied Energy*, 97, 491-497.
- Sokhansanj, S., Mani, S., Stumborg, M., Samson, R., Fenton, J. 2006. Production and distribution of cereal straw on the Canadian prairies. *Canadian Biosystems Engineering*, 48, 3.
- Solantausta, Y., Beckman, D., Bridgwater, A., Diebold, J., Elliott, D. 1992. Assessment of liquefaction and pyrolysis systems. *Biomass and Bioenergy*, 2(1-6), 279-297.
- Solantausta, Y., Beckman, D., Bridgwater, A.V., Diebold, J.P., Elliott, D.C. 1992. International Energy Agency Bioenergy Agreement Progress and Achievements 1989-1991 Assessment of liquefaction and pyrolysis systems. *Biomass and Bioenergy*, 2(1), 279-297.
- Sorenson, C.B. 2010. A comparative financial analysis of fast pyrolysis plants in Southwest Oregon.
- Soria-Verdugo, A., Morato-Godino, A., Garcia-Gutierrez, L.M., Garcia-Hernando, N. 2017. Pyrolysis of sewage sludge in a fixed and a bubbling fluidized bed – Estimation and

- experimental validation of the pyrolysis time. *Energy Conversion and Management*, 144, 235-242.
- Sun, Y., Cheng, J. 2002. Hydrolysis of lignocellulosic materials for ethanol production: a review. *Bioresource Technology*, 83(1), 1-11.
- Swanson, R.M., Platon, A., Satrio, J.A., Brown, R.C. 2010. Techno-economic analysis of biomass-to-liquids production based on gasification. *Fuel*, 89, Supplement 1(0), S11-S19.
- Syntroleum. Synthetic fuels technology for a clean future, <http://www.syntroleum.com/profiles/investor/fullpage.asp?BzID=2029&to=cp&Nav=0&LangID=1&s=0&ID=11912>. Accessed: October 2013.
- Tang, Z., Lu, Q., Zhang, Y., Zhu, X.F., Guo, Q.X. 2009. One Step Bio-Oil Upgrading through Hydrotreatment, Esterification, and Cracking. *Industrial & Engineering Chemistry Research*, 48(15), 6923-6929.
- The University of California Davis, The University of California Berkeley. California Renewable Diesel Multimedia Evaluation, [http://www.arb.ca.gov/fuels/multimedia/RenewableDieselTierI\\_DftFinal.pdf](http://www.arb.ca.gov/fuels/multimedia/RenewableDieselTierI_DftFinal.pdf). Accessed: October 2013.
- Thilakaratne, R., Brown, T., Li, Y., Hu, G., Brown, R. 2014. Mild catalytic pyrolysis of biomass for production of transportation fuels: a techno-economic analysis. *Green Chemistry*, 16(2), 627-636.
- Thompson, J.D., Klepac, J., Sprinkle, W. 2012. Trucking characteristics for an in-woods biomass chipping operation. *Proceedings of the 2012 Council on Forest Engineering Annual Meeting: Engineering New Solutions for Energy Supply and Demand*.
- Torri, I.D.V., Paasikallio, V., Faccini, C.S., Huff, R., Caramão, E.B., Sacon, V., Oasmaa, A., Zini, C.A. 2016. Bio-oil production of softwood and hardwood forest industry residues through fast and intermediate pyrolysis and its chromatographic characterization. *Bioresource Technology*, 200(Supplement C), 680-690.
- Trippe, F., Fröhling, M., Schultmann, F., Stahl, R., Henrich, E., Dalai, A. 2013. Comprehensive techno-economic assessment of dimethyl ether (DME) synthesis and Fischer–Tropsch synthesis as alternative process steps within biomass-to-liquid production. *Fuel Processing Technology*, 106(0), 577-586.

- Tsai, W.T., Lee, M.K., Chang, Y.M. 2007. Fast pyrolysis of rice husk: Product yields and compositions. *Bioresource Technology*, 98(1), 22-28.
- Tyson. Welcome to Tyson Renewable Energy, <http://renewableenergy.tyson.com/>. Accessed: October 2013.
- United Nations. 2018. National greenhouse gas inventory data for the period 1990–2015, available at <https://unfccc.int/sites/default/files/resource/docs/2017/sbi/eng/18.pdf>. Accessed on 15 October 2018.
- United States Environmental Protection Agency. Renewable fuels: regulations & standards, <http://www.epa.gov/otaq/fuels/renewablefuels/regulations.htm>. Accessed: October 2013.
- Várhegyi, G., Antal, M.J., Jakab, E., Szabó, P. 1997. Kinetic modeling of biomass pyrolysis. *Journal of Analytical and Applied Pyrolysis*, 42(1), 73-87.
- Varma, A.K., Mondal, P. 2016. Physicochemical characterization and pyrolysis kinetic study of sugarcane bagasse using thermogravimetric analysis. *Journal of Energy Resources Technology*, 138(5), 052205.
- Venderbosch, R.H., Ardiyanti, A.R., Wildschut, J., Oasmaa, A., Heeresb, H.J. 2010. Stabilization of biomass-derived pyrolysis oils. *Journal of Chemical Technology and Biotechnology*, 85(5), 674-686.
- Venkatesh, M., Ravi, P., Tewari, S.P. 2013. Isoconversional Kinetic Analysis of Decomposition of Nitroimidazoles: Friedman method vs Flynn-Wall-Ozawa Method. *Journal of Physical Chemistry A*, 117(40), 10162-10169.
- Verma, P., Sharma, M.P., Dwivedi, G. 2016. Impact of alcohol on biodiesel production and properties. *Renewable and Sustainable Energy Reviews*, 56, 319-333.
- Vosesoftware. 2015. Model Risk, Monte Carlo Simulation, available at <http://www.vosesoftware.com/contactus.php>.
- VoseSoftware. 2018. Model Risk – Monte Carlo Simulation, available at <https://www.vosesoftware.com/index.php>. Accessed on 12 February 2018.
- VTT Technical Research Centre of Finland. Stability of fast pyrolysis bio-oils and upgraded products, <http://www.gastechnology.org/tcbiomass2013/tcb2013/04-Oasmaa-tcbiomass2013-presentation-Thur.pdf>, Accessed: October 2013.
- Vyazovkin, S., Wight, C.A. 1999. Model-free and model-fitting approaches to kinetic analysis of isothermal and nonisothermal data. *Thermochimica Acta*, 340-341(Supplement C), 53-68.

- Wang, X., Kersten, S.R., Prins, W., van Swaaij, W.P. 2005. Biomass pyrolysis in a fluidized bed reactor. Part 2: Experimental validation of model results. *Industrial & engineering chemistry research*, 44(23), 8786-8795.
- Wang, Y., He, T., Liu, K., Wu, J., Fang, Y. 2012. From biomass to advanced bio-fuel by catalytic pyrolysis/hydro-processing: Hydrodeoxygenation of bio-oil derived from biomass catalytic pyrolysis. *Bioresource Technology*, 108(0), 280-284.
- Ward, J.W. 1993. Hydrocracking processes and catalysts. *Fuel Processing Technology*, 35(1-2), 55-85.
- Warnecke, R. 2000. Gasification of biomass: comparison of fixed bed and fluidized bed gasifier. *Biomass and Bioenergy*, 18(6), 489-497.
- Wen, C., Yu, Y. 1966. A generalized method for predicting the minimum fluidization velocity. *AIChE Journal*, 12(3), 610-612.
- Wildschut, J., Arentz, J., Rasrendra, C.B., Venderbosch, R.H., Heeres, H.J. 2009a. Catalytic hydrotreatment of fast pyrolysis oil: Model studies on reaction pathways for the carbohydrate fraction. *Environmental Progress and Sustainable Energy*, 28(3), 450-460.
- Wildschut, J., Iqbal, M., Mahfud, F.H., Melian-Cabrera, I., Venderbosch, R.H., Heeres, H.J. 2010a. Insights in the hydrotreatment of fast pyrolysis oil using a ruthenium on carbon catalyst. *Energy & Environmental Science*, 3(7), 962-970.
- Wildschut, J., Mahfud, F.H., Venderbosch, R.H., Heeres, H.J. 2009. Hydrotreatment of fast pyrolysis oil using heterogeneous noble-metal catalysts. *Industrial & Engineering Chemistry Research*, 48(23), 10324-10334.
- Wildschut, J., Melian-Cabrera, I., Heeres, H.J. 2010b. Catalyst studies on the hydrotreatment of fast pyrolysis oil. *Applied Catalysis B-Environmental*, 99(1-2), 298-306.
- Wong, A., Zhang, H., Kumar, A. 2016. Life cycle assessment of renewable diesel production from lignocellulosic biomass. *The International Journal of Life Cycle Assessment*, 21(10), 1404-1424.
- World Energy Council. 2017. World energy resources bioenergy 2016, available at [https://www.worldenergy.org/wp-content/uploads/2017/03/WEResources\\_Bioenergy\\_2016.pdf](https://www.worldenergy.org/wp-content/uploads/2017/03/WEResources_Bioenergy_2016.pdf). Accessed on 29 July 2017.

- Wright, M.M., Brown, R.C., Boateng, A.A. 2008. Distributed processing of biomass to bio- oil for subsequent production of Fischer- Tropsch liquids. *Biofuels, bioproducts and biorefining*, 2(3), 229-238.
- Wright, M.M., Dugaard, D.E., Satrio, J.A., Brown, R.C. 2010. Techno-economic analysis of biomass fast pyrolysis to transportation fuels. *Fuel*, 89, S2-S10.
- Wu, W.X., Mei, Y.F., Zhang, L., Liu, R.H., Cai, J.M. 2014. Effective Activation Energies of Lignocellulosic Biomass Pyrolysis. *Energy & Fuels*, 28(6), 3916-3923.
- Yaman, S. 2004. Pyrolysis of biomass to produce fuels and chemical feedstocks. *Energy Conversion and Management*, 45(5), 651-671.
- Yang, Y., Gilbert, A., Xu, C. 2009. Hydrodeoxygenation of bio-crude in supercritical hexane with sulfided CoMo and CoMoP catalysts supported on MgO: A model compound study using phenol. *Applied Catalysis A: General*, 360(2), 242-249.
- Yao, F., Wu, Q., Lei, Y., Guo, W., Xu, Y. 2008. Thermal decomposition kinetics of natural fibers: Activation energy with dynamic thermogravimetric analysis. *Polymer Degradation and Stability*, 93(1), 90-98.
- Yildiz, S., Gezer, E.D., Yildiz, U.C. 2006. Mechanical and chemical behavior of spruce wood modified by heat. *Building and Environment*, 41(12), 1762-1766.
- Yoshimura, Y., Sato, T., Shimada, H., Matsubayashi, N., Nishijima, A. 1991. Influences of oxygen-containing substances on deactivation of sulfided molybdate catalysts. *Applied Catalysis*, 73(1), 55-63.
- Zhang, H., Shao, S., Jiang, Y., Vitidsant, T., Reubroycharoen, P., Xiao, R. 2017. Improving hydrocarbon yield by two-step pyrolysis of pinewood in a fluidized-bed reactor. *Fuel Processing Technology*, 159, 19-26.
- Zhang, Q., Chang, J., Wang, T., Xu, Y. 2007. Review of biomass pyrolysis oil properties and upgrading research. *Energy Conversion and Management*, 48(1), 87-92.
- Zhang, S., Yan, Y., Li, T., Ren, Z. 2005. Upgrading of liquid fuel from the pyrolysis of biomass. *Bioresource Technology*, 96(5), 545-550.
- Zhang, S.P., Yan, Y.J., Ren, J.W., Li, T.C. 2003. Study of hydrodeoxygenation of bio-oil from the fast pyrolysis of biomass. *Energy Sources*, 25(1), 57-65.
- Zhang, Y., Brown, T.R., Hu, G., Brown, R.C. 2013. Techno-economic analysis of two bio-oil upgrading pathways. *Chemical Engineering Journal*, 225, 895-904.

- Zhao, C., He, J., Lemonidou, A.A., Li, X., Lercher, J.A. 2011. Aqueous-phase hydrodeoxygenation of bio-derived phenols to cycloalkanes. *Journal of Catalysis*, 280(1), 8-16.
- Zhu, Y., Albrecht, K.O., Elliott, D.C., Hallen, R.T., Jones, S.B. 2013. Development of hydrothermal liquefaction and upgrading technologies for lipid-extracted algae conversion to liquid fuels. *Algal Research*, 2(4), 455-464.
- Zhu, Y., Bidy, M.J., Jones, S.B., Elliott, D.C., Schmidt, A.J. 2014. Techno-economic analysis of liquid fuel production from woody biomass via hydrothermal liquefaction (HTL) and upgrading. *Applied Energy*, 129(Supplement C), 384-394.
- Zhu, Z., Sathitsuksanoh, N., Vinzant, T., Schell, D.J., McMillan, J.D., Zhang, Y.H.P. 2009. Comparative study of corn stover pretreated by dilute acid and cellulose solvent- based lignocellulose fractionation: Enzymatic hydrolysis, supramolecular structure, and substrate accessibility. *Biotechnology and bioengineering*, 103(4), 715-724.

# Appendix A

## Material and energy balance for fast pyrolysis and hydroprocessing technology

**Table A1: Stream table for fast pyrolysis and hydroprocessing technology**

	BIOC HAR	BIOM ASS	BIO- OIL	DIES EL	GASOL INE	GASES OUT	WASTE WATER	WATER OUT
Mass Flow kg/hr								
BIOMASS	0	166666	0	0	0	0	0	0
WATER	0	0	15738	0	0	0	24366	69542
CO	0	0	0	0	0	7344	0	0
H2	0	0	0	0	0	336	0	0
ETHANE	0	0	0	0	0	0	0	0
PROPANE	0	0	0	0	0	430	0	0
BUTANE	0	0	0	0	558	21	0	0
METHANE	0	0	0	0	0	413	0	0
CO2	0	0	0	0	0	9380	3	0
CHAR	16589	0	0	0	0	0	0	0
MEHEXANE	0	0	2717	0	0	0	0	0
SQUARIC	0	0	2025	0	0	0	0	0
BENTRIOL	0	0	1500	0	0	0	0	0
MEPHENOL	0	0	2497	0	0	0	0	0
BENZOIC	0	0	2077	0	0	0	0	0
VINYLPHE	0	0	2161	0	0	0	0	0
SYRINGOL	0	0	8708	0	0	0	0	0
C8H8N2O3	0	0	91	0	0	0	0	0
C11H14O4	0	0	923	0	0	0	0	0
DIMEPROP	0	0	112	0	0	0	0	0
ISOEUGEN	0	0	3106	0	0	0	0	0
VANILLIN	0	0	3295	0	0	0	0	0
PHENOL	0	0	8740	0	0	0	0	0
GUAIACOL	0	0	8918	0	0	0	0	0
HEXANE	0	0	0	0	823	0	0	0
2,3,3-TRIMETHYL-1- BUTENE	0	0	0	0	104	0	0	0
2,3,3-TRIMETHYL-1- BUTENE	0	0	0	783	975	0	0	0
N-BUTYLCYCLOHEXANE	0	0	0	135	86	0	0	0
1-METHYL-2- ETHYLBENZENE	0	0	0	1189	1018	0	0	0
DECALIN	0	0	0	1367	494	0	0	0
2,6- DIMETHYLNAPHTHALENE	0	0	0	4535	251	0	0	0

	<b>BIOC HAR</b>	<b>BIOM ASS</b>	<b>BIO- OIL</b>	<b>DIES EL</b>	<b>GASOL INE</b>	<b>GASES OUT</b>	<b>WASTE WATER</b>	<b>WATER OUT</b>
1,2,4-TRIETHYLBENZENE	0	0	0	2388	453	0	0	0
BICYCLOHEXYL	0	0	0	239	28	0	0	0
DIPHENYL	0	0	0	2540	257	0	0	0
DIAMANTANE	0	0	0	791	97	0	0	0
PHENANTHRENE	0	0	0	2159	16	0	0	0
N-DECYLCYCLOPENTANE	0	0	0	339	17	0	0	0
1,2,3,4- TETRAHYDRONAPHTHALE NE	0	0	0	351	93	0	0	0
P-XYLENE	0	0	0	138	100	0	0	0
1-TRANS-3,5- TRIMETHYLCYCLOHEXAN E	0	0	0	1642	3013	0	0	0
METHYLCYCLOHEXANE	0	0	0	11	4021	0	0	0
<b>Total Flow kg/hr</b>	<b>16589</b>	<b>166666</b>	<b>62610</b>	<b>18605</b>	<b>12404</b>	<b>17924</b>	<b>24370</b>	<b>69542</b>
Temperature C	480		19.99	202.4	163.785	19.9995		
Pressure bar	1.013	1.0132	5	2	1.08	1.082	1	172
Enthalpy kcal/kg	123.584		1437.	9.334	259.559			
			78	041	8	-1501.69	-3791.055	3841.913

**Table A2: Summary of discounted cashflow of 2000 dry t d<sup>-1</sup> renewable diesel plant**

Year	-3	-2	-1	0	1	2	3	4	5	6	7	8	9	10
<b>Capital Cost (\$)</b>	8.45E+07	1.48E+08	1.90E+08											
<b>Raw Material Cost (\$)</b>				1.25E+08	1.04E+08	1.08E+08	1.12E+08	1.16E+08	1.20E+08	1.24E+08	1.28E+08	1.33E+08	1.37E+08	1.42E+08
<b>Operating Labor Cost (\$)</b>				8.42E+06	8.67E+06	8.93E+06	9.20E+06	9.48E+06	9.76E+06	1.01E+07	1.04E+07	1.07E+07	1.10E+07	1.13E+07
<b>Maintenance Cost (\$)</b>				1.27E+07	1.31E+07	1.35E+07	1.39E+07	1.43E+07	1.47E+07	1.51E+07	1.56E+07	1.61E+07	1.65E+07	1.70E+07
<b>Utilities (\$)</b>				1.12E+07	1.15E+07	1.19E+07	1.22E+07	1.26E+07	1.30E+07	1.34E+07	1.38E+07	1.42E+07	1.46E+07	1.51E+07
<b>Operating Charges (\$)</b>				2.10E+06	2.17E+06	2.23E+06	2.30E+06	2.37E+06	2.44E+06	2.51E+06	2.59E+06	2.67E+06	2.75E+06	2.83E+06
<b>Plant Overhead (\$)</b>				1.06E+07	1.09E+07	1.12E+07	1.15E+07	1.19E+07	1.22E+07	1.26E+07	1.30E+07	1.34E+07	1.38E+07	1.42E+07
<b>G and A Cost (\$)</b>				1.36E+07	1.21E+07	1.25E+07	1.29E+07	1.34E+07	1.38E+07	1.43E+07	1.48E+07	1.54E+07	1.59E+07	1.64E+07
<b>Waste Water Cost (\$)</b>				1.42E+03	1.46E+03	1.51E+03	1.55E+03	1.60E+03	1.65E+03	1.70E+03	1.75E+03	1.80E+03	1.85E+03	1.91E+03
<b>Camping Cost (\$)</b>				1.27E+07	1.33E+07	1.40E+07	1.47E+07	1.54E+07	1.62E+07	1.70E+07	1.78E+07	1.87E+07	1.97E+07	2.07E+07
<b>Product Revenue (\$)</b>				2.47E+08	2.07E+08	1.94E+08	2.04E+08	2.14E+08	2.25E+08	2.36E+08	2.48E+08	2.60E+08	2.74E+08	2.87E+08
<b>Net Revenue (\$)</b>	-8.45E+07	-1.48E+08	-1.90E+08	5.09E+07	3.14E+07	1.23E+07	1.56E+07	1.93E+07	2.32E+07	2.74E+07	3.19E+07	3.68E+07	4.19E+07	4.75E+07
<b>Present Value for 10% return (\$)</b>	-1.13E+08	-1.79E+08	-2.09E+08	5.09E+07	2.86E+07	1.01E+07	1.17E+07	1.32E+07	1.44E+07	1.55E+07	1.64E+07	1.71E+07	1.78E+07	1.83E+07
<b>Diesel cost (\$/L)</b>				0.99	1.00	1.02	1.05	1.07	1.09	1.11	1.13	1.15	1.18	1.20
<b>Gasoline cost (\$/L)</b>				0.94	0.95	0.97	0.99	1.01	1.03	1.05	1.07	1.10	1.12	1.14

**Table A2: Summary of discounted cashflow of 2000 dry t d<sup>-1</sup> renewable diesel plant (Contd..)**

<b>Year</b>	<b>11</b>	<b>12</b>	<b>13</b>	<b>14</b>	<b>15</b>	<b>16</b>	<b>17</b>	<b>18</b>	<b>19</b>
<b>Capital Cost (\$)</b>									
<b>Raw Material Cost (\$)</b>	1.47E+08	1.52E+08	1.58E+08	1.63E+08	1.69E+08	1.75E+08	1.81E+08	1.87E+08	1.94E+08
<b>Operating Labor Cost (\$)</b>	1.17E+07	1.20E+07	1.24E+07	1.27E+07	1.31E+07	1.35E+07	1.39E+07	1.43E+07	1.48E+07
<b>Maintenance Cost (\$)</b>	1.76E+07	1.81E+07	1.86E+07	1.92E+07	1.98E+07	2.03E+07	2.10E+07	2.16E+07	2.22E+07
<b>Utilities (\$)</b>	1.55E+07	1.60E+07	1.64E+07	1.69E+07	1.74E+07	1.80E+07	1.85E+07	1.91E+07	1.96E+07
<b>Operating Charges (\$)</b>	2.91E+06	3.00E+06	3.09E+06	3.18E+06	3.28E+06	3.38E+06	3.48E+06	3.58E+06	3.69E+06
<b>Plant Overhead (\$)</b>	1.46E+07	1.50E+07	1.55E+07	1.60E+07	1.64E+07	1.69E+07	1.74E+07	1.80E+07	1.85E+07
<b>G and A Cost (\$)</b>	1.70E+07	1.76E+07	1.82E+07	1.89E+07	1.95E+07	2.02E+07	2.09E+07	2.17E+07	2.24E+07
<b>Waste Water Cost (\$)</b>	1.97E+03	2.02E+03	2.09E+03	2.15E+03	2.21E+03	2.28E+03	2.35E+03	2.42E+03	2.49E+03
<b>Camping Cost (\$)</b>	2.17E+07	2.28E+07	2.39E+07	2.51E+07	2.64E+07	2.77E+07	2.91E+07	3.05E+07	3.20E+07
<b>Product Revenue (\$)</b>	3.02E+08	3.17E+08	3.32E+08	3.49E+08	3.67E+08	3.85E+08	4.04E+08	4.24E+08	4.46E+08
<b>Net Revenue (\$)</b>	5.35E+07	5.99E+07	6.67E+07	7.40E+07	8.18E+07	9.01E+07	9.90E+07	1.08E+08	1.18E+08
<b>Present Value for 10% return (\$)</b>	1.87E+07	1.91E+07	1.93E+07	1.95E+07	1.96E+07	1.96E+07	1.96E+07	1.95E+07	1.94E+07
<b>Diesel cost (\$/L)</b>	1.22	1.25	1.27	1.30	1.33	1.35	1.38	1.41	1.43
<b>Gasoline cost (\$/L)</b>	1.16	1.19	1.21	1.23	1.26	1.28	1.31	1.34	1.36

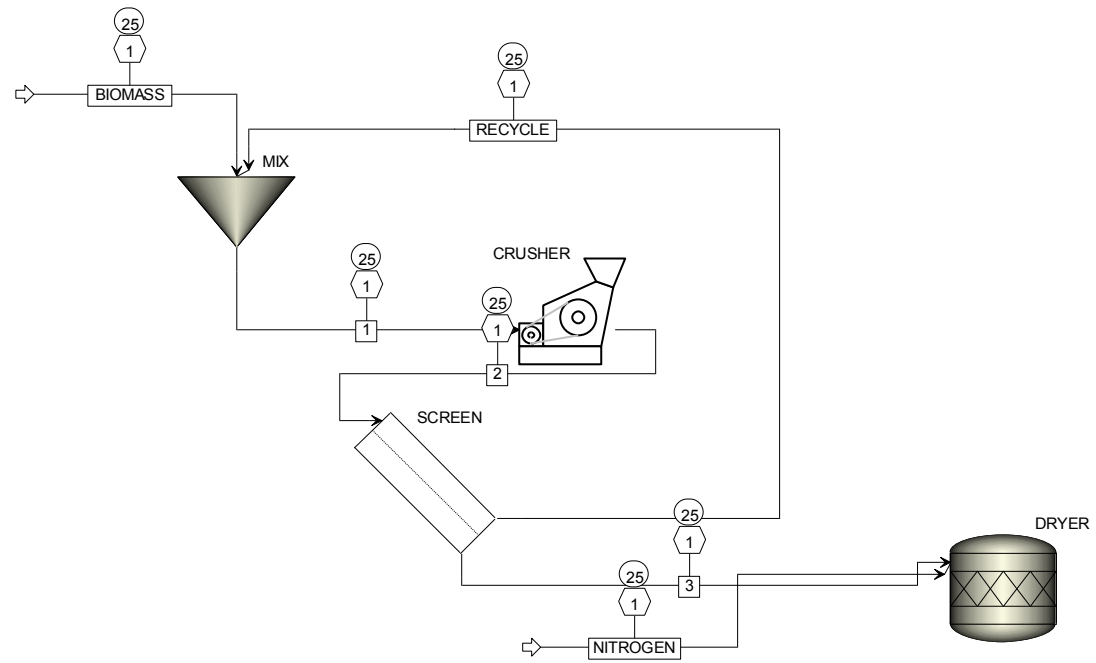


**Figure A1: Aspen Plus® flow sheet for biomass pretreatment**

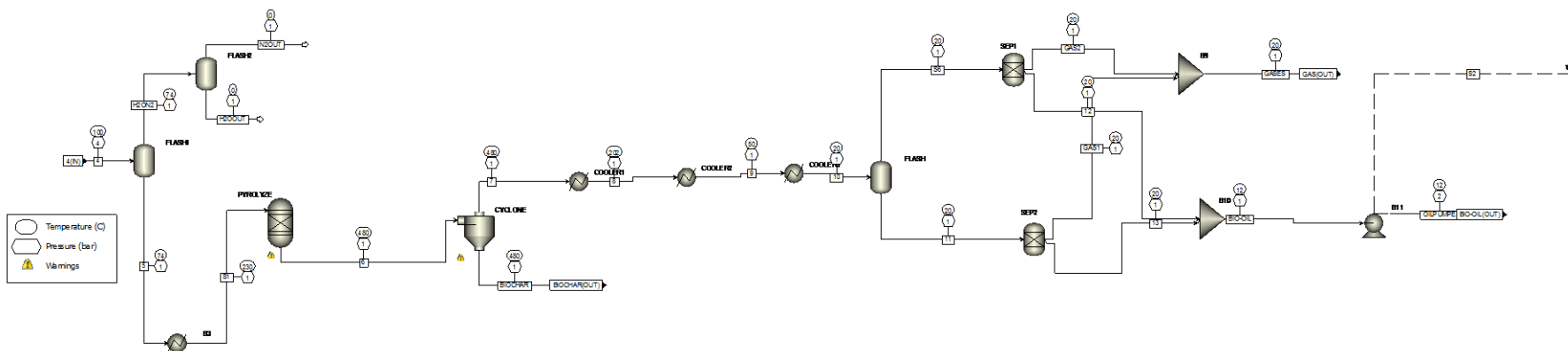


Figure A2: Aspen Plus® flow sheet for biomass pyrolysis

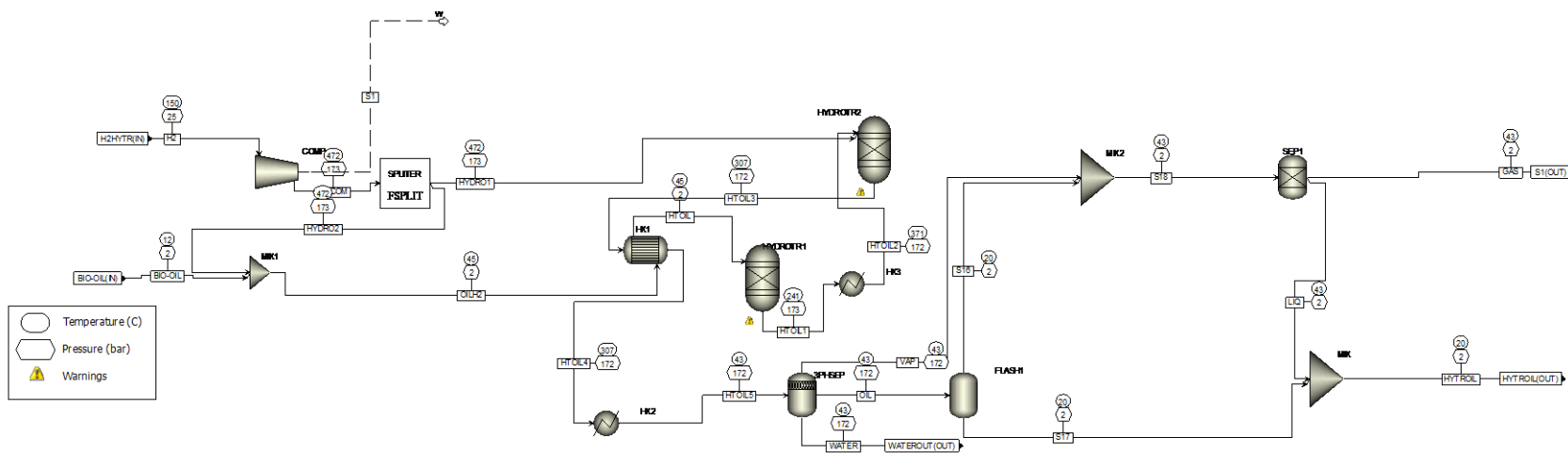


Figure A3: Aspen Plus® flow sheet for hydrotreating of bio-oil

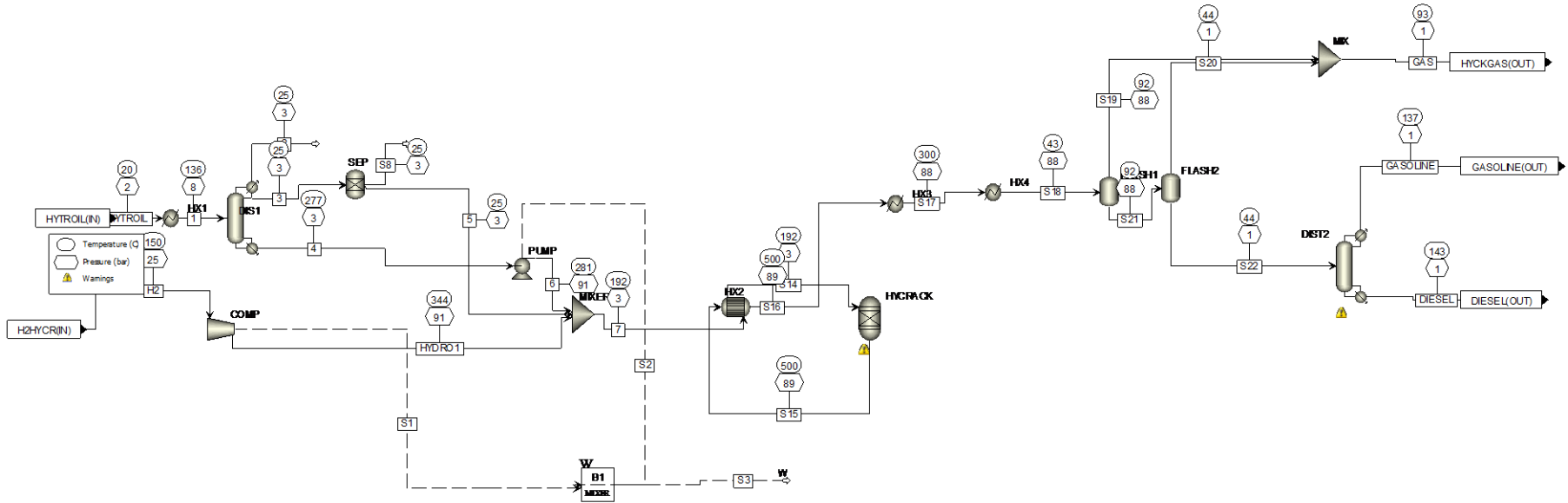
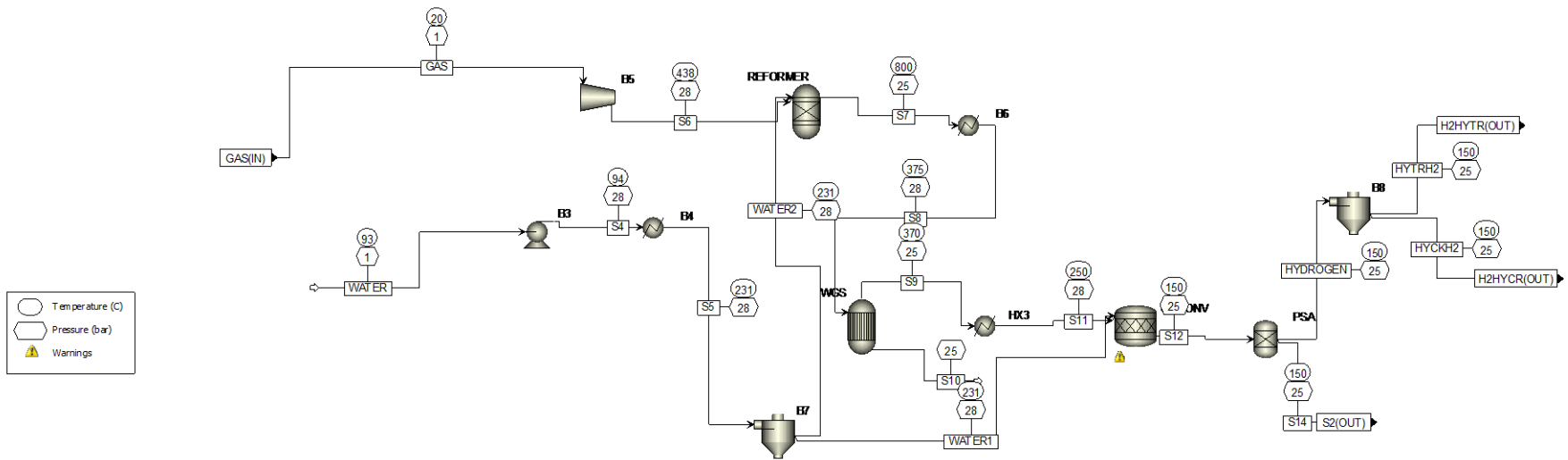


Figure A4: Aspen Plus® flow sheet for hydrocracking and fractionation unit to produce diesel and gasoline



**Figure A5: Aspen Plus® flow sheet for reforming unit**

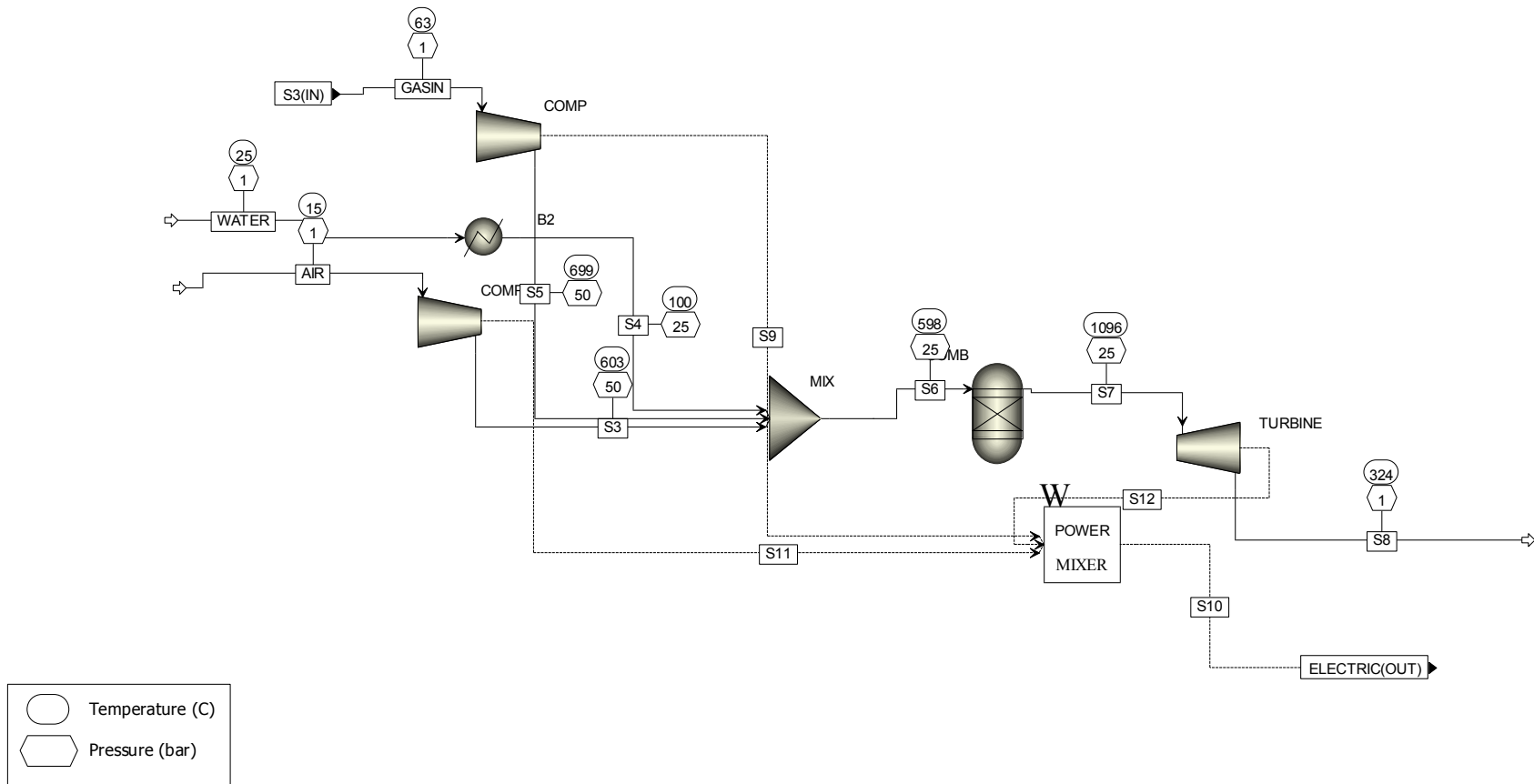


Figure A6: Aspen Plus® flow sheet for electricity generation unit

## Appendix B

Derivation for:

### Scenario 1: Truncated

Calculation of angle  $\phi$ :

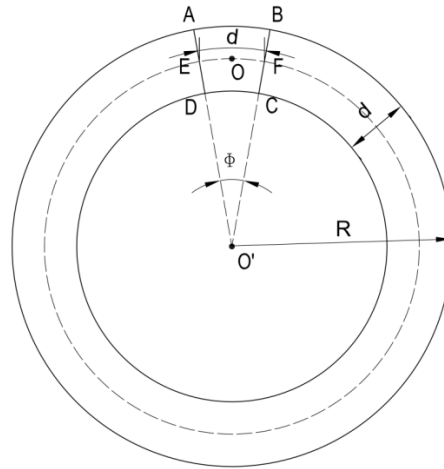


**Figure B1: Truncated scenario**

The perimeter of the dotted circle is given by Equation (B1):

$$P = 2\pi * \left(R - \frac{d}{2}\right) \quad (B1)$$

The perimeter  $P$  creates an angle  $2\pi$  at the center. So, angle  $\phi$  (radian) is estimated by Equation (B2):

$$\phi = 2\pi * \left(\frac{d}{P}\right) = 2\pi * \frac{d}{2\pi \left(R - \frac{d}{2}\right)} \quad (\text{B2})$$

$$= \frac{d}{\left(R - \frac{d}{2}\right)} = \frac{d}{\left(R_0 + \frac{d}{2}\right)}$$

where  $R = \left(R - \frac{d}{2}\right) = \left(R_0 + \frac{d}{2}\right)$  as shown in the Figure B3

The area of the ring created by R and R-d is  $A_d$  as represented by Equation (B3)

$$A_d = \pi R^2 - \pi(R - d)^2 = 2\pi R d - \pi d^2 \quad (\text{B3})$$

The area of segment ABFCED is  $A_s$  (Figure B1) and is given in Equation (B4)

$$A_s = \frac{A_d \phi}{2\pi} = \frac{2\pi R d - \pi d^2}{2\pi} * \frac{d}{\left(R - \frac{d}{2}\right)} = d^2 \quad (\text{B4})$$

### **Bio-oil transportation distance**

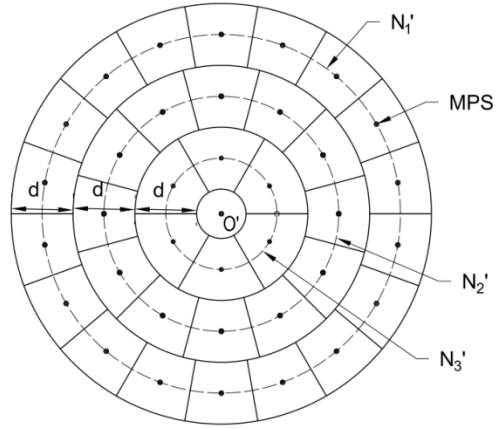


**Figure B2: Bio-oil transportation distance in truncated scenario**

The number of all truncated segments in the 1<sup>st</sup> ring can be calculated using Equation (B5).

$$N_1' = \frac{\text{Perimeter of dotted circle } N_1'}{d} \quad (\text{B5})$$

$$= \frac{2\pi \left( R - \frac{d}{2} \right)}{d}$$

The number of all truncated segments in the 2<sup>nd</sup> ring can be calculated by using Equation (B6).

$$N_2' = \frac{\text{Perimeter of dotted circle } N_2'}{d} \quad (\text{B6})$$

$$= \frac{2\pi \left( R - \frac{3d}{2} \right)}{d}$$

The bio-oil transportation distance for all truncated segments located in the 1<sup>st</sup> ring can be calculated by using Equation (B7).

$$D_1 = N'_1 * \left(R - \frac{d}{2}\right) = \frac{2\pi \left(R - \frac{d}{2}\right)}{d} * \left(R - \frac{d}{2}\right) \quad (\text{B7})$$

$$= \frac{2\pi \left(R - \frac{d}{2}\right)^2}{d}$$

The bio-oil transportation distance for the d squares located in the 2<sup>nd</sup> ring can be calculated by using Equation (B8)

$$D_2 = N'_2 * \left(R - \frac{3d}{2}\right) = \frac{2\pi \left(R - \frac{3d}{2}\right)}{d} * \left(R - \frac{3d}{2}\right) \quad (\text{B8})$$

$$= \frac{2\pi \left(R - \frac{3d}{2}\right)^2}{d}$$

## Biomass transportation distance

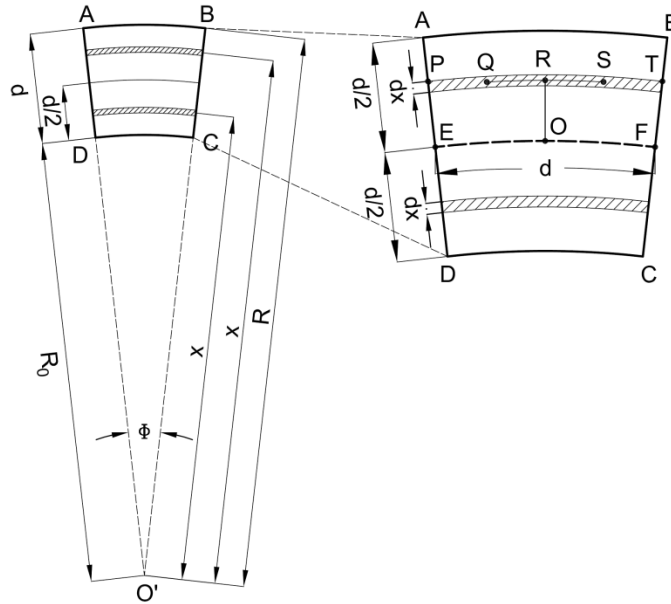


**Figure B3: Biomass transportation distance in truncated scenario**

For the small area  $dx$  in the first segment,  $ABFE$  (outer arc to MPS), the distance travelled by the truck to transport the biomass to the MPS unit is calculated by Equation (B9):

$$\text{Biomass transportation distance by truck} = d_1 \quad (\text{B9})$$

$$= (QR + RO) + (SR + RO) = 2 * (QR + RO)$$

$$= 2 * \left[ \left( x * \frac{\phi}{4} \right) + \left( x - R_0 - \frac{d}{2} \right) \right]$$

$$= 2 * \left[ \left( \frac{d}{(R_0 + \frac{d}{2})} * \frac{x}{4} \right) + \left( x - R_0 - \frac{d}{2} \right) \right]$$

For the small area  $dx$  in the second segment,  $EFCD$  (MPS to inside arc) the path followed by the truck to transport the biomass to the MPS unit is calculated by Equation (B10):

$$\text{Biomass transportation distance by truck} = d_2 \quad (\text{B10})$$

$$= 2 * \left[ \left( \frac{d}{\left(R_0 + \frac{d}{2}\right)} * \frac{x}{4} \right) + \left( R_0 + \frac{d}{2} - x \right) \right]$$

The area of the small strip  $dx$  is given in Equation (B11):

$$dA = (PR + RT)dx = 2 * PR * dx = 2 * \frac{\phi}{2} * x * dx = \frac{d}{\left(R_0 + \frac{d}{2}\right)} * x * dx \quad (11)$$

The truck capacity for biomass transportation is 20 green tonnes per trip and a yield of 84 dry tonnes of forest biomass is assumed. The area required to collect biomass for one trip is estimated with Equation (B12) and the number of trips required to deliver the biomass is given in Equation (B13).

$$\text{Area required for each truck trip} = \frac{\text{Capacity of truck}}{\text{Whole tree yield}} = \frac{10 \text{ ha}}{84 \text{ trip}} \quad (\text{B12})$$

$$\text{Number of truck trips required for the area} = \frac{dA}{10/84} \quad (\text{B13})$$

$$= \frac{84 dA}{10} \text{ trip/ha}$$

The total distance travelled by truck and the number of trips for the area  $dA$  in segments 1 and 2 are given in Equation (B14) and Equation (B15), respectively.

$$dd_1 = \frac{84 dA}{10} * 2 * \left[ \left( \frac{d}{\left(R_0 + \frac{d}{2}\right)} * \frac{x}{4} \right) + \left( x - R_0 - \frac{d}{2} \right) \right] \quad (\text{B14})$$

$$= 2 * \frac{84}{10} * \left[ \left( \frac{d}{\left(R_0 + \frac{d}{2}\right)} * \frac{x}{4} \right) + \left( x - R_0 - \frac{d}{2} \right) \right] * \frac{d}{\left(R_0 + \frac{d}{2}\right)} * x dx$$

$$dd_2 = 2 * \frac{84}{10} * \left[ \left( \frac{d}{\left(R_0 + \frac{d}{2}\right)} * \frac{x}{4} \right) + \left( R_0 + \frac{d}{2} - x \right) \right] * \frac{d}{\left(R_0 + \frac{d}{2}\right)} * x dx \quad (\text{B15})$$

To calculate the average biomass transportation distance for the whole area  $AMBCND$ , Eqn. (14) and Eqn. (15) are integrated from  $R_0+d/2$  to  $R_0+d$  and  $R_0$  to  $R_0+d/2$ , respectively. The total average distance travelled by truck can be estimated by summing the two integrations, which are estimated in Equation (B16).

(B16)

$$\begin{aligned}
D &= \int_{R_0+\frac{d}{2}}^{R_0+d} dd_1 + \int_{R_0}^{R_0+\frac{d}{2}} dd_2 \\
&= \left[ \int_{R_0+\frac{d}{2}}^{R_0+d} 2 * \frac{84}{10} * \left[ \left( \frac{d}{R_0+\frac{d}{2}} * \frac{x}{4} \right) + \left( x - R_0 - \frac{d}{2} \right) * \frac{d}{R_0+\frac{d}{2}} * x dx \right] \right. \\
&\quad \left. + \left[ \int_{R_0}^{R_0+\frac{d}{2}} 2 * \frac{84}{10} * \left[ \left( \frac{d}{R_0+\frac{d}{2}} * \frac{x}{4} \right) + \left( R_0 + \frac{d}{2} - x \right) * \frac{d}{R_0+\frac{d}{2}} * x dx \right] \right] \right] \\
&\Rightarrow D \\
&= \left[ \frac{7d^3(6d^2 + 17dR_0 + 12R_0^2)}{5(d + 2R_0)^2} \right] \\
&\quad + \left[ \frac{7d^5}{10(d + 2R_0)^2} + \frac{7d^4}{10(d + 2R_0)} + \frac{21d^4R_0}{5(d + 2R_0)^2} \right. \\
&\quad \left. + \frac{42d^3R_0^2}{5(d + 2R_0)^2} + \frac{63d^3R_0}{5(d + 2R_0)} + \frac{84d^2R_0^2}{5(d + 2R_0)} - \frac{42d^2R_0}{5} \right] \\
&\Rightarrow D = \frac{7d^3}{10(d + 2R_0)^2} [13d^2 + 40dR_0 + 36R_0^2] + \frac{7d^3}{5(d + 2R_0)} \left[ \frac{d}{2} + 3R_0 \right]
\end{aligned}$$

## Scenario 2: Radial scenario

### Biomass transportation distance

For the small area  $dr$  in the first segment (from the center to the centroid), the distance travelled by the truck to transport the biomass to the MPS unit is calculated by Equation (B17):

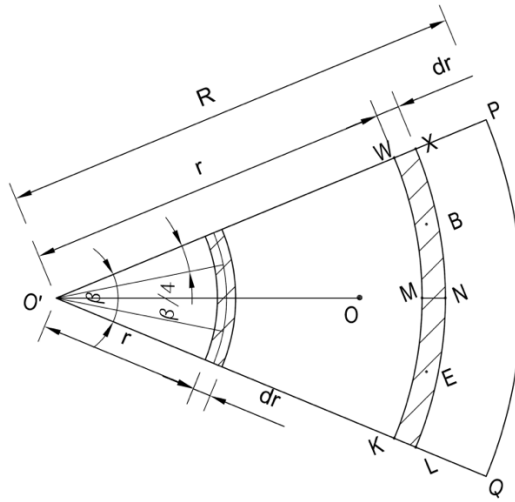


**Figure B4: Biomass transportation distance in radial scenario**

$$\text{Biomass transportation distance by truck} = d_1 \quad (\text{B17})$$

$$= (BN + NO) + (EN + NO) = 2 * (BN + NO)$$

$$= 2 * \left[ \left( r * \frac{\beta}{4} \right) + (r - R') \right]$$

For the small area  $dr$  in the second segment (from the centroid to the end of the arc), the path followed by the truck to transport the biomass to the MPS unit is calculated by Equation (B18):

$$\text{Biomass transportation distance by truck} = d_2 \quad (\text{B18})$$

$$= 2 * \left[ \left( r * \frac{\beta}{4} \right) + (R' - r) \right]$$

The area of the small strip  $dr$  is given in Equation (B19):

$$dA = \frac{\pi(r + dr)^2}{Nm} - \frac{\pi r^2}{Nm} = \frac{2\pi r dr}{Nm} \quad (\text{B19})$$

Like the truncated configuration, the number of truck trips is estimated using Eqn. 13. The total distance travelled by truck and the number of trips for the area  $dA$  in segments 1 and 2 are given in Equation (B20) and Equation (B21), respectively.

$$\begin{aligned} dd_1 &= \frac{84 dA}{10} * 2 * \left[ \left( r * \frac{\beta}{4} \right) + (r - R') \right] \quad (\text{B20}) \\ &= 2 * \frac{84}{20} * \frac{2\pi r dr}{Nm} * \left[ \left( \frac{2\pi r}{4Nm} \right) + \left( r - \frac{2R}{3} \right) \right] \end{aligned}$$

$$\begin{aligned} dd_2 &= \frac{84 dA}{10} * 2 * \left[ \left( r * \frac{\beta}{4} \right) + (R' - r) \right] \quad (\text{B21}) \\ &= 2 * \frac{84}{20} * \frac{2\pi r dr}{Nm} * \left[ \left( \frac{2\pi r}{4Nm} \right) + \left( \frac{2R}{3} - r \right) \right] \end{aligned}$$

To calculate the average biomass transportation distance for the whole area  $QO'P$ , Equation (B20) and Equation (B21) are integrated from  $R'$  to  $R$  and  $\theta$  to  $R'$ , respectively. The total average distance

travelled by truck can be estimated by summing the two integrations, which are estimated in Equation (B22).

$$\begin{aligned}
 D &= \int_{R'=\frac{2R}{3}}^R dd_1 + \int_0^{R'=\frac{2R}{3}} dd_2 && \text{(B22)} \\
 &= \int_{R'=\frac{2R}{3}}^R 2 * \frac{84}{10} * \frac{2\pi r}{Nm} \\
 &\quad * \left[ \left( \frac{2\pi r}{4Nm} \right) + \left( r - \frac{2R}{3} \right) \right] dr \\
 &\quad + \int_0^{R'=\frac{2R}{3}} 2 * \frac{84}{10} * \frac{2\pi r}{Nm} \\
 &\quad * \left[ \left( \frac{2\pi r}{4Nm} \right) + \left( \frac{2R}{3} - r \right) \right] dr \\
 &= \frac{2 * 84 * 2\pi}{10 * Nm} * \frac{R^3}{27} \left[ \left( \frac{9 * 2\pi}{4Nm} \right) + \frac{8}{3} \right]
 \end{aligned}$$